FUEL ELEMENT PERFORMANCE MAPS FOR NUCLEAR REACTOR OPERATIONAL DECISIONS

by

OTHON LUIZ PINHEIRO DA SILVA

B.S. in Naval Architecture and Marine Engineering
at Escola Politecnica da Universidade de São Paulo (Brasil)
1966

SUBMITTED IN PARTIAL FULFILLMENT
OF THE REQUIREMENTS FOR THE DEGREE OF
NUCLEAR ENGINEER
SIMULTANEOUSLY WITH THE DEGREE OF
MASTER IN SCIENCE IN MECHANICAL ENGINEERING
at the
MASSACHUSETTS INSTITUTE OF TECHNOLOGY

December 1977
(i.e. February, 1978)

Signature of the Author _____
Department of Nuclear Engineering
December , 1977

Certified by _____
Thesis Supervisor

Certified by _____
Thesis Reader

Accepted by _____
Chairman, Department Committee on
Graduate Students

ABSTRACT

FUEI EIEMENT PERFORMANCE MAPS FOR NUCLEAR REACTOR CPERATIONAI DECISIONS

by

OTHON LUIZ PINHEIRO DA SILVA

Submitted to the Department of Nuclear Engineering on December 22, 1977 in partial fulfillment of the requirements for the degree of Nuclear Engineer simultaneously with the degree of Master in Science in Mechanical Engineering

This thesis study includes a historical review of Light Water Reactor fuel failure causes. Pellet cladding interaction, being the current major cause of fuel failure, is treated in some detail: the treatment includes an analysis and summary of most of the important related published experimental and power reactor data. Two methods of fuel failure prediction (one in development, the other in validation) are described. Finally using simple models and available computer codes a method is presented that suggests the nuclear fuel operational limits from pellet cladding interaction (specialized to Pressurized Water Reactors).

Thesis Supervisor: John E. Meyer
Professor of Nuclear Engineering.

Thesis Reader: David D. Lanning

Professor of Nuclear Engineering.

ACKNOWLEDGEMENTS

I wish to express my sincere gratitude to Professor John E. Meyer, for his patience and advice throughout this project, and to Professor David D. Lenning who kindly was the Thesis Reader.

The computer expenditures to this project were supported via MIT Energy Laboratory by Northeast Utilities Service Company, New England Electric System, Yankee Atomic Electric Company, Public Service Electric and Gas Company (NJ) and was greatly appreciated.

I am greatful to the Brazilian Navy, whose fully support made possible to study and participate in this wonderful technical environment of the Massachusetts Institute of Technology.

Special thanks to my friend Gilberto de Andrade for his encouragement and help. The colaboration of Su Chiang Shu Faya in implementing computer codes in Multics System was very valuable.

My most sincere appreciation to Maria Celia, my wife, and to my daughters, who provided a lifetime of love, encouragement and support.

To my parents

TABLE OF CONTENTS

CHAPTER 1

INTRODUCTION

Experience with water cooled power reactors has shown that rates of power increase below 5% per minute, value encountered in some reactor specifications (39), might cause fuel failures after sufficiently high burnup.

Currently recommended rates of power ascension, soak periods and threshold levels of local power are provided by the fuel vendors and there is a noticeable variation among them (26); it has been also observed that vendors periodically revise these recommendations. The calculations or experimental data that stand behind such recommendations are often proprietary data and consequently not reported to the utilities. Generally, all the utility is told in essence is that the fuel has been demonstrated to have a lower probability of failure if the vendors recommendations are followed.

These recommendations tend to reduce the plant capacity factors since they tend to limit the rate at which power can be changed. Losses (46) from 1/2 to 7% in capacity factor have been reported with very significant associated costs and loss of operational flexibility; it was estimated (45) that the slower-than-design-allowable maneuvers might cost a utility up to $7 million per year per plant.

The method applied in this thesis to develop Fuel Performance Maps provides a technical reasoning to interpret and perhaps eventually permit selective violations of the vendors

recommendations.

This thesis study has included an extensive survey in the available published material about test reactor experiments, power reactor fuel experience, fuel failure related laboratory experiments and methods of fuel failure prediction. The basic concepts and information from the survey were applied in simple but significant illustrative examples. Computer codes from the public domain were used for these calculations after modifications to calibrate and reproduce numerically the evidences encountered in fuel experience.

The final result of this work suggests plant maneuvering practices close to the existing practices. However, this method also provides to the operator an easy understanding and permits an interpretation of what might be happening in the reactor in terms of pellet cladding interaction. Eventually this method can lead to improvements in terms of plant maneuvering flexibility since it suggests higher ramp rates at the beginning of power increase maneuvers when the cladding behavior is essentially elastic and the stresses are probably below the level that can cause stress corrosion cracking; higher ramp rates are also permitted whenever there is a high probability of fuel and cladding not being in hard contact. The method also provides a way to estimate when in time this contact occurs for the first time with new fuel and the power level in which the contact first occurs when going up in power after decrease maneuver.

This thesis starts with a general review of the fuel failure causes since the early power reactors (Chapter 2);

explains with some datail the pellet cladding interaction mechanism (Chapter 3); describes briefly the existant in development methods of fuel failure prediction (Chapter 4), and finally presents the basis of Fuel Performance Maps with some numerical examples (Chapter 5).

This thesis study considers only non accident normal reactor operation conditions.

CHAPTER 2

FUEL FAILURES

This chapter provides a review of the defect mechanisms of Light Water Reactors (LWR) fuels. The aims are to show briefly that the principal causes of fuel failure are generally understood and also to indicate some of the remedies adopted to prevent failures.

In general,(17) the good performance record of nuclear fuels has been a good one. Although additional reductions in fuel failure might imply only small potential savings in fuel supply costs, any reduction in coolant activity can have a broad impact on plant capacity (11) by simplifying plant maintenance and reducing periods of limited plant operation to maintain acceptable environmental impact.

2.1 - FUEL FAILURE DEFINITION AND CLASSIFICATION

It is possible to classify fuel failures in the following way (7):

Class A:

TYPE I - Defected Cladding - Generally defined as a fuel pin (actually an assembly containing fuel pin), in which cladding integrity is breached causing leakage of fission products to the system.

Reactors normally operate with much less than 1% of the rods

failed at the end of fuel life. The leakage detection is performed indirectly from off gas or coolant sampling activity (I^{131}).

TYPE II - Forced Fuel Removal

This category encompasses fuel behavior out of ordinary, in which clad is not breached but fuel is unsafe for others reasons and fuel removal is forced.

As an example of this category, we have densification causing excessive power peaking and pin bowing which reduces the margin for minimum critical heat flux ratio (MCHFR).

Class B: Other Abnormal Behavior

Abnormal fuel behavior which is potentially costly, including behaviors not well understood altough neither defected nor unsafe.

It causes concern, because of its potential failure mechanism. This category includes duct bow, nodular corrosion, non interference bow, etc.

2.2 - FUEL FAILURES IN LWR

The goals of fuel design, fabrication and plant operation have been to minimize class A occurences while maximizing the burnup of fuel. This has been done within the framework of design limits for: steady state, transient and accident conditions. In practice, this has been a hard long task, mainly because at the beginning the contributing causes of fuel

failure mechanism were not well known or well characterized.

The role of the material limitations as creep, corrosion and embrittlement were not well known and are still subject to speculation.

Manufacturing practices, limitations in quality assurance and quality control also interacted with fuel failure phenomena.

Historically one can divide the fuel failure in the following way:

1) Early failures;
2) Epidemic failures;
3) Current failures and future concerns.

2.2.1 - Early Failures

As occured in the others types of industries, the step of going from a prototype to a commercial utilization presented some problems, some of the problems are mentioned ensuingly:

Design Related:

a) Fretting/corrosion - Vibration induced wear of pin against object. As example of this category we have (7):
   - Bypass cross flow enhanced vibration of peripheral rods at Jose Cabrera Plant (Spain);
   - Boron curtain interference in some BWR;
   - Foreign material interference as wire mesh from steam dryer (Grundreminngen BWR Plant); and bolt from core support structure (PWR, Stade).

b) Rod Bow - Caused by in pile stress relieving, leading to rod bow against ducts (BWR) this was remedied using annealed

clad tubing (51).

c) Inadequate Plenum Volume - Causing pin bursting, it was due to lack of data on fission gas release. (7, 51)

d) Inadequate Gap Size - Causing hard pellet clad interaction and consequent longitudinal split. This was caused by lack of data on fuel swelling. (41, 51)

e) Faulty End Cap Design - Improper end cap design was one of the causes of end cap failures, that was for a while the major contributor to fuel failures. (7, 10)

Manufacture Related Failures

Manufacturing defects are probably the most easily appreciated, since all manufacturing processes are prone to such defects. There has been though, a very small number of in pile defects that might be caused by fuel fabrication, one reason for such low incidence is the simplicity of design which makes the fuel 100% susceptible to non destructive testing (17); there were, though, some exceptions:

a) Pellet Loading - Cracked pellet, wrong enrichments.

b) Clad Flaws - Clad manufactured with variety of through-wall defects as partial cracks precipitates, inclusions.

Although few defects have been attributed to these, they constitute source of trouble, which might be improved by better manufacturing procedures and quality control (7).

c) End Cap Welds - For a while a major contributor to fuel failure, improvements in welding techniques and quality control remedied this situation. (10)

d) Fuel Pellet Fabrication Processes - Proper selection of the powder preparation process, adequate granulometry, and improved sintering temperature have proven to be very important to fuel in pile performance. (42)

e) Moisture - Moisture that remained on the fuel after incomplete drying contributed to clad hydriding failures. (34, see also section 2.2.2)

Unforeseen Failure Mechanisms

This category emphasizes the importance of in reactor testing:

a) Intergranular attack of stainless steel cladding of the very early BWRs, remedied by Zircaloy cladding. (51)

b) Fretting zirconium grid - rapid in pile deformation of zirconium grid contributed to fretting the change to inconel solved the problem. (7) Combustion Engineering still uses Zircaloy grid but design so as to account for spring relaxation. (52)

c) Crud deposition - crud deposition, mainly Fe_3O_4 with Mg, Mn, N, Cr, Co deposited from colloidal suspension in the primary coolant and precipitated by the radiation environment.

This is not a deleterious effect, unless it impeds heat transfer by becoming too thick or non porous. It tends to cause clad overheating which accelerates corrosion.

Instances of large crud deposits due to vortex shedding, were remedied by proper spacer design.

Cu, Mg, Ca transform normally porous crud into dense. Improvements have been made by improving water chemistry and by removing Cu-bearing materials from primary loop. (53)

2.2.2 - Epidemic Failures

Fuel failure rates have been low about 0.1% per cycle (7), however, certain types of failures have led to high rates. During 1969 and 1970, hydriding was the single major contribution, while in 1971 densification appeared to be the major problem.

Internal Hydriding (Ref. 7, 34)

In the late 1960s BWR and PWR (predominantelly BWR) began to show accelerated defects in early fuel life (0.5 to 5MWd/kg). Detected rod defects were associated with H_2 nodules or blisters, which cracked to form a penetrating defected ("sunburst") - Fig. 2.1 .

The location of the sunburst was found to be random in each pin and also in random pin distribution in core.

Experiments (34) indicated that Zr-2 and Zr-4 could have the zirconium content attacked locally to form bulk hydriding ($Zr\ H_2$) with as little as 0.1mg of Hydrogen, and also that the hydrogen could be supplied by water (1mg).

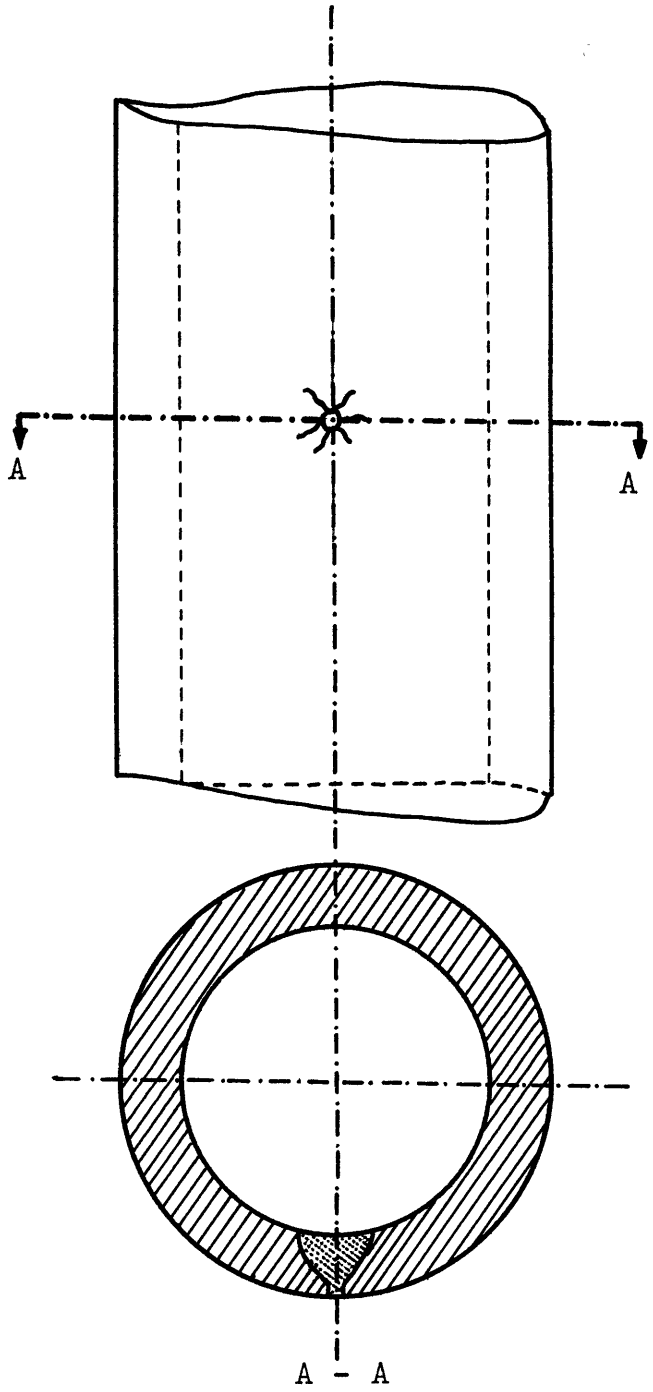

Fig. 2.1 - "Sunburst" Defect (Ref 7)

Despite this evidence, failures were not foreseen. Investigation subsequent showed the mechanism to occur as follows:

1) Hydrogen bearing impurities in fuel attacks inside clad, locally, where the oxide film is broken down.

2) For hydrogen pressures greater than 10Pa (10^{-4}atmospheres); the arrival rate is greater than the diffusion rate away from the zone of attack, which causes the solubility limits to be exceeded.

3) When bulk hydrides form the higher specific volume of Zr H_2 result in internal stresses (Zr H_2 specific volume 0.00182m^3/kg while Zr specific volume is 0.00154m^3/kg). These high internal stresses may cause cracking and failure.

4) The number of sites of primary hydriding are few per rod, but reaction procedes rapidly once initiated, using up available hydrogen.

The local breakdown of oxide film may occur from:abrasion of autoclaved film, pellet interaction and chemical breakdown flourine (F^-) contamination accelerates hydriding.

Hydrogen Sources

a) H_2 trapped in pores or soluble in matrix from sintering process.

b) Hydrocarbon impurities caused by fabrication process.

c) Moisture (major source): UO_2 is an excellent dessicant. The change to lower density fuel increased the moisture content due to higher surface area and more open porosity.

d) There have been instances of H entering Zr by corrosion of the outside surface in hotter regions of the rod, migrating down the temperature gradient to weld zone causing severe hydriding without defecting. (54)

The remedy to avoid hydriding has been:

a) Adequate burnout of hydrocarbons in fabrication.

b) Hot vaccum outgas pellets.

c) Use of getters in fuel pin, that preferentially reacts with hydrogen preventing Zircaloy hydriding.

d) Autoclave cladding 72 hours at 400°C (General Electric) to buildup a protective internal oxide layer (34) versus no autoclave Exxon who claims that multiple scratching of autoclaved surface leads to hydriding. (43)

Densification and Clad Flattening (Ref. 7, 14, 3, 17)

In the mid 1960s, Bettis Lab reported UO_2 fuel swelling and also the relation with burnup.

Fuel vendors (including G.E. and Westinghouse) reduced the fuel density to 90-93% of TD, considering that the porosity would accomodate swelling, but unfortunatelly this density reduction led to fuel failure due to densification.

The densification of fuel pellets has been observed during relatively short term irradiation, causing decrease in their volume and corresponding shrinkage in pellet diameter and

length.

As consequence of the volumetric reduction, the column of pellets gets shorter and there is an increase in gap size. Mechanical interaction between the fuel rod cladding and pellets may cause the hang up of a fuel pellet in the cladding tube, thus preventing the settling of an upper part of the fuel pellet column onto the top of the reduced length pellet column below.

Once these axial gaps are present, there is the tendency for the Zircaloy cladding to suffer a local buckling collapse in the region of the gap.

Early observations whose importance were not fully appreciated:

. Columnar grain growth (reported in 1969-1970).
. Resolution of fission gas bubbles (reported in 1969-1970).
. Closure in reactor of fabricated pores smaller than one micron.
. Clad ovalization under external pressurization also known from early fuel profilometry and diametral scans.

Example of reported problems in utilities (7):

- Ginna Reactor

a) Using unpressurized Westinghouse pellets, critical in 1969.
b) First shutdown, leakers removed.
c) Coolant activity was observed in the second cycle (April 1972) observed flattened sections and leakages in the pins. It was observed absence of fuel in 1/2 to 4 inches(10 to 100mm) toward upper 40% of core.

. Point Beach 1: Shutdown in September of 1972 with 3% of rods flattened.

. A.B. Robinson 2: Local power monitors indicated flux peaks (absence of pellets in stacks)in 1% of rods.

In older and lower rated cores and in stainless steel cladded cores, no flattening was observed nor in BWR (lower coolant pressure).

Summary of In Reactor Observation on Sintering

a) Fuel sintering occurred towards upper core in rods of higher power.
b) Frequency of occurrence of fuel sintering inversely related the degree of pressurization.
c) In most of the cases, cracking and leaking occurred near the edges of fully flattened sections.

Summary of Hot Cell and Analytical Investigation on Sintering(7)

a) The weight of all rods within the specifications (gaps not due to forgotten pellets).
b) γ-rays and X-rays scans, indicated fuel gaps in uncollapsed rods.
c) Profilometry indicated ovalization both in gapped and ungapped regions, being the highest ovalization at the top.
d) Calculations and measurements of Zircaloy cladding growth indicated that the length change of clad was not sufficient to account for gap sizes.
e) Density measured indicated 92-96% TD showing higher densifi-

cation at periphery.

f) Non isotropic phenomena.

Probable Mechanism of Fuel Failure Caused by Sintering (14,7,17)

Based in hot cell observation, plant data and analytical studies the flattening mechanism appears to be:

a) Low density fuel (90% TD) undergoes densification early in life as result of closure of small pores - Fig. 2.2 .

b) The fuel stack begins to decrease when the linear heat generation rate (q') and fuel temperature increase.

c) Pellets may be cocked or wedged where the clad creepdown hangs pellet up (see Fig. 2.3).

d) The lower part of the stack shrinks from hung pellet producing an axial gap.

e) The clad continues to creep down flattens and collapses into gap.

Probably the densification and flattening were not observed in earlier fuels in test reactors because it was used higher density fuels and the pellet stack had a length of only 3ft (1m) instead of 14ft (4m) as it is in reactor.

Effects of Densification and Clad Flattening on Fuel Performance (3)

The fuel densification affects the heat transfer from the pellet to the surrounding cladding and to the cooling water. As the pellets densify and shrink in their dimmensions, the size of the small radial gap between the sides of the pellet

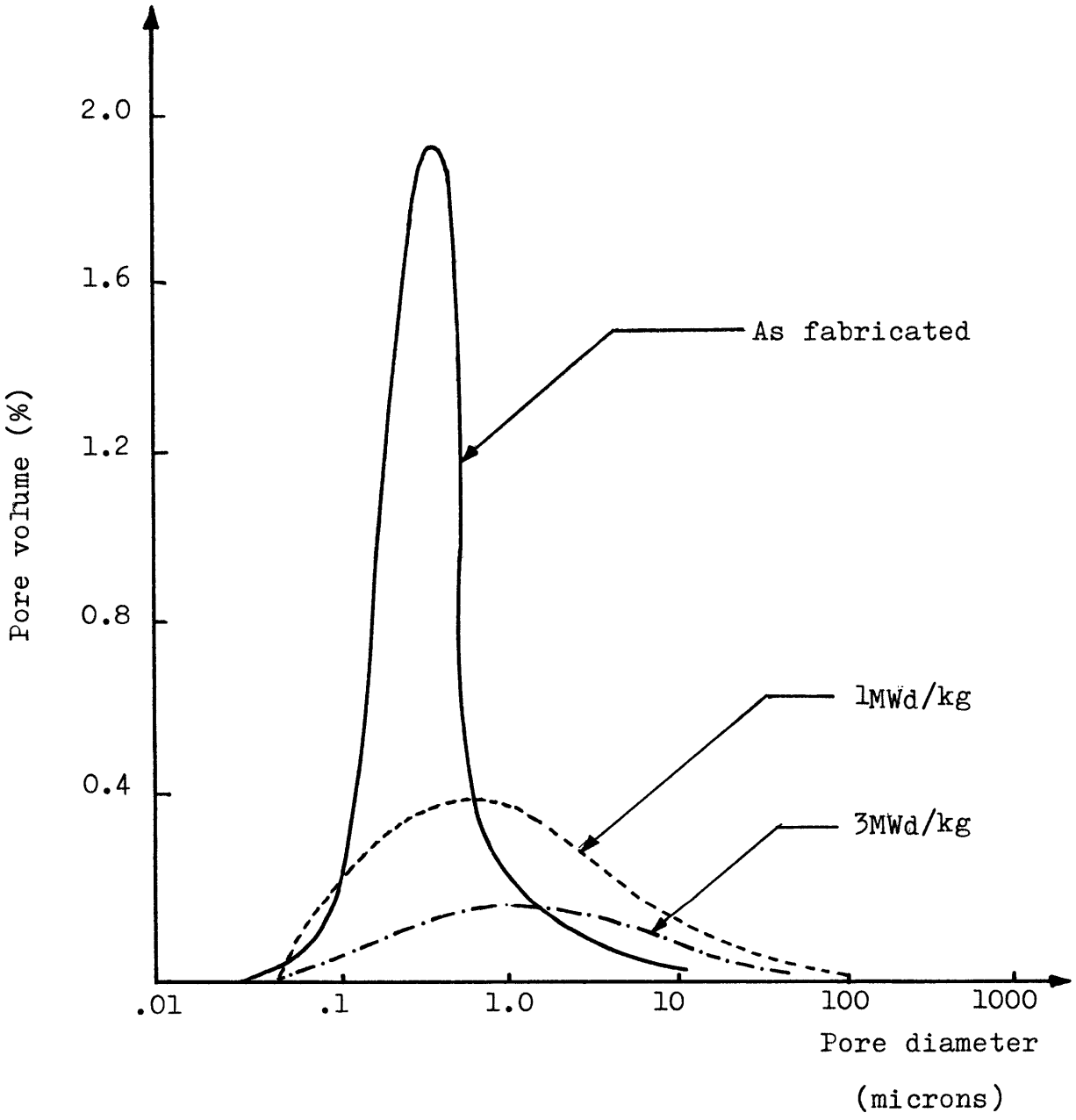

Fig. 2.2 - Effect of Irradiation on Porosity Distribution in an Instable UO_2 Fuel (Ref 7)

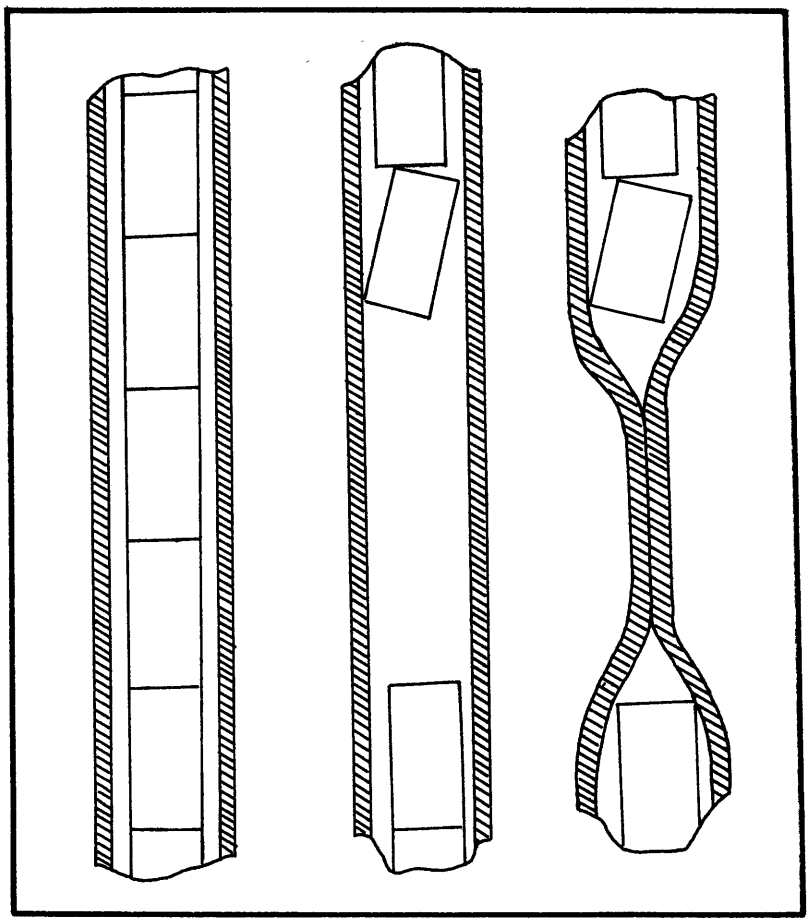

Fig. 2.3 - Cladding Colapse into Axial Gap
(Ref 7)

and the cladding increases. Later, as the cladding creeps down towards the pellet under the influence of the outside coolant pressure, there is a decrease in the gap dimension. These gap changes during reactor operation must, of course, influence the fuel element behavior during both normal and abnormal situations.

The local stresses and deformations induced in the collapsed cladding section, severely endanger the integrity of the fuel rod.

Another important effect of the fuel densification phenomena are the local changes in heat generation rate of the reactor core. The replacement of fuel by gas filled space within the fuel rod has an effect of neutron flux distribution in the reactor core. The effect is to increase the fission rate in fuel pellets adjacent to the gap, creating localized increases in the power distribution. When clad collapses down to the axial gap section, there are additional effects to be considered. One effect of the collapse is that a part of the formerly present gas filled space is now replaced by coolant water. This has a further effect on neutron thermalization, which further increases the power locally.

Normally the consequences of fuel densification and clad flattening are:

a) plant outage for replacement of large flattened and/or defected rods.

b) decrease power rating of the plant when detecting undefected flattened rods. The power derating is to guarantee that local power peaks remain within the specified range and also

to guarantee adequate margins with respect to minimum critical heat flux ratio (MCHFR). The derating of the plant might also be imposed by loss of coolant accident calculations (LOCA) since due to the radial gap increase, there is an increase in the energy stored in the fuel.

Design Changes to Avoid Fuel Densification and Clad Flattening Problems

a) Westinghouse have gone from 90% theoretical density (TD) in UO_2 pellet to more than 94% TD (4).
b) Pressurized water reactors adopted internal helium prepressurization of fuel rods, which alleviates the pressure differential on clad with favorable effects on creepdown. The internal fuel pressurization at the beginning of life at room temperature, seems to be within the 200-400 psi (1400 to 2800 kPa)range, and is usually an important proprietary data since the amount of internal prepressurization plus the fission gas release affects the end of life reliability of the fuel.
c) Exxon (43) uses a thicker clad, higher radial gap, and inconel springs in plenum. The inconel springs retain better the mechanical properties and seem to work maintaining the pellet stack integral during densification, probably the spring action is successful partially due to thicker clad, (since the pellet clad contact following creepdown could resist axial force).
d) These and other design changes have virtually eliminated the flattening problems. For example, changes in fuel density

in powder preparation and in sintering techniques has lead to a more adequate pore size initial distribution lowering substantially the fuel densification problems (42).

2.2.3 - Current and Future Concerns

As explained before, the observations and measurements taken from the irradiated fuel elements in test reactors and power reactors lead to a better understanding of fuel behavior. As consequence, design changes, improvements in fabrication techniques and new quality control and quality assurance procedures have been adopted and have given minimization in the so called "early failures" of fuel elements. Similar improvements have caused virtual elimination of problems caused by hydriding, fuel densification and clad flattening (epidemic failures).

Unfortunately, judging by the results of the observation measurements during refueling and at pool side in the last two years, there are remaining concerns with respect to fuel failure that we are going to classify in the following way:

Current minor concerns in LWR fuel

Current major concerns in LWR fuel

Future concerns

Current Minor Concerns in LWR Fuel:

a) Nodular corrosion (7)

White circular oxide patches with approximately 200 to 500 microns in diameter and 10-100 microns in depth which form in Zircaloy pins and ducts (PWR and BWR) after long exposure

(post transition oxidation), causing wall thinning.

b) Fuel Rod Bow

Significant fuel rod bow has been observed with more incidence in Westinghouse PWR reactors and may be caused by large grid force effect in the lower half of the core. The potential consequence is excessive subchannel area reduction (observed up to 50%) and decrease in margins with respect to minimum critical heat flux ratio (MCHFR).

c) Clad Fatigue (17, 12, 55)

Although cladding failure by fatigue has been demonstrated in stainless steel clad experimental rods and has been mentioned as a possible defect mechanism Zircaloy clad power reactor rods, it has not yet been blamed for any fuel failures in power reactors. However, there is some concern that the need for nuclear reactors to provide a load following capacity (as when they constitute a larger fraction of the generating system, or when by any reason the non-nuclear part of the grid becomes less elastic to power changes) could lead to an incidence of cladding fatigue failures.

In the experimental rods that failed the cladding consisted of extremely thin (0.1mm) stainless steel which collapsed onto the fuel forming a sharp longitudinal ridge (55) . When the fuel was raised in power its expansion stretched the cladding, reversing the strain at the crest of the ridge. On reducing power the original ridge reformed

(two rods failed after about twenty of such power cycles). Test more representative of actual power reactor fuel rods using strain gauges attached to Zircaloy cladding, had shown that the cladding did not deform plastically into longitudinal ridges (Reference 17) under the coolant pressure. The resulting measurements showed that for large power cycles the amplitude of the strain cycle in the cladding was only 0.1%, indicating that many cycles could occur without fatigue failure. Other tests performed have shown the absence of fuel failures even after several hundred power cycles.

Current Major Concerns in LWR Fuel

The interaction between fuel and clad, both chemical and mechanical (and especially combined chemical/mechanical) is considered to be the major concern nowadays. Failures from such interactions are presently controlled by limiting the power ramping and thereby also causing reduction in the capacity factor of the plant. Pellet clad interaction is also a major cause of fuel failure during some postulated transient and accident conditions.

Although a fuel rod consists, in essence, of only fuel and clad assembled in a simple cylindrical geometry, its in service behavior is very difficult to analyse in detail. The fuel is a porous medium whose composition varies in space and time, and within which many chemical species are generated by fission. In its hot central region it may deform plastically but in the cooler outer region it cracks. The observed cracks

exhibit a random nature superimposed on a pattern due to thermal stresses and mechanical stresses. These complications assure that it is very difficult to analyse rigorously the fuel failure from first principles, even though it seems possible to explain qualitatively most of the observed failures.

The pellet clad interaction PCI as cause of failure was first observed and reported in CANDU reactors (7), and shortly thereafter, it was observed to play an important role in LWRs with Zircaloy cladding. Being a central point in this thesis, the PCI will be discussed in some detail in the next chapter.

Future Concerns

Existing fuel rods belong to a generation for which a lot of work was performed to achieve pellet shapes and dimension that minimize the stresses during pellet clad interaction (see also Sec. 3.1.1). Also, enormous development has occurred in ceramics technology and one can say that there is now a better understanding of swelling, gas release, and fuel cracking mechanisms. Similar advances have occurred with densification and hydriding problems. It seems that there exists a reasonable understanding of the fuels designed and manufactured to attain today's design limits and parameters, and to work in reactors which also have certain operating limits.

In future, we can expect new fuel designs to be associated with new defect mechanisms and the existing designs to be pushed beyond their present limits of demonstrated good performance (e.q. in load following operation).

It is therefore imperative that all members of the nuclear

fuel industry remain vigilant,in design,in exercising a high level of quality control during manufacture, in adequately testing the design concepts before commiting them to power reactors, and in rigorously controlling in-service conditions.

CHAPTER 3

PELLET CLADDING INTERACTION

The presence of defected fuel in the nuclear reactor core can have a significant impact on plant capacity.

Fuel failure modes of recent concern, like hydride failures and clad collapse by densification have been overcomed by changes in design and in the production specifications, without appreciable influence on fuel economy. However, experiences with water cooled reactor fuel rods have shown that a power increase (ramp) can cause cladding failure after a sufficiently high burnup. These fuel rod defects are attributed to pellet cladding interaction (PCI), and persist as a limitation even though the current design of fuel pins has been made to reduce such problem.

At the beginning of life of the fuel element, when power is raised, the as fabricated fuel/cladding gap is available to accommodate differential thermal expansion. Later in the fuel working life, however, if the power is increased from a low level to a high level, the Zircaloy cladding is somewhat embrittled by irradiation damage while the clearences have been, at least partly, taken up by cladding creepdown, fuel swelling and diametral movement of fuel fragments. Furthermore, the discontinuous nature of the stack of pellets and cracked individual pellets contributes to produce localized cladding stress concentration. Also among the fission product species generated in the fuel is iodine that can cause stress corrosion

cracking (18, 3) of the Zircaloy.

This chapter describes the contributing mechanisms of pellet cladding interaction (PCI) aiming to give a general picture of this problem. It is, however, important to point out that most data on PCI have been obtained from laboratory and test reactor experiments and it seems that there are a lot more details to be known about the sequence of the fundamental events in PCI cracking mechanism. This situation is due in part to the masking of the datails in cladding fracture caused by localized factors and also because of complexities of stress and the internal fuel pin environamental histories encountered in operation; the problem is further complicated by the uncertainties in reproducing in laboratories and even in test reactors the same phenomena that occur in power reactors real life.

3.1 - FUEL CLADDING CONTACT

Designers generally have tried to avoid or minimize the direct contact of fuel and cladding in Light Water Reactors (LWR) by choosing self standing cladding tubes and providing the maximum fuel pellet-cladding gap and cladding thickness that the balance among heat transfer, fuel internal temperature and material properties, reactor physics and economical considerations would permit. Experiences however, have shown that for Zircaloy-UO_2 fuel pins, in most of the situations, the fuel pellet contact is unavoidable. The following mechanisms

contribute to such contact:

1. Differential thermal expansion
2. Fuel swelling
3. Cladding creepdown
4. Fuel cracking and radial relocation

3.1.1 - Differential Thermal Expansion

When the fuel rod is subject to the neutron flux and generates power the radial temperature profile is approximately parabolic. The initial gap width changes because of the relative thermal expansion of the fuel and the cladding. Although the thermal expansion coefficient of the cladding is comparable to that of the fuel, the temperature rise of the fuel is considerably greater than that of the cladding. The net result is a reduction in the gap as soon as the reactor goes to power.

The change in gap width is not constant along the axial dimension of the pellet. If the pellet initially is a perfect cylinder, when applied the temperature field it distorts so that the flat end faces bulge out and the curved surface bends outward ("hourglassing", Fig. 3.1) the rim being displaced much more than the beltline of the cylinder curved surface. This is observed experimentally in good agreement with calculations.

The axial expansion of an unrestrained stack of cylindrical fuel pellets is different than would be expected applying (generalized) plane strain theory; for unit length-to-diameter ratio pellet the axial expansion is about twice the amount

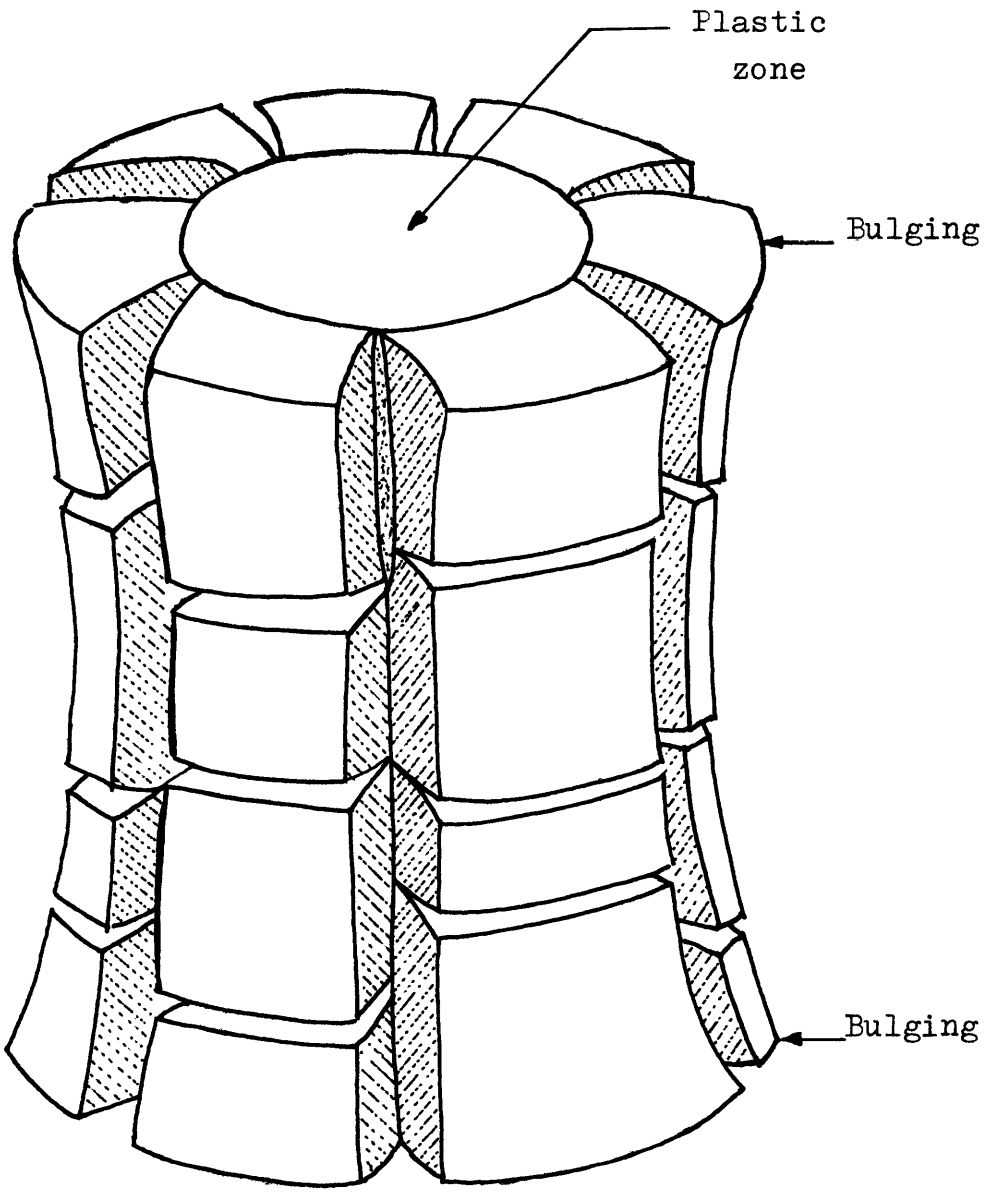

Fig. 3.1 - Ceramic Pellet Condition During Irradiation

(Ref 52)

calculated by plane strain theory. This large axial elongation of fuel pellet stacks is due to end-face bulging of the individual pellets and has been minimized by some manufacturers using "dished" pellets (Fig. 3.2); the dished shaped leaves room for longitudinal expansion of the hotter regions near the center of the fuel pellet.

The dishing, however, may give rise to appreciably larger diametral expansion at the end of the rim of the fuel pellet. This, as will be mentioned later, aggravates the ridging of the fuel element cladding, and can be alleviated by proper shaping the pellet profile (tapering or chamfering near the ends).

It was observed (14) that the ridging of the pellet increases with the linear heat generation ratio (LHGR) and pellet height to diameter ratio (Fig. 3.3).

3.1.2 - Fuel Swelling

Swelling is defined as the fractional increase in the volume of the fuel with respect to the volume of the as-fabricated fuel.

The fission process produces twice as many atoms of fission products as the number of uranium (or plutonium) atoms fissioned. Fuel swelling, though, is due to the replacement of heavy metal atoms by fission product atoms and is commonly considered as the sum of a contribution due to inert fission gases and another arising from all other (solid) fission products.

The solid-fission-product gives a relatively small contribution to swelling and is found (2) to be about 0.32% per atom

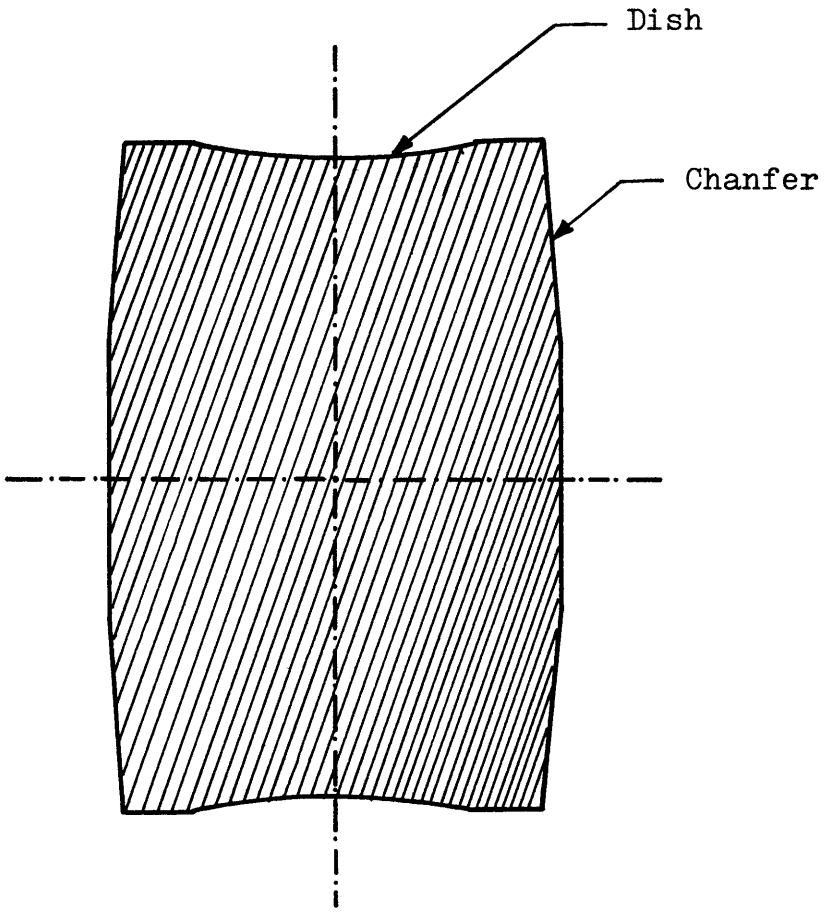

Fig. 3.2 - Fuel Pellet Initial Shape

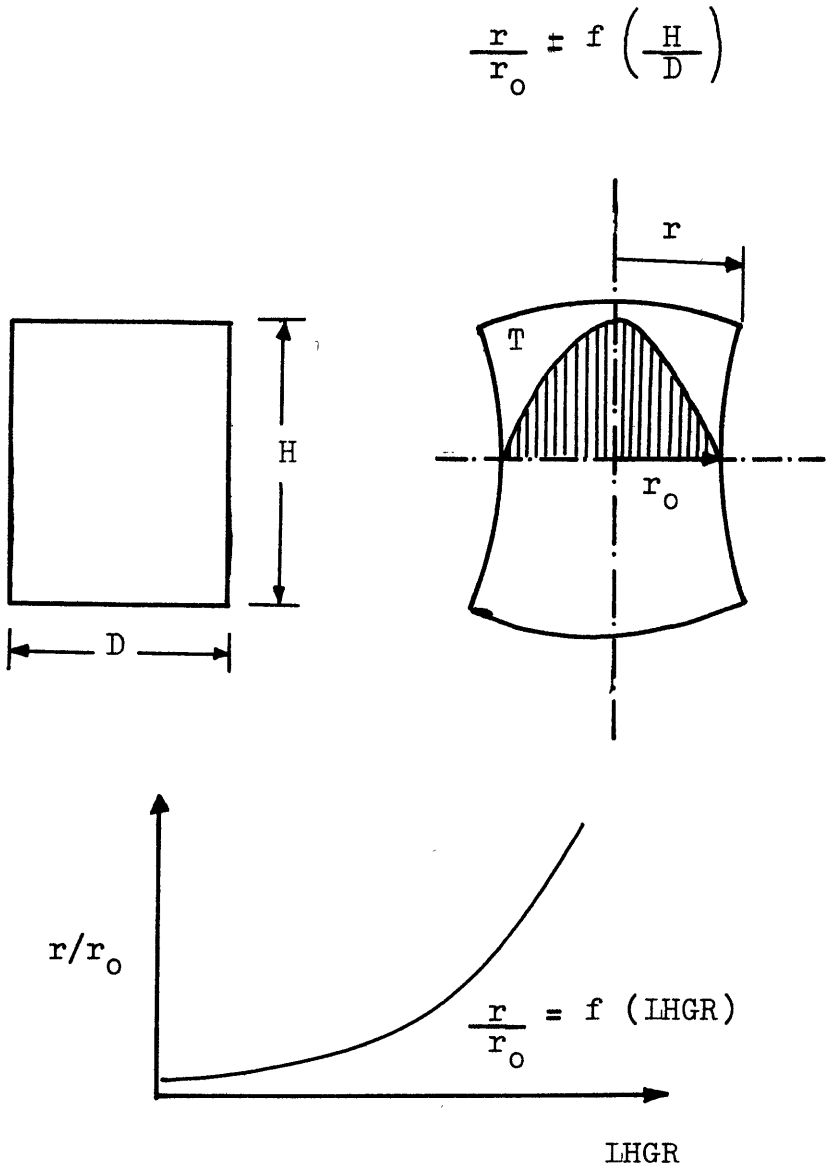

Fig. 3.3 - Pellet Hourglassing (Ref. 7)

percent burnup (0.089 MWd/kg).

The fission products xenon and krypton, due to their virtually complete insolubility in the fuel matrix, and the fact that their normal pure state is a gas rather than a solid have a unique status among the other fission products. Due to their insolubility, being kinetically possible, they are rejected from fuel matrix; being gas (in normal state) they are either released to the gaseous atmosphere within the fuel pin, or precipitated as bubbles of gas within the fuel body.

The density of the gas in such bubbles is considerably lower than that of the solid fuel. Gas atoms residing in these bubbles occupy more volume than either the fissile atoms they replaced or fission-product atoms that segregate as solid phases. The concentration of fission gases, after certain accumulation, leads to swelling of the fuel to a larger degree than the volume expansion that would occur if the xenon and krypton had remained dispersed on the atomic scale of the fuel matrix.

In the undisturbed structure of the fuel, however, the fission gases are quite immobile in the solid (because of the low temperature, less than 1200°C), and consequently, they are not released in large quantities, and the expansion they cause is comparable to that of other solid fission products. In the undisturbed region both release and swelling are low. In the equiaxed-grain-growth region (if it happens) gas release is appreciable, but large swelling can occur because a significant fraction of gases is retained in the fuel as bubbles. In the columnar-grain region, nearly all fission gases are released as

soon as they are formed, and the gas swelling is quite small.

The IWR power reactors normally work in such way that fission density, burnup and fuel temperatures are too low to produce fuel restructuring, and the complex series of phenomena that are now recognized as occuring in highly rated fuels. An exception of this trend occurred at Maine Yankee Reactor (3) where fuel densification took place causing an increase in fuel-cladding gap clearance, and worse heat transfer conditions. This heat transfer degradation lead the pellets to work in a higher temperature regime producing fuel restructuring and higher gas release (further worsening the heat transfer conditions).

As it can be seen in Fig. 3.4, swelling does not play an important role as a major contributor to fuel contact up to relatively high burnups. The same conclusion is shown in Fig. 3.5.

3.1.3 - Cladding Creepdown and Ovalization

Considering most of the present fuel designs, it is appropriate to consider the creepdown of the Zircaloy cladding as the major contributing cause for fuel pellet-cladding gap closure.

Post irradiation examination of a large number of fuel rods of average burnups up to 40 MWd/kg revealed characteristic dimmensional changes of Zircaloy cladding and UO_2-pellet columns as summarized in Fig. 3.5 .

Stehle et al (5) suggests that by creep under coolant pressure, which is enhanced by the fast neutron flux, the mean

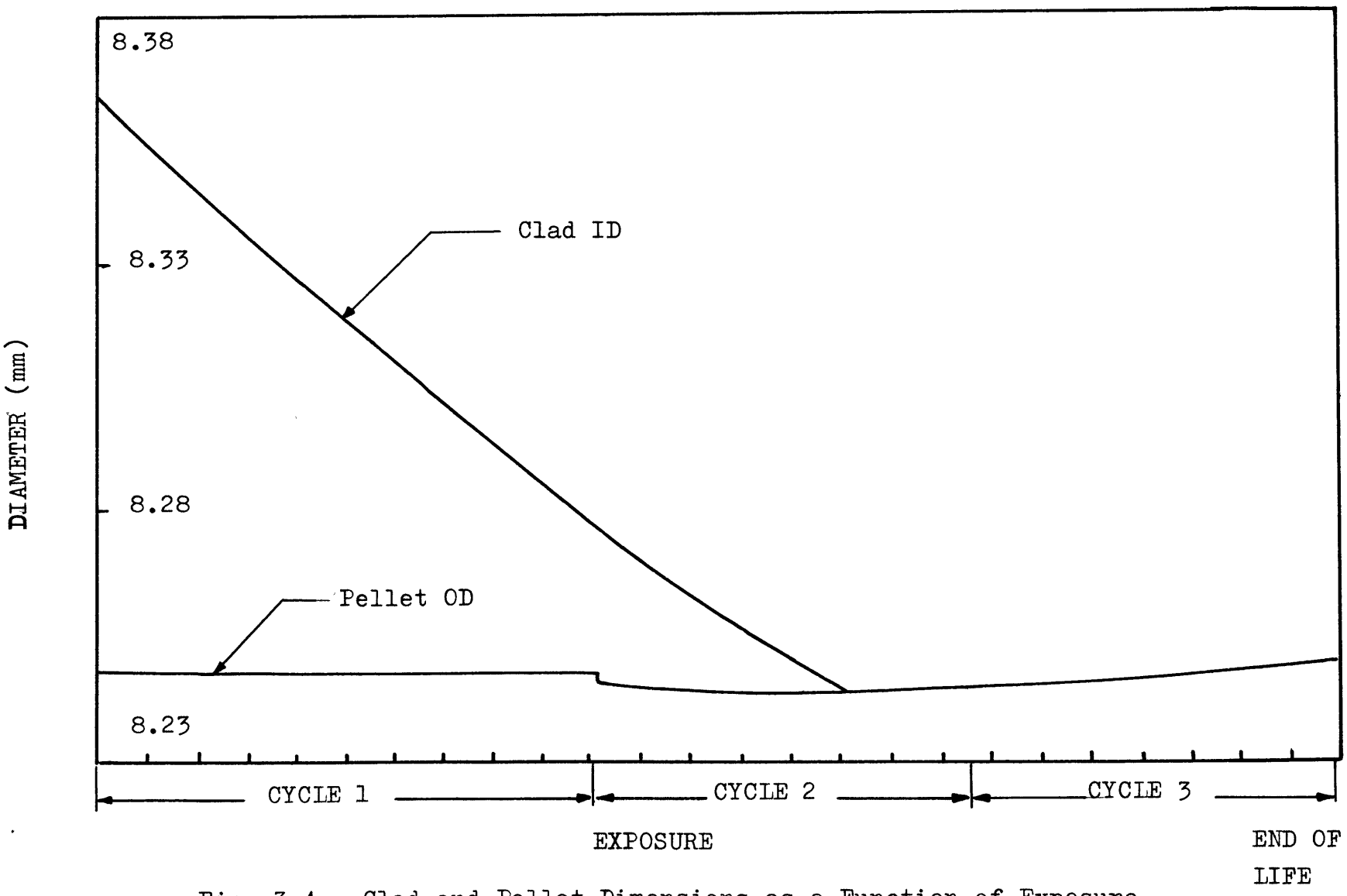

Fig. 3.4 - Clad and Pellet Dimensions as a Function of Exposure

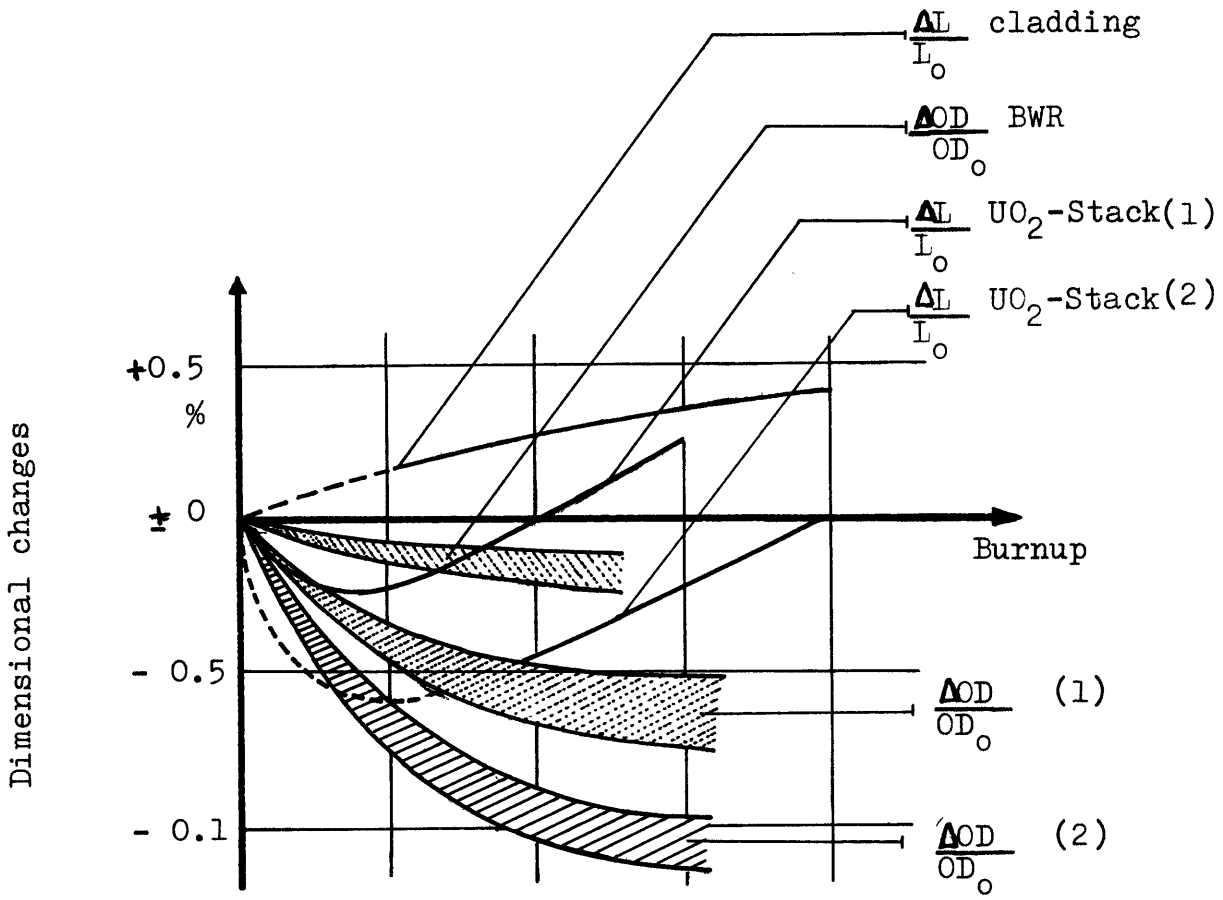

(1) PWR prepressurized

(2) PWR unprepressurized

Fig. 3.5 - Dimensional Changes of Light Water Fuels Rods (Ref 5)

outer diameter of the cladding decrease according to the following empirical relation

$$\left(\frac{\Delta OD}{OD_o}\right) = \text{constant} \cdot t^{0.45}$$

where: t = time

OD_o = initial outside diameter of the cladding

This is, of course, a very empirical relation that does not consider the initial ovality and whose constant depends on stress, temperature, material properties and fast flux, whose variation during the life time of a fuel rod are not taken into account. This is however, an experimentally derived correlation that reflects the effect of the creep during the early stage of operation (it does not include the later influence of the supporting action of the UO_2 pellets).

As can be seen in the Fig. 3.6 the in pile behavior of the fuel element shows that the ovality increases while the rod outer diameter decreases until UO_2 pellets support the cladding. Initial support occurs in this design when the outer diameter decrease is about 0.5%. It was also observed that at this point in time the development of circumferential ridges across the pellet interfaces starts. Further decreases in cladding diameter causes increasing ridges and decreasing ovality as the amount of cladding resting on the UO_2 pellets increases.

It is intersting to observe, with regard to creepdown of the cladding tubes, that in this study (5) the diameter (even

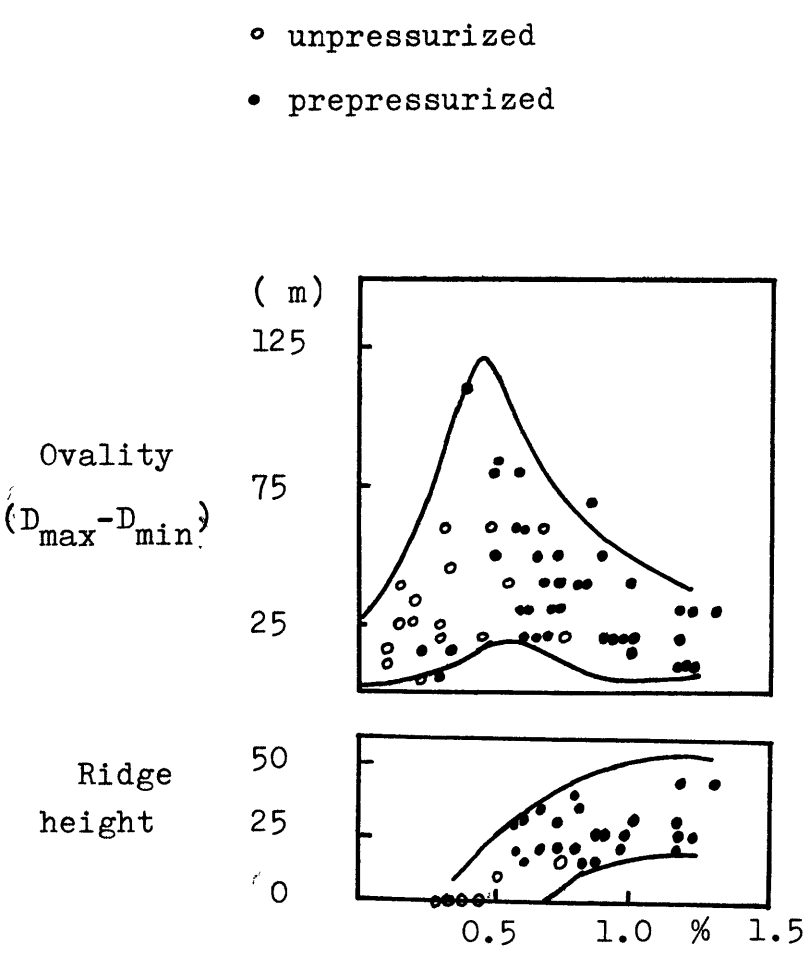

Fig. 3.6 - Ovality and Ridge height Versus Decrease of Outer Diameter (Ref. 5)

across the ridges) is always below the initial diameter of the tube.

Prepressurization of PWR fuel rods delays the creepdown and ovalization of the cladding tubes, as can be seen in Figs. 3.5 and 3.6 .

The theoretical solution of the creep buckling problems of thin-walled shells combines the difficulties encountered in shell analysis with those arising from the non-linear nature of the creep problem. For this reason only few solutions resting on diverse simplifying assumption have been suggested in this field among them BUCKLE, TCOV and CINCEER computer codes (7). The BUCKLE code is used in this thesis (Chapter 5).

3.1.4 - Pellet Cracking and Radial Relocation

When the fuel rod is first brought to power, each fuel pellet will normally develop cracks due to thermal stresses. The pellet center tends to expand more than its periphery due to the existance of a center to surface temperature gradient. To accomodate this excess center expansion, radial cracks first form in the colder peripheral material. Then, with the continued increase in the heat output further expansion of the pellet center causes additional cracks and further opening of existing cracks.

Pellet cracking and fuel densification are competing gap closure mechanisms. The pellet cracking tends to decrease the as fabricated gap, while fuel densification tends to increase it. These two mechanisms are usually completed after a few hundred hours of irradiation.

Recent studies show that pellet cracking and healing and the resultant fuel relocation give substantial closure of the initial as fabricated pellet-to-cladding gap.

For example, measurements (8) of UO_2 pellet diameter on fuel rod cross section at different burnups indicate clearly pellet cracking and radial relocation phenomena. Additional experiments performed at Kraftwerk Union Aktiengesellschaft (KWU), Germany (5) have shown that the gap between pellet and cladding is reduced in about 40% in early operation due to the radial relocation of the cracked pellet. It was, also observed a decrease in rod diameter up to burnup of 40MWd/kg (U). The magnitude of the decrease showed that pellet relocation is a reversible phenomena, and that pellets reconstitute almost completely.

3.2 - MECHANICAL INTERACTION

The combination of the effects of differential thermal expansion, pellet swelling, densification and radial relocation determines at what point in time (for a determined power history) gap closure occurs.

At the beginning of life, pellet cracking and fuel densification are probably the dominant mechanisms, the pellet cracking tends to decrease the gap while fuel densification tends to increase it. Clad creep gradually reduces the gap size until it closes completely after significant period of irradiation. Fuel swelling, in existing fuels manufactured

according to latest specifications, only affects substantially the pellet dimension at the end of fuel life (Fig. 3.4).

When the gap is closed, and the fuel is in firm contact with the cladding, the latter will be forced to follow the thermal expansion of the pellet when the reactor goes up in power. The hoop and axial stresses of the cladding (usually in compression before starting the ramp) tend to change from compression to tension and the values reached will depend on the magnitude of the power increase and the rate at which this power increase is carried.

Numerous direct in-reactor measurements (12) have shown that the deformation characteristics of the fuel pin in the axial and radial direction follow the same general pattern. This characteristic behavior is indicated in Fig. 3.7 that considers a fuel pin that has an open gap initially and the gap closes during the power increase.

As we are going to see later on, in some reactor situations, the gap could be large enough to remain open up to the end of the power increase, preventing the fuel cladding direct contact. This situation tends to happen at the beginning of the fuel residence in-reactor. At the second half of the fuel life in reactor the firm contact at the beginning of the power increase seems to be the most probable situation (as long as the pre-ramp power has been maintained for some time), (4, 5).

Fig. 3.7 shows that up to certain load, when the gap is still open, the cladding elongates according to its own coefficient of expansion; when the oxide fuel, by its thermal expansion, has filled the gap and is in firm contact with the

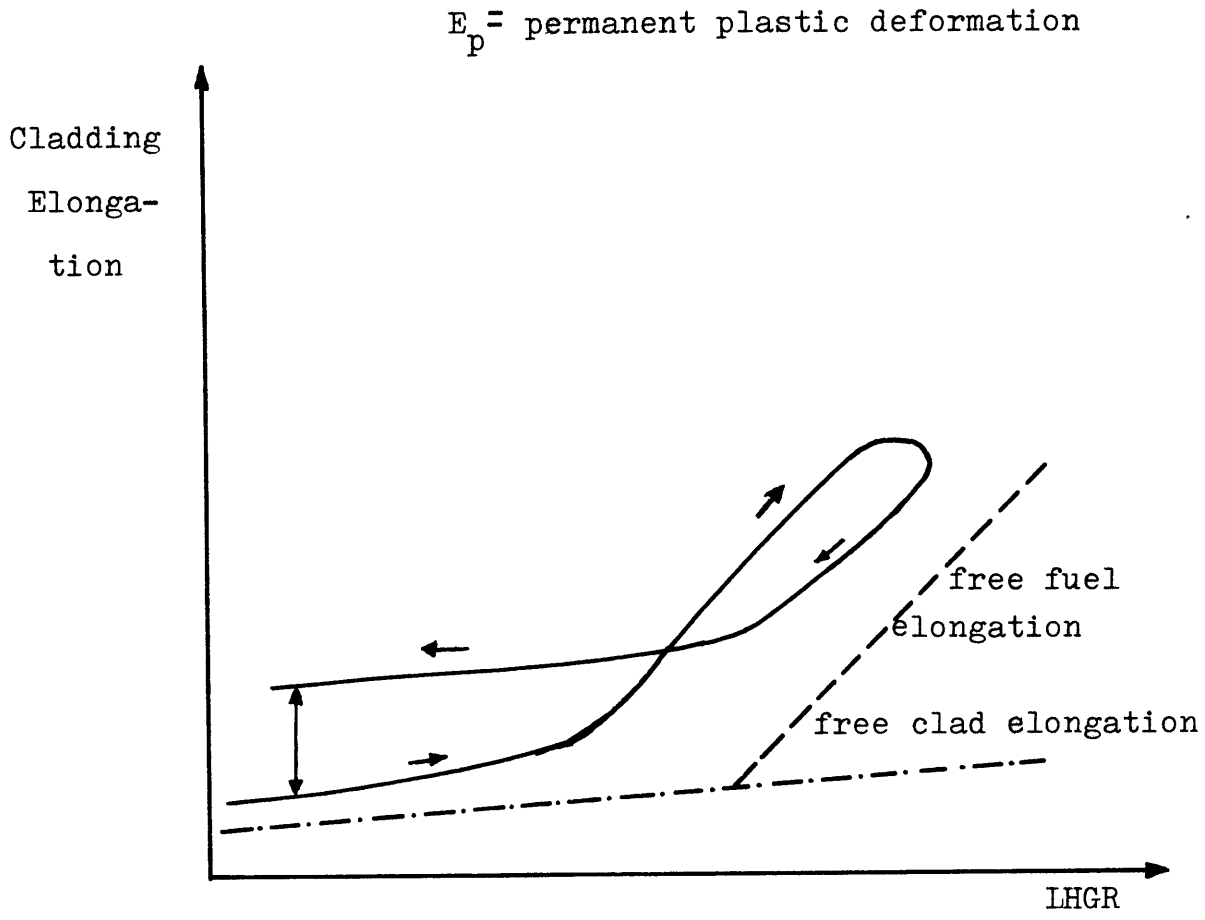

Fig. 3.7 - Cladding Elongation In-pile (12)

cladding, the cladding will be forced to follow the thermal expansion of the fuel. At higher heat loads, the expansion curve might bend off a little, indicating that relaxation takes place.

On the way down in power a small hysteresis loop is formed. The cladding first follows the contraction of the pellet, then the cladding looses contact and contracts freely. In this figure a small amount of plastic deformation is indicated. On the next increase in power the rod will deform approximately according (but not necessarily equally) the curve it followed on the way down. The exact shape of this deformation trace depends somewhat upon the manner of carrying out the power cycle.

In the absence of creep of the cladding and pellet, and any other change in shape and size (swelling for example) in the pellet, once a fuel pin has been through a power cycle no additional strains and permanent deformations would be inflicted unless the previous maximum power level is exceeded. This behavior, however, may not occur, since a progressive extension of the cladding, due to the ratchetting phenomena may develop, as will be explained at section 3.2.1 .

Local stress and strain concentration caused by fuel cracks and other discontinuities in fuel pellets play a very important role in pellet cladding mechanical interaction as will be explained in paragraph 3.2.2 .

3.2.1 - Ratchetting of Fuel and Cladding

Progressive extension of fuel rods has been observed under cyclic conditions of reactor power (14, 19).

The exact picture of the governing mechanism under which ratchetting can occur, is complicated by the very diverse conditions under which fuel pellets interact with the cladding; this problem will be discussed here only in a qualitative way.

Suppose that a fuel rod is subjected to a ramp in power and a return to zero power as shown in Fig. 3.7. The fuel gap is originally open and a "permanent" cladding axial deformation remains when the reactor returns to a lower power level and the gap is again open. When hard contact ceases, a relative movement between the fuel stack and the cladding tends to occur as the mutual axial forces are removed. The fuel will tend to consolidate by gravity as soon as the conatct with the clad is lost.

In a cycle, fuel and clad are once more brought into contact by increase in power or by cladding creepdown; the contact will then take place in a relative position, different from the previous cycle and when the power is increased another increment in axial deformation might take place. This cyclic relative movement between the fuel and clad can be defined as a ratchetting process.

There are many parameters which can have an influence on the ratchetting characteristics of a fuel element. Some of these factors are fuel geometry, such as pellet dishing; initial sizing of fuel-clad gap, cracking pattern of the fuel, and anisotropic properties of the cladding since it alters the

creep performance of the cladding (Ref. 48).

3.2.2 - Stress Concentration in Cladding

Experiments, measurements and analysis of the fuel rods after refueling of power reactors (15, 23) have shown evidences of cladding deformation and symptoms of local stress concentration in the cladding. Analysis of fuel failures have also shown (21) that there is a decisive tendency for the cracks to start in regions where the stresses might be, for some reason, well above the average stresses in the cladding.

For the sake of discussion let us consider the two most common types of stress concentration mechanisms in cladding; those caused by hard contact of the pellet (which has its shape changed with temperature) and those caused by fuel pellet cracks or pellet interfaces. It is also possible to consider the occurence of stress concentration caused by the existence of a chip between the fuel and the cladding.

Stress Concentration Caused by Pellet Changes in Shape with Temperature. Ridging Phenomena.

As was mentioned in paragraph 3.1.1 , the fuel pellet does not retain its original shape if subjected to in reactor operating temperatures. In the event of direct pellet cladding contact, the stresses in the cladding next the more prominent regions of the fuel (usually next to corners and edges of the pellets) tends to reach higher values leading to local plastic deformations, as can be seen in Fig. 3.8 . The creepdown of region of the cladding not supported by the fuel pellet tends

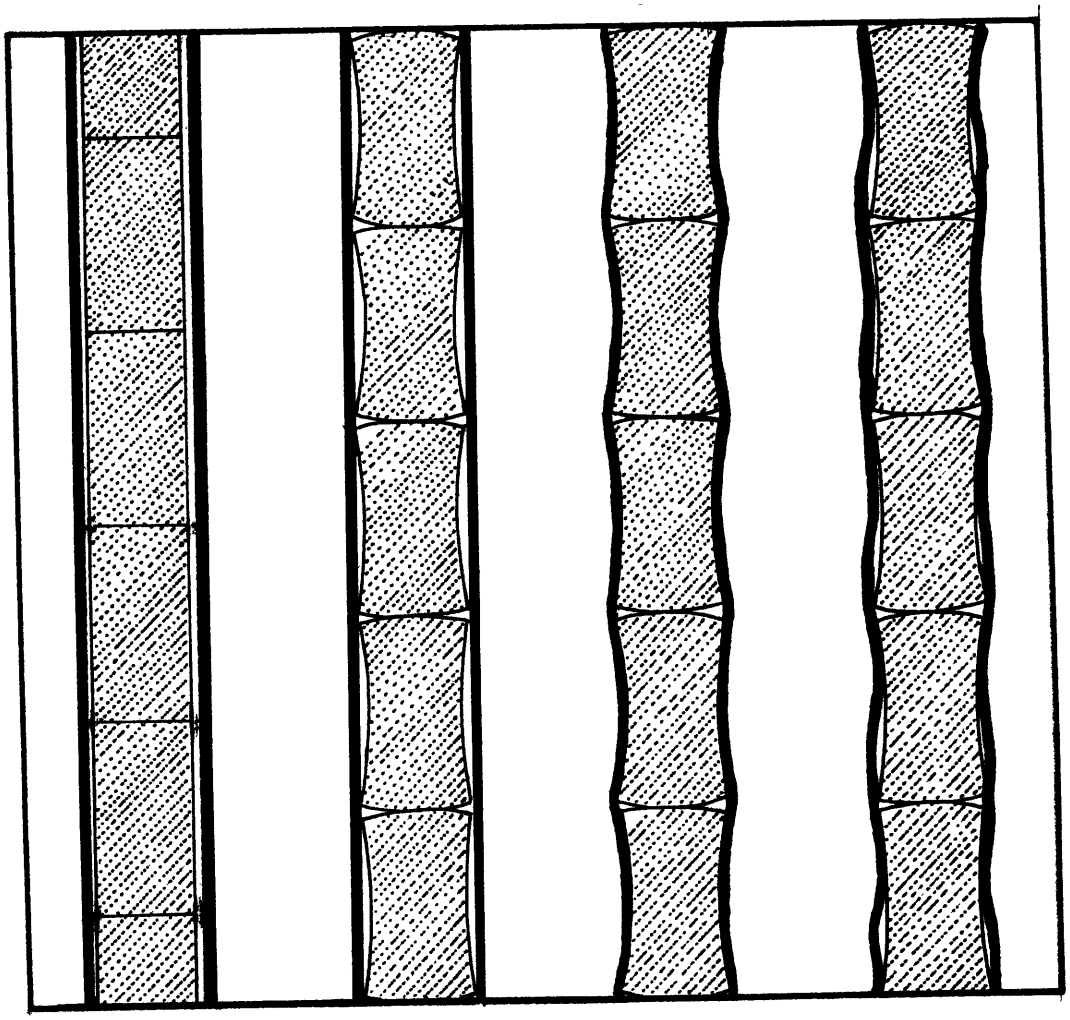

Fig. 3.8 - Interaction Between Fuel and Cladding

to help, salient, and consolidate this deformation and the fuel pin can achieve a "bamboo" shape. This phenomena has been called ridging or "bambooing" of the cladding in the technical literature.

Experience shows that very frequently the initiation of flaws occurs at those salient "bamboo" rings, and it is considered (14, 15) that ridging is detrimental to the endurance of the fuel element.

The severity of the ridging depends upon several parameters as fuel pressurization, pellet shape and dimmensions, original gap, cladding thickness and anisotropy.

Measurements of the diametral deformation of the cladding conducted at Halden, Norway (20) whose results are shown at Fig. 3.9 indicates the local diametral deformation of the cladding along the fuel rod. The rod on which those measurements were taken had fully annealed cladding and dished pellets. Fig. 3.10 , also results of experiments performed at Halden Reactor (20), shows the tendency of the cladding to get higher deformations at pellet interfaces, same results are shown in Fig. 3.11 , from Maine Yankee Core I measurements.

Stress Concentration by Fuel Cracks

The presence of radial and transverse cracks in ceramic fuel pellets has an important bearing on the stresses and strains produced in the fuel cladding during in-reactor service and in some circunstances it might be the primary effect on integrity of the cladding (16, 21).

When the reactor power is increased, during the expansion

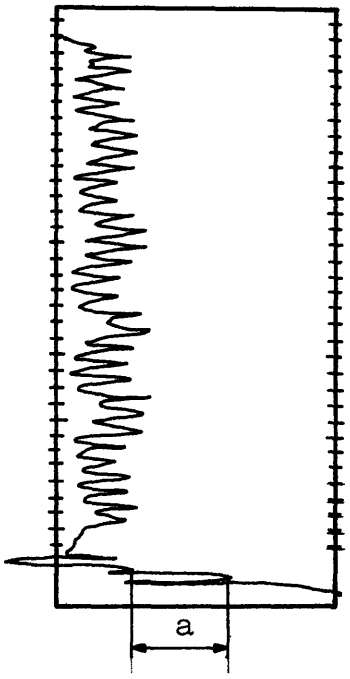

Fig. 3.9 - Measurements of the Diametral Deformation of the Cladding at Full Power (1^{st} Power Cycle) Conduced at Halden (20)

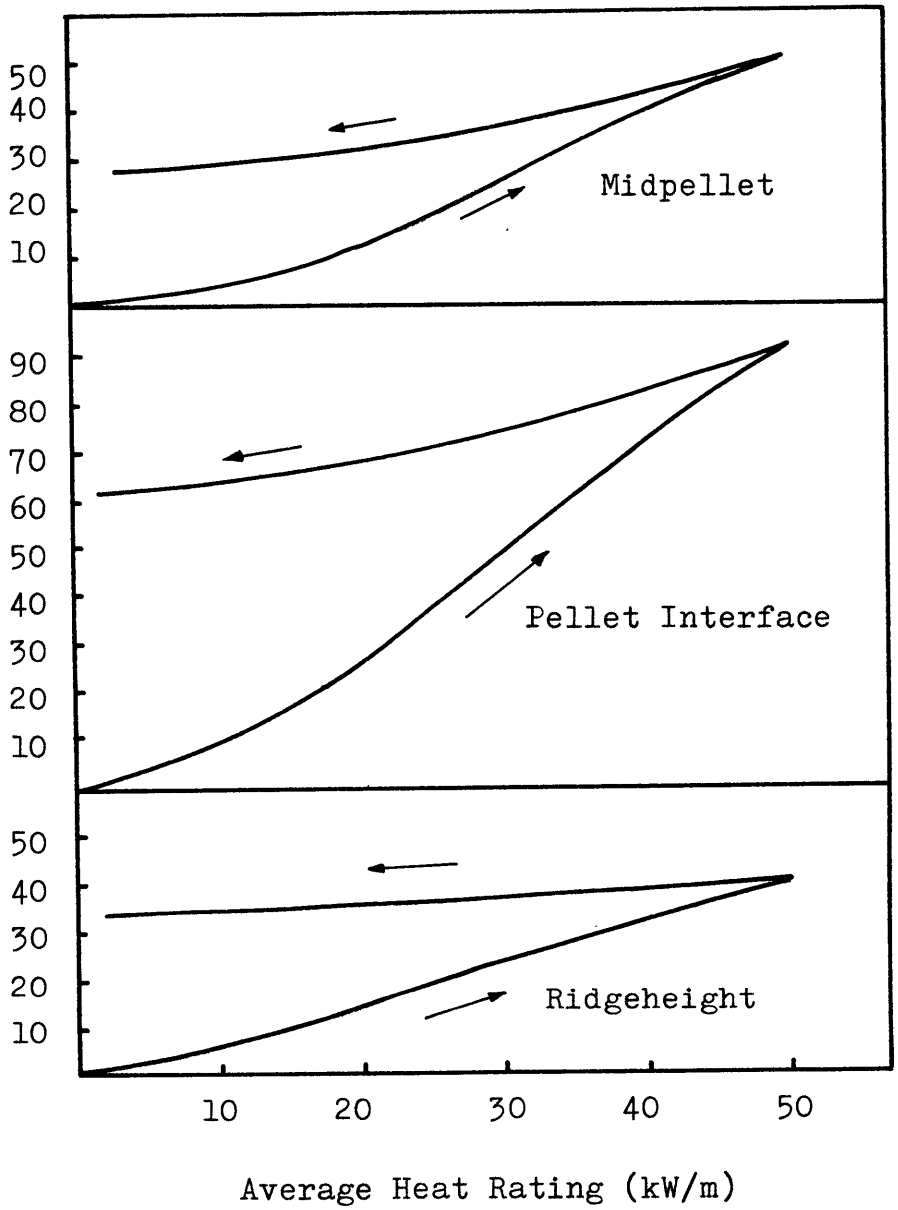

Fig. 3.10 - Diametral Deformations (Ref 20)
The curves represent mean deformation value over the rod length.

a = approximate pellet length (15.9mm)

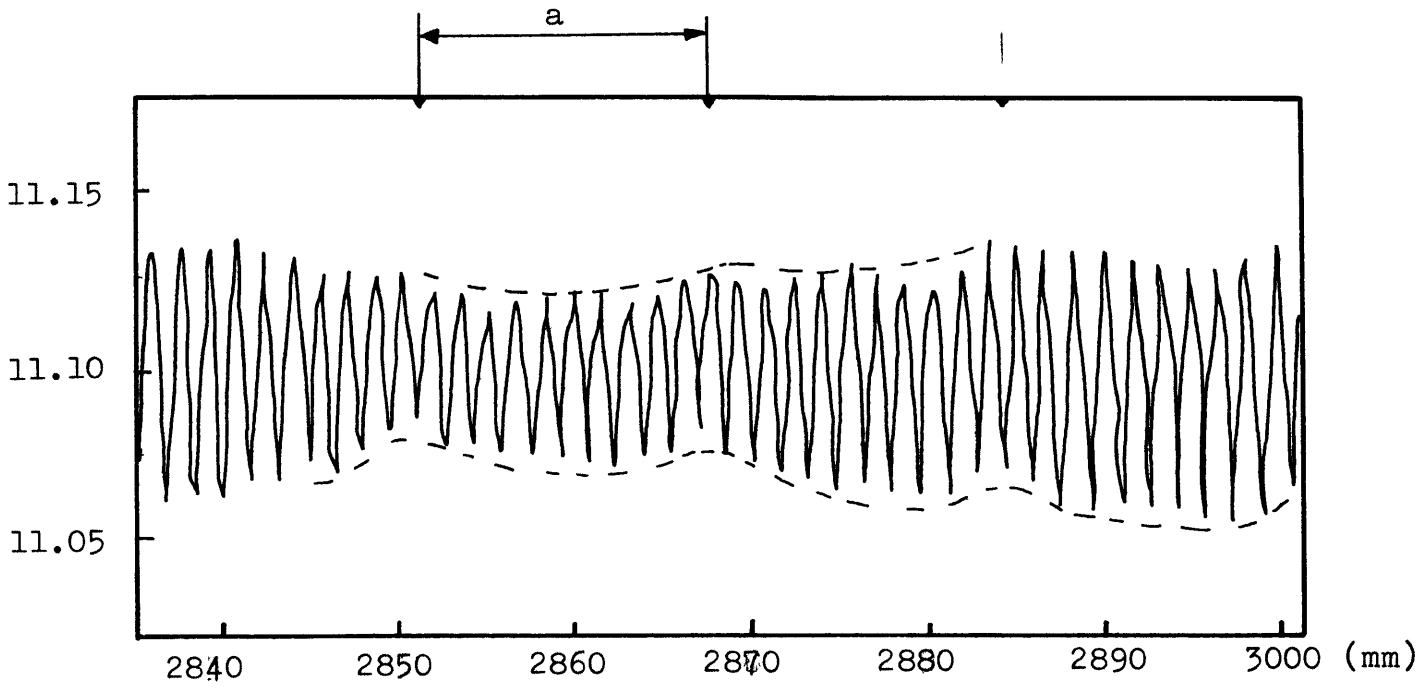

Fig. 3.11 - Spiraling Trace of the Diameter, Portion of Profilometer Trace Showing Ridging (from Ref 3)

of the fuel pellets, the radial cracks in it open up and cause strain in the adjacent cladding if the fuel pellet and cladding are in direct hard contact. There is, though, a tendency for strain concentration in arcs of cladding adjacent to pellet cracks.

According to analysis performed by J.H.Gittus et al (21) the coefficient of friction between fuel and clad, the angle between adjacent radial pellet cracks, and the creep properties of the clad have, in theory, strong effects upon the tendency for cladding strain to be concentrated over opening pellet cracks. Confirmation of the correctness of these deduction has been obtained (in the same work) from laboratory experiments in which cladding has been stretched by cracked pellets that move by action of an expanding mandrel.

It should be emphasized, at this point, that the power ramps on reactor tend to produce, in the tangencial direction of the cladding, an effect similar to the test cracked pellet and expanding mandrel.

Assuming that the coefficient of friction between fuel and clad and angle between adjacent pellet cracks are not rate dependent, the creep properties of the cladding tend to play a very important role (in the event of hard contact) in the local strain, and stress concentration.

From Gittus studies (21) it is possible to extrapolate the importance of the "cracking pattern" of the fuel and to infer that the achievement of a cracking pattern as uniform as possible also helps in reducing the tangential peak to average ratio of the stresses.

With respect to reducing the frictional forces, Canadian studies (18) have proven that the utilization of a graphite layer between fuel and cladding tends to improve the fuel performance characteristics. There is, however, some controversy about the graphite layer role since it may work also to isolate the cladding from the internal corroding environment of the fuel pin. It is also possible that the graphite barrier might be eventually detrimental if the graphite coating does not provide a fully coating of the cladding internal surface and local stresses and corrosive attack occur at breaks in the coating.

In some local regions of the cladding there may be a superposition of the stress concentration (30) mechanism discussed in item 3.2.2 with the stress concentration caused by fuel cracks in pellets and over pellet interfaces (23). Reference 30 relates an experiment in Halden Reactor: "A general correspondence of cracks in the cladding with cracks in UO_2 is seen, also the wider cracks in the cladding coincide with matching cracks in the two pellets".

3.3 - STRESS CORROSION CRACKING

Fuel failures due to PCI have in common the fact that they occur only after some burnup and when the fuel temperatures are sufficiently high to release volatile fission products. A delay time varying from a few minutes to some hours is often seen between the power rise and defect formation(10).

Most of data on PCI have been obatained from laboratory

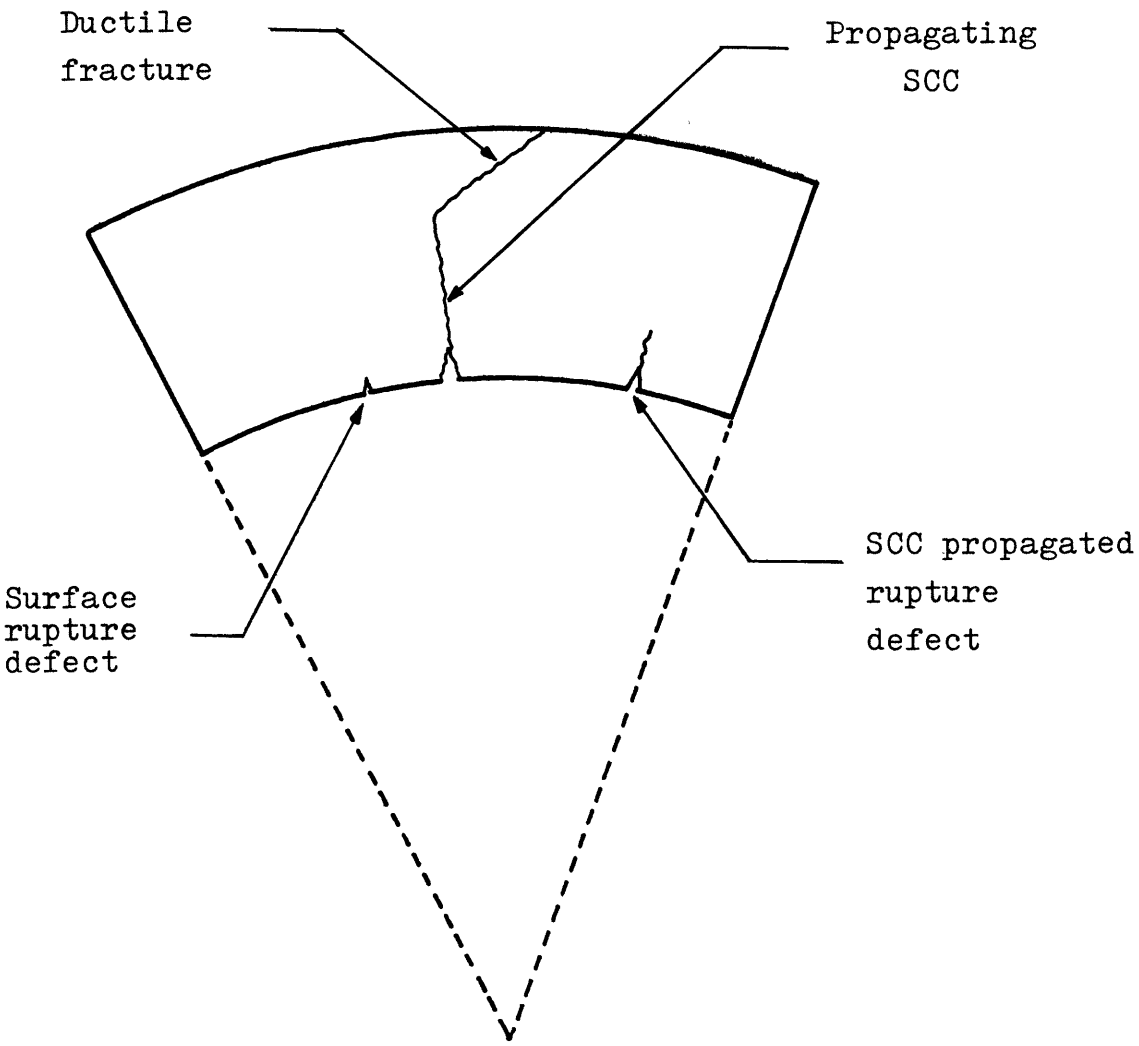

Fig. 3.12 - SCC Failure Sequence (from Ref 25)

tests, test reactor experiments (11), and Heavy Water Reactors; so far, the sequence of fundamental metallurgical events is not completely known in pellet cladding interaction cracking in prototypic Light Water Reactor fuel.

The Canadians were the first to report and appear to be convinced by in-pile and out-of-pile evidence (11) that CANDU Reactors power ramp related failures involve iodine-assisted stress corrosion cracking (SCC) (33).

Examination of the fracture surface of cracks of the failed pins of test reactors, as well as the Maine Yankee Power Reactor (3, 18), have shown similarities with SCC laboratory tests on Zircaloy. Fig. 3.12 provides a sketch showing the general trend of the crack surface where three zones normally identified are shown (3, 11, 18, 25).

These three zones are characterized in the following way:

a) The crack face immediately adjacent to the inside clad surface exhibits surface characteristics atributed to contact with an oxidizing medium that may have to come from in-reactor environment.
b) The next zone is the continuation of the initial crack, the fracture appears to be free of oxidation and exhibited characteristic flat cleavage ascribed to iodine stress corrosion based on out reactor tests.
c) The third zone has a fracture surface distinctly different from the original crack face; it seems that this is the fracture zone caused by the mechanical opening of the original crack, and it is characterized by the ductile dimpling associated with such a cracking process.

Furthermore, the extensive analysis carried on Maine Yankee Reactor (Power Reactor, PWR) have shown also (3) that all the cladding cracks were of transgranular nature with no evidence of twins or slips in or around the cracks; this morphology along with their tight nature, and their orientation with respect to the hoop stress direction (90 degrees), and their branching characteristics is consistent with stress corrosion cracking. Similar results are reported in Halden Reactor(BWR) experiments (18, 20).

The evidence reported above makes the hypothesis of failure by SCC stronger than the hypothesis of failure by local plastic instability, in most of the fuel failures.

The recognition that SCC is the prevalent failure mechanism leads the research towards a better understanding of SCC. Important part of this research include the chemical characterization of the fuel, as well as the nature of the species or compounds that contributes to SCC at working temperatures of the cladding; and the definition of the stress and strain regime necessary for failure.

Works published by Garlick (1), Vinde and Lunde (18), Busby et al (31), JC Wood et al (35) reflect the efforts to determine stress or strain limits (or both), the chemical concentration, and the species that produce SCC.

At this point it is important to recognize that we are just at the "tip of the iceberg" since relatively little is known about the stresses that locally occur in cladding during power ramps, the dynamics of the fuel chemistry, and the details of the crack propagation model.

The following sections contain a brief review of some published results of the experiments performed to determine the stress threshold and the chemical components necessary to produce SCC.

3.3.1 - Fuel Pin Internal Chemical Environment

When Zircaloy was first used as cladding material, it was postulated (18) that stress corrosion should probably not occur because the elementary iodine could not be present according to thermodynamic calculations of the fission product chemistry. This argument was proven to be wrong, first because the available thermodynamic information were not sufficient to be applied to an irradiated system, and second because elementary iodine is not the only constituent that can cause stress corrosion cracking in Zircaloy (18).

The chemical state of the fission products in fuel pins is poorly known. However, Vinde (18) and Garlick (1) in order to investigate whether elementary iodine is necessary for SCC, performed some tests and found that the failure by SCC of Zircaloy occured also in presence of zirconium iodide after about the same time of exposure under the same stress regime. It is therefore, clear that elementary iodine is not uniquely responsible for stress corrosion of Zircaloy. Vinde and Lund experiments also found that neither cesium iodide alone nor any combination with water or air caused stress corrosion.

The presence of an irradiation field can cause the formation of normally unstable products. In the environment inside the fuel cladding elementary iodine is an unstable

product having, though the possibility of existence. Also free radicals may occur from other sources than iodine and zirconium iodide.

It is still unknown (11) whether the crack forming environment always exists inside the cladding after a certain burnup or if it depends on power history or the achievement of determined temperature in the fuel (function of local power level). It is known (11, 18) that fission gases tends to release burst wise at power changes which open up cracks in the fuel; it is suspected (33) that at such time, a very short period of more intense cladding attack occurs before the elementary iodine combines with cesium (rubidium etc.) to form cesium iodide.

CC Busby (31) performed long duration out-of-pile tests which have shown that (for temperatures of 360°C and 400°C) as little as 0.05 to 1.0g/m^2 of Zircaloy-4 surface is sufficient to reduce the "stress threshold" for hoop stress to 145 to 165 MPa (21 to 24 ksi).

The same tests have shown also that stress corrosion cracking appears to be essentially independent of iodine concentration in the range of 0.8 to 1g/m^2.

3.3.2 - Critical Stress to Produce Stress Corrosion Cracking

Researchers(1, 18, 31, 35) seem to agree that for a determined heat treatment, temperature, strain and time of exposure, the stress level must be above a critical threshold in order for SCC to occur.

Although researchers agree in the existence of such

threshold, they do not necessarily agree with the magnitude of the threshold and the variable (time, strain rate, maximum strain, etc.) to correlate with.

Garlick (1) proposes for this threshold the 0.2% proof stress in a biaxial test, measured in a closed end tubing of the same material subjected to a hydraulic burst test. Vinde and Lunde (18) although finding a stress threshold in a stress versus time plot they suggest that strain rate versus maximum strain might be a better criterion. Wood (35) points out the importance of internal stresses, an argument that Garlick (1) tends to disregard because of irradiation effects. Bubsy et al (31) performing long duration tests found that for test times upon 6000 to 8000 hours stress corrosion cracking was not observed for stresses below the range of 145 to 165 MPa (21 to 24 ksi) for Zircaloy-4 stress relieved. There are a general agreements that Zircaloy-4 and Zircaloy-2 have similar properties concerning stress corrosion cracking, and that SCC does not normally occur for Zircaloy below 240^{o}C.

The laboratory techniques normally used for SCC test are inert gas-iodine pressurization and expanding mandrel.

In the inert gas-iodine pressurization, Zircaloy tubes containing iodine (or zirconium iodide) are internally pressurized with argon at elevated temperature under closed end conditions.

In expanding mandrel tests a short length Zircaloy tube is stressed in iodine vapor by expansion of tightly-fitting mandrel. An alternate "composite mandrel" test is also used, where a split uranium dioxide annulus is forced against the

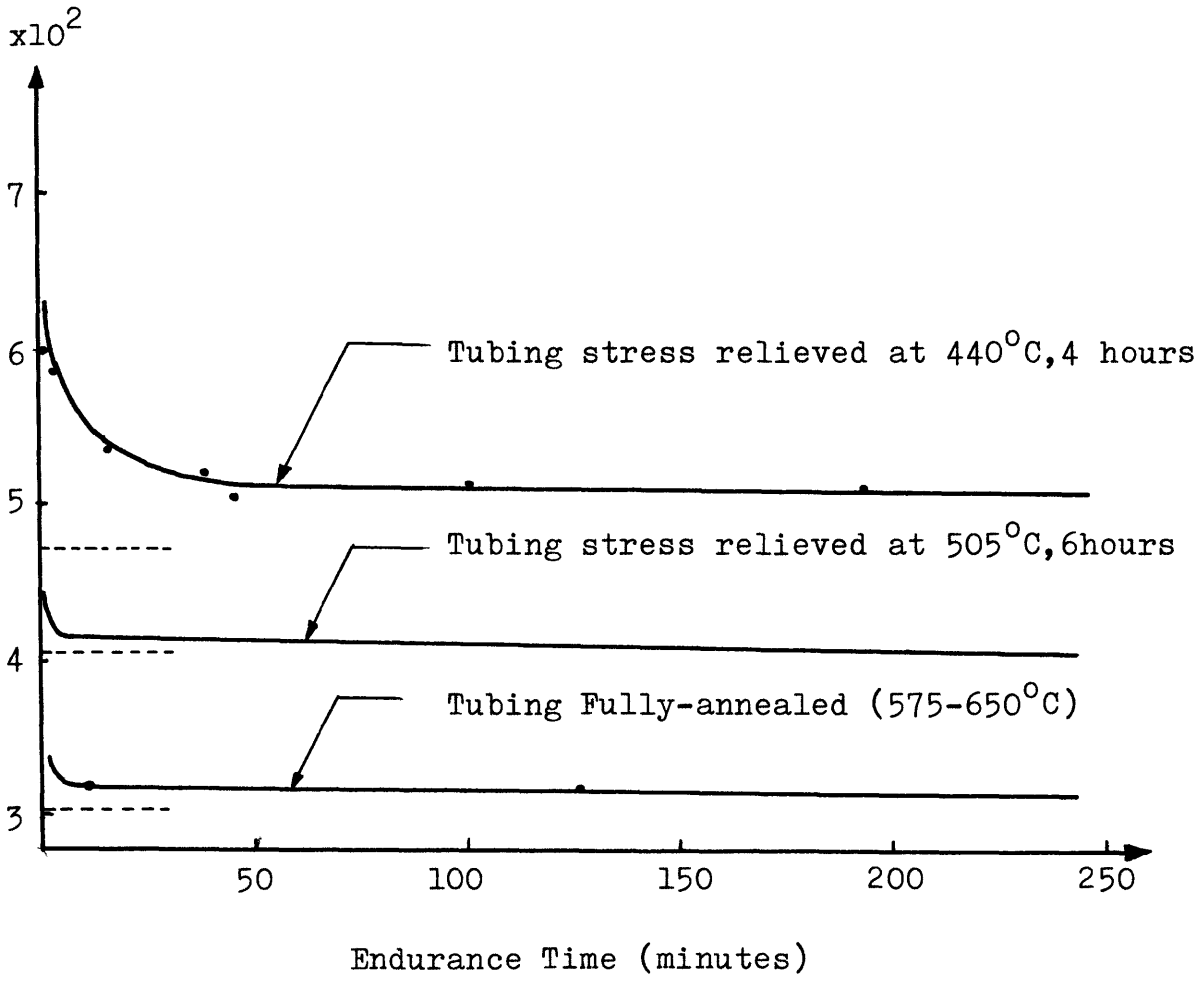

Fig 3.13 - Endurance Curves for Unirradiated Zircaloy Tubing Internally Pressurized with Iodine at 330°C (Ref 1)

1) unannealed

2) annealed (520°C)

3) annealed (590-700°C)

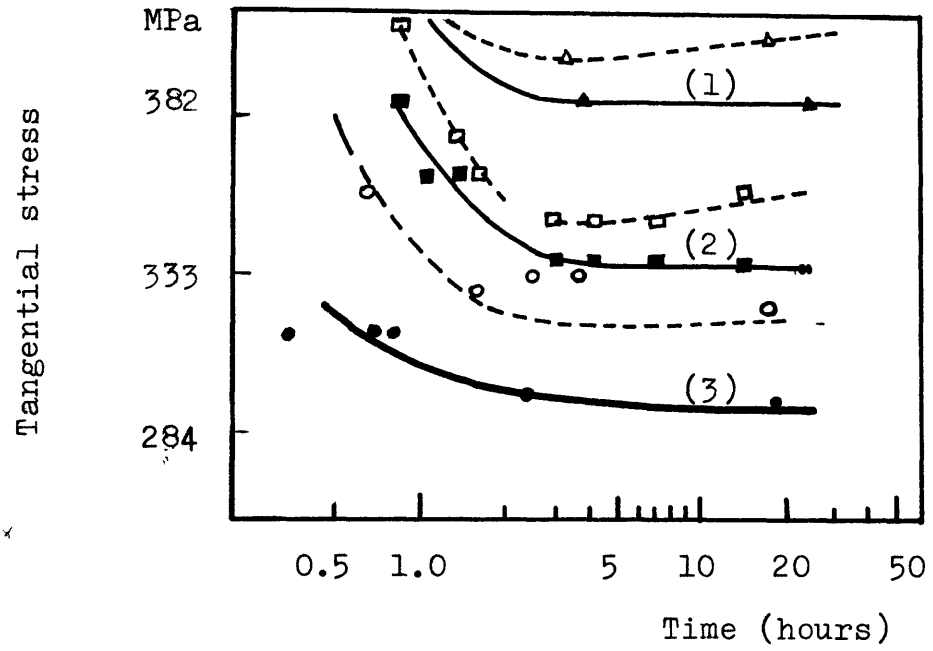

Fig. 3.14 - Time to Failure as Function of Stress (Ref.18)
Initial stress is given by closed points and solid lines, while stress at failure is given by open points and dotted lines.

Fig. 3.15

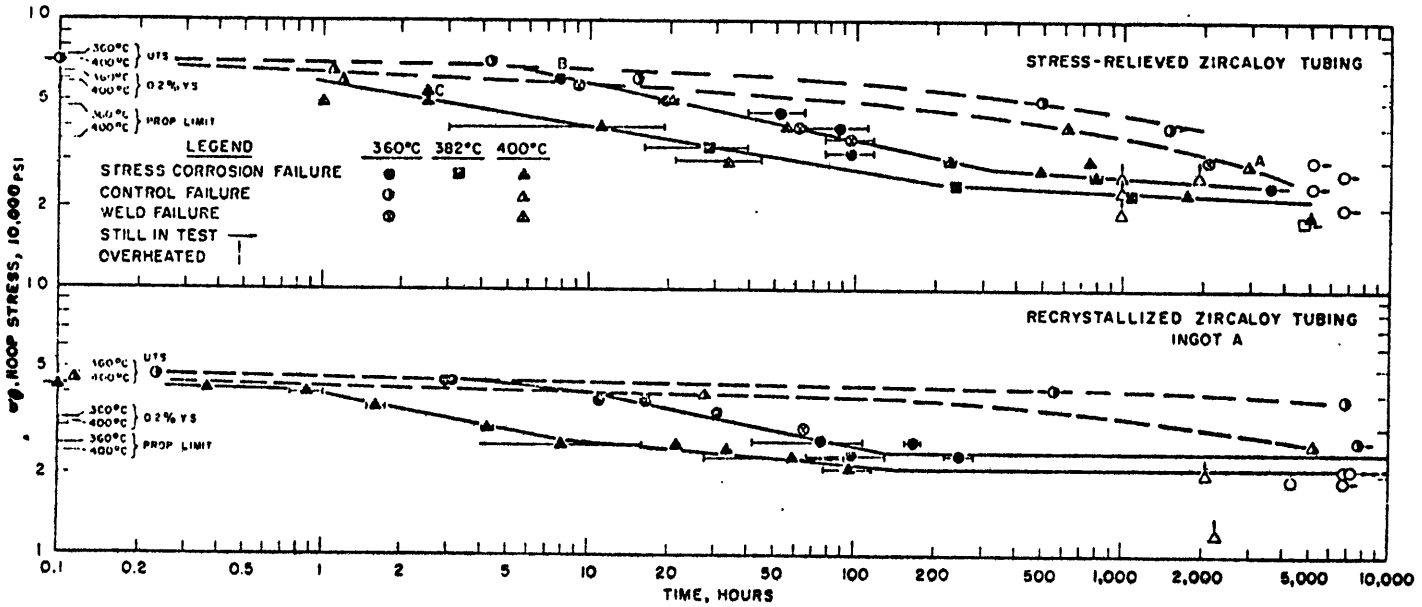

Iodine stress corrosion and stress rupture failure curves for stress-relieved and recrystallized Zircaloy-4 tubing.

(Ref. 31)

Zircaloy tubing. This test intends to reproduce the effect of the cracks of the fuel over the cladding and has a disavantage in that local stresses to failure are not well known.

Figs. 3.13, 3.14, 3.15 are reproductions of published results of inert gas-iodine experiments of Garlick (1), Vinde and Lunde (18) and Busby (31). The expanding mandrel test have shown that if the applied stress is allowed to relax by creep, stress corrosion cracking may not happen (18). It is important to point out that all of these experiments refer to time to failure and not to time to generate an incipient crack size that might later lead to failure.

3.4 - REMARKS ABOUT THE CHAPTER

As it has been pointed out in this chapter, the picture of PCI failures is not yet completely clear. There seems to be a qualitative understanding of most of the details of PCI phenomena. Quantitative uncertainties however, still persist and at this point one can not consider that the models applied are really numerically adequate and sufficiently precise to represent reality.

There are uncertainties about almost all mechanisms that contribute to PCI. However there are three areas where a better understanding would possibly indicate measures to avoid PCI failures and relax some of the limitations in LWR maneuvering flexibility:

a) Internal chemistry: chemical conditions for crack initiation at microscopic level in radiated cladding.

b) Cladding properties, in particular creep, effect of anisotropy on creep, cladding tube creep down under reactor conditions, local stress relaxation.

c) Cracking and relocation mechanisms; effects of pellet cracks on cladding stress concentration and effects of broken fuel fitting back together (accomodation) on forces reductions.

CHAPTER 4

EXISTING METHODS TO ASSESS FAILURES FROM PELLET CLAD INTERACTION

New licencing requirements have as a goal, the reduction, to a minimum practicable level, of contamination of the environment and radiation exposure of plant personnel (26). Fuel malperformance under less stringent restrictions has already proven enormously costly to victim utilities. A step increase in the associated costs of fuel malperformance, will result from more stringent regulatory limitations and the rising cost of replacement power.

The above described panorama, and the fact that utilities that are following vendor recommendations for plant maneuvers recognize some loss in plant availability, provide the incentive for development of studies on fuel performance and failure. As a consequence, there is a worldwide effort of the sectors of nuclear community concerned with fuel performance to improve the understanding of fuel failure mechanisms. As part of this effort, there is a systematic buildup of a statistical bank of information (25) and a continuous analysis that eventually will lead to further improvements in fuel design and recommendations to plant maneuvers that exploit completely but safely the fuel capabilities.

As a natural consequence of these efforts, methods of failure prediction are being developed. For LWR at least two methods have been suggested: the Scandpower Power Shock method

(POSHO) and the Cladding Flaw Growth Index (CFGI). These methods are summarized in the remainder of this chapter.

4.1 - THE CLADDING FLAW GROWTH INDEX

The cladding flaw growth index (CFGI) is an anlytic logic system developed with the intention of defining the state of the reactor core with respect to the probability of loss of fuel rod cladding hermeticity (49). The logic for computing the probability of cladding failure as function of axial location along each fuel rod depends on calculated linear heat generation rate (LHGR) variation of this specified length of the fuel rod as a function of irradiation. It also assumes that the probability of failure depends on current power maneuver and on all previous power change events. So, according to this method, failure can result from a cumulative process.

4.1.1 - CFGI Basic Methodology (49)

The CFGI basic methodology is:

. Divide the fuel rod into a number of axial nodes; approximate the actual duty cycle by a series of constant power states, such that the power (P) variations along the node can be neglected during each exposure state. Thus the power history (duty cycle) for the ith node is described by [Pi(Ei->Ei+1),Ei], where the notation indicates that at exposure Ei the nodal power is Pi and remains constant at

that value up to the beginning of the subsequent exposure Ei+1.

. Compute the set of [Pi(Ei→Ei+1),Ei] for each axial node using core simulation (Nodal neutronics core simulator).

. Input the set of [Pi(Ei→Ei+1),Ei] into a failure probability algorithm to compute (and update) the failure propensity for each axial node.

The author of the method (Reference 49) points out that the computer "bookeeping" requirements of this method are quite substantial since power, exposure, CFGI, cumulative CFGI and failure probability are to be stored and manipulated.

The cladding failure sequence in this method is separated into three major steps:

1) Fissure of cladding inside diameter oxide layer.
2) Initiation of the flaw in the Zircaloy substrate.
3) Chemically assisted flaw extension and shear-mode propagation through the cladding wall.

4.1.2 - Minimum Linear Heat Generation Rate for Interaction

The initial diametral gap does not persist throughout the irradiation lifetime of the fuel rod, since it decreases due to clad creepdown, pellet relocation towards the cladding and pellet swelling. The method postulates a minimum interaction linear heat generation rate (Fig. 4.1) that is defined as the onset uniform-surface contact pressure (hard contact) between

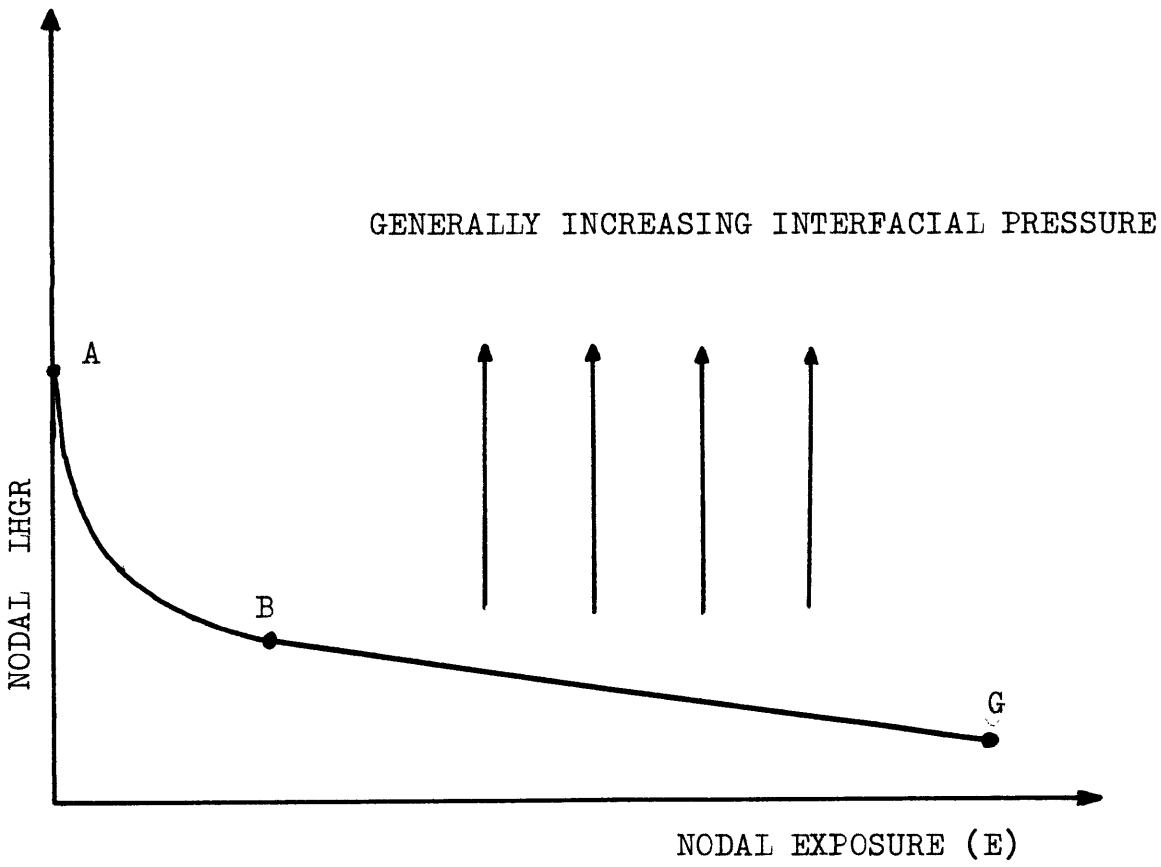

Fig. 4.1 - Variation of the Minimum Interaction Linear Heat Generation Rate (LHGR) With Exposure (Ref. 49)

fuel and cladding; the curve does not attempt to account for pellet stack offset, tilting, chipping or in general any non-cylindrical aspects of fuel pellet behavior.

The point where the curve intersects the ordinate, corresponds to uniform closure of the "as fabricated gap" by fuel gap thermal expansion; and the ordinate value of the curve decreases with exposure.

4.1.3 - Changes of the Linear Heat Generation Rate for Interaction

The method considers that the change in the dimensions of the fuel rods during irradiation is caused by inward creep of the cladding due to the coolant pressure and the radially outward and axial distortion due to fuel-cladding differential thermal expansion. The fuel clad mechanical interaction can occur at different cladding strain rates, with the possibility of short-term plastic strain resulting from a rapid increase in power or the opportunity of outward creep if elastic cladding stresses are maintained for a longer period of time. These transient changes are designated "dynamic interactios".

As it can be seen in Fig. 4.2, when the increasing node power shown at E_o reaches the minimum interaction LHGR curve (point B), uniform fuel-clad mechanical interaction begins. The point C is an LHGR value slightly less than the power increase terminal LHGR shown. The B-C type of increase in the interaction LHGR is refered to as fuel rod conditioning.

The decrease in interaction power (deconditioning) during the E_o to E_1 state of steady power operation is due to creep

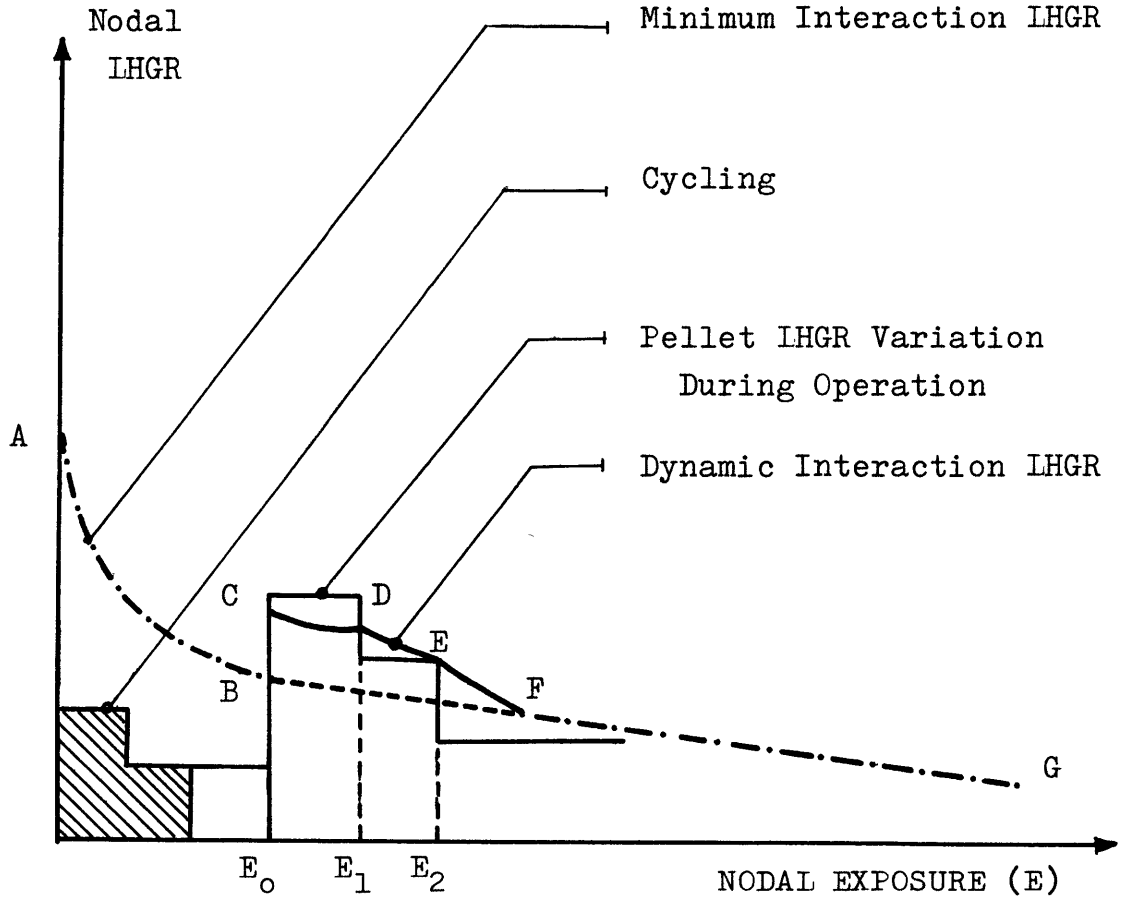

Fig. 4.2 - Dynamic Interaction Linear Heat Generation Rate (Ref. 49)

induced by coolant pressure and further stress relaxation.

When the power decreases at exposure $E_1(E_1-E_2)$ the fuel thermal contraction causes a further decay of the interaction power.

4.1.4 - Cladding Flaw Growth Index

The index is an integral function that describes the severity of a power increase event as compared to an event certain to cause failure.

In the Fig. 4.3, there is a second set of coordinates with the origin at the dynamic interaction linear heat generation rate; where the function F(P) is plotted, this function represents the behavior of a variable (e.g. Cladding hoop stress), which is felt to be important in cladding failure and is computed using an integral fuel rod modeling code.

With the assumption that the failure process is cumulative both the magnitude and location of the peak of the function F(P) changes with the exposure. Chemical effects are accounted for by increasing the peak value of the F(P) with increasing exposure to account for any corrosive weakening or extension of the flaw.

4.1.5 - Rate of Power Increase

To account for the possibility of stress relaxation during a slow rise in LHGR a relationship is used to attenuate the severity of CFGI. Such a weighting function is described by the curve in Fig. 4.4; the shape of this curve assumes that there is a ramp rate below which no detrimental mechanical

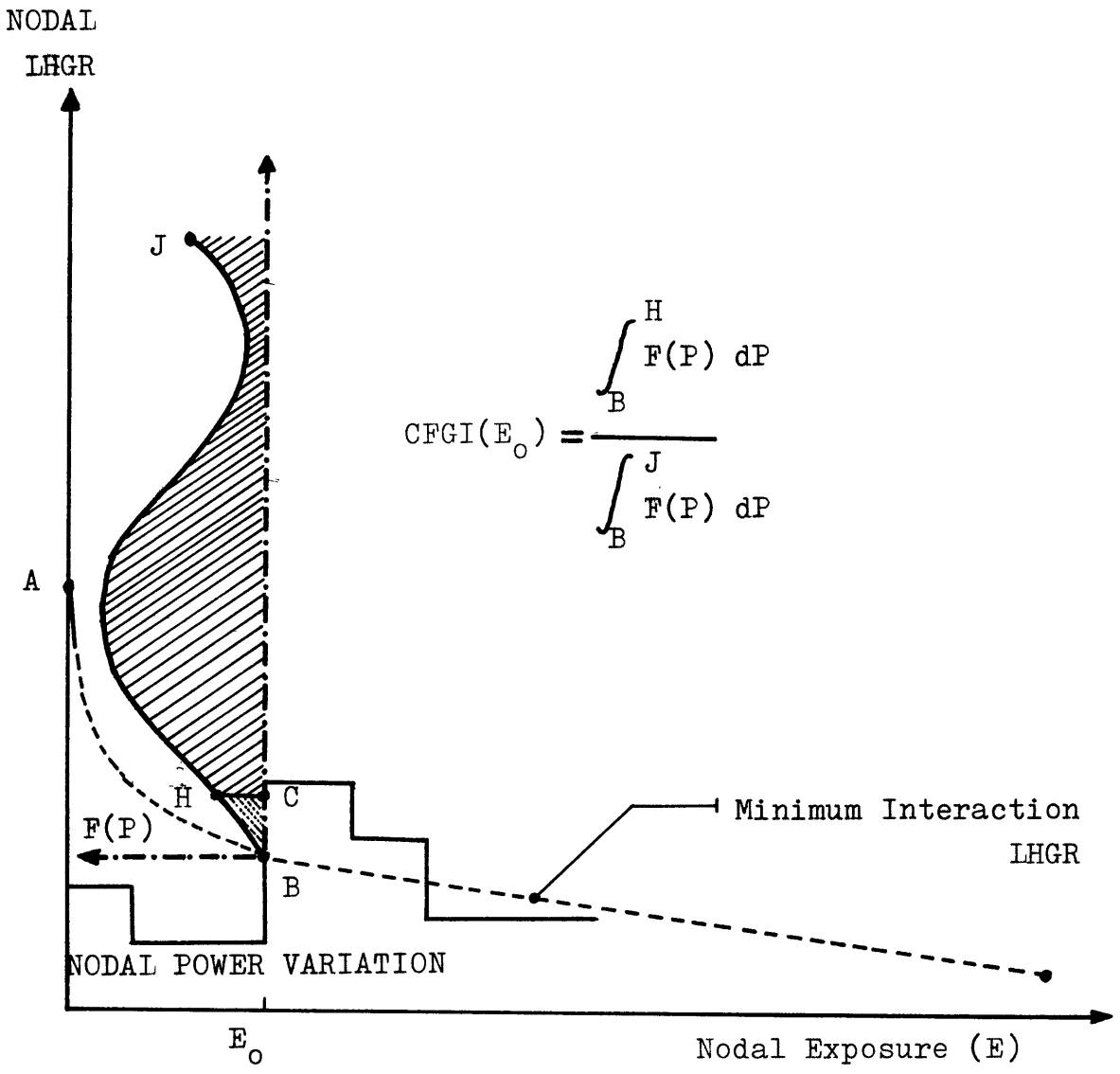

Fig. 4.3 - Evaluation of the Cladding Flaw Growth Index for a Power Increase at E_o (Ref. 49)

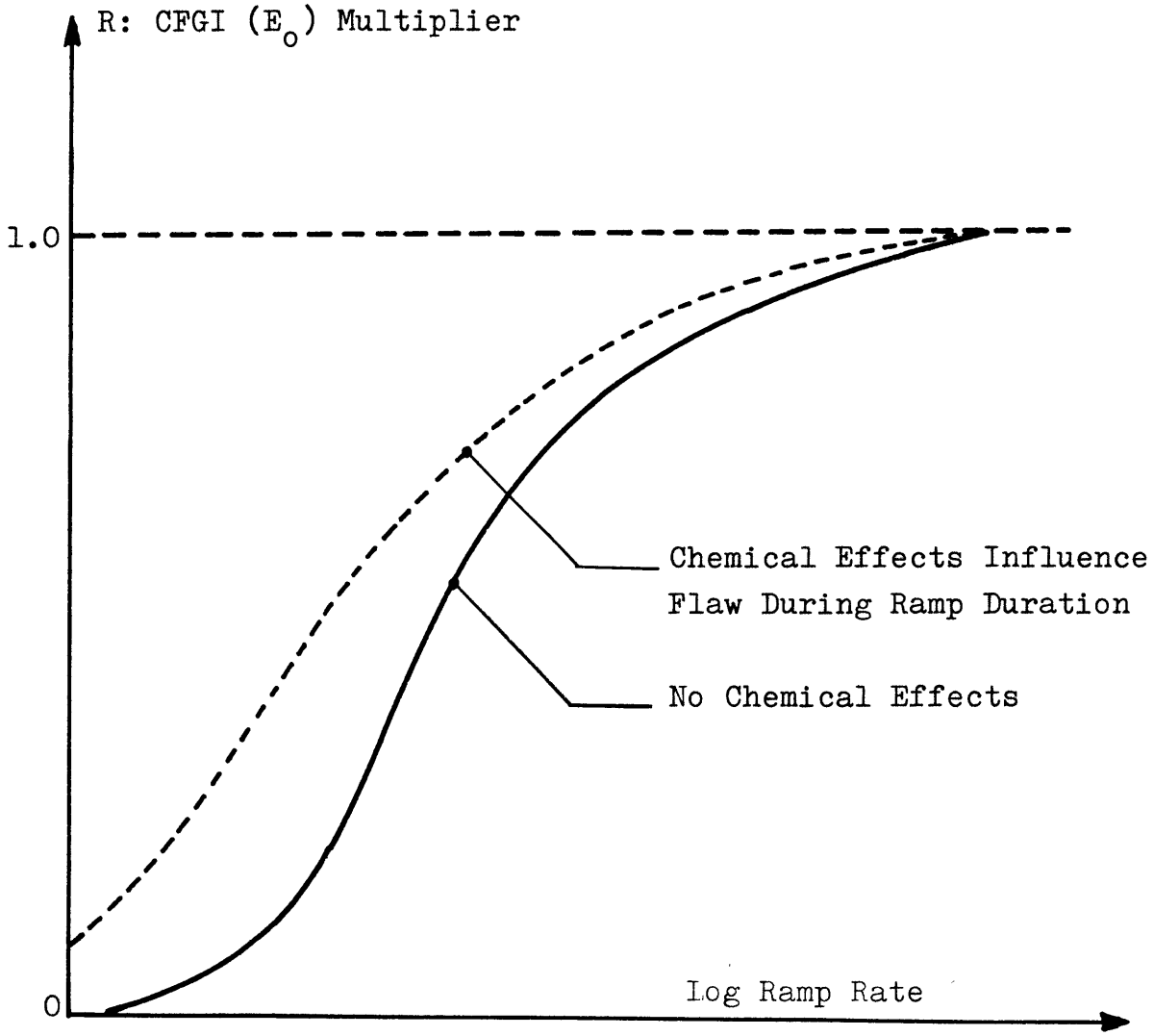

Fig.4.4- Cladding Flaw Growth Index Weighting to Account for Differences in Cladding Stress Buildup at Different Ramp Rates (Ref. 49)

interaction occurs. The curve rises to unity for rates at which no stress relaxation occurs during the increase maneuver. The dashed curve suggests that if chemical effects influence the flaw behavior during the ramp duration, the CFGI should be attenuated to a lesser degree.

4.1.6 - Cladding Nodal Failure Probability

The procedure for calculating the CFGI from the F(P) curve is shown in Fig. 4.3 ; the normalized CFGI is calculated from the relative areas under curve F(P).

The Fig. 4.5 shows how the nodal failure probability is calculated from the power increase starting from the minimum interaction LHGR curve. The ordinate of this probability graph consists of straight sum of all previous power increase normalized and weighted index values, and the abcisa is the instantaneous value for the power increase of concern. Implicit in this logic is the assumption that failure can be a cummulative event.

Since refueling shutdown nondestructive tests for failure are most frequently done on a bundle and not on a rod basis, this method calculates the bundle failure probability based on fuel rod cladding nodal failure probabilities.

Utilization of the CFGI Method

The method is suggested to be used to help in orienting the leak detection procedures indicating the most probable failed bundles, this is claimed to be important since it has been observed that old leaks can be hard to locate by sipping

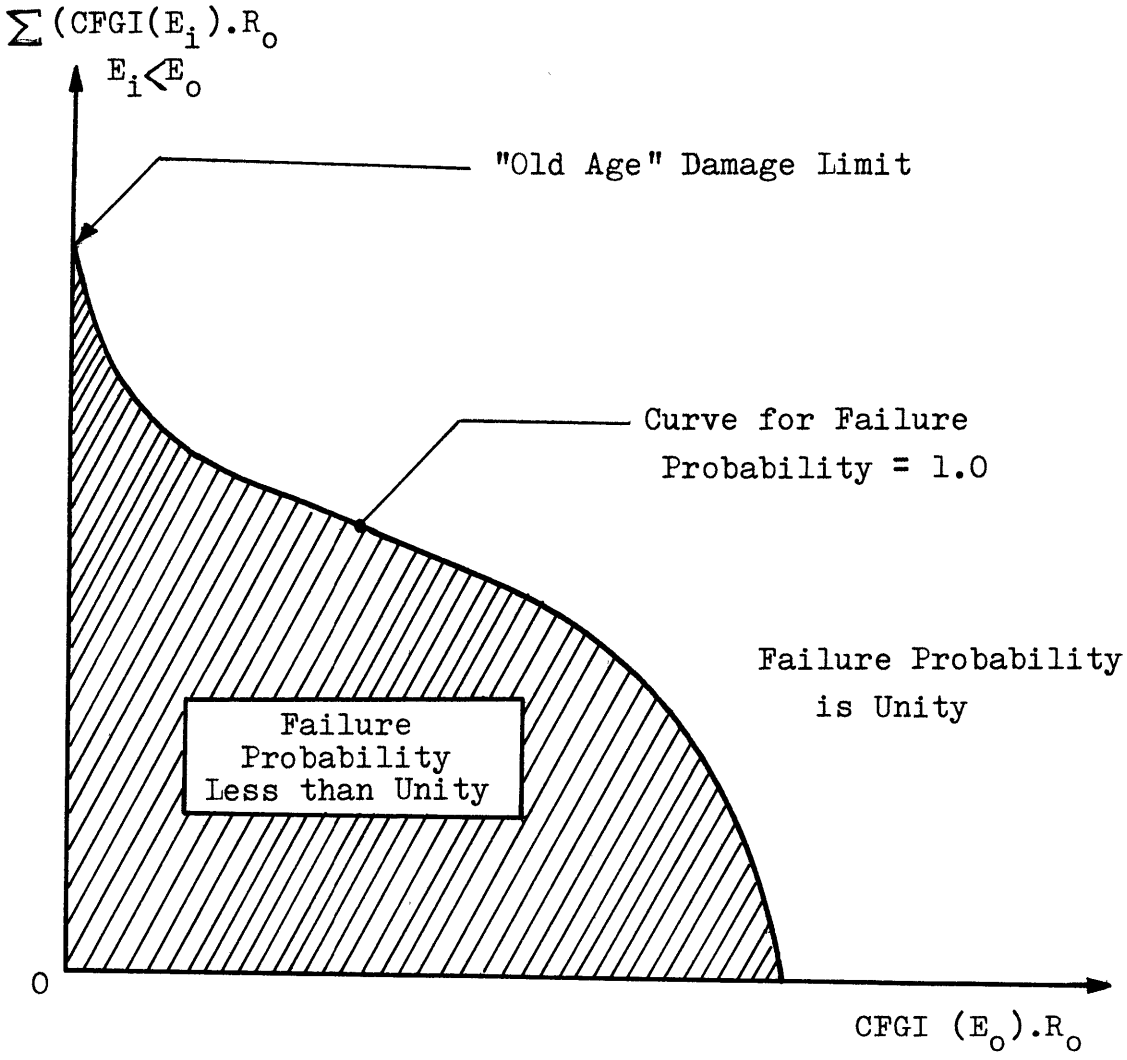

Fig. 4.5 - Fuel Rod Nodal Failure Probability as a Function of the (instantaneous) Value of CFGI at E_o and the Prior Accumulated CFGIs for Power Increases $E_i < E_o$ (49)

process because the cladding fissure has closed due to crud or other buildup or the entire inventory of fission products is not available to release, due to imperfect axial communication of the internal fuel rod void. The sipping process can thus preferentially locate cladding failures that occurred late in the reactor cycle. The method alerts to the likelihood of bundle failure helping in sipping failed/non failed discrimination process.

Certainly the main goal of the method is to predict the power maneuver scenario, which minimizes (or keeps at an acceptable level) the change in failure probability. At the time of issuing the EPRI NP-324-SR (49) the CFGI approach had not been implemented. The shapes of the curves and the calculation sequence were presented as being plausible. However, details of deriving and using the curves must await the results of ongoing research sponsored by EPRI (Ref. 49).

4.2 - SCANDPOWER'S EMPIRICAL FUEL PERFORMANCE MODEL (46,47,50) (Power Shock model)

Fuel tests in experimental reactors have established that high burnup fuel will fail if subjected to a sufficiently large and rapid increase relative to its historically normal operating value. This type of power increase is referred by the authors of the method as a power shock (POSHO),including is its meaning both the magnitude and rate of application of the power increase, relative to an historical power. The authors

of the method claim that the failure is by local clad overstraining; as explained in Chapter 3, there is some controversy about this conclusion. However, the method may still be appropriate for making operational decisions, even if the assigned failure mechanisms are not correct.

The POSHO method is an empirical model for failure probability of a unit length of fuel (or number of pellets)as a function of the design of the fuel and the power "shock" history combined with a method of statistically describing the shock distributions resulting from various modes of light water power reactor operation. The method aims to predict the number of local cracks, rod failures and the number of assemblies containing failed pins after any period of time, for any selected fuel, reactor, and operating mode combinations.

4.2.1 - The Fuel Performance Model

The basic assumption in the POSHO Model is that the reason for failure is local clad over-straining, resulting from stresses produced in the clad by thermal expansion of the fuel pellet during positive local or total power changes. Stress corrosion, as a major contributing factor in the failure process is not explicity considered by the POSHO Model and that might cause it to underestimate the effect of a "shock" of low magnitude if the failure is chemically assisted (it is also conceivable that adjustments can be made to account for this effect).

According to this method, thermal expansion of the fuel pellets is transmited to the cladding only if the linear heat

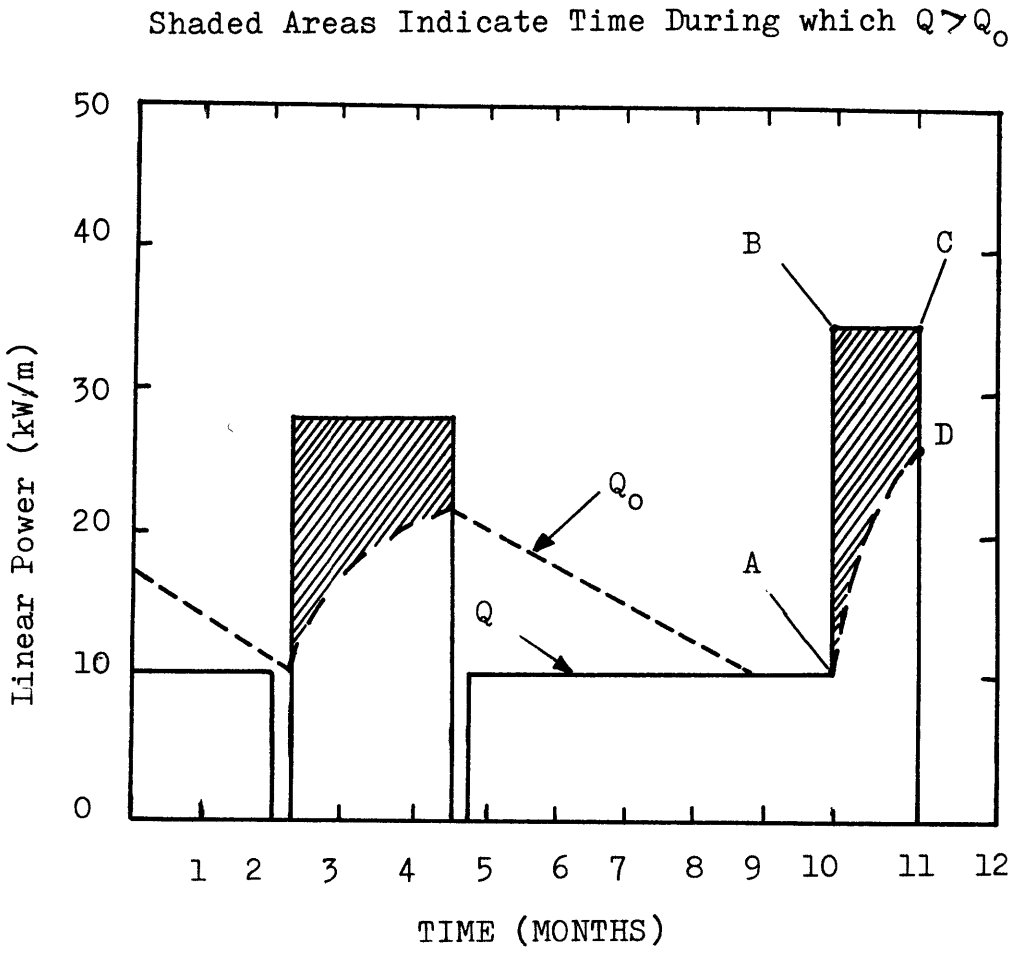

Fig. 4.6 - Tracking the Interaction Level, Q_o, for a Local Power Variation, Q, with Time (Ref. 47)

generation rate (Q) exceeds the interaction threshold level(Q_o) for which the fuel expands radially to contact cladding. The value of Q_o is, however, a dynamic quantity which changes throughout the operating cycle, mainly depending on the actual power Q relative to Q_o. (Refer to Fig. 4.6)

The tracking of Q_o with time is done by two functions which simulate the dimensional change process of the fuel.

A "fuel conditioning correlation" is used when the local power Q is greater than the interaction threshold power Q_o, when is considered that the clad is in hoop tension and the fuel subjected to a radial compressive load which tends to compact the pellets.

A "fuel de-conditioning correlation" is used when the operating power Q is less than the interaction threshold Q_o, which means that there is a radial gap between the fuel and the clad; in this situation, the fuel is assumed to relocate outwards and/or clad creepdown occurs reducing Q_o, which approaches Q as a limit if Q is held constant.

Figure 4.6 , illustrates how the interaction threshold power density Q_o moves toward the local power Q for a section of a fuel rod where considerable power shock has occurred during two events. The power shock for any event is defined as the maximum value by which Q exceeds Q_o.

Figure 4.7 pictorializes the process by which failure probability is found in POSHO. The coordinates of the interaction threshold, Q_o, and the shock magnitude $\Delta Q = (Q-Q_o)$, locate the probability of failure for the fuel segment in question. The solid lines, with reference labels A to D, show

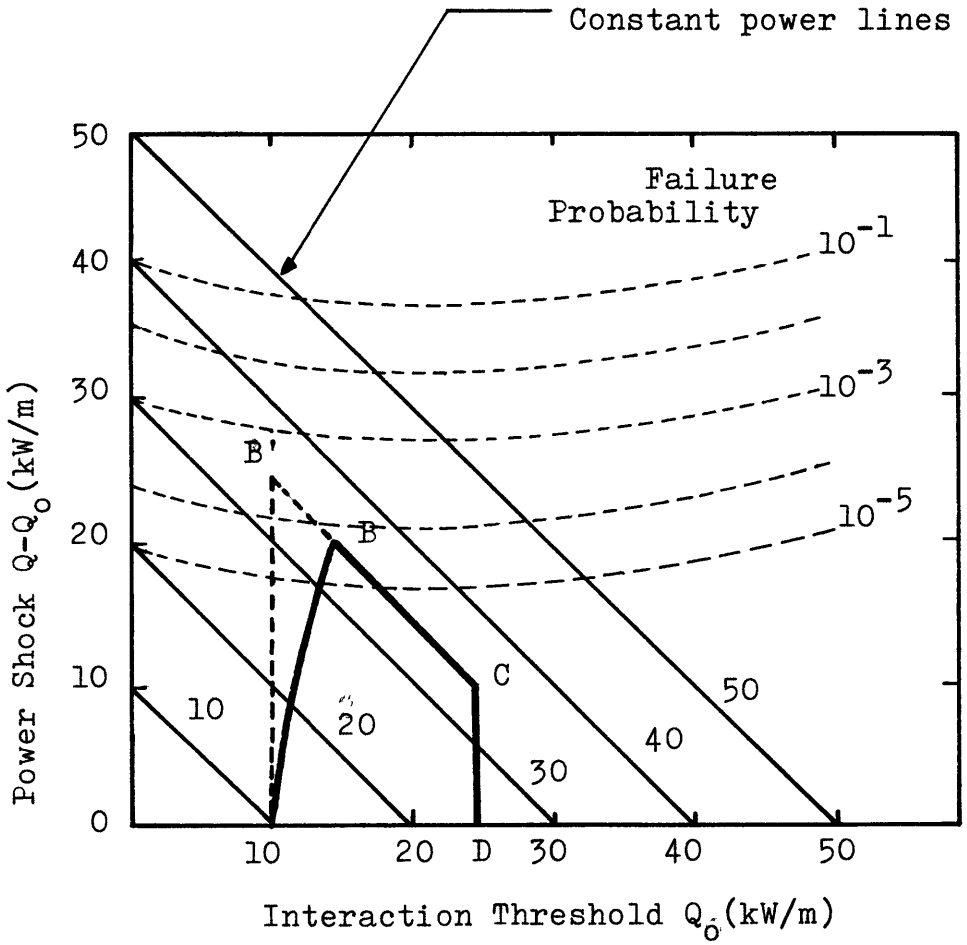

Fig. 4.7 - "POSHO" Computation of Failure Probability (Ref 47)

how the locus of failure probability moves during the power shock event of Fig. 4.6 , with conditioning taking place. The vertical dashed line (A-B') shows the locus of failure probability if the power rise were instantaneous.

For an instantaneous power rise, from 10 kW/m to 35 kW/m the power shock, $Q-Q_o$, would be 25 kW/m, since Q_o-Q = 10 kW/m initially. For this shock the probability of failure would be approximately $5x10^{-4}$ (Point B' no Fig. 4.7). For a real shock ascension the value of Q_o would increase during the time the power shock was taking place. This is represented by the heavy solid curve between points A and B. Thus, the power shock is less than the total power change; in this case the power shock is 20 kW/m and the probability of failure is reduced to approximately $5x10^{-5}$ (point B on Fig. 4.7). While the power, Q, is constant between points B and C at a level of 35 kW/m, the interaction threshold power, Q_o, increases to approximately 25 kW/m. Since the power shock for this event if defined as the maximum value by which the power, Q, exceeds the interaction threshold power, Q_o, and the probability of failure for this event is associated with the 20 kW/m shock (i.e. $5x10^{-5}$). The failure probability does not change regardless of the time spent at the increased power level. If the power ascension were slower than depicted, then the probability of failure would be less, since Q_o would be increasing over a longer period of time. Point D indicates the value of the interaction threshold power, Q_o=25 kW/m, reached at the time power, Q, was reduced to zero from point C.

4.2.2 - Fuel Management System

The power shock model requires, as input, information about all "power shocks" created in the reactor core during operation; the fuel performance model (POSHO), has been integrated in a Fuel Management System (FMS) in a subsystem called Fuel Duty Cycle Analysis whose functional diagram is shown in Fig. 4.8 . In an operating plant the information about power shocks may be obtained "on line" from the process computer.

There is a computer program called "PRESTO", which is a three-dimensional core simulator with xenon transient dynamics, allowing simulation on specific events on a time scale of hours or following core burnup over weeks. PRESTO simulates a simplified cycle and is designed such that it will adequately reproduce the power shock in the core during identified events. The events that are believed to produce power shocks are mainly: changes in total power, control rod motions and shift in power distribution caused by increase or decrease in the concentration of xenon.

RECORD is a two-dimensional fuel assembly burnup computer program, which provides all required nuclear data for the simulator PRESTO and relative pin power for the fuel assembly as function of burnup. RECORD treats the fuel assembly reactor physics with detail and accounts for lattices heterogenities.

Relative pin power distributions are combined with the nodal power distribution and the total power history to produce a continuous power history for 4 groups of pins in each node.

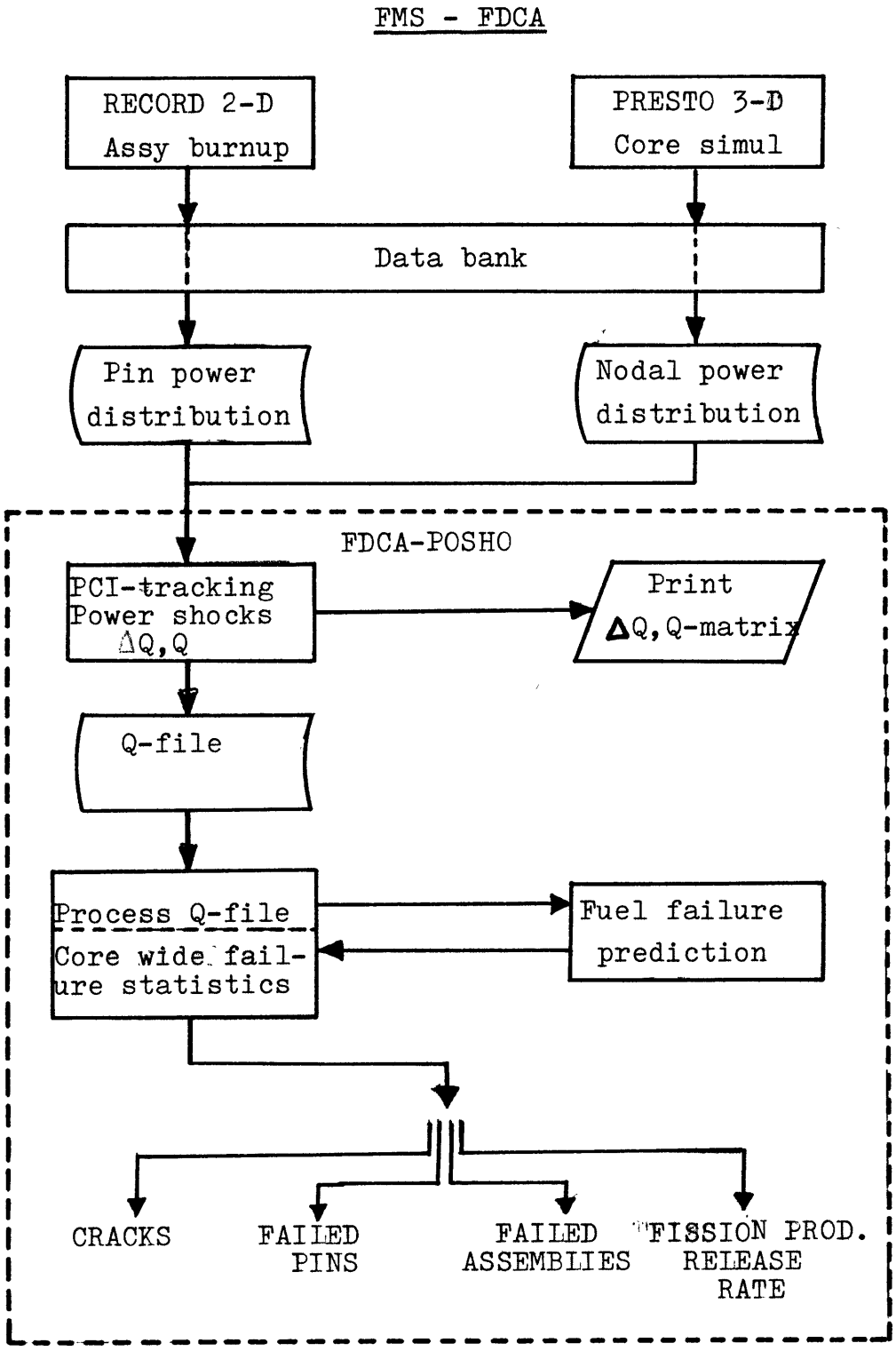

Fig. 4.8 - Functional Diagram of the FDCA System Incorporating the POSHO Logic (Ref 47)

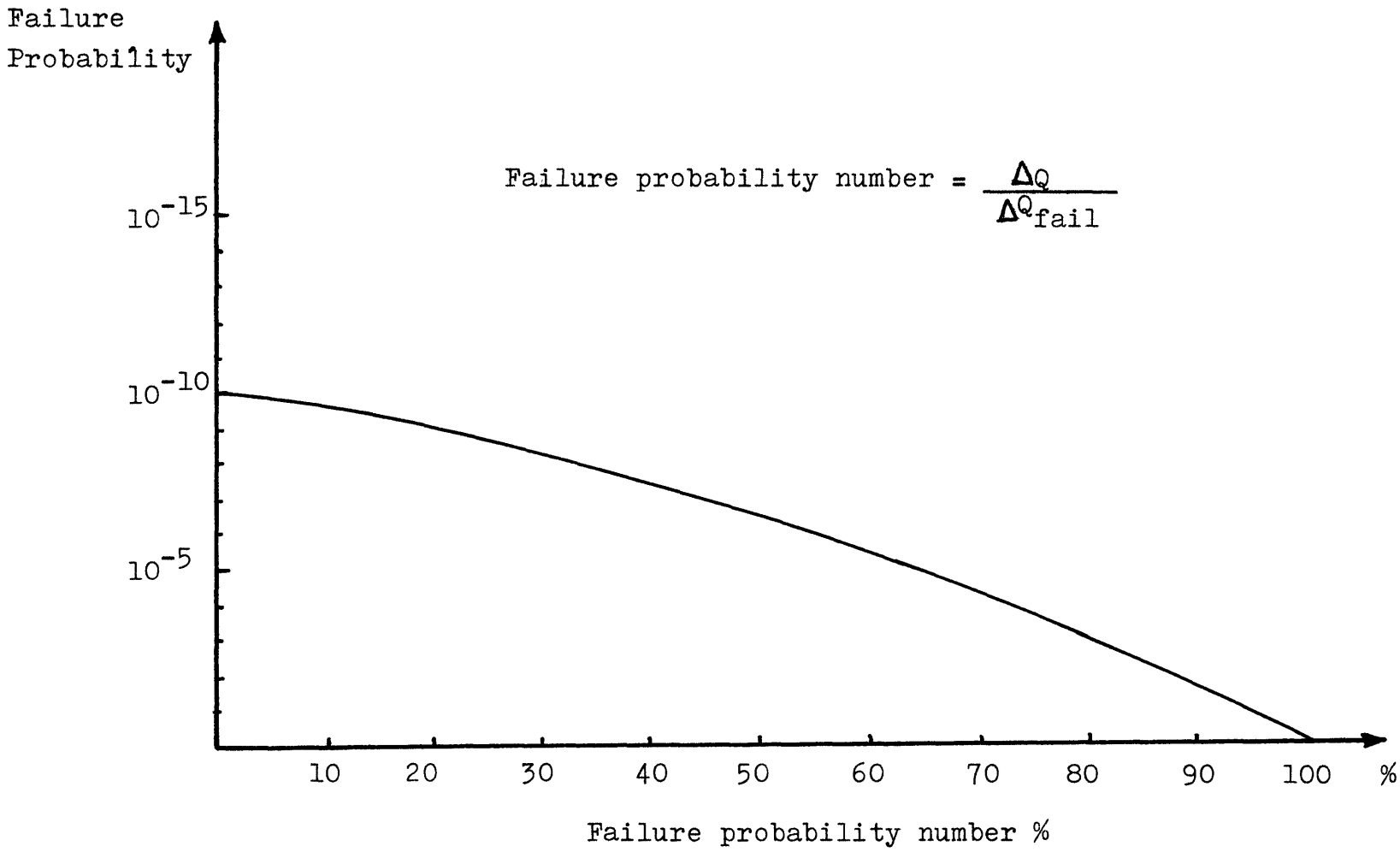

Fig. 4.9 - Probability of Failure Versus Failure Probability Number (Ref 50)

The corresponding PCI interaction level and power shocks are calculated during each power ramp and stored in a permanent file, the ΔQ, Q file, together with the actual power history.

For each pin group in each node, the probability for fuel failure is evaluated by the POSHO Model. The crack probabilities are integrated for each pin group in the assembly to give the expected number of failed pins and assemblies for each event and as function of time.

The failure probability is calculated applying the failure probability number in the failure probability function (Fig. 4.9). The failure probability number is determined dividing the power increment ΔQ (at initial power Q) by the power increment certain to cause failure.

The power shock certain to produce failure is determined experimentally. Example of values of power shock certain to produce failure is given in Fig. 4.10. "The adjustments of the curve up or down depend on design parameters such as clad thickness, fuel density, pellet length, dishing, diametral gap size, etc. and are based on axial and diametral in-reactor strain measurements done at Halden" (50).

Determination of the fuel conditioning correlation and adjustment of the power shock certain to cause failure to "creep advantage" (50) are based on equations developed on the basis of experimental results from the Halden Reactor; Fig.4.11 shows an example of how the $Q-\Delta Q$ "certain to failure" increases at slower power ramps.

The rate at which Q_o decreases (deconditioning rate) is experimentally derived from Halden Reactor experiments and is

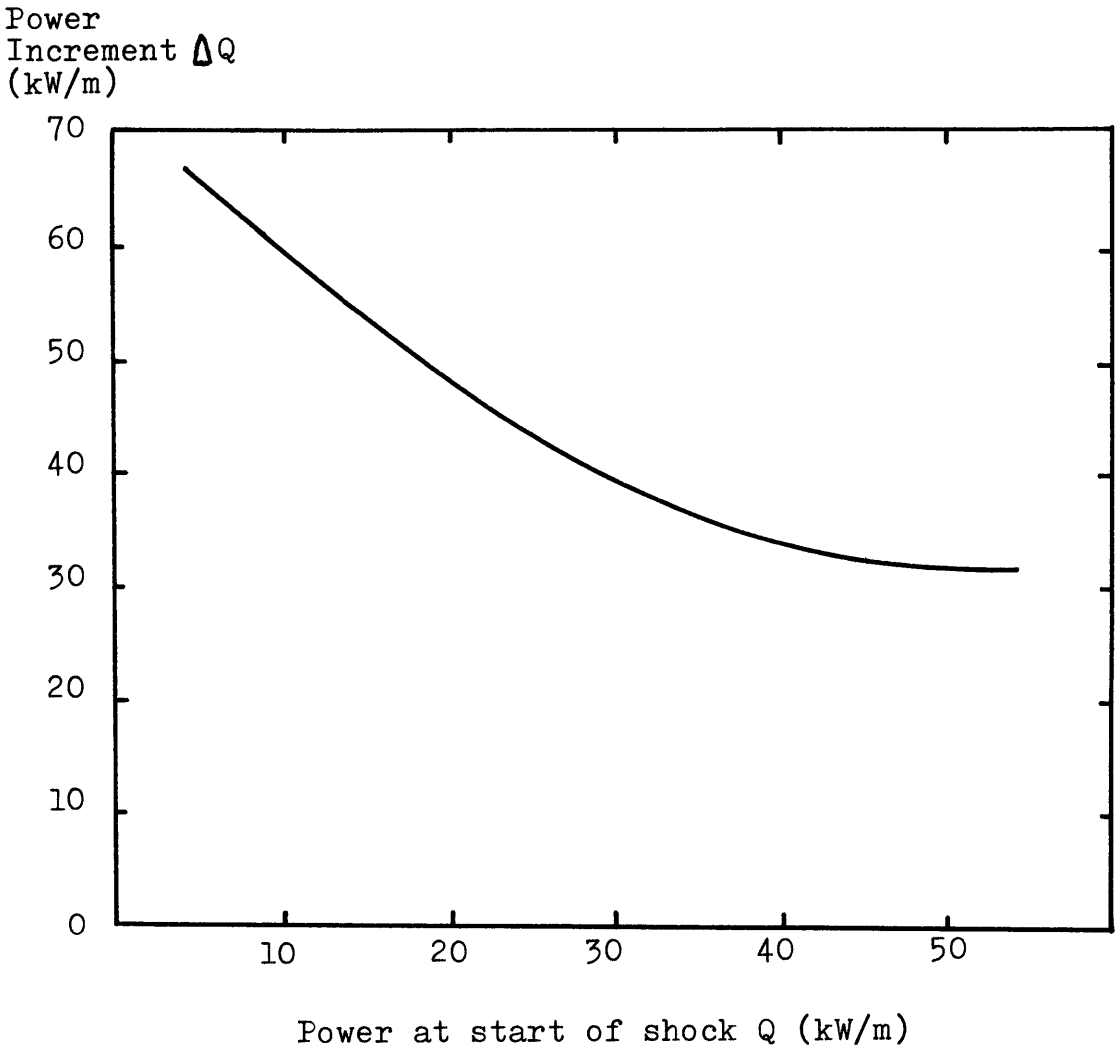

Fig. 4.10 - Q-ΔQ for Certain Failure (Ref. 50)

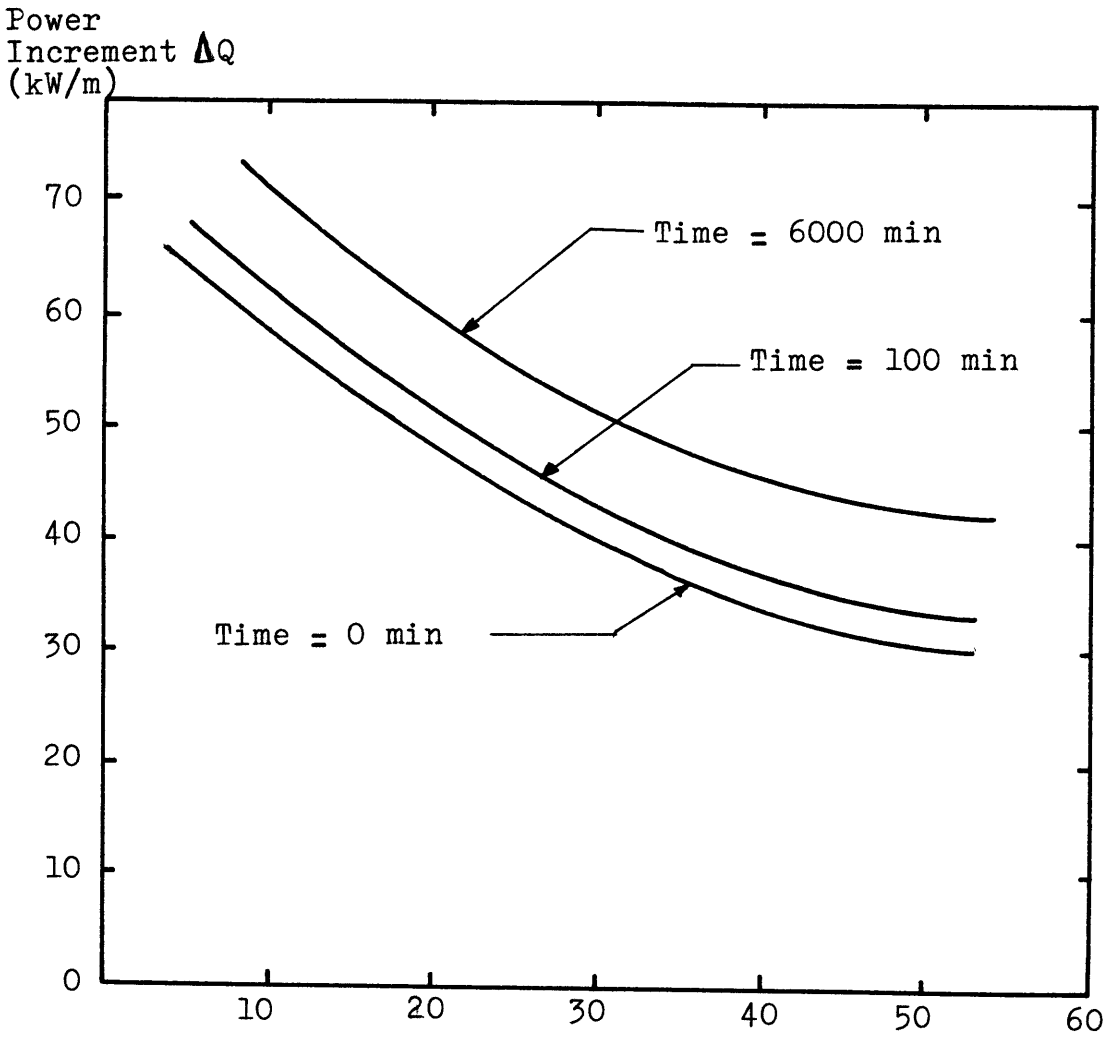

Fig. 4.11 - Effect of Time Over Which ΔQ Occurs on "lines of certain failure" (Ref 50)

given by (50):

$$-\frac{dQ_o}{dt} = 0.03\left(\frac{Q^2}{400}\right)$$

where:

t is time (days)

Q and Q_o are linear heat generation rates (W/cm)

With EPRI sponsorship, this method finished this year, the first cycle of validation in power reactors (Quad Cities BWR and Maine Yankee PWR). The model is in the process of being further improved. In addition it will be necessary to develop a large data base, essential for statistical treatment of the PCI phenomenon, based on informations from both USA and European utilities (47).

CHAPTER 5

FUEL PERFORMANCE MAPS

5.1 - INTRODUCTION

Experience with water cooled reactors has been discussed in previous chapters and has shown that power maneuvers can cause cladding fractures after a sufficiently high burnup. Analysis and studies identified pellet cladding interaction (PCI) as being the major cause for such failures. Therefore, PCI is considered the prime limiting factor when establishing a fuel performance criteria which influence allowable maneuvers.

Chapter 3 described with some detail the PCI phenomena, and point out that, so far, there are uncertainties that still remain on the different areas related to PCI. It is not the purpose of this thesis research study to solve any of the existing uncertainties; they will only be solved with continuing research and experimentation.

The study of this thesis relies on published analyses of power reactor fuel experience, test reactor experiments and related laboratory experiments and is intended to provide:

- a set of calculations that gives allowable ramp rates for maneuvers and numbers for conditioning and deconditioning phenomena;

- a treatment sufficiently simple so that it is easily understood and is suitable for plant operator training (or even, with more validation, suitable for operational use);

- actual numerical results for an illustrative example, rather than the schematic descriptions often found in the existing literature; and

- thoughts on limitations and suggestions for work to extend the method.

5.2 - BASIS OF THE METHOD

For most existing LWR at the beginning of life (BOL), the fuel-clad gap is open but gradually diminishes until complete closure occurs, usually during the second in reactor residence cycle. This behavior tends to be true for prepressurized rods with current techniques of fuel fabrication (ruling out the possibility of drastic densification). It is in general agreement that fuel failure by pellet cladding interaction cannot occur if the existing gap is greater than the maximum pellet diameter increase during the power ramp. Consequently it is important to know when in the life of the fuel, the gap is closed. The next section (5.3) explains the calculational procedure to estimate gap closure.

If the gap is closed, whenever the reactor goes up in power the thermal expansion of the fuel pellet causes tensile

stresses in the cladding, the magnitude of these stresses depending upon the rate and magnitude of the reactor power increase. These stresses are to be kept below a determined level to avoid stress corrosion cracking.

5.3 - PROCEDURE TO CALCULATE GAP CLOSURE

A fuel performance code available at MIT, the LIFE 1-LWR* (Ref 17) does not consider two important mechanisms of gap closure in UO_2-Zircaloy LWR fuel rods: pellet cracking/relocation, and cladding creepdown, the two mechanisms that chief contributors to gap closure. To circumvent this problem it was decided to use the BUCKLE code to calculate the cladding tube creepdown, using input data taken from LIFE 1-LWR output.

LIFE 1-LWR is an adaptation of LIFE 1, a fast reactor fuel performance code, and retains its original swelling and gas release models. Results from early runs showed the necessity to calibrate these models against available data. At this point it was chosen to base calculations with Angra-1 Westinghouse 16x16 fuel pins (identical to Westinghouse 17x17) since all the non proprietary data were easily at hand.

The first task was to calibrate the swelling and gas release models against Westinghouse information provided in Figs. 5.1 and 5.2 (Ref 4).

The GASOUT (gas release) and SWELL (swelling) modified subroutines are presented in the appendix 1 of this thesis.

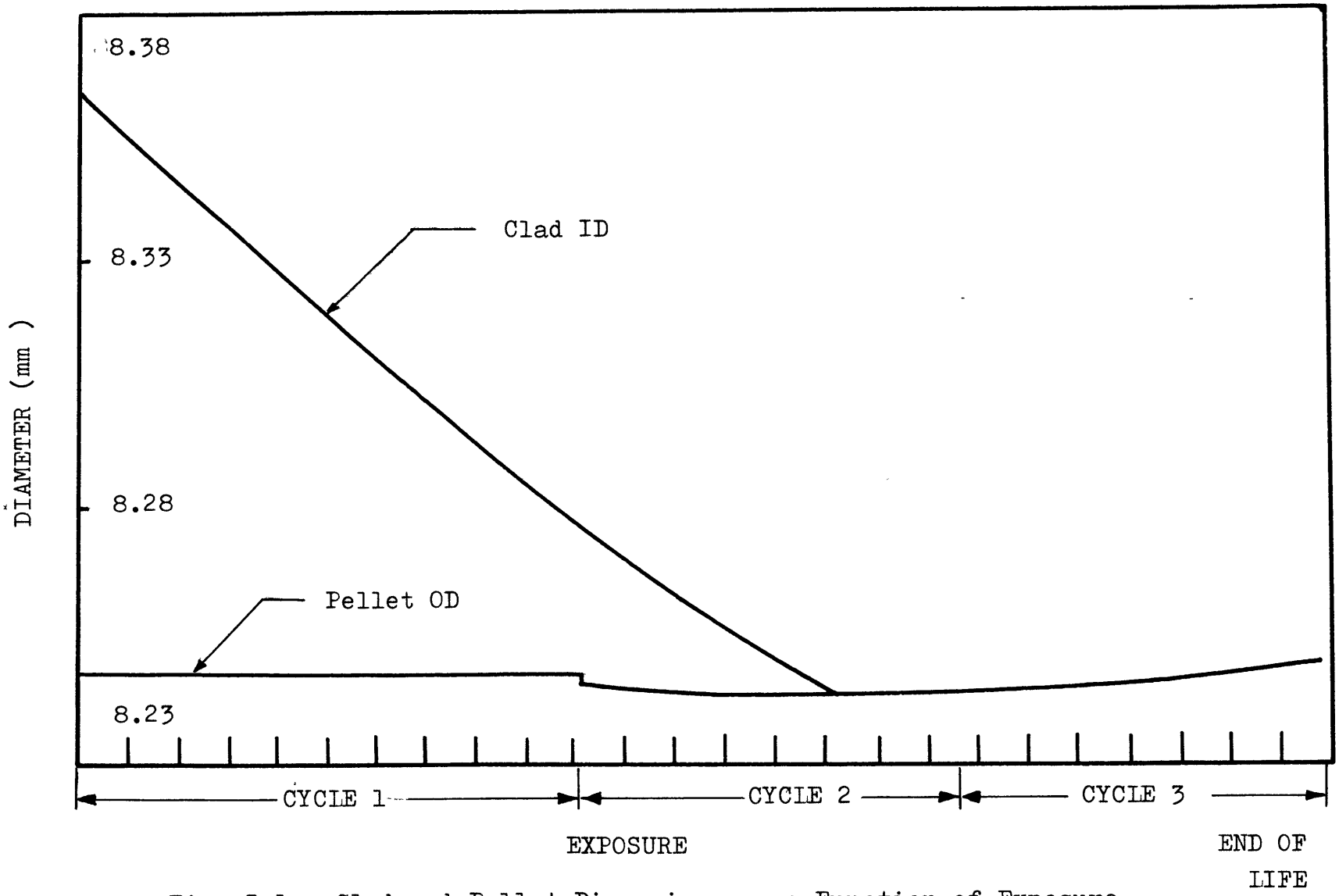

Fig. 5.1 - Clad and Pellet Dimensions as a Function of Exposure

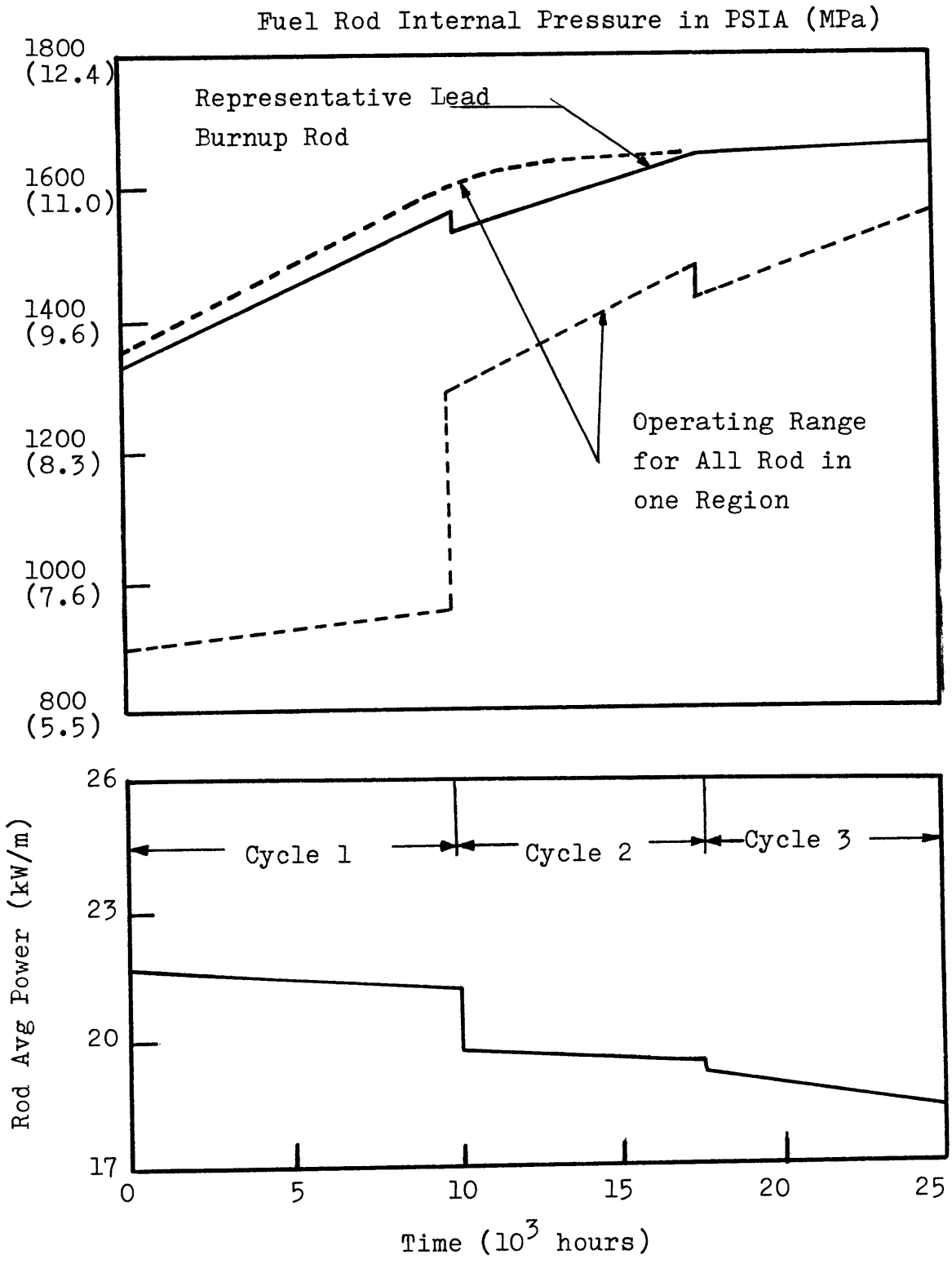

Fig. 5.2 - Internal Pressure and LHGR for the Lead Burnup Rod as Function of Time (Ref 4)

The process of calibration was to adopt multipliers (as input data) to adjust the existing model, and to use as power history the "representative" fuel rod power history presented in Fig. 5.2c. The results of this calibration work is presented in Fig. 5.3 and Fig. 5.4 .

After this LIFE 1-LWR calibration was performed, the output results: plenum pressure and cladding temperature and hot dimensions were used as input to BUCKLE and this code was calibrated to provide the fuel/clad gap closure at the same point in time at the Westinghouse data presented in Fig. 5.1a. The results of this work presented in Fig. 5.5 and calibration details in appendix 2.

In the Fuel Performance Maps, the time to close the gap is considered to be time at which the average reduction internal radius of the cladding, (calculated by the BUCKLE code) is equal the fuel/clad radial gap in the maximum expected hot spot under normal operation conditions, calculated by LIFE 1-LWR.

It was assumed that the fuel pellet diameter in the hot spot, calculated by LIFE (without creepdown or relocation) provides a pellet diameter increase that may be too large and if so, that tends to compensate for the non-existance of pellet ridging and relocation models in this code.

* CYGRO - 3C is also available, but only for U.S. citzens.

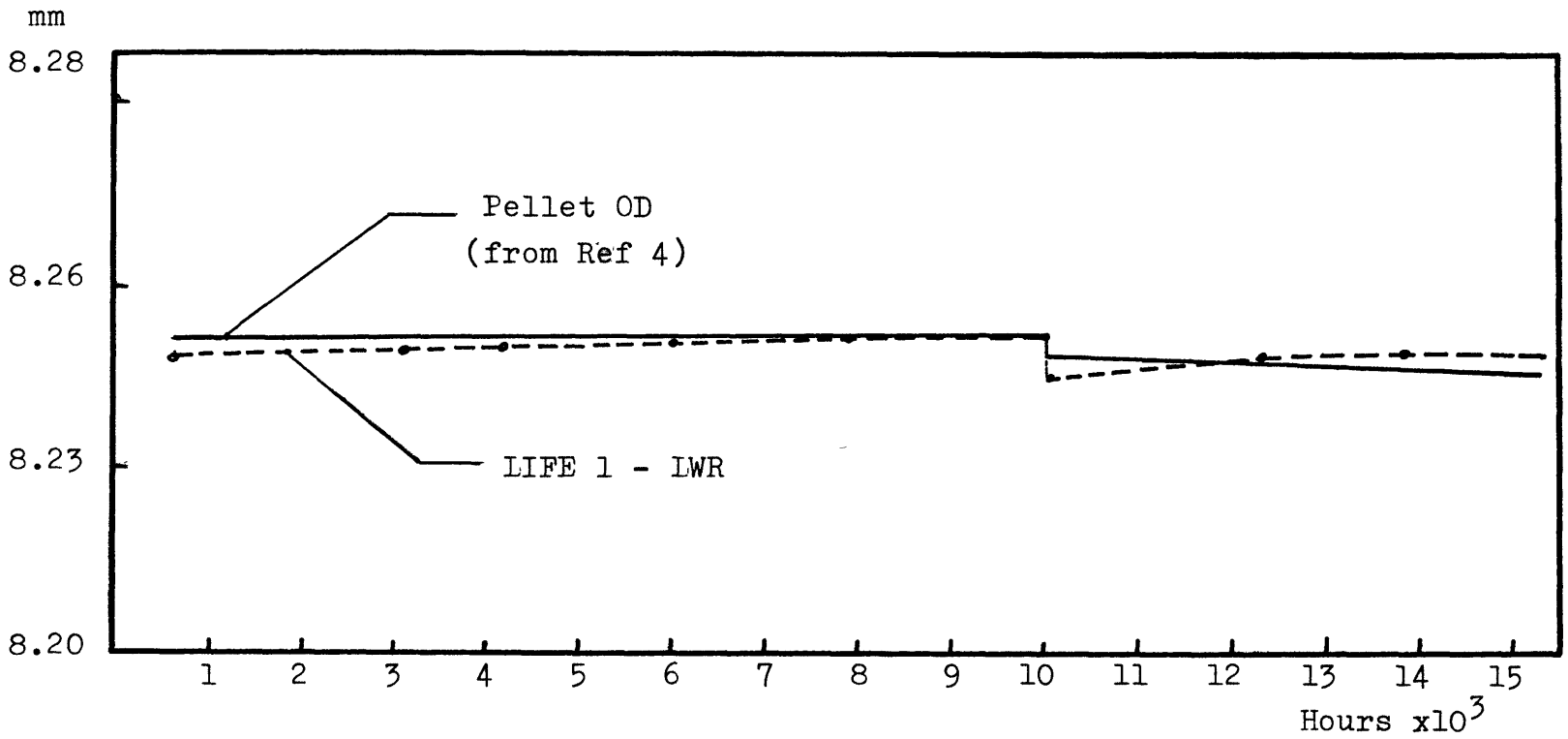

Fig. 5.3 Swelling Calibration Results

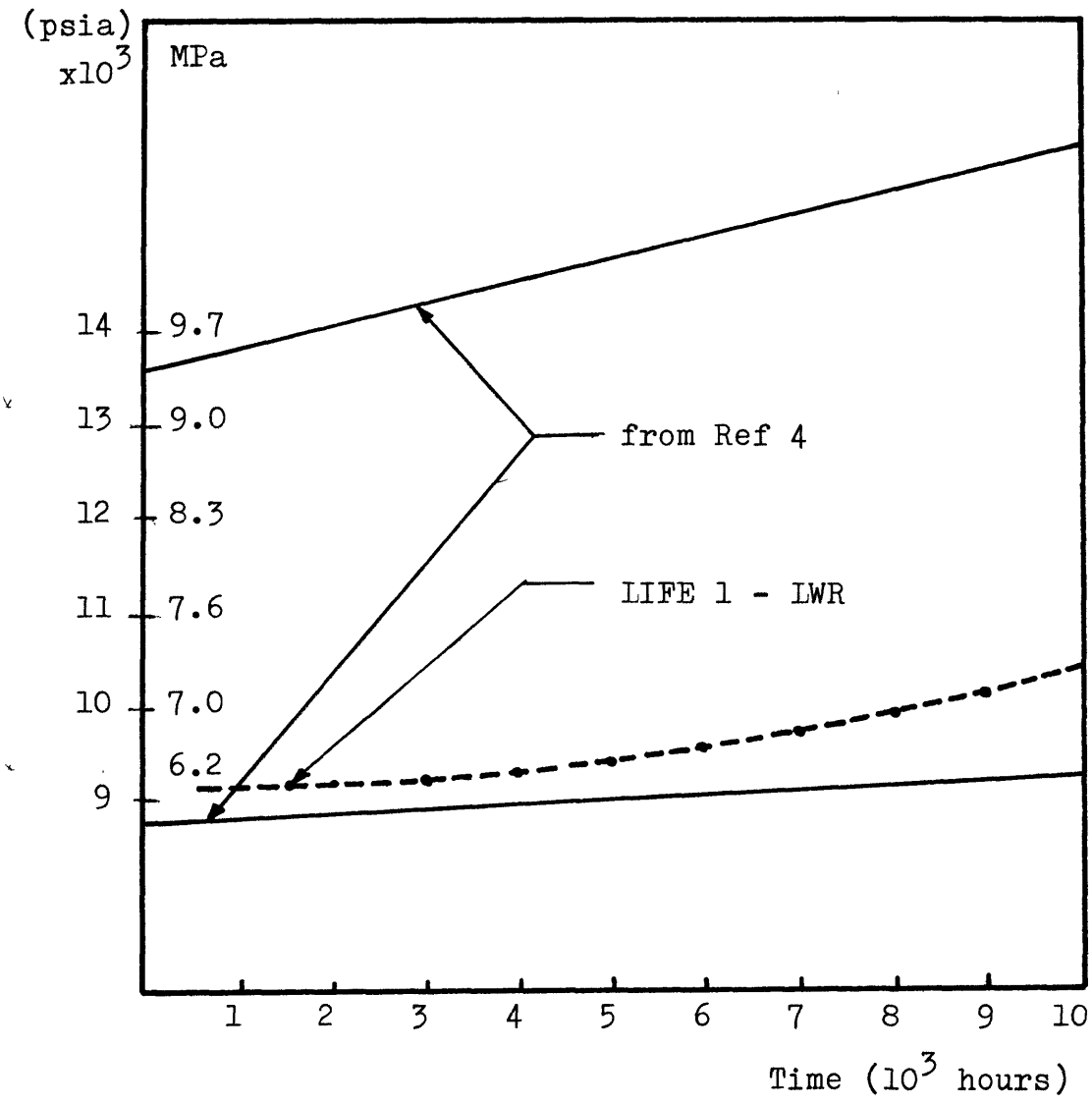

Fig. 5.4 - Gas Release Calibration Results

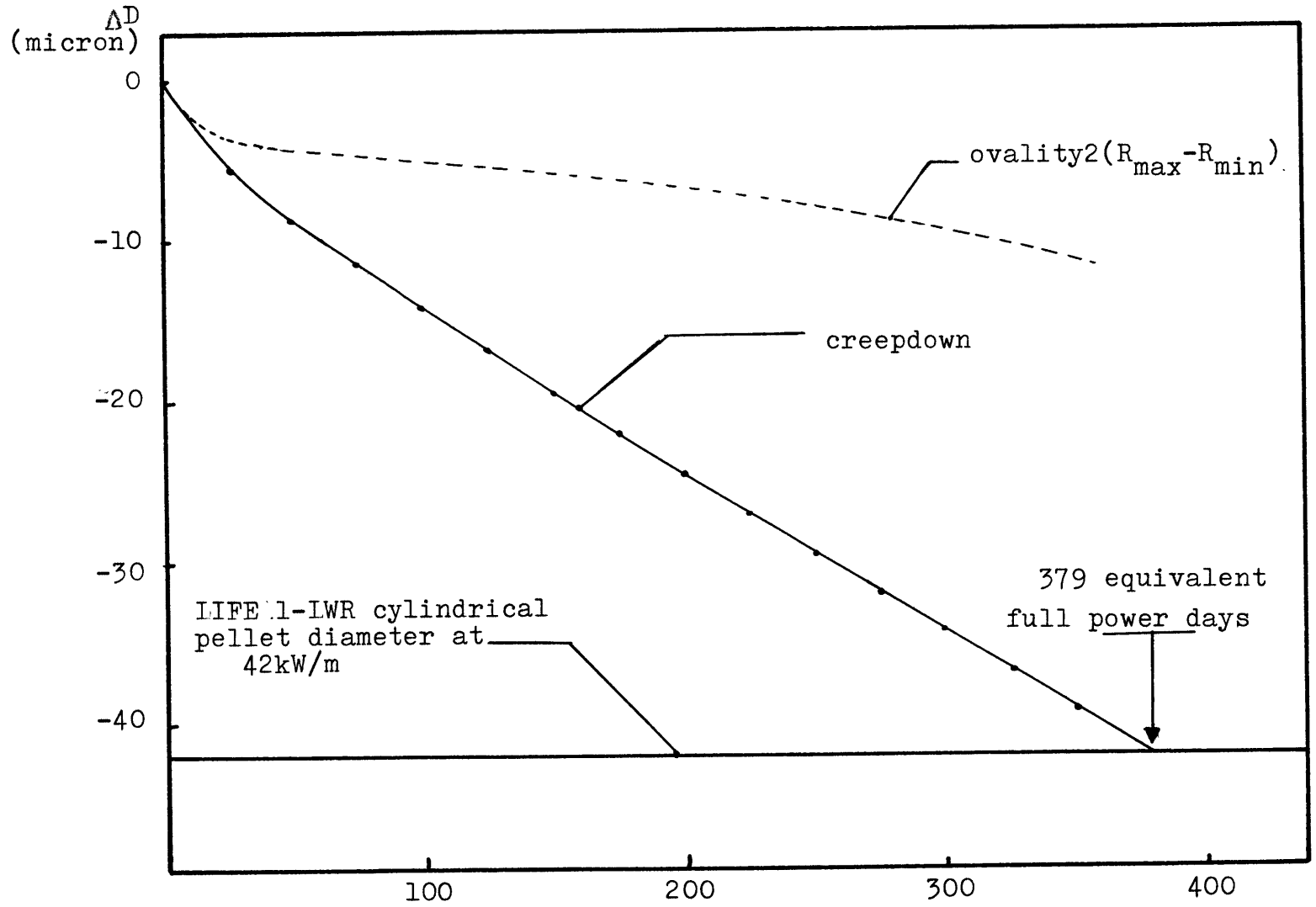

Fig. 5.5 - Results of BUCKLE Code Calibration

5.4 - PROCEDURE TO IMPOSE GAP CLOSURE IN LIFE COMPUTER RUNS

As was mentioned earlier, the LIFE computer code does not consider cladding creepdown. Experiments (4,5) have shown that the fuel cladding gap really closes at sufficiently high burnup after a gradual decrease in the cladding diameter until the cladding is supported completely by UO_2 pellets.

As definition, from now on, whenever the cladding rests completely upon the UO_2 pellets, for a determined linear heating generation ratio (LHGR), the fuel pin will be considered "conditioned" for such LHGR. When the fuel is conditioned for a certain power level, and the reactor undergoes a power increase, the pellet thermal expansion may cause the cladding stresses to increase and depending on the magnitude and rate or power increase to achieve stresses that may cause cladding failure by SCC.

In order to calculate those stresses, it was necessary to modify the LIFE code to introduce changes that permit an "artificial" conditioning. The subroutines RSTART, DTANEW and the altered MAIN program are also included in the appendix 3. The subroutine RSTART permits stopping the computer run at any previously determined (by BUCKLE code) point in time and prints all the necessary cards for reinitiation. The subroutine DTANEW allows to continue the computer run at the same point in time, but with the cladding dimensions artificially altered to contact the fuel.

It is considered that hard contact exists, when the cladding inside radius is equal the pellet outside radius;

this situation is achieved after an iterative process, since whenever the cladding diameter decreases towards the elimination of the gap, there is an improvement in the heat transfer conditions that leads to a decrease in the fuel temperature and consequently a decrease in pellet diameter, re-opening the gap.

At this point a conservative assumption was adopted that there is not an increase in the cladding wall thickness as consequence of the cladding tube creepdown process.

5.5 - LIFE MODIFICATIONS TO HANDLE POWER RAMPS

After some numerical experiments with LIFE in its original version, it was concluded that it was not adequate to work with ramp rates of the magnitude the power reactors are designed to operate and provide the necessary numerical convergence. In order to adequately calculate power ramp rates with fuel in the "conditioned" condition further modifications had to be performed in the MAIN program and also in the subroutines TIMETR and CREEC. The modified subroutines are also listed in appendix 3.

The subroutine TIMETR selects the size of the time step. Numerical experiments have proven that with the original TIMETR, this selection was not always adequate, there were though, introduced modifications to optimize the selection of the time step in order to provide convergence in the calculation with every ramp rate. These modifications were

performed after testing code sensitivity in several runs.

Having solved the numerical convergence problem, it was noticed that the numerical results for cases with different power rates, starting with the fuel pin in the same initial conditions (in-contact) gave always the same value in stresses for the same power level, no matter the ramp rate applied; in other words, the code giving an elastic deformation (with no creep) and hence distictions did not exist for different ramp rates.

Knowing from reactor experience (32, 11, 12, 17) that very small concentration to the fission products that contribute to stress corrosion are necessary for the occurrence of such phenomena, it was assumed that chemically the fuel internal environment would be always able to produce SCC. This assumption leads naturally to the hypothesis that the magnitude of the stresses achieved, as consequence of the power ramp, are the solely responsible for the existance or not of the SCC. The consequence of this hypothesis was to emphasize the importance of improvements in the stress calculational model in order to make it sensitive to differences in power ramp rates.

Different models were considered to obtain a time dependency that could lead to appreciable changes in stresses in the type span of a normal power ramp. By an elimination process, it was decided to consider three possible contributing factors: swelling of the fuel pellet, creepdown of the fuel and creep of the cladding.

Experimental evidences as Fig. 5.1 and Fig. 3.5 (4, 5)

have proven that swelling in modern fuel probably would not cause an increase in diameter sufficient to alter the magnitude of the cladding stresses.

Experiments have demonstrated the low swelling of LWR fuel in normal operational conditions (5), and was considered not to be an important participant in the short term process of an up power ramp.

The short term processes in the fuel that might be important in an up power ramps are:

- inward creeping of the bridging annulus (Fig. 5.6) material.
- better fitting of cracked or broken pieces of the fuel that lead to creep compaction of the fuel pellet.

There are still some uncertainties with respect to Zircaloy cladding creep behavior under reactor working conditions. Liu and Bement (13) point out that among the existing experimental correlations discrepancies up to three orders of magnitude exist. They also explain that the values of the variables that enter in those correlations are average values, and this is inevitable, because during a long reactor test, the fluctuations in temperature, pressure, stress and flux histories are just too complex to be considered. In addition, since the up power ramp causes a newly applied stress, primary creep effects may be important. Under such circunstances it appeared to be reasonable to work in the cladding creep subroutine ot obtain the desired numerical sensitivity to different ramp rates.

The original LIFE code used the Watkins and Wood correlation. It was decided to change to the model suggested

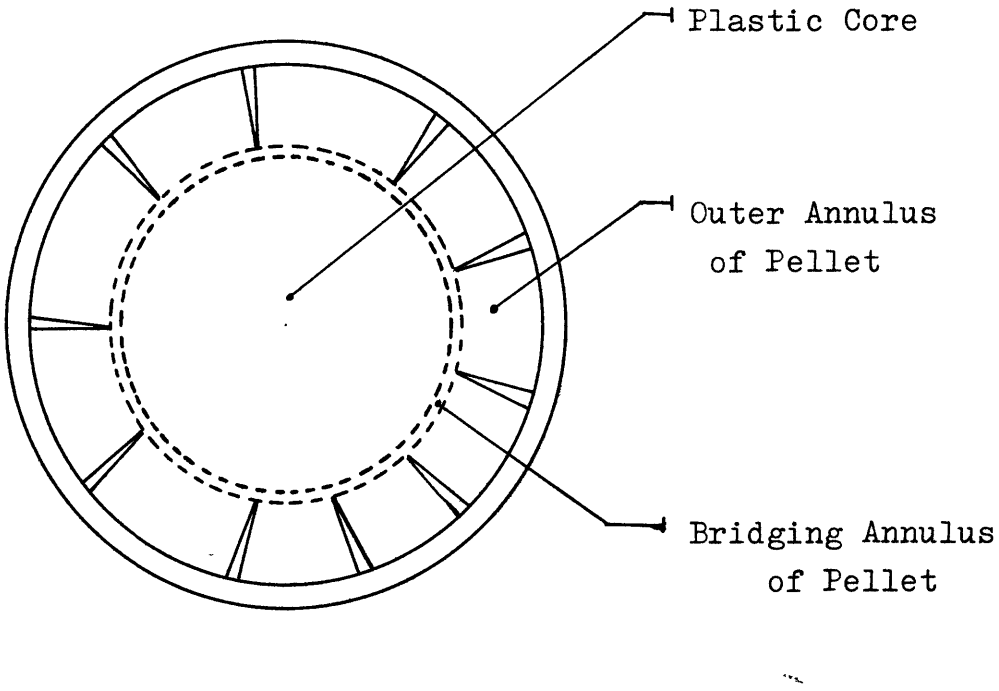

Fig. 5.6 - Pellet Cracking Distribution Model (Ref 19)

by Liu and Bement and implemented for calculation purposes by M. Kramen. As consequence, the original CREEC subroutine was changed by the CREEC subroutine taken from reference 38. It was decided, after some numerical experiments, to apply a creep enhancement factor of one hundred during the ramp rate. This enhancement factor is intended to provide for:

- extra creep attributed to the difference between the average stresses and strain from life calculation and the local stress and strain near potential failure locations;
- creep and refitting effects in the fuel pellet; and
- primary creep effects.

5.6 - FAILURE AND CONDITIONING CRITERIA

The failure and conditioning criteria are presented in Fig. 5.7 which is an average hoop stress versus time plot.

A maximum allowable ramp rate is adopted as a ramp that causes an average hoop stress, in the maximum linear heat generation region of the fuel, 50% below the minimum threshold stress found by Vinde and Lunde in their stress corrosion tests: 2965 Mpa (43000 psi) (Ref 18). The fuel is considered conditioned for a determined power level in the time necessary for the cladding average hoop stress (in the maximum local LHGR region)to decay by creep relaxation to 50% of the stress threshold defined by Busby (31) in his long duration stress corrosion experiments: 165 MPa (24000 psi) (Ref 31). The 50% corresponds to the application of a stress

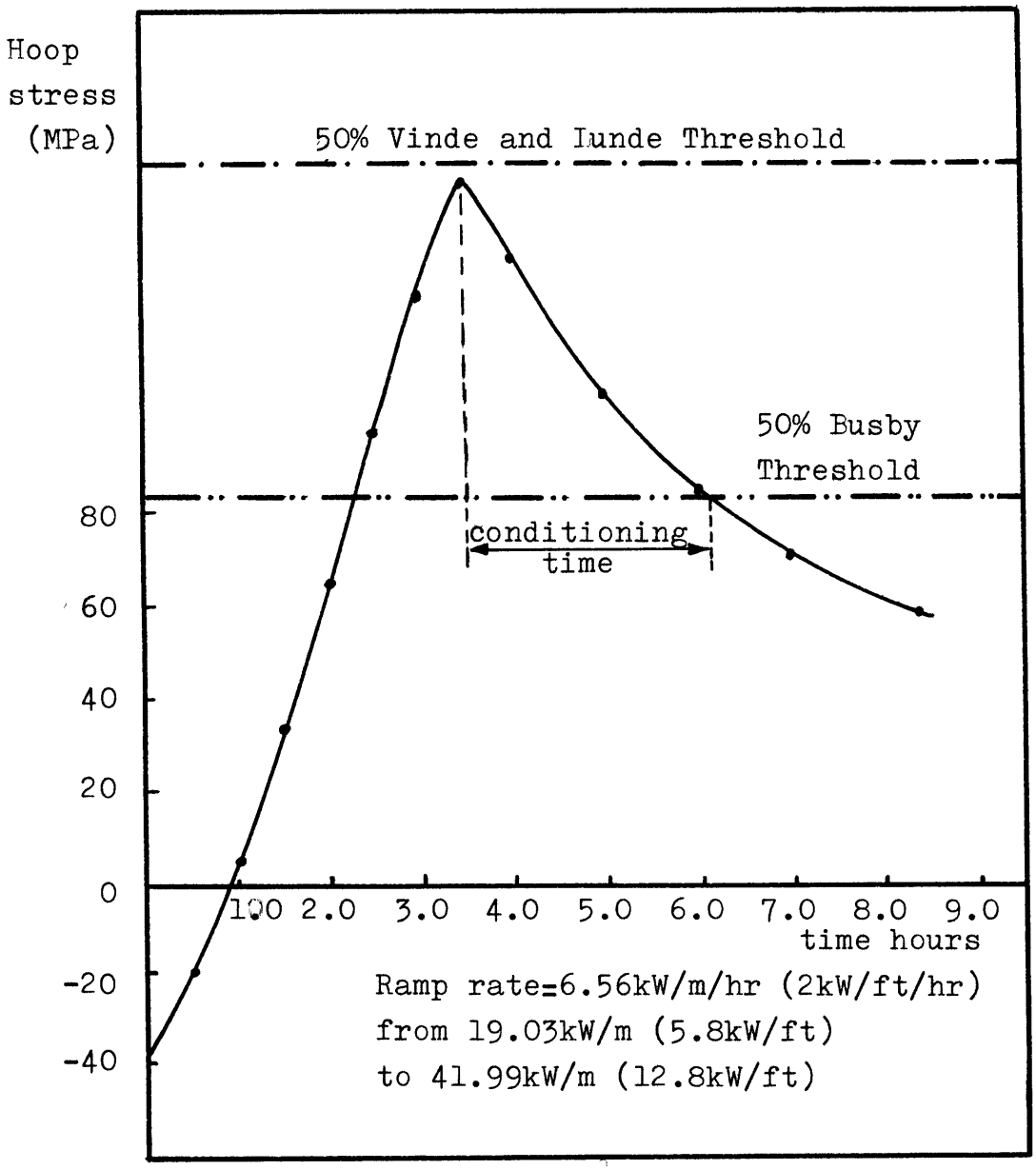

Fig. 5.7 - Failure and Conditioning Criteria

concentration factor equal 2 since it is considered that the existence of stress concentration near cracks and ridging zones are very important in SCC failure and (as explained before) those are the preferential regions for cracking initiation.

In the calculational procedure the fuel in the conditioned situation rests on the pellet stack along the complete length of the stack; for simplification most of the calculation are based on the maximum LHGR existing along the full length of the stack. This is a simple and probably a conservative procedure. One can not guarantee, however, that this would reproduce the normal worse condition for the local stress, even considering the "safety coefficient" (stress concentration factor) of 100%.

5.7 - CALCULATION OF THE DECONDITIONING RATE

If the fuel is conditioned for a determined power level, and there is a power decrease maneuver, there will be a decrease in the fuel temperature and consequently a contraction in the fuel pellet diameter and possibly reopening the gap. If the reactor is maintained for a while in this lower power level, the gap will not continue indefinitely open. At the moment of the new gap aperture, the cladding starts very slowly to buckle down and after a while, a considerable amount of the clad will rest again upon the UO_2 pellets.

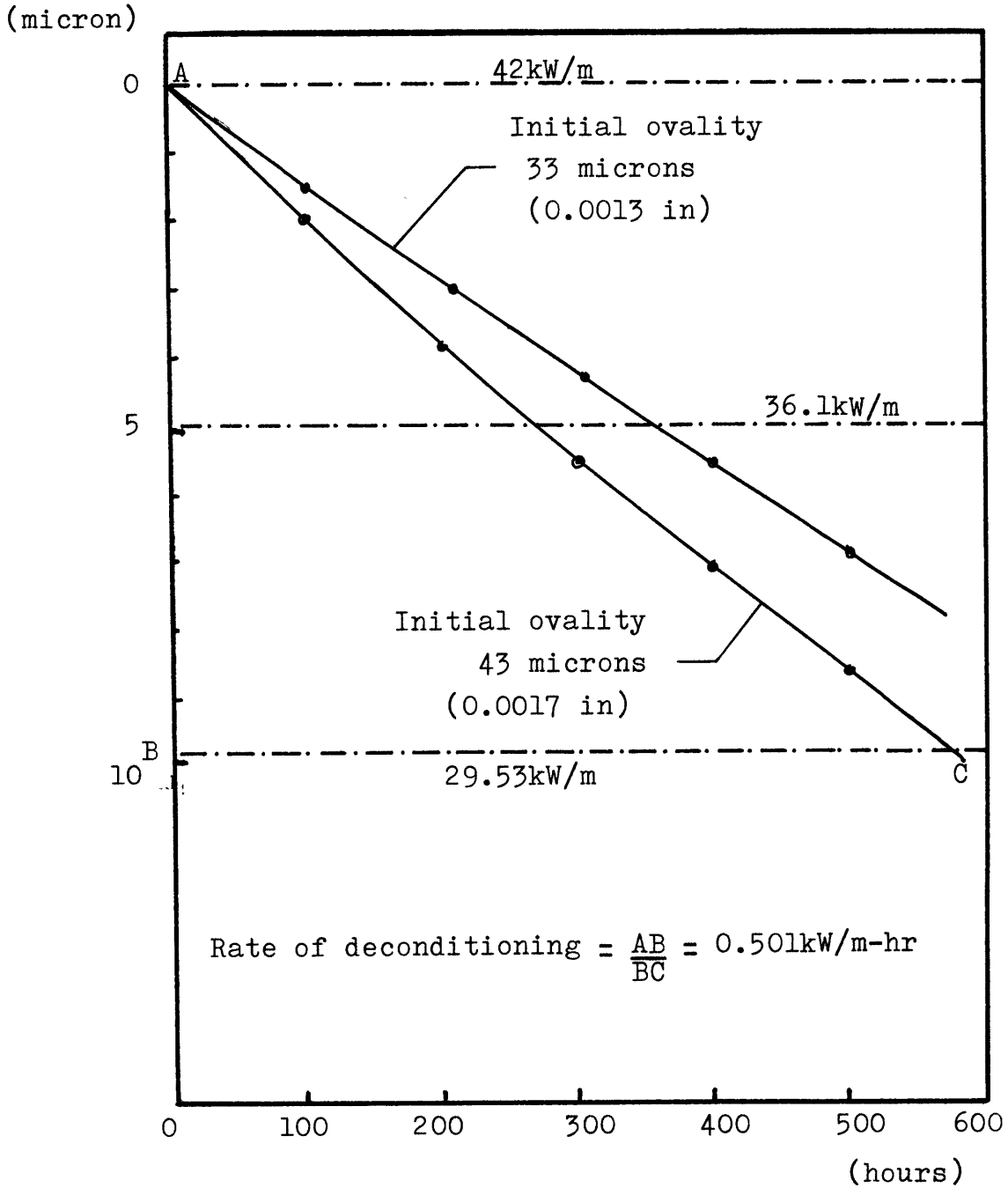

Fig. 5.8 - Deconditioning Rate

Experience shows that at sufficiently high burnup, when the fuel rests upon the cladding the ovality of the fuel pin is much greater than the initial ovality at BOL, and also as consequence of the reversibility of the relocation mechanism, the fuel pellets have also an oval shape given, at least to some extent, by the shape of the cladding in the buckle down process. This larger initial ovality at gap reopening might lead to a cladding inward radial rate of displacement, by increase in ovality, greater than the rate of decrease in the average radius by creepdown, used as criteria for first gap closure.

The rate of deconditioning is calculated using as input in BUCKLE the ovality suggested by experience (5). When the inward radial increase in ovality (BUCKLE) has the same value of the decrease in fuel pellet radius (calculated by LIFE) caused by reduction in LHGR, it is considered that the fuel rod is conditioned again for this reduced power level. The rate of deconditioning is considered to be the power difference between the initial and final conditioned situations divided by the time span between the two events, as it is explained in Fig. 5.8 . This criteria leads to numbers comparable to the Scandpower experimental correlation given in Reference 50.

5.8 - FUEL PERFORMANCE MAP AND MANEUVERING TABLE

Fig. 5.9 presents the fuel performance map. It is a plot

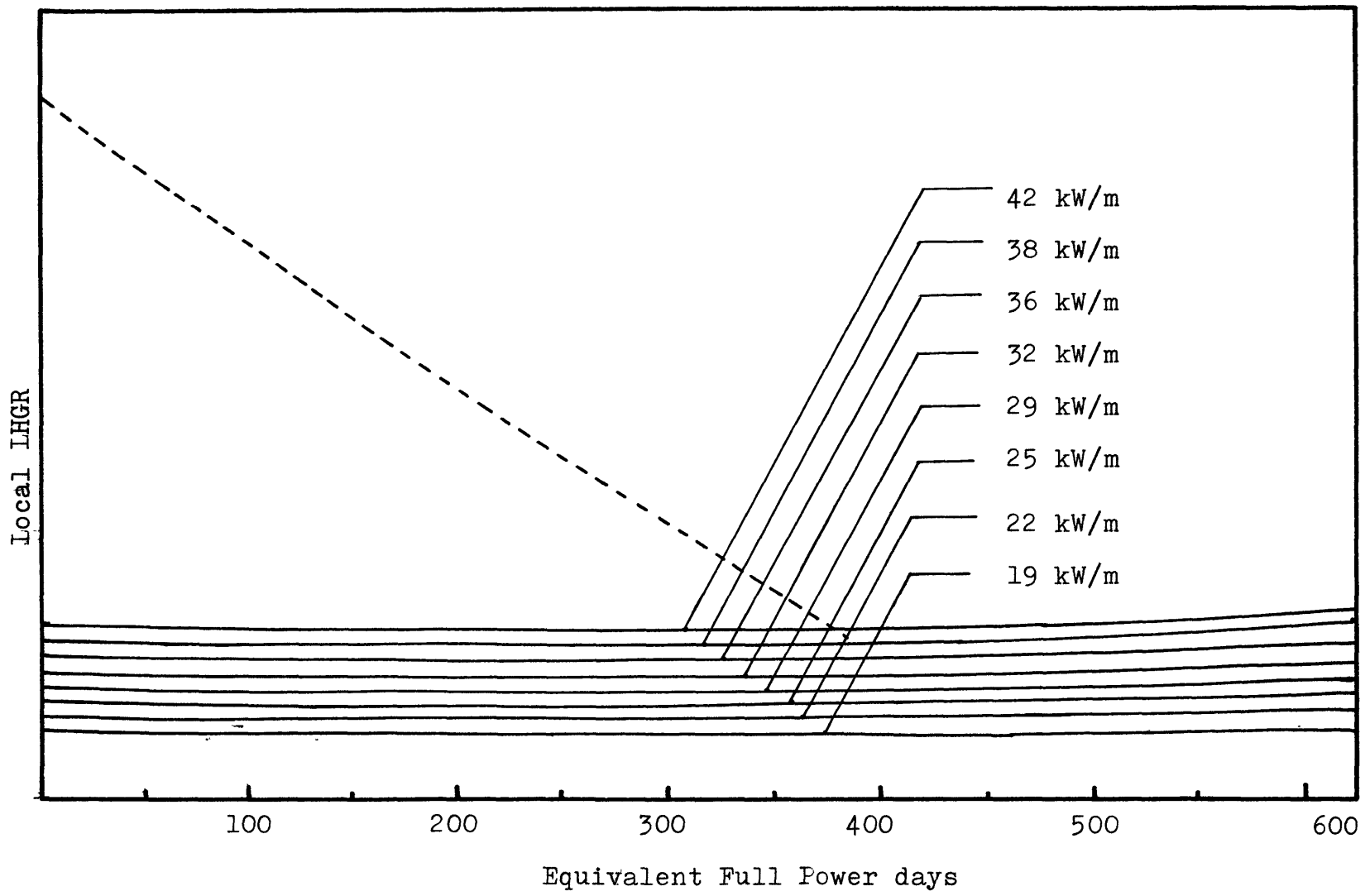

Fig. 5.9 - Fuel Performance Map

in terms of local peak heat generation rate and equivalent full power days of operation. In order to consider an intermediate power an interpolation between curves has to be performed.

This plot is nothing more than the locus of the fuel pellet diameter translated in terms of LHGR versus equivalent full power days (EFPD, defined in Appendix 1).

The dotted closing gap line is the locus (in terms of LHGR) of the position of the cladding inside diameter at beginning of the fuel life. It is considered that the fuel pin, whenever the gap is open, can handle the maximum ramp rate permissible by the system, which for PWRs is usually dictated by the maximum rate of boron dissolution, or the maximum allowable rate of change of power in the secondary loop (Ref 40).

Usually, only a new plant works with all fresh batches of fuel in the core in its beginning of a cycle. The normal situation is the existence of at least one batch working in the "close gap region" of the map. This is, though, the most important region of the map in terms of restricting the plant maneuvering flexibility by fuel performance limitations. The map allows to keep track of the history of the fuel performance and might eventually be an easy guide to plant operation.

The Fuel Performance Map is to be used in combination with the "Fuel Maneuvering Table" (Fig. 5.10) that suggests the allowable maneuvering rates for the different situations plotted in the fuel performance map. It is suggested a

MANEUVERING TABLE (550 TO 600 EFPD)					
from \ to	42 kW/m	41 kW/m	40 kW/m	39 kW/m	38 kW/m
kW/m	kW/m-hr →	—	—	—	—
38.7	M	M	M	M	—
35.4	M	M	M	M	M
32.2	M	M	M	M	M
28.9	M	M	M	M	M
25.6	82	65	M	M	M
22.3	13	33	M	M	M
19.0	6.6	13	33		

M = Maximum System allowable Ramp Rate

Rate of deconditioning= 0.501kW/m-day

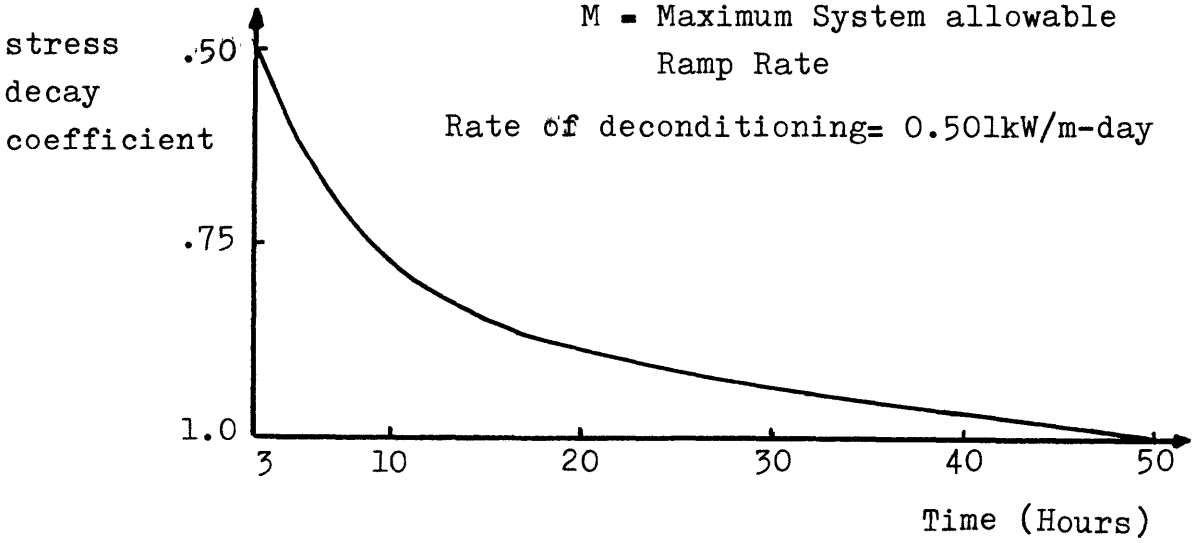

Fig. 5.10 - Maneuvering Table

maneuvering table for each group of fifty equivalent full power days in fuel cycle.

The maneuvering table considers as starting point (in terms of power) the fuel in "fully" conditioned situation and provides the maximum allowable ramp rates for local LHGR that has to be translated in terms of reactor power.

A fuel is considered in fully conditioned situation in a power level $\hat{q}$, if:

- it has been working at this power level during the last 50 hours (see Appendix 1),
- it was deconditioned from a conditioned higher power level,
- it has worked at a higher power level for at least 24 hours.

For times of residence in the power level $\hat{q}$ smaller than 50 hours, the ramp rates suggested in the table have to be multiplied by the "stress decay coefficient" presented in the Fig. 5.10 .

The ramps presented in Fig. 5.10 are calculated according the failure criteria mentioned in section 5.6 . The reason for applying the stress decay coefficient is to compensate the fact that whenever the fuel is not "fully conditioned", the cladding might be subjected to a tension hoop stress.

The table presents also the recommended rate of deconditioning which is calculated as explained in item 5.7 .

The rate of deconditioning multiplied by the time elapsed since the maneuver of reducing power provides the power level at which the pellet tends to contact the cladding. It is considered that up to this power level, the reactor can be maneuvered going up in power with the maximum allowable ramp

rate permitted by the system.

The calculation procedure to achieve the performance maps and maneuvering table are presented in Appendix 1, and an example of application in Section 5.10 .

5.9 - HOT SPOT CONSIDERATION

The present method emphasizes the importance of a good fuel management in minimizing fuel failures by PCI. There is a premium in reducing the maximum local linear heat generation ratio, since the reduction of this maximum causes a reduction in the "power shock" that the fuel suffers in power maneuvers.

The core of one reactor (after the third load) contains fuel batches with different average burnups, and operating under different local power levels; as explained before, to each batch is associated one Performance Map and the plotting is performed based in the number of equivalent full power days of the reactor that the batch in question have participated, which is a rough estimate of the integral energy produced by this batch.

There is always an inherent uncertainty in the calculation of the hot spot factor, since it changes with core life, power level, etc. One hot spot factor could be considered for each fuel batch. However it is recommended that the maximum expected hot spot factor (in normal operation) be used for the three batches. This assumption tends to be conservative.

5.10 - EXAMPLE OF APPLICATION OF THE FUEL PERFORMANCE MAPS AND MANEUVERING TABLE

A simple example of application of Fuel Performance Maps will be presented in this section.

Suppose one have a power reactor in the following situation:

	Depletion per cycle in EFPD			Total Batch Depletion (EFPD)
1st batch	225	215	210	550
2nd batch	—	215	210	425
3rd batch	—	—	210	210

Suppose the reactor has been operated for long time at 77% of full power and the power is reduced to 53% for 30 days and one wish to know how fast can the power be increased to 100%.

Hypothesis:

Core average LHGR at 100% power = 17.95 kW/m

Hot spot factor = 2.34

LHGR at hot spot when at 100% power = 17.95x2.34=42kW/m

Maximum LHGR at 77% = 0.77 x 42.0 = 32.34 kW/m

Maximum IHGR at 53% = 42 x 0.53 = 22.26

It is important to remember that the batch to be considered is the most depleted batch.

In the fuel performance map (Fig. 5.11) the pellet performance behavior is plotted in terms of power, as being

the path A-B-C, since there is an immediate reduction in the pellet diameter when the power is reduced (AB).

The cladding deconditioning is plotted as AD. The rate of deconditioning is 0.501 kW/m-day (from Fuel Performance Map).

Number of EFPD to close gap = $\frac{32.34 - 22.26}{0.501}$ = 20.12 EFPD

The fuel rod after 20.12 EFPD is conditioned for: 53% of full power.

Entering with 22.26 kW/m in the maneuvering table (Fig. 5.10), we can select 13 kW/m-hr as being the allowable ramp rate to increase the power to 100%.

Suppose now, that instead of going to 100% power, by some reason, the reactor has to stay 10 hours at 60% of full power and then, it is decided to continue the power increase to 100%. How fast can it be?

The fuel is not "fully conditioned" for 60% (25.6 kW/m), and cannot use directly the table recommended power ramp rate.

Entering with 10 hours in the "stress decay coefficient" curve (Fig. 5.10), one would pick 0.76 as the applicable stress decay coefficient and the adequate ramp rate to go to 100% power would be:

82 kW/m-h x 0.76 = 62.3 kW/m-h

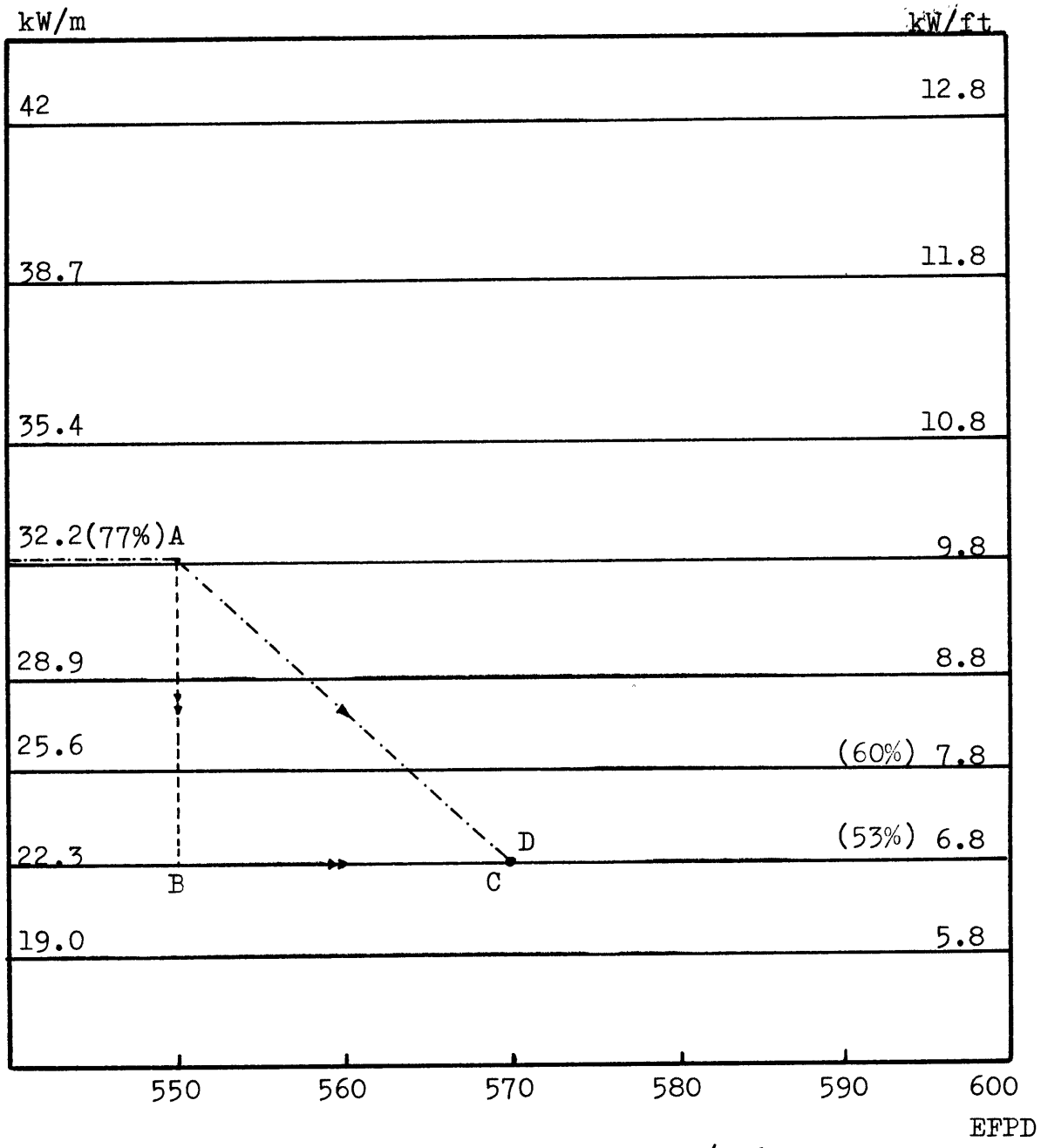

Rate of deconditioning = 0.501kW/m-day

Fig. 5.11 - Fuel Performance Map (550 - 600 EFPD)

CHAPTER 6

CONCLUSION AND SUGGESTION FOR CONTINUING WORK

The method presented in this chapter has the virtue of giving numerical values useful in reactor operation, and obtaining such numbers from simple models and available computer codes. The method seems easy to be implemented and provides to the reactor operator the feeling of the fuel performance concerning pellet cladding interaction. The method is considered to be a practical approach but needs to undergo a validation period before actual usage.

The fuel performance maps and maneuvering charts have to be prepared for each fuel design. The method has the advantage of being relatively non expensive and previously prepared, which makes it adequate as a backup system in the event of adoption, by the utilities, of a more sophisticated "on-line" system for fuel failure prediction.

6.1 - LIMITATIONS OF THE METHOD

Being a precalculated method, it does not consider the actual fuel power history. An artificial history is employed a full power until close to the considered point, then a period of lower power until the considered point (see Appendix 1 Fig. A1.1). This history is not necessarily the worse performance condition. The application of the maximum linear

heat generation ratio along the full length of the rod was considered as a "limit in worst condition". This assumption brought some simplification and might not represent the worse possible real situation.

Due to the fact that LIFE 1-LWR does not consider the local stress concentration, a coefficient of two was applied in the adopted SCC failure limit. This factor is applied on the average clad stress and is to compensate also the fact that LIFE model for the pellet is a long solid cylinder with no cracks, and no hourglassing.

The enhancement of two orders of magnitude in the creep to compensate for local relaxation is also an artificial adjustment that leads to reasonable results but needs validation in reactor trials or by comparison with more detailed analysis.

6.2 - SUGGESTION FOR FURTHER WORK

Improvements in the method are suggested to include the effects of pellet cracks and hourglassing and to incorporate the creepdown and buckling mechanisms for initial gap closing and fuel rod deconditioning in the available fuel performance code.

The validation by comparing the method to results of real reactor experiments is necessarily desirable.

APPENDIX 1

CALCULATIONAL PROCEDURE TO ACHIEVE THE FUEL PERFORMANCE MAPS AND MANEUVERING TABLE

A1.1 - FUEL PERFORMANCE MAPS

Example: Procedure to calculate the fuel performance map at 550 equivalent full power days (EFPD).

a) Run the calibrated LIFE code in constant 100% average core power ($\bar{q}$ = 17.95 kW/m) with a set of axial shape factors that gives 42 kW/m in the hot spot, stopping and printing cards for re-starting again at point A (13180 hrs) as shown in Fig. A1.1 .

b) By adopting a LHGR of 42 kW/m in the full active length of the fuel rod start a group of runs indicated in Fig. A1.1, stopping each run in a different power level at 13200 hrs (550 days). At this point there are a group of points (each one in a power level) that can be used for re-starting (see Fig. A1.1 points B1, B2, B3, B4, ...B8).

c) At each point B re-starts again using the cladding inside diameter equal the pellet outside diameter, altering the cladding outside diameter to maintain the same wall thickness. Perform a short run (2 hours) only to check the gap closure.

The gap will reopen since those improvements in the heat transfer condition lead to a decrease in the pellet diameter. Re-start the computer run with the new value of the pellet

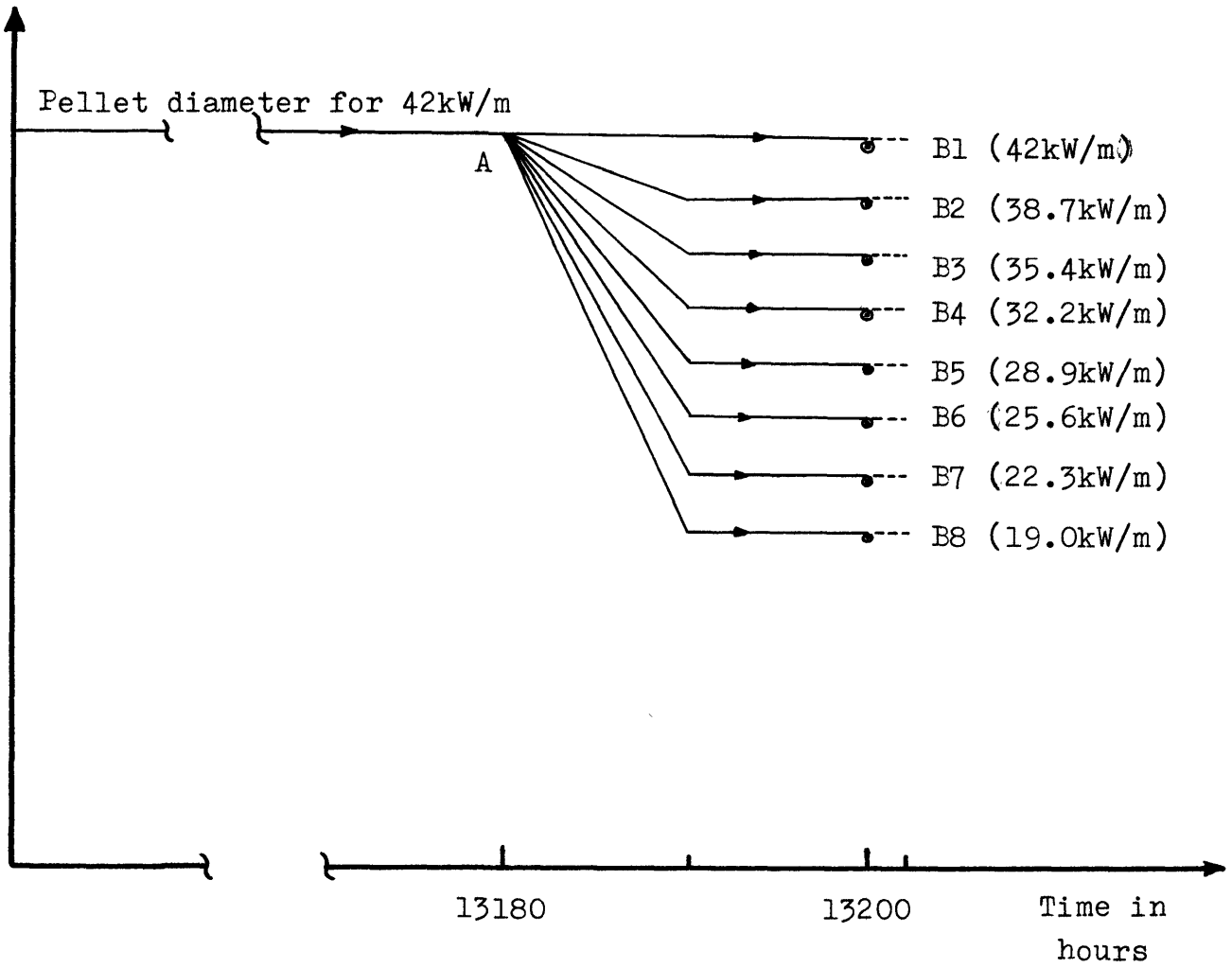

Fig. A1.1 - Procedure to Achieve Fuel Performance Maps

diameter; repeat this operation until gap closure is achieved (about 3 computer trials). In such situation, the fuel rod is considered conditioned and the pellet diameter will be plotted in the fuel performance map.

The fuel performance is, in reality, a diameter versus time graph for a set of LHGR.

A1.2 - CLOSING GAP LINE

The fuel rod internal pressure history at 100% power, and cladding initial hot dimensions taken from LIFE are used as input to BUCKLE with the initial ovality suggested at reference 5 (5 to 20 microns). The decrease in the average internal diameter (BUCKLE) output is plotted in the fuel performance map. When the curve of decrease in cladding inside diameter (starting at initial hot cladding diameter) encounters the line correspondent to the hot spot diameter at 100% power (calculated by LIFE) the gap is considered closed (Fig. 5.5).

A1.3 - MANEUVERING TABLE

With the fuel conditioned for different power levels (at determined depletion in EFPD); starting from each point in power, a set of ramp rates are tried up to 100% power (42kW/m).

From the output is taken the necessary data to plot a

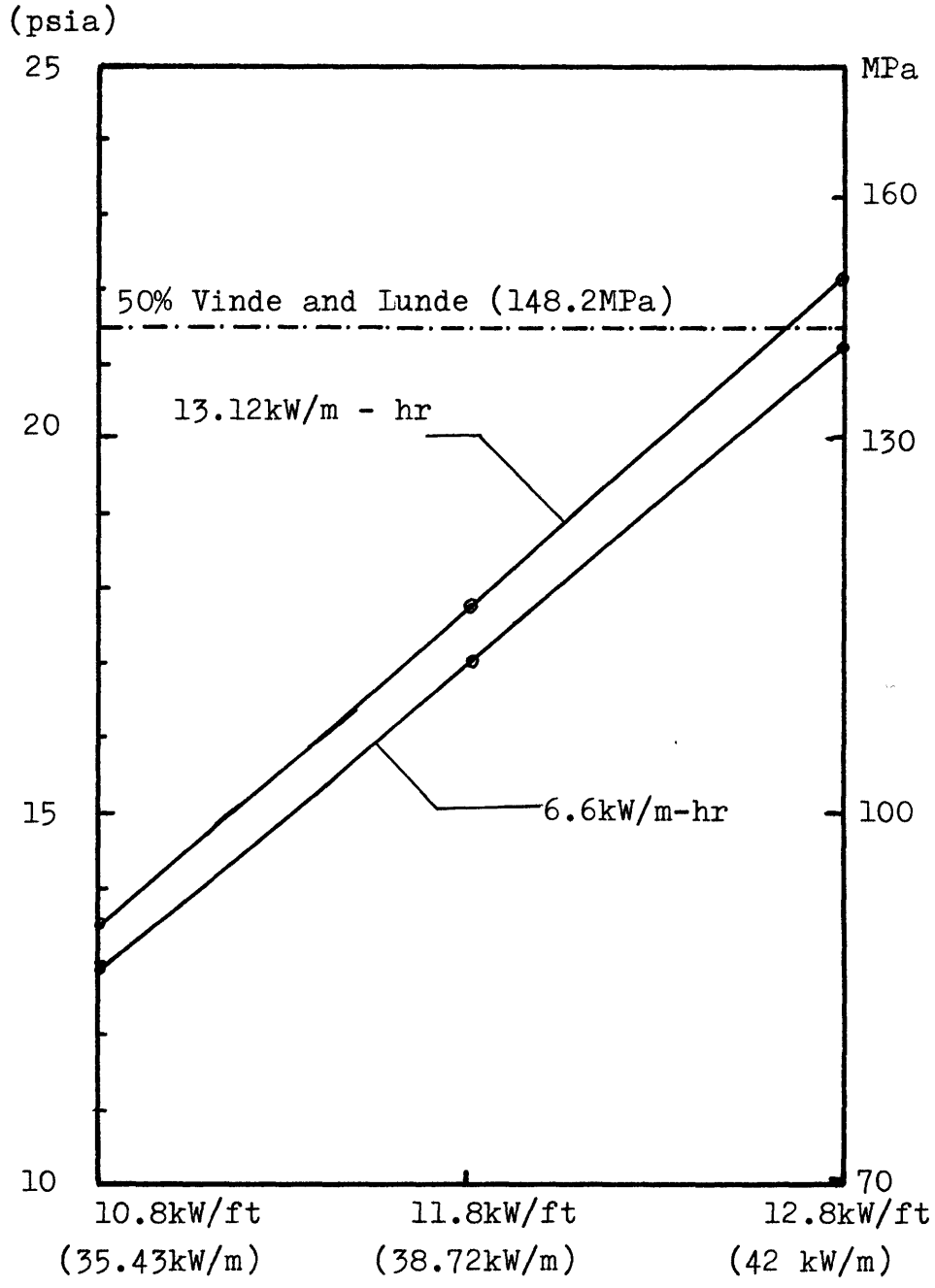

Fig. A1.2 - Stress X IHGR for Different Power Ramp Rates Starting at 19kW/m

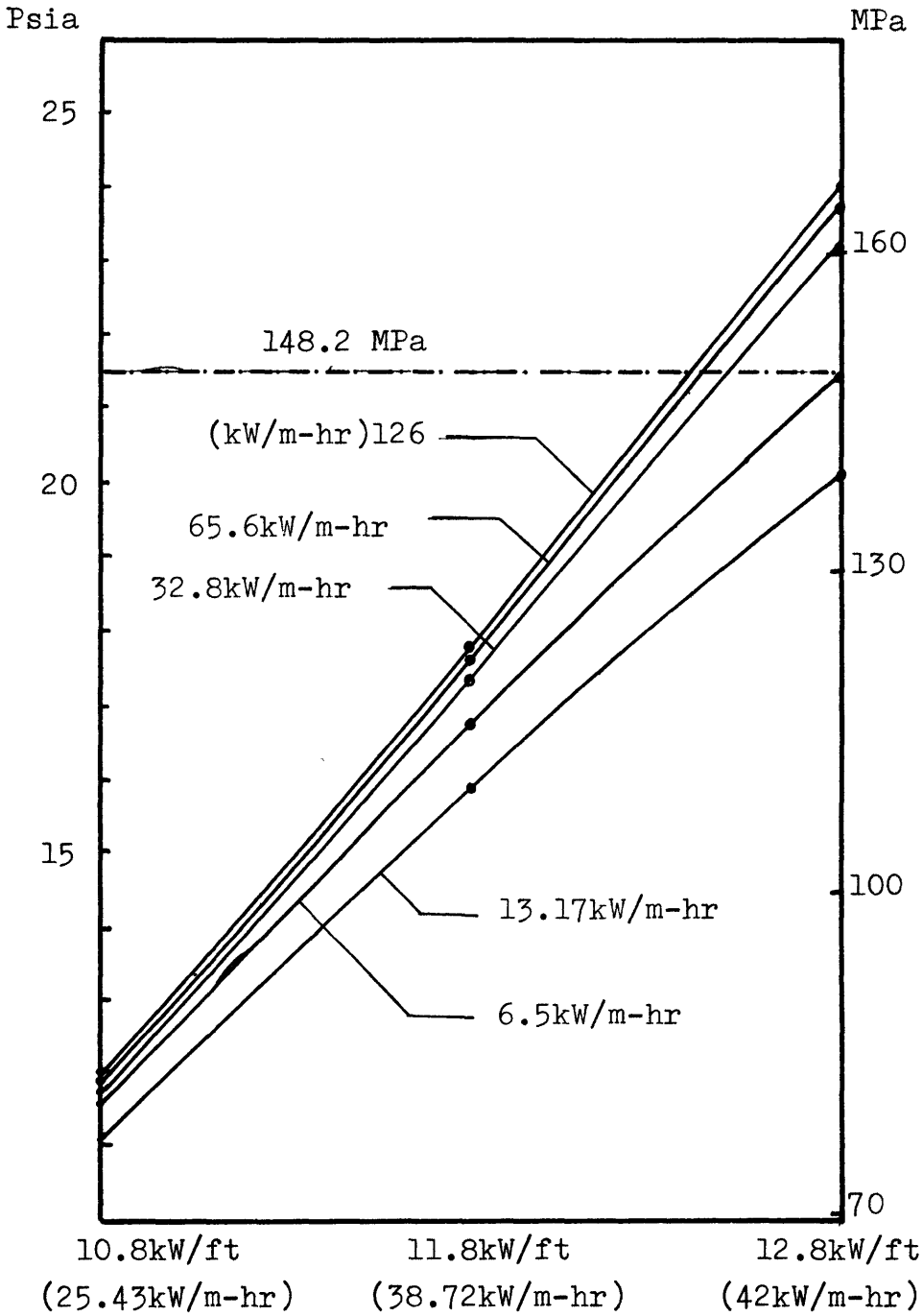

Fig. A1.3 - Stress X LHGR for Different Power Ramp Rates Starting at 22.31 kW/m

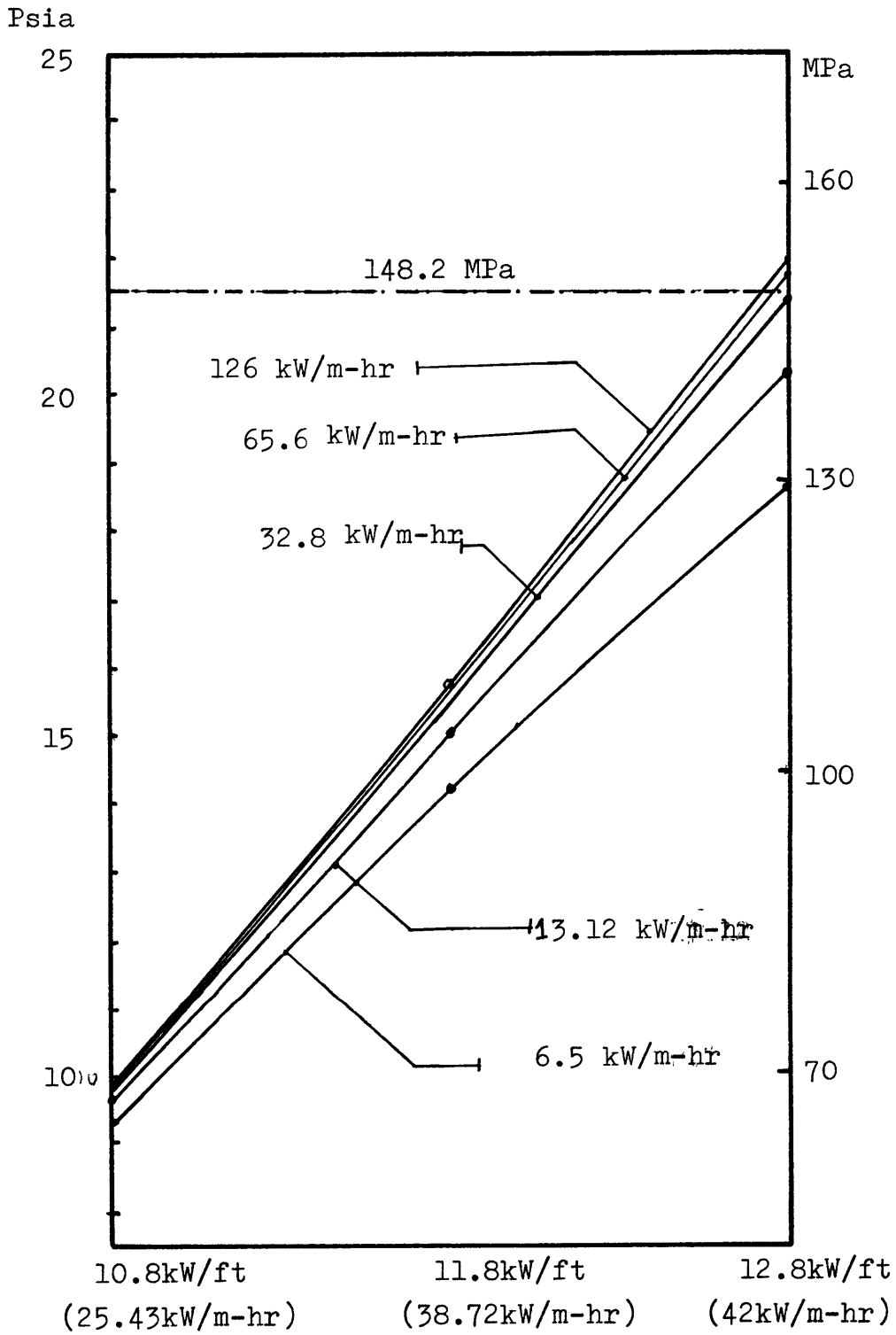

Fig. A1.4 - STRESS X LHGR FOR DIFFERENT POWER RAMP RATES STARTING AT 25.6 kW/m

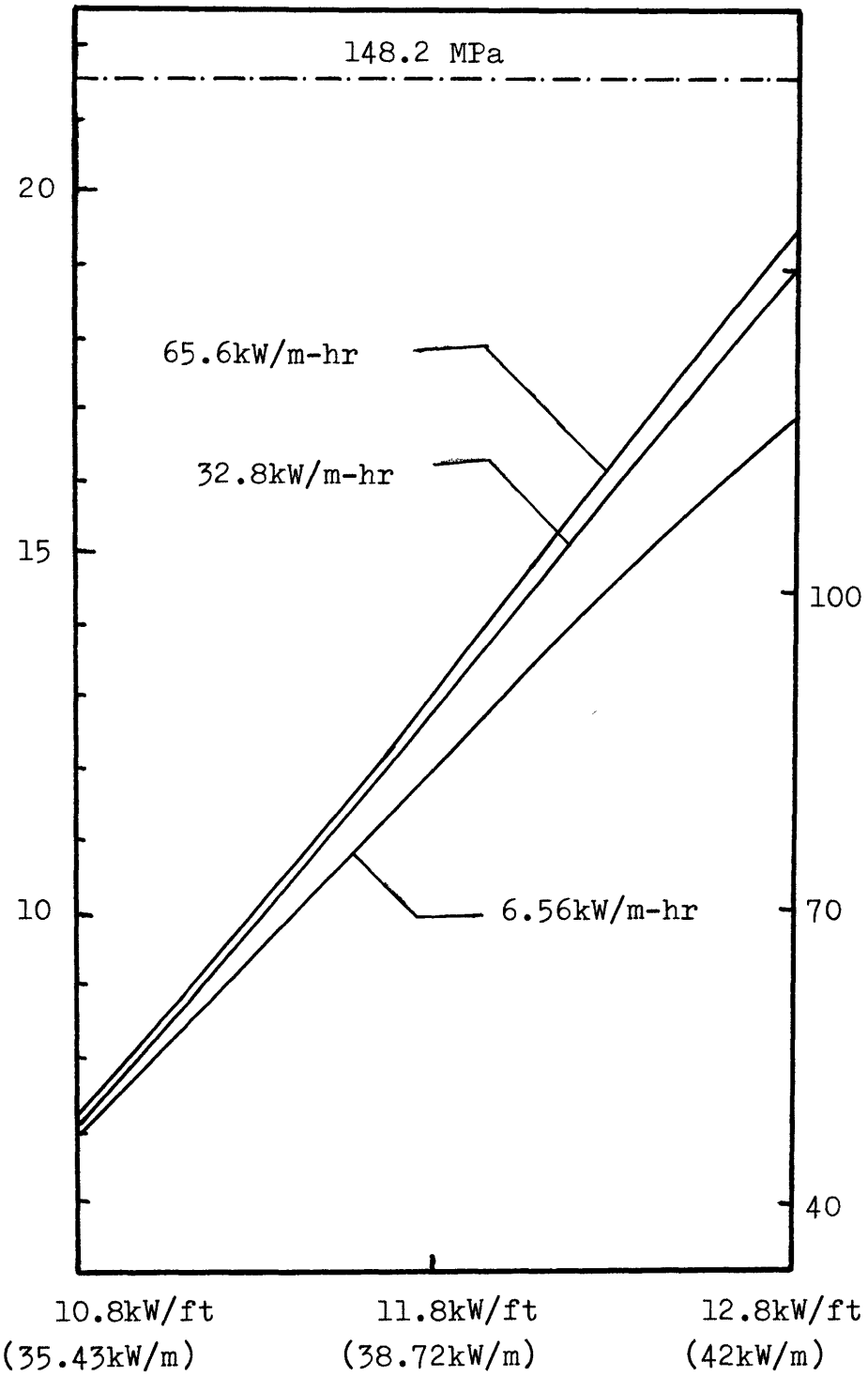

Fig. A1.5 - Stress X IHGR for Different Power

stress x power curve (Figs. A1.2, A1.3, A1.4, A1.5). Applying the failure criteria explained in section 5.6 the allowable ramp rates are selected.

A1.4 - DEFINITION OF EQUIVALENT FULL POWER DAYS

$$\text{Equivalent full power days} = \int_0^t \frac{\bar{q}\ dt}{24 \times 17.94}$$

Where: t = time in hours

17.94 = average LHGR at 100% power (5.47 kW/ft)

$\bar{q} = \frac{\text{Reactor Power}}{n.L}$

n = number of fuel rods

L = active length of the fuel rod

A1.5 - STRESS DECAY COEFFICIENT CURVE

This curve is derived maintaining the fuel at constant power after a ramp rate (with enhancement creep) and plotting the stress relaxation (as in Fig. 5.7).

APPENDIX 2

CODE CALIBRATION PROCEDURE

A2.1 - BUCKLE CODE CALIBRATION

The BUCKIE uses the Watkins and Wood creep correlation:

$$\dot{e}_c = \left[1 + AK \exp(-Kt)\right] BF^{0.85} \exp(-Q/RT) \sinh(Cs)$$

Where: A, K, B, C = constants

t = time of operation (hrs)

s = stress

$\dot{e}_c$ = creep strain rate

F = fast neutron flux

R = Universal gas constant

Q = ativation energy

T = Temperature (^{o}K)

The code was changed to MULTICS (Honeywell) system. Applying different multipliers to the constants A, K, B, C and testing the sensibility for alterations in the different multipliers it was concluded that small alterations in the constant C would lead to large variations in the results. It was decided to actuate in the C multiplier in order to calibrate it(according the criteria explained in section 5.3). With the value 1.1 in such multiplier, the code was considered calibrated.

A2.2 - LIFE 1 -LWR CALIBRATION

Most of the datails of the calibration are explained in Appendix C with comment cards previously to the modification.

GAS RELEASE MODEL (Gasout subroutine)

The LIFE 1 - IWR uses the original gas release model of LIFE 1, that specifies fractional gas release rates for each of the three fuel zones. The fractional gas release rates are proper for fast reactor, and when applied to LWR results in excessive gas release. The use of multipliers to adjust the release rates lead to results comparable to data presented in Fig. 5.2 (Ref 4).

SWELLING MODEL (Swell subroutine)

LIFE code assumes the gaseous fission products in the undisturbed region to be essentially incompressible, and therefore, they contribute to swelling in that region in a manner similar to solid fission products. It was used a multiplier (SACAN 3) to adjust to this kind of swelling.

In the equiaxed and columnar zones (artificially used to permit the utilization of this code) it was used very small radius 0.001, and 0.002 even though it was decided to adjust the swelling model of those zones, that is:

$$\left(\frac{\Delta V}{V}\right) = \frac{nRT}{V(P_I + P_i')}$$

altered to: $\left(\frac{\Delta V}{V}\right) = \left(\frac{nRT}{VP}\right)$ SACAN 2

Where: SACAN 2 adjuster multiplier

ΔV_i = change in volume of the ith region,

V_i = original volume of the ith region,

n_i = number of gas moles remaining in the region

$\bar{T}_i$ = average temperature of the gas, assumed equal to the average temperature of the region,

$P_i = \frac{1}{3}(\sigma_r^i + \sigma_\theta^i + \sigma_z^i)$, i.e., one-third the sum of the average stresses in the ith region,

P_i' = a constant similar to the usual surface-tension coreection term, only applying here to the entire ith region rather than to a single bubble,

R = unirvesal gas constant.

The solid swelling was also adjusted by the multiplier SACAN 1.

The adjustment was performed comparing with Fig. 5.1 (Ref 4).

```
C***  LIFE CODE, LIFE-1LWR VERSION
C *** NN = NUMBER OF AXIAL SECTIONS
C *** EPR,EPC,EPZ ARE THE TOTAL STRAINS AT T+DELT BASED ON DIMENSIONS
C *** AT TIME T
C *** TPR, TPC,TPZ ARE THE TOTAL PLASTIC STRAINS AT TIME T
C *** DPR,DPC,DPZ ARE THE INCREMENTAL PLASTIC STRAINS DURING DEL T
C *** TSR,TSC,TSZ ARE THE TOTAL SWELLING STRAINS AT TIME T
C *** DSR,DSC,DSZ ARE THE INCREMENTAL SWELLING STRAINS DURING TIME DELT
C *** SIGR,SIGC,SIGZ ARE THE STRESS COMPONENTS
C *** RVB IS THE RADIUS OF THE CENTRAL VOID
C *** R1B IS THE OUTSIDE RADIUS OF THE COLUMNAR GRAIN REGION
C *** REB IS THE OUTSIDE RADIUS OF THE EQUIAXED GRAIN REGION
C *** RUB IS THE OUTSIDE RADIUS OF THE UNDISTURBED REGION
C *** RCA IS THE INSIDE RADIUS OF THE CLAD
C *** R4B IS THE OUTSIDE RADIUS OF THE CLAD
C *** NN = TOTAL SECTIONS  NN-1 ARE FUEL , PLUS 1 PLENUM SECTION
      REAL*8 RFO,DUB,DUBO,DHO,RH,RHH,RHOP,XM6,XMM6,XM,DP,CX2,CX3,C,
     1ROT,ROO,RIT,RIO,XARG
      DIMENSION TMPA(5),PRSA(5),SPHT(5,5),WCON(5,5),WVIS(5,5),WVOL(5,5)
      DIMENSION RHOP(10,3),XM(3)
      COMMON/A1/NI,NN,ITERNO,NT,NOK,IPOCAS
      COMMON/A2/AFNA,FL,CL,PTOP,PO,FKA1,FKB1,FKC1,FKA2,FKB2,FKC2,FA11,
     *FA12,FA21,FA22,FA31,FA32,CK1,CK2,CA1,CA2,GASI,TIT,PRG,DP,TV1,
     *TOGAS,SMEP,DSMX1,TIT1,TVZJ1,TVZJ2,FLO,CLO,POWA1,PPOW,PTOUT,
     *PTIN,CIM,DELTO,SF,SC,SSF,SSC,Z
      COMMON/A3/ EPR(10,4),EPC(10,4),EPZ(10,4),DPR(10,4),DPC(10,4),
     1DPZ(10,4),TPR(10,4),TPC(10,4),TPZ(10,4),DSR(10,4),DSC(10,4),
     2DSZ(10,4),TSR(10,4),TSC(10,4),TSZ(10,4),UDISP(10,6),WDISP(10,4),
     3SIGR(10,4),SIGC(10,4),SIGZ(10,4),RVB(10),R1B(10),REB(10),RUB(10),
     4RCA(10),R4B(10),RHO(3),      TIME(1500),SS(10,4),QSF(10),
     5POW(10),TCLO(10),R(10,7),T(10,7),TBC(10),ATBC(10),A(7),ALF0(3),
     6ALF1(3),CM1(2),DHR(2),DXM(3),TRLR(4),RLR(4),TB(3),ATB(3),TL(15),
     7RL(15),XML(3),DXM6(10,3),RLR6(10,4),TLR6(10,4),TBF6(10,3),ATBF6(10
     8,3),TL6(10,15),RL6(10,15),GAS(10),EQEP(4),EQSIG(4),SIGMA(4),
     9ARTI(4),G(4),GNU(4),EQSI2(4),DEPR(10,4),DEPC(10,4),DEPZ(10,4),
     AXM6(10,3),TBM(3),ATBM(3),TLR(4),F(14),SIG(4),RH(10,3),FD(10,3),
```

```
     BDER(10,4),DEC(10,4),DEZ(10,4),SWS(10,3),GS(10,3),W(3),
     CEPRO(10,4),EPCO(10,4),EPZO(10,4),FA(3),R4BI(10),SWS6(10,3),
     DXPC(10,4),DDS(4),      XMM6(10,3),RHH(10,3),DERO(10,4),DECO(10,4)
      COMMON/A4/
     EDEZO(10,4),DMAX(3),                  GSO(10,3),CM(2),SIGRO(10,4),
     FSIGCO(10,4),SIGZO(10,4),RUBO(10),RCAO(10),R4BO(10),
     GPRS(10,4),PRSO(10,4),BM(4),EB(3),EBO(10,4),DEB(10,4),HG1(10),
     HFM(10),FMM(10),DUB(10),DHO(3),DUBO(10),CPRS(4),PRT(10),PPRG(10),
     IDXX(3),HC1(10),TNA(10),TCPO(10),TCPI(10),FLNC(10),FLNCO(10),
     JGDT(15),XPR12(10),XPR23(10),
     KXPRG(10),IIRW(10),F7(10,14),EBG(10,3),EHP(10,3),EHP6(10,3)
      COMMON/A5/TITLES(20)
      COMMON/A6/RHOZON(3),PNTDLT(10)
      COMMON PI,N3
      COMMON/GRAPH/IGRAPH,KONVER
      COMMON/SACC/SAC1,SAC2,SACAN1,SACAN2,SACAN3,SAC3
      CALL READ2 (TMPA,PRSA,SPHT,WCON,WVIS,WVOL)
      READ (5,1000) ISCASE
C **  BEGIN THE CALCULATION FOR EACH SEPARATE CASE
  5   CONTINUE
      READ (5,2000) TITLES
      WRITE(6,3000) TITLES
C
C
C      ADDED INPUT DATA ARE IN SUBROUTINE DTANEW
C
      CALL       DTANEW(ISEIKO,IPCAR,KONOP,LIMIT,SLIMIT,TLIMIT,TAUCRE,
     * SAC1,SAC2,SACAN1,SACAN2,SACAN3,QGLHO1,QGLHO2,QGLHO3,QGLHO4,SAC3)
C
C
      ITOCA=1
      ISTRSS=1
      ITLIMT=1
      READ(5,10) NI,NN,ITERNO,NT,NOK
      N3 = NT+1
C***  NT IS NOT LARGER THAN 14
```

```
      CALL READ1(EPR,EPC,EPZ,DPR,DPC,DPZ,TPR,TPC,TPZ,
     1DSR,DSC,DSZ,TSR,TSC,TSZ,SIGR,SIGC,SIGZ,WDISP,UDISP,RVB,R1B,
     2REB,RUB,RCA,R4B,NN,AFNA)
      READ(5,20)  FL,CL,PTOP,PO,FKA1,FKB1,FKC1,FKA2,FKB2,FKC2,FA11,FA12,
     1FA21,FA22,FA31,FA32,CK1,CK2,CA1,CA2
      READ(5,20) (RHO(I),I=1,3),RHOC
      READ(5,20) (RHOZON(I),I=1,3)
      READ (5,20)  (QSF(N),N=1,NN)
      READ (5,20)  (CM1(L),L=1,2),(DHR(L),L=1,2)
      READ (5,20) GASI
      READ(5,20) (F(J),J=1,NT)
C
C
C      REINITIALIZATION OPTION
C
C
      IF(LIMIT)20000,20001,20000
20000 READ(5,10)IGRAPH,KONVER,IDELTP,JST,KNS
      READ(5,20)TIME(1),PRG,QSFF,PI,DP
      QSF(NN)=QSFF
      READ(5,20)C,TV1,TOGAS,SMEP,DSMX1
      READ(5,20)TIT1,TVZJ1,TVZJ2
      CALL BEGINR(NN,XM6,RHO,C,R1B,RVB,REB,RUB,RH,RHOP,
     1SWS,GS,PRS,DEB,EBO,DER,DEC,DEZ,EPRO,EPCO,EPZO,DELTO,DUBO,RCAO,
     2R4BO,R4BI,R4B,RCA,FLO,FL,CLO,CL,JKL,MNO,POWA1,PPOW,PPRG,PTOUT,
     3PTIN,FM,DERO,DECO,DEZO,I,J,K,L,M,N,IT,CIM,IM,SF,SC,SSF,SSC,ALFO,
     4ALF1,FA11,FA12,FA21,FA22,FA31,FA32,DUB,FLNCO,NT,SIGRO,
     5SIGCO,SIGZO,EHP,PRSO,EHP6,SWS6)
      CALL RITE2       (NN,NI,ITERNO,NT,NOK,RVB,R1B,REB,RUB,RCA,R4B,
     1FL,CL,PTOP,PO,FKA1,FKB1,FKC1,FKA2,FKB2,FKC2,FA11,FA12,FA21,FA22,
     2FA31,FA32,CK1,CK2,CA1,CA2,CM1,DHR,RHO,RHOC,F,QSF,TOGAS,AFNA)
      READ(5,1000) IPOCAS
      GO TO 500
20001 CONTINUE
      IGRAPH = 0
      KONVER = 0
```

```
      TIME(1) =0.
      PRG = 0.
      QSF(NN) = 0.
      PI = 3.1415927
      DP = PI
      C = DP*2.54*2.54
      TV1 = 1.0                                                    8/14
      TOGAS = GASI
      IDELTP = 0
      CALL BEGIN(NN,XM6,RHO,C,R1B,RVB,REB,RUB,RH,RHOP,
     1SWS,GS,PRS,DEB,EBO,DER,DEC,DEZ,EPRO,EPCO,EPZO,DELTO,DUBO,RCAO,
     2R4BO,R4BI,R4B,RCA,FLO,FL,CLO,CL,JKL,MNO,POWA1,PPOW,PPRG,PTOUT,
     3PTIN,FM,DERO,DECO,DEZO,I,J,K,L,M,N,IT,CIM,IM,SF,SC,SSF,SSC,ALFO,
     4ALF1,FA11,FA12,FA21,FA22,FA31,FA32,DUB,FLNCO,NT,SIGRO,
     5SIGCO,SIGZO,EHP,PRSO,EHP6,SWS6)
      CALL RITE2       (NN,NI,ITERNO,NT,NOK,RVB,R1B,REB,RUB,RCA,R4B,
     1FL,CL,PTCP,PO,FKA1,FKB1,FKC1,FKA2,FKB2,FKC2,FA11,FA12,FA21,FA22,
     2FA31,FA32,CK1,CK2,CA1,CA2,CM1,DHR,RHO,RHOC,F,QSF,TOGAS,AFNA)
      SMEP = 1.E-06
      DSMX1 = 10.
      TIT1 = -2.
      TVZJ1 = TLEFT(1.)/100.
      TVZJ2 = TVZJ1
      JST = 0
      KNS = -1
      READ (5,1000) IPOCAS
  500 IF(JKL-1)83,83,82
   82 TIME(IT) = TIME(IT+1)
      TIME(IT+1) = TIME1
      TOUT = TOUT1
      TIN = TIN1
      POWAV = POWA1
      JKL = 1
      GO TO 74
   83 IT = IT+1
C***  TLEFT IS A LOCAL ANL FUNCTION
```

```
      IPOCAS = IPOCAS -1
      IF(IPOCAS.LT.0) GO TO 1003
      READ (5,80) TIME(IT+1),POWAV,TIN,TOUT
C
C
C      TINCRE IS THE UPPER BOUND VALUE FOR DELT IN SUBROUTINE TIMETR
C      OPTION USED IF ISEIKO=1 AND TIME(I+1).GE.TAUCRE
C
C
      TANG=ABS((POWAV-POWA1)/(TIME(I+1)-TIME(I)))
      RAZAO=0.5*TANG
      IF(RAZAO.LT.0.2) RAZAO=0.2
      TINCRE=0.02/RAZAO
      IF(TINCRE.LT.0.01) TINCRE=0.01
      KONVRG = 1
      KUTSTP = 0
      NEWTIM = 1
      JCRR = 0
   25 TCON = (TOUT-TIN)/POWAV
   27 IF(TIME(IT+1)-TIME(IT)-.001) 565,566,566
  565 TIME(IT+1) = TIME(IT) + 0.001
      JCRR = 1
  566 IF(POWAV-.001 ) 567,568,568
  567 POWAV = 0.001
      JCRR = 1
  568 IF(TOUT-TIN-2.) 569,14,14
  569 TOUT = TIN+2.
      JCRR = 1
   14 TIME1 = TIME(IT+1)
      TOUT1 = TOUT
      TIN1 = TIN
      JKLM = 1
      NDTIME = 10
      IF(POWAV-POWA1) 71,72,73
   71 JKLM = 2
      NDTIME = 3
```

```
      GO TO 73
   72 JKLM = 3
      NDTIME = 5
   73 POWA1 = POWAV
      NDTIM1 = NDTIME
   74 DELT = TIME(IT+1)-TIME(IT)
      JINX = 0
      ICV = 1
      SUMDS1 = 0.
      SDEP2 = 0.
      CALL TIMITR (DELT,DELTO,TIME(IT),TIME(IT+1),POWAV,PPOW,TOUT,PTOUT,
     1 TIN,PTIN,JKI,JKLM,KUTSTP,KONVRG,NEWTIM,NDTIME,NDTIM1,
     2TINCRE,ISEIKO,TAUCRE)
   84 JPLEN = 1
      IDELTP = IDELTP + 1
      PNTDLT(IDELTP) = DELT
      IF (IDELTP.NE.10 .AND. JKL.NE.1)  GO TO 5000
      WRITE(6,4000) (PNTDLT(J),J=1,IDELTP)
 4000 FORMAT (1X,10(1PE10.3,1X))
      IDELTP = 0
 5000 JBM = 0
      SF = 0.
      SC = 0.
      DO  505  J=1,NN
      X = RCA(J)
      Y = R4B(J)
      IF(MNO-1) 44,44,45
   44 DUB(J) = DUBO(J)+UDISP(J,4)
      RCA(J) = RCA(J)+UDISP(J,5)
      R4B(J) = R4B(J)+UDISP(J,6)
      GO TO 46
   45 RUB(J) = DUB(J)
      RCA(J) = RCAO(J)
      R4B(J) = R4BO(J)
   46 RCAO(J) = X
      R4BO(J) = Y
```

```
      SF = SF+EPZ(J,1)
      SC = SC+EPZ(J,4)
  505 CONTINUE
      FL = FL*(1.+(SF-EPZ(NN,1))/(NN-1.))
      CL = FL*(1.+(SC-EPZ(NN,4))/(NN-1.))+(CL-FL)*(1.+EPZ(NN,4))        9/9
C***  PLASTIC AND SWELLING INCREMENTS FROM LAST TIME STEP NOW ADDED TO
C***  FUEL ELEMENT DIMENSIONS
      CT = DELT/DELTO
      DO 184  J = 1,NN
      DO 184  K = 1,4
      DER(J,K) = DER(J,K)*CT
      DEC(J,K) = DEC(J,K)*CT
      DEZ(J,K) = DEZ(J,K)*CT
      DEB(J,K) = (DER(J,K)+DEC(J,K)+DEZ(J,K))/3.
  184 CONTINUE
C *** CHECK ALL UNITS
      CALL GOLDN (POWAV,QSF,TOUT,TIN,NN,R4B,POW,TCLO,AFNA,FL,
     1HC1,TNA,TMPA,PRSA,SPHT,WCON,WVIS,WVOL,PO)
      DO 525  J=1,NN
      CALL CLTMP(J,POW,TCLO,R4B,RCA,CK1,CK2,CA1,CA2,R,T ,TBC,ATBC)
  525 CONTINUE
C *** MUST GO FROM CLAD TO FUEL WITH GAP H
      DO 535 I=1,NN
      TCI = T(I ,1)
      QFLO = POW(I)*284.6
C *** QFLO NOW IN BTU/IN/HR
      PRG = PPRG(I)
C *** NEXT CALCULATE HG, THE LO GAP CONDUCTANCE
      A3 = .08483/12.
      A4 = .00009111/12.
      XKO = A3+A4*TCI
      RO = RCA(I)
      RI = DUB(I)
      IF(RO-RI-.00001) 301,302,302
  301 RI = RO-.00001
  302 HG = (XKO+SQRT(XKO*XKO+A4*QFLO*ALOG(RO/RI)/PI))/(2.*RO*ALOG(RO/RI
```

```
     1))
      HG1(I) = HG
C *** HG NOW IN BTU/HR/IN/IN/DEGF
      TFO = TCI+QFLO/(HG*2.*PI*RO)
      IF(I-NN) 189,535,535
 189  WFO = POW(I)
      RFO = DUB(I)
      RHOT=10.96
      BT = 0.5
C *** SET RHOT AND BT IN FLTMP CALC
      IF(MNO-1) 47,47,175
 47   DO 471 K = 1,3
 471  RH(I,K) = RHOP(I,K)
      IF(MNO-1) 176,176,175
 175  DO 177 J = 1,3
      XM6(I,J) = XMM6(I,J)
 177  CONTINUE
 176  DP = 1.
      DO 531 J = 1,3
      XM(J) = XM6(I,J)/(DP+EPZ(I,J))
      IF(J-2) 461,462,463
 461  CX2 = (DP+(UDISP(I,2)-UDISP(I,1))/(R1B(I)-RVB(I)))*(DP+(UDISP(I,2)
     1+UDISP(I,1))/(R1B(I)+RVB(I)))
      GO TO 464
 462  CX2 = (DP+(UDISP(I,3)-UDISP(I,2))/(REB(I)-R1B(I)))*(DP+(UDISP(I,3)
     1+UDISP(I,2))/(REB(I)+R1B(I)))
      GO TO 464
 463  CX2 = (DP+(UDISP(I,4)-UDISP(I,3))/(RUB(I)-REB(I)))*(DP+(UDISP(I,4)
     1+UDISP(I,3))/(RUB(I)+REB(I)))
 464  CX3 = (DP+EPZ(I,J))*CX2
      IF(MNO-1) 48,48,49
 48   RH(I,J) = RH(I,J)/CX3
 49   DHO(J) = RH(I,J)
      RHO(J) = DHO(J)
      IF(MNO-1) 178,178,531
 178  XMM6(I,J) = XM6(I,J)
```

```
      RHH(I,J) = RH(I,J)*CX3
  531 CONTINUE
      N3 = NT+1
      LJ = 2
C***  N3 IS IN COMMON FOR MAIN AND FLTMP
      CALL FLTMP(WFO,TFO,RFO,RHOT,DHO,XM,ALF0,ALF1,NOK,BT,FKA1,FKB1,
     1FKC1,FKA2,FKB2,FKC2,CM1,DHR,F,NT,LJ,DXM,TLR,RLR,TBM,ATBM,TL,RL,FA
     2,I,GDT,JBM,RHOZON)
      CX2 = XM6(I,1)+XM6(I,2)+XM6(I,3)
      U = 1.+EPZ(I,3)
      H = CX2/U
      DO 180 K = 1,NT
  180 F7(I,K) = F(K)
      DO 533  J=1,3
      DXM6(I,J) = DXM(J)
      TBF6(I,J) = TBM(J)
      ATBF6(I,J) = ATBM(J)
      XM6(I,J) = XM6(I,J)+DXM6(I,J)*3600.*DELT
      FD(I,J) = FA(J)                                              7/25
  533 CONTINUE
      XM6(I,3) = CX2-XM6(I,1)-XM6(I,2)
      CX2 = CX2/40.                                                1/11
      CX3 = CX2/5.
      IF(XM6(I,3)-CX3) 499,506,506
  499 XM6(I,2) = XM6(I,2)+XM6(I,3)-CX3
      XM6(I,3) = CX3
  501 IF(XM6(I,2)-CX3) 502,506,506
  502 XM6(I,1) = XM6(I,1)+XM6(I,2)-CX3
      XM6(I,2) = CX3
  506 DXX(3) = XM6(I,3)-XMM6(I,3)
      DXX(1) = XM6(I,1)-XMM6(I,1)
      DXX(2) =DABS(XM6(I,2)-XMM6(I,2))
      IF(XM6(I,2)) 504,504,494
  494 IF(DXX(3)+CX2 ) 504,498,498                                  1/11
  361 IF(DXX(2)-0.1*XM6(I,2)) 503,504,504
  498 IF(DXX(1)-CX2) 361,361,504
```

```
 504  JBM = 1
 503  DO 516 K = 1,3
      EBG(I,K) = (EPR(I,K)+EPC(I,K)+EPZ(I,K))-3.*ATBF6(I,K)-SWS6(I,K)
 516  GSO(I,K) = GS(I,K)
      GST = GS(I,1)+GS(I,2)+GS(I,3)
      GS(I,3) = GS(I,3)*XM6(I,3)/XMM6(I,3)
      GS(I,1) = GS(I,1)+GS(I,2)*(XM6(I,1)-XMM6(I,1))/XMM6(I,2)
      GS(I,2) = GST-GS(I,1)-GS(I,3)
      RVB(I) = RLR(1)
      R1B(I) = RLR(2)                                                    7/25
      REB(I) = RLR(3)                                                    7/25
 190  DO 534 J = 1,4                                                     7/25
      RLR6(I,J) = RLR(J)
      TLR6(I,J) = TLR(J)
 534  CONTINUE
      DO 536 J = 1,N3                                                    7/25
      TL6(I,J) = TL(J)
      RL6(I,J) = RL(J)
 536  CONTINUE
  535 CONTINUE
      DO 515 J=1,NN
 509  SS(J,1) = (R1B(J)-RVB(J))*(R1B(J)+RVB(J))
      SS(J,2) = (REB(J)-R1B(J))*(REB(J)+R1B(J))
      SS(J,3) = (DUB(J)-REB(J))*(DUB(J)+REB(J))
      SS(J,4) = (R4B(J)-RCA(J))*(R4B(J)+RCA(J))
  515 CONTINUE
C     FUEL REGIONS = NN-1
      NF = NN-1
      GTO = TOGAS                                                        8/28
      CALL GASOUT(SS,NF,FL,DELT,GAS,TOGAS,GS,POW,FD,JPLEN,IT,EBG)
  537 CALL PLENP (NN,RLR6,TLR6,R,T,TOUT,FL,CL,TOGAS,PLPR)
      FL = FLO
      CL = CLO
      DO 538  J = 1,NN
      RUB(J) = DUBO(J)
      X = RCA(J)
```

```
      Y = R4B(J)
      RCA(J) = RCAC(J)
      R4B(J) = R4BO(J)
      RCAO(J) = X
      R4BO(J) = Y
      ROT = DUB(J)
      RO0 = DUBO(J)
      RIT = REB(J)
      DO 931  M = 1,3
      K = 4-M
      EX = (EPC(J,K)+EPR(J,K))/2.
      CX2=DP+EX
      CX3 = RO0*CX2
      XARG =              (RIT/2.)**2 +CX3*(CX3-ROT)
      IF(XARG.LE.0.) XARG=0.
      RI0 = (RIT/2.+DSQRT(XARG))/CX2
      RO0 = RI0
      IF(K-2) 101,102,103
  103 ROT = REB(J)
      REB(J) = RI0
      RIT = R1B(J)
      GO TO 931
  102 ROT = R1B(J)
      R1B(J) = RI0
      RIT = RVB(J)
      GO TO 931
  101 RVB(J) = RI0
  931 CONTINUE
      SS(J,1) = (R1B(J)-RVB(J))*(R1B(J)+RVB(J))
      SS(J,2) = (REB(J)-R1B(J))*(REB(J)+R1B(J))
      SS(J,3) = (RUB(J)-REB(J))*(RUB(J)+REB(J))
      SS(J,4) = (R4B(J)-RCA(J))*(R4B(J)+RCA(J))
  538 CONTINUE
      IM = 0
      SDPM = 0.
C *** CHOOSE AXIAL REGION FOR DEFORMATIONS
```

```
      DO 999 J=NI,NN
      RW = 1.                                                          9/19
      RW1 = 1.                                                         9/26
      CHKN = 1.                                                        9/26
      SDDP1 = 0.09                                                     9/24
      I1 = 0
      IRW = 0
      PR12 = 0.
      PR23 = 0.
      DO 440  K = 1,3
      ATB(K) = ATBF6(J,K)
      RHO(K) = RHH(J,K)
      IF (ISCASE.EQ.1)  RHO(K) = RH(J,K)
      TBM(K) = TBF6(J,K)
  440 CONTINUE
      TB1 = TBC(J)
      CALL XLAME (TB1,TBM,G,GNU,J,NN,RHO,RHOT)
      DO 441  K = 1,4
      BM(K) = G(K)*(2. + 2.*GNU(K))/(1. - 2.*GNU(K))
  441 CONTINUE
      SDDPM = 0.09
  539 DO 953 I=1,ITERNO
C *** ITERNO IS MAX. ITERATIONS ALLOWED
      IF (I1 .GT. 0)  GO TO 528
      TVZJ = TLEFT(1.)/100.
      DO 410 K = 1,4
      DDS(K) = 1.0E+06
  410 CONTINUE
      IX = 0
  528 CONTINUE
      I1 = I1 + 1
      IF (J .GE. NN)  GO TO 572
      DO 442  K = 1,3
      EB(K) = (EPR(J,K) + EPC(J,K) + EPZ(J,K))/3. - ATBF6(J,K)
      IF (I1 .EQ. 1)  EB(K) = EB(K) + DEB(J,K)
  442 CONTINUE
```

```
      CALL SWELL(SIGR,SIGC,SIGZ,J,TBF6,SS,POW,DELT,GS,FL,NF,TSR,TSC,
     1TSZ,SWS,SWS6,DSR,DSC,DSZ,FD,PRS,BM,EB,I1,PRSO,RHOT,RHO,EHP,
     2 EHP6,ATB)
C**** FLUX CALCULATED FOR THERMAL REACTOR
C**** FLUX IN N/CM**2-SEC
  572 TFLUX = (2.417E+12)*POW(J)
      IF (TFLUX .LE. 0.0)  TFLUX = (2.417E+12)*POW(J-1)
      FLUX = 0.148*TFLUX
C**** FLUX IS THE FAST NEUTRON FLUX
      IF (I1 .GT. 1)  GO TO 306
      FLNC(J) = FLNCO(J) + TFLUX*DELT*3600.
      DSR(J,4) = 0.0
      DSC(J,4) = 0.0
      DSZ(J,4) = 0.0
  306 K$ = 1
      IF (J .GE. NN)  K$ = 4
      DO 546  K = K$,4
      EB1 = (EPR(J,K) + EPC(J,K) + EPZ(J,K))/3.
      DPR6 = EPR(J,K) - TPR(J,K) - EB1
      DPC6 = EPC(J,K) - TPC(J,K) - EB1
      DPZ6 = EPZ(J,K) - TPZ(J,K) - EB1
      IF (I1 .GT. 1)  GO TO 186
      DEB1 = (DER(J,K) + DEC(J,K) + DEZ(J,K))/3.
      DPR6 = DPR6 + DER(J,K) - DEB1
      DPC6 = DPC6 + DEC(J,K) - DEB1
      DPZ6 = DPZ6 + DEZ(J,K) - DEB1
  186 CALL EQUIEP(DPR6,DPC6,DPZ6,EPSEQ)
      SIGR6 = SIGRO(J,K)
      SIGC6 = SIGCO(J,K)
      SIGZ6 = SIGZO(J,K)
      CALL EQUISI (SIGR6,SIGC6,SIGZ6,SIGEQ)
      EQSIG(K) = SIGEQ
      G6 = G(K)
      IF (K .EQ. 4)  GO TO 544
      TBF67 = TBF6(J,K)
      X     = ATBF6(J,K)
```

```
      ATB(K) = X                                                        7/16
      D = (100.)*RHO(K)/RHOT
      CALL CREEF(SIGEQ,EPSEQ,FLUX,TBF67,DELT,SIGNW,G6,FC,D)
      GO TO 545
  544 TBF67 = TBC(J)                                                    7/7
      X     = ATBC(J)                                                   7/14
      TAH=TIME(IT+1)
      CALL CREEC(SIGEQ,EPSEQ,FLUX,TBF67,DELT,SIGNW,G6,FC,TAH,KNS,
     1QGLHO1,QGLHO2,QGLHO3,QGLHO4,TAUCRE,ISEIKO)
  545 SIGMA(K) = SIGNW
      IF(SIGNW) 303,303,304
  303 JBM = -1
      KNG = K
  304 EQEP(K) = EPSEQ*FC
      ARTI(K)=   X   *SS(J,K)/2.                                        7/14
      DPR(J,K) = DPR6*FC
      DPC(J,K) = DPC6*FC
      DPZ(J,K) = DPZ6*FC
  546 CONTINUE
      DO 541 K=1,4                                                      7/8
      TPR(J,K) = TPR(J,K) + DPR(J,K)                                    7/8
      TSR(J,K) = TSR(J,K) + DSR(J,K)                                    7/8
      TPC(J,K) = TPC(J,K) + DPC(J,K)                                    7/8
      TSC(J,K) = TSC(J,K) + DSC(J,K)                                    7/8
      TPZ(J,K) = TPZ(J,K) + DPZ(J,K)                                    7/8
  541 TSZ(J,K) = TSZ(J,K) + DSZ(J,K)                                    7/8
      CALL       VZJRWW (J,NN,TPR,TPC,TPZ,TSR,TSC,TSZ,ATB,ATBC,RVB,R1B,
     1REB,RUB,RCA,R4B,ARTI,SS,FL,CL,RHO,RHOC,G,GNU,PLPR,PO,PTOP,PR12,
     2PR23,PRG,EPZC,EPZ,EPZM,EPZ4,FM,FMM,IRW,U41,U42)
      IF(J-NN) 480,481,481
C *** NCW COMPUTE DISPLACEMENTS ETC.
  480 CALL DISPL(TPR,TPC,TSR,TSC,TSZ,ATBC,ATBF6,RVB,R1B,REB,RUB,RCA,
     1R4B,G,GNU,J,PLPR,PR12,PR23,PRG ,PO,EPZM,EPZ4,U11,U12,U22,U32,     7/8
     2U41,U42,SS)
  481 CALL  STRAIN       (RVB,R1B,REB,RUB,RCA,R4B,U11,U12,U22,U32,U41,
     1U42,PLPR,PR12,PR23,PRG,PO,TPR,TPC,TPZ,TSR,TSC,TSZ,ATBC,ATBF6,
```

```
     2EPZM,EPZ4,G,GNU,ARTI,J,NN,EPC,EPR)
      IF (J-NN) 932,942,942
 932  UDISP(J,1) = U11
      UDISP(J,2) = U12
      UDISP(J,3) = U22
      UDISP(J,4) = U32
 942  UDISP(J,5) = U41
      UDISP(J,6) = U42
C *** NOW COMPUTE STRESSES
      CALL STRESS(FPR,EPC,EPZ,ATBF6,ATBC,TPR,TPC,TPZ,TSR,TSC,TSZ,G,GNU,
     1SIGR,SIGC,SIGZ,EQSI2,J,NN,CPRS)
C *** COMPARE EQUIVALENT STRESSES AND ITERATE
      CALL COMPO(EPR,EPC,EPZ,EQEP,J,DPR,DPC,DPZ,SIGMA,EQSI2,
     1DDS,DSMX1,NN,ID,RW,PRS,SDEP,G,GNU,IRW,SDEP1,CPRS,TPR,TPC,TPZ,
     2SUMDS,SMEP,SS,DELT)
      IF(JBM) 93,496,495
  93  ID = -1
C ***INCLUDE STARRED FORMAT CARDS WHEN AUXILIARY OUTPUT DESIRED *****
C *** WRITE(6,122) ***
C*122 FORMAT(1X,'SIGMA(',I1,') NEGATIVE,THEREFORE,')  ***
      GO TO 975
 495  ID = -1
C *** WRITE(6,121) ***
C*121 FORMAT(1X,'RADIAL ZONE MASSES CHANGE TOO MUCH, THEREFORE,') ***
      GO TO 975
 496  IF(ID) 420,945,955
 420  IF(SDEP-2.*SMEP) 986,986,975
 986  DSMX1 = (DSMX1+SUMDS)/2.
      SMEP = (SMEP+SDEP)/2.
      IF(SMEP-.00010) 975,975,908
 908  SMEP = .00010
      GO TO 975
 945  MNO = 1
      IF(I-ITERNO) 949,975,975
  975 CONTINUE
C *** WRITE(6,985) J,I,DSMX1,SMEP,SUMDS,SDEP ***
```

```
C*985 FORMAT(6X,'DIVERGENT IN AXIAL SECTION',I3,' AFTER',I3,
C ***1'  ITERATIONS'/15X,'GO TO DT/2'/6X,'DSMX1 =',E10.3,' SMEP =',
C ***2E10.3,/6X,'SUMDS =',E10.3,' SDEP=',E10.3) ***
      ICV = 0
  427 POWAV = PPOW + (POWAV-PPOW)/2.                                    9/21
      TOUT = PTOUT + (TOUT - PTOUT)/2.                                  9/22
      TIN = PTIN + (TIN - PTIN)/2.                                      9/22
      TIME(IT+1) = TIME(IT+1)-DELT/2.                                   9/21
      DELT = DELT/2.                                                    9/25
      JKL = 2
      JPLEN = 2
      MNO = 2
      KONVRG = 0
      KUTSTP = KUTSTP + 1
      IF(DSMX1-0.5) 964,949,949
  949 DO 198 K = 1,4                                                    7/25
      TPR(J,K) = TPR(J,K) - DPR(J,K)                                    7/8
      TSR(J,K) = TSR(J,K) - DSR(J,K)                                    7/8
      TPC(J,K) = TPC(J,K) - DPC(J,K)                                    7/8
      TSC(J,K) = TSC(J,K) - DSC(J,K)                                    7/8
      TPZ(J,K) = TPZ(J,K) - DPZ(J,K)                                    7/8
  198 TSZ(J,K) = TSZ(J,K) - DSZ(J,K)                                    7/8
      IF(MNO-1) 952,952,961
  961 DO 989 K = 1,4
      DER(J,K) = DERO(J,K)
      DEC(J,K) = DECO(J,K)
      DEZ(J,K) = DEZO(J,K)
      SIGR(J,K) = SIGRO(J,K)
      SIGC(J,K) = SIGCO(J,K)
      SIGZ(J,K) = SIGZO(J,K)
      PRS(J,K) = PRSO(J,K)
  989 CONTINUE
      DO 401 L = 1,NN
      DO 401 K=1,4
      EPR(L,K) = EPRO(L,K)
      EPC(L,K) = EPCO(L,K)
```

```
 401  EPZ(L,K) = EPZO(L,K)
      TOGAS = GTO                                                    8/28
      DO 990 K = 1,3                                                 8/28
      DO 990 L = 1,NF                                                120970
  990 GS(L,K) = GSO(L,K)
      J1 = J - 1
      IF ( J1 ) 84,84,31
   31 DO 32 L = 1,J1
      DO 32 K = 1,4
      TPR(L,K) = TPR(L,K) - DPR(L,K)
      TSR(L,K) = TSR(L,K) - DSR(L,K)
      TPC(L,K) = TPC(L,K) - DPC(L,K)
      TSC(L,K) = TSC(L,K) - DSC(L,K)
      TPZ(L,K) = TPZ(L,K) - DPZ(L,K)
   32 TSZ(L,K) = TSZ(L,K) - DSZ(L,K)
      GO TO 84
 952  PRS(J,1) = CPRS(1)
      PRS(J,4) = CPRS(4)
      IF(IX) 953,953,539
  953 CONTINUE
 955  CONTINUE
      CALL CONVG(J,I1,SDEP,PR12,PR23,PRG,IRW,IM,SDPM,SUMDS,
     1CPRS,PRS,SUMDS1,SDEP2,NN,SIGRO,SIGCO,SIGZO,SIGR,SIGC,SIGZ,DEB,EB,
     2EBO,ATBF6,PRSO,DER,DEC,DEZ,EPR,EPC,EPZ,EPRO,EPCO,EPZO,DERO,DECO,
     3DEZO,DELTO,DELT,TVZJ,PRT,MNO,CIM)
C ***INCLUDE STARRED FORMAT CARDS WHEN AUXILIARY OUTPUT DESIRED *****
C *** WRITE(6,987) J,I,SUMDS,SDEP ***
C *** WRITE(6,200) PR12,PR23,PRG ***
C*987 FORMAT(6X,'CONVERGED IN AXIAL SECTION',I3,' AFTER',I3,' ITERATIONS
C ***1'/6X,'SUMDS=',E10.3,' SDEP=',E10.3) ***
C*200 FORMAT('0','INTERFACE PRESSURES PR12,PR23,PFC NEXT',/2X,2E20.8)
      XPR12(J) = PR12
      XPR23(J) = PR23
      XPRG(J) = PRG
      IIRW(J) = IRW
      IF(SIGC(J,4).GE.SLIMIT) ISTRSS=0
```

```
C
C
C       STICK OR SLIP FUEL-CLAD CONTACT OPTION
C
C
      IF(IRW.NE.0) ITOCA=0
      IF(IRW.EQ.-1.AND.KONOP.NE.0) ITOCA=1
      KONVER=KCNVER+1
  999 CONTINUE
      TIT = TIME(IT+1)
      TVZJ = TLEFT(1.)/100.
C *** WRITE(6,708) KONVER,TIT,POWAV,TOUT,TIN,DELT,J,TVZJ
C*708 FORMAT('0','STEP NO.',I4,' TIME(HRS)',F10.3,' , POWAV(KW/FT)',
C ***1F10.3,' , TOUT(F)',F10.3,' , TIN(F)',F10.3/' DELT=',E11.5,
C ***2', AXIAL SECTION =',I2,' TLEFT =',F7.2,'SEC.')
      DTVZJ2 = TVZJ2-TVZJ
      TVZJ2 = IVZJ
C
C
C       FUEL-CLAD GAP CLOSURE STOP OPTION
C
C
      IF(ITOCA.EQ.0.AND.LIMIT.EQ.0) GO TO 490
C
C
C       STRESS LIMIT STOP OPTION
C
C
      IF(ISTRSS.EQ.0) GO TO 490
C
C
C       TIME LIMIT STOP OPTION
C
C
      IF(TLIMIT-TIT)11116,11116,11117
11116 ITLIMT=0
```

```
      GO TO 490
11117 CONTINUE
      IF(TVZJ-2.*DTVZJ2) 911,911,912
 911  JST = 1
      GO TO 490
 912  IF(JKL-1) 490,490,913
  913 IF (POWAV - PPOW) 497,909,497
  497 IF (TIT - TIT1 - 5.) 491,490,490
 909  IF(SDPM-.000001) 508,508,493
  508 IF (ISCASE.EQ.2)  GO TO 491
      IF (TIT-TIT1-500.) 491,490,490
  493 IF (ISCASE.EQ.2)  GO TO 491
      IF (TIT-TIT1-200.) 491,490,490
  490 CALL       RITE3(NN,R4B,POW,TCLO,R,T,TBC,ATBC,HG1,RUB,RHOT,RH,
     1XMM6,EPZC,N3,F,DXM6,TLR6,RLR6,TBF6,ATBF6,TL6,RL6,GS,TOGAS,PLPR,
     2IT,TIT,POWAV,TOUT,TIN,TVZJ,SIGR,SIGC,SIGZ,EPR,EPC,EPZ,UDISP,DPR,
     3DPC,DPZ,TPR,TPC,TPZ,DSR,DSC,DSZ,TSR,TSC,TSZ,FL,CL,SF,SC,RCA,
     4REB,RVB,R1B,R4BI,DELT,HC1,TNA,SWS6,FLNC,
     5F7,DSMX1,SMEP,XPR12,XPR23,XPRG,IIRW,IM,SDPM,EHP6,GASI,JCRR)
C
C
C      OPTION TO PRINT CARDS FOR PROGRAM REINITIALIZATION
C
C
      IF(ITLIMI.EQ.0) GO TO 11115
      IF(ITOCA)11113,11114,11113
11114 IF(LIMIT)11113,11115,11113
11115 IF(IPCAR.NE.0) GO TO 1003
C
C
C      SUBROUTINE RSTART PUNCHES CARDS FOR PROGRAM REINITIALIZATION
C
C
      CALL       RSTART(XM,RHOP)
      GO TO 1003
11113 IF(ISTRSS.EQ.0)GO TO 11115
```

```
      DTVZ = TVZJ1 - TVZJ
      TVZJ1 = TVZJ
  910 TIT1 = TIT
  491 DO 402  J = 1,NN
      FM(J) = FMM(J)                                                  10/26
      PPRG(J) = PRT(J)
      FLNCO(J) = FLNC(J)
      DO 187  K = 1,3
      EHP(J,K) = EHP6(J,K)
  187 SWS(J,K) = SWS6(J,K)
      DO 402  K = 1,4
      EBO(J,K) = (EPR(J,K)+EPC(J,K)+EPZ(J,K))/3.
      EPRO(J,K) = EPR(J,K)
      EPCO(J,K) = EPC(J,K)
  402 EPZO(J,K) = EPZ(J,K)
      PPOW = POWAV
      PTOUT = TOUT                                                    9/22
      PTIN = TIN                                                      9/22
      KNS =  1
      IF(JST) 500,500,403                                             4/1
  403 IF ( TVZJ  - 100.) 964,500,500                                  4/1
C *** GO TO NEXT TIME STEP
  964 WRITE(6,213) JINX,DSMX1,DTVZJ2
 1003 CONTINUE
      ISCASE = ISCASE - 1
      IF(ISCASE.NE.0) GO TO 5
      STOP
   10 FORMAT(8I10)
   20 FORMAT(5E15.8)
   80 FORMAT(4E15.8)
  213 FORMAT (' ',10X,'EXECUTION TERMINATED BECAUSE JINX =',I3,
     1' OR DSMX1 =',F8.4,' OR DTVZJ2 =', F5.2)
 1000 FORMAT(2I10)
 2000 FORMAT(20A4)
 3000 FORMAT('1',20A4)
      END
```

```
      SUBROUTINE RSTART(XM,RHOP)
      REAL*8 RFO,DUB,DUBO,DHO,RH,RHH,RHOP,XM6,XMM6,XM,DP,CX2,CX3,C,
     1ROT,RO0,RIT,RI0,XARG
      DIMENSION RHOP(10,3),XM(3)
      COMMON/A1/NI,NN,ITERNO,NT,NOK,IPOCAS
      COMMON/A2/AFNA,FL,CL,PTOP,PO,FKA1,FKB1,FKC1,FKA2,FKB2,FKC2,FA11,
     *FA12,FA21,FA22,FA31,FA32,CK1,CK2,CA1,CA2,GASI,TIT,PRG,DP,TV1,
     *TOGAS,SMEP,DSMX1,TIT1,TVZJ1,TVZJ2,FLO,CLO,POWA1,PPOW,PTOUT,
     *PTIN,CIM,DELTO,SF,SC,SSF,SSC,Z
      COMMON/A3/ EPR(10,4),EPC(10,4),EPZ(10,4),DPR(10,4),DPC(10,4),
     1DPZ(10,4),TPR(10,4),TPC(10,4),TPZ(10,4),DSR(10,4),DSC(10,4),
     2DSZ(10,4),TSR(10,4),TSC(10,4),TSZ(10,4),UDISP(10,6),WDISP(10,4),
     3SIGR(10,4),SIGC(10,4),SIGZ(10,4),RVB(10),R1B(10),REB(10),RUB(10),
     4RCA(10),R4B(10),RHO(3),      TIME(1500),SS(10,4),QSF(10),
     5POW(10),TCLO(10),R(10,7),T(10,7),TBC(10),ATBC(10),A(7),ALF0(3),
     6ALF1(3),CM1(2),DHR(2),DXM(3),TRLR(4),RLR(4),TB(3),ATB(3),TL(15),
     7RL(15),XML(3),DXM6(10,3),RLR6(10,4),TLR6(10,4),TBF6(10,3),ATBF6(10
     8,3),TL6(10,15),RL6(10,15),GAS(10),EQEP(4),EQSIG(4),SIGMA(4),
     9ARTI(4),G(4),GNU(4),EQSI2(4),DEPR(10,4),DEPC(10,4),DEPZ(10,4),
     AXM6(10,3),TBM(3),ATBM(3),TLR(4),F(14),SIG(4),RH(10,3),FD(10,3),
     BDER(10,4),DEC(10,4),DEZ(10,4),SWS(10,3),GS(10,3),W(3),
     CEPRO(10,4),EPCO(10,4),EPZO(10,4),FA(3),R4BI(10),SWS6(10,3),
     DXPC(10,4),DDS(4),      XMM6(10,3),RHH(10,3),DERO(10,4),DECO(10,4)
      COMMON/A4/
     EDEZO(10,4),DMAX(3),                    GSO(10,3),CM(2),SIGRO(10,4),
     FSIGCO(10,4),SIGZO(10,4),RUBO(10),RCAO(10),R4BO(10),
     GPRS(10,4),PRSO(10,4),BM(4),EB(3),EBO(10,4),DEB(10,4),HG1(10),
     HFM(10),FMM(10),DUB(10),DHO(3),DUBO(10),CPRS(4),PRT(10),PPRG(10),
     IDXX(3),HC1(10),TNA(10),TCPO(10),TCPI(10),FLNC(10),FLNCO(10),
     JGDT(15),XPR12(10),XPR23(10),
     KXPRG(10),IIRW(10),F7(10,14),EBG(10,3),EHP(10,3),EHP6(10,3)
      COMMON/A5/TITLES(20)
      COMMON/A6/RHOZON(3),PNTDLT(10)
      COMMON PI,N3
C
C
```

```
C       SUBROUTINE RSTART PUNCHES CARDS FOR PROGRAM REINITIALIZATION
C
C
      WRITE(7,2000) TITLES
      WRITE(7, 10)NI,NN,ITERNO,NT,NOK
      WRITE(7,20)((EPR(N,M),M=1,4),N=1,NN)
      WRITE(7,20)((EPC(N,M),M=1,4),N=1,NN)
      WRITE(7,20)((EPZ(N,M),M=1,4),N=1,NN)
      WRITE(7,20)((DPR(N,M),M=1,4),N=1,NN)
      WRITE(7,20)((DPC(N,M),M=1,4),N=1,NN)
      WRITE(7,20)((DPZ(N,M),M=1,4),N=1,NN)
      WRITE(7,20)((TPR(N,M),M=1,4),N=1,NN)
      WRITE(7,20)((TPC(N,M),M=1,4),N=1,NN)
      WRITE(7,20)((TPZ(N,M),M=1,4),N=1,NN)
      WRITE(7,20)((DSR(N,M),M=1,4),N=1,NN)
      WRITE(7,20)((DSC(N,M),M=1,4),N=1,NN)
      WRITE(7,20)((DSZ(N,M),M=1,4),N=1,NN)
      WRITE(7,20)((TSR(N,M),M=1,4),N=1,NN)
      WRITE(7,20)((TSC(N,M),M=1,4),N=1,NN)
      WRITE(7,20)((TSZ(N,M),M=1,4),N=1,NN)
      WRITE(7,20)(( SIGR(N,M),M=1,4),N=1,NN)
      WRITE(7,20)(( SIGC(N,M),M=1,4),N=1,NN)
      WRITE(7,20)(( SIGZ(N,M),M=1,4),N=1,NN)
      WRITE(7,20)((WDISP(N,M),M=1,4),N=1,NN)
      WRITE(7,20)((UDISP(N,M),M=1,6),N=1,NN)
      WRITE(7,20)  (RVB(N),N=1,NN)
      WRITE(7,20)  (R1B(N),N=1,NN)
      WRITE(7,20)  (REB(N),N=1,NN)
      WRITE(7,20)  (RUB(N),N=1,NN)
      WRITE(7,20)  (RCA(N),N=1,NN)
      WRITE(7,20)  (R4B(N),N=1,NN)
      WRITE(7,20)AFNA
      WRITE(7,20)  FL,CL,PTOP,PO,FKA1,FKB1,FKC1,FKA2,FKB2,FKC2,FA11,FA12,
     1FA21,FA22,FA31,FA32,CK1,CK2,CA1,CA2
      WRITE(7,20)(RHO(I),I=1,3),RHOC
      WRITE(7,20)(RHOZON(I),I=1,3)
```

```
WRITE(7,20)   (QSF(N),N=1,NN)
WRITE(7,20)   (CM1(L),L=1,2),(DHR(L),L=1,2)
WRITE(7,20)GASI
WRITE(7,20) (F(J),J=1,NT)
IGRAPH=0
KONVER=0
IDELTP=0
JST=0
KNS=-1
WRITE(7,10)IGRAPH,KONVER,IDELTP,JST,KNS
QSFF=QSF(NN)
WRITE(7,20)TIT,PRG,QSFF,PI,DP
WRITE(7,20)C,TV1,TOGAS,SMEP,DSMX1
WRITE(7,20)TIT1,TVZJ1,TVZJ2
WRITE(7,20) (DUB(N),N=1,NN)
WRITE(7,20) (XM6(N,1),N=1,NN)
WRITE(7,20) (XM6(N,2),N=1,NN)
WRITE(7,20) (XM6(N,3),N=1,NN)
WRITE(7,20) ((RH   (N,K),K=1,3),N=1,NN)
WRITE(7,20) ((RHOP(N,K),K=1,3),N=1,NN)
WRITE(7,20) ((SWS (N,K),K=1,3),N=1,NN)
WRITE(7,20) ((SWS6(N,K),K=1,3),N=1,NN)
WRITE(7,20) ((GS   (N,K),K=1,3),N=1,NN)
WRITE(7,20) ((PRS  (N,K),K=1,4),N=1,NN)
WRITE(7,20) ((PRSO(N,K),K=1,4),N=1,NN)
WRITE(7,20) ((DEB  (N,K),K=1,4),N=1,NN)
WRITE(7,20) ((EBO  (N,K),K=1,4),N=1,NN)
WRITE(7,20) ((DER  (N,K),K=1,4),N=1,NN)
WRITE(7,20) ((DEC  (N,K),K=1,4),N=1,NN)
WRITE(7,20) ((DEZ  (N,K),K=1,4),N=1,NN)
WRITE(7,20) ((SIGRO(N,K),K=1,4),N=1,NN)
WRITE(7,20) ((SIGCO(N,K),K=1,4),N=1,NN)
WRITE(7,20) ((SIGZO(N,K),K=1,4),N=1,NN)
WRITE(7,20) ((EHP  (N,K),K=1,4),N=1,NN)
WRITE(7,20) ((EPRO (N,K),K=1,4),N=1,NN)
WRITE(7,20) ((EPCO (N,K),K=1,4),N=1,NN)
```

```
      WRITE(7,20)((EPZO (N,K),K=1,4),N=1,NN)
      WRITE(7,20)(DUB(J),J=1,NN)
      WRITE(7,20)(DUBO (J),J=1,NN)
      WRITE(7,20)(FLNCO(J),J=1,NN)
      WRITE(7,20)(PPRG (J),J=1,NN)
      WRITE(7,20)(RCAO (J),J=1,NN)
      WRITE(7,20)(R4BO (J),J=1,NN)
      WRITE(7,20)(R4BI (J),J=1,NN)
      WRITE(7,20)(FM(I),I=1,NN)
      WRITE(7,20)((DERO(I,J),J=1,4),I=1,NN)
      WRITE(7,20)((DECO(I,J),J=1,4),I=1,NN)
      WRITE(7,20)((DEZO(I,J),J=1,4),I=1,NN)
      WRITE(7,20)FLO,CLO,POWA1,PPOW,PTOUT
      WRITE(7,20)PTIN,CIM,DELTO,SF,SC
      WRITE(7,20)SSF,SSC,Z,ALF0(1)
      WRITE(7,20)ALF1(1),ALF0(2),ALF1(2),ALF0(3),ALF1(3)
      EHP61=EHP6(NN,1)
      EHP62=EHP6(NN,2)
      EHP63=EHP6(NN,3)
      WRITE(7,20)EHP61,EHP62,EHP63
      I=1
      J=1
      K=1
      L=1
      M=1
      N=1
      WRITE(7,10)I,J,K,L,M,N
      JKL=1
      MNO=1
      IM=0
      IT=0
      WRITE(7,10)JKL,MNO,IM,IT
      WRITE(7,1000) IPOCAS
   10 FORMAT(8I10)
   20 FORMAT(5E15.8)
 1000 FORMAT(2I10)
```

```
 2000 FORMAT(20A4)
      RETURN
      END
      SUBROUTINE  CREEC(SIGOLD,EPSNEW,FLUX,TEMAV,DELT,SIGNEW,G6,FC,TAH,
     1KNS,QGLHO1,QGLHO2,CW,QGLHO4,TAUCRE,ISEIKO)
      IT=0
      SIGNEW=0.
C     TEMAV IS T IN F
C     TEMAV1 IS T IN K
C     TEMAV2 IS T IN C
      TEMAV1=(TEMAV+460.)*5./9.
      TEMAV2=(TEMAV-32.)*5./9.
C
C     OBTAIN PROPER T RELATION
      IF (TEMAV-450.) 59,60,60
   60 T=TEMAV
      T1=TEMAV1
      T2=TEMAV2
      GO TO 63
   59 T=450.
      T1=(450.-32.)*5./9.+273.15
      T2=T1-273.15
   63 CONTINUE
C
C     OBTAIN PROPER COLD WORK RELATION
      IF (CW-10.) 70,71,71
   70 CW1=.2
      GO TO 75
   71 IF (CW-45.) 72,72,73
   72 CW1=1.
      GO TO 75
   73 CW1=7./5.
   75 CONTINUE
C
C     SECONDARY CREEP FOR INTERMEDIATE STRESSES, NON-STRESS
C     DEPENDENT TERMS
```

```
      A1=2.5*6218.47
      A2=5.E+11
      A3=(4770.-1.906*T)*1000
      FM=0.597
      FN=1.827
      Q1=-17920.81
      R=1.987
      AA1=CW1*A1*(FLUX/A2)**FM*EXP(Q1/(R*T1))
C     PRIMARY CREEP FOR INTERMEDIATE STRESSES, NON-STRESS DEPENDENT TERM
      B1=4.581E-10*T2-8.221E-8
      B2=1.655E-3*T2-1.297
      B3=1.5E-2*T2
      B4=9.663E-5
      IF (TAH-10.) 50,51,51
   50 TIME=10.
      GO TO 52
   51 TIME=TAH
   52 BB1=B1*TIME**B2
C     CREEP FOR HIGH STRESSES, NON-STRESS DEPENDENT TERMS
C     OBTAIN PROPER COLD WORK RELATION
      IF (CW-10.) 80,81,81
C     ANNEALED CLAD PROPERTIES GIVEN FOR CLAD WITH APPRECIABLE
C     FAST FLUENCE
   80 C1=2.87E+4
      C2=6.70E-4
      Q2=-62000.
      E1=3.7276E-17
      E2=3.2894E-4
      GO TO 85
   81 IF (CW-45.) 82,82,83
   82 C1=190.
      C2=4.30E-4
      Q2=-43000.
      E1=3.7871E-16
      E2=2.7742E-4
      GO TO 85
```

```
   83 C1=6.1
      C2=2.80E-4
      Q2=-31000.
      E1=5.1795E-15
      E2=2.1929E-4
   85 CONTINUE
      CC1=C1*EXP(Q2/(R*T1))
      FCO = 0.
      IF(EPSNEW) 20,20,22
  20  FC = 1.
      EPSNEW = 1.E-30
      SIGNEW = EPSNEW*G6*3.
      GO TO 25
 22   IF(SIGOLD) 310,310,312
 310  SIGOLD = 100.
  312 SIG=SIGOLD
  399 SIGB=SIG*QGLHO4
      IF(TAUCRE.GT.TAH) SIGB=SIG
C
C     CALCULATE CREEP RATE AND D(CREEP RATE)/D(STRESS)*STRESS
C     STRESS DEPENDENT SECONDARY CREEP AT INTERMEDIATE STRESSES
      IF(AA1.LE.0.) AA1=0.
      IF(SIGB.LE.0.) SIGB=0.
      IF(A3.LE.0.) A3=0.
      AA2=ALOG(AA1)+FN*ALOG(SIGB)-FN*ALOG(A3)
      AA2=EXP(AA2)
      IF(TAH.GT.TAUCRE) AA2=AA2*QGLHO1
      AA21=AA2*FN
C     STRESS DEPENDENT PRIMARY CREEP AT INTERMEDIATE STRESSES
      BB2=BB1*EXP(B3+B4*SIGB)
      BB21=BB2*B4*SIGB
C     STRESS DEPENDENT CREEP AT HIGH STRESSES
      CC2=CC1*EXP(C2*SIGB)
      IF(TAH.GT.TAUCRE) CC2=CC2*QGLHO2
      CC21=CC2*C2*SIGB
C
```

```
C      DOMINANT CREEP
       IF (AA2-BB2) 53,53,54
   53  IF (BB2-CC2) 55,55,56
   55  FCN=CC2
       FC1=CC21
       GO TO 57
   56  FCN=BB2
       FC1=BB21
       GO TO 57
   54  IF (AA2-CC2) 55,55,58
   58  FCN=AA2
       FC1=AA21
   57  CONTINUE
C
C      OBTAIN PROPER T RELATION
       IF (TEMAV-450.) 61,62,62
   61  DD1=1.E-10
       DD2=0.
       EE1=E1*EXP(E2*SIGB)
       EE2=EE1*E2*SIGB
       IF (DD1-EE1.LT.0.) DD1=EE1
       IF (DD1-EE1.LT.0.) DD2=EE2
       IF(FCN.LE.0.) FCN=0.
       IF(DD1.LE.0.) DD1=0.
       FF1=ALOG(FCN)
       FF2=ALOG(DD1)
       FCN=EXP(FF2+TEMAV*(FF1-FF2)/450.)
       FC1=DD2+TEMAV*(FC1-DD2)/450.
   62  CONTINUE
C
C      CALCULATE CREEP RATE*D(TIME) AND D(CREEP RATE)/D(STRESS)*S*D(TIME)
       FCN=FCN*DELT
       FC1=FC1*DELT
C****  NOW DETERMINE IF CREEP STRAIN INCREMENT A GOOD ESTIMATE
       X7 = ABS(FCN-FCO)/FCN
       FCO = FCN
```

```
      X = SIG
      SIG=ABS(SIG*(EPSNEW-FCN+FC1)/(FC1+SIG/G6/3.))
      IF(IT-100) 2,2,1
    1 WRITE (6,10) IT,X,SIG,FCN,X7
   10 FORMAT('0',' ***NUMERICAL GUESS OF CREEP WAS NOT SATISFACTORY AFTE
     1R',I4,' EXTRAPOLATIONS',/2X,'PREVIOUS SIGMA =',E15.8,' LAST SIGMA
     2=',E15.8,/2X,'FINAL CREEP =',E15.8,' HAS AN ESTIMATED FRACTIONAL E
     3RROR =',E15.8/)
      GO TO 401
    2 IF(X7-.0001) 26,399,399
   26 X8 = ABS(SIG-X)
      IF(X8-.5) 401,399,399
  401 SIGNEW = SIG
   24 FC = FCN/EPSNEW
   25 CONTINUE
      IF(KNS) 27,29,29
   27 KNS=0
   29 RETURN
      END
      FUNCTION TLEFT(TIML)
C     ********************
C     ***** FUNCTION TLEFT(TIML) ADDED TO ACCOUNT FOR ANL FUNCTION ****
C     ********************
C ****
C ****  SYS5.FORTLIB.SUBR TIMING RETURNS CPU TIME IN 100TH SECONDS.
C ****
      CALL TIMING(JLEF)
      TUSE = FLOAT(JLEF)
C ****
C ****  INITIAL TIME VALUE SET AT 400 SECONDS, THUS ALLOWING ONE TIME
C ****   STEP EXECUTION AFTER A 5 MINUTE CPU TIME LIMIT.
C ****
      TLEFT = TIML*40000. - TUSE
      IF (TLEFT .LT. 0.0)  TLEFT = 0.0
      RETURN
      END
```

```
      FUNCTION WPROP(TMP,PRS,TMPA,PRSA,PROP,JPMAX,KPMAX)
C     WPROP IS A LINEAR INTERPOLATION OF TABULATED WATER PROPERTIES
C     TMP -- INDEPENDENT TEMP VARIABLE
C     PRS -- INDEPENDENT PRESS. VARIABLE
C     TMPA -- DEPENDENT VARIABLE TEMP ARRAY
C     PRSA -- DEPENDENT VARIABLE PRESS. ARRAY
C     JPMAX -- NUMBER OF POINTS IN  PRESS. ARRAY
C     KPMAX -- NUMBER OF POINTS IN TEMP ARRAY
      DIMENSION TMPA(KPMAX),PRSA(JPMAX),PROP(JPMAX,KPMAX)
      JW=0
      KW=0
      JP=1
      KP=1
      IF (PRS.LT.PRSA(1)) GO TO 200
      DO 100 JW=1,JPMAX
      JP=JW
      IF (PRS-PRSA(JW)) 300,200,100
  100 CONTINUE
  200 CONTINUE
      IF (TMP.LT.TMPA(1)) GO TO 550
      DO 500 KW=1,KPMAX
      KP=KW
      IF (TMP-TMPA(KW)) 600,550,500
  500 CONTINUE
  550 WPROP=PROP(JP,KP)
      RETURN
  600 WPROP2=PROP(JP,KP)
      WPROP1=PROP(JP,KP-1)
      GO TO 900
  300 IF (TMP.LT.TMPA(1)) GO TO 700
      DO 650 KW=1,KPMAX
      KP=KW
      IF (TMP-TMPA(KW)) 800,700,650
  650 CONTINUE
  700 WPROP=PROP(JP-1,KP)+(PROP(JP,KP)-PROP(JP-1,KP))*
     1(PRS-PRSA(JP-1))/(PRSA(JP)-PRSA(JP-1))
```

```
      RETURN
  800 PRR=(PRS-PRSA(JP-1))/(PRSA(JP)-PRSA(JP-1))
      WPROP2=PROP(JP-1,KP)+(PROP(JP,KP)-PROP(JP-1,KP))*PRR
      WPROP1=PROP(JP-1,KP-1)+(PROP(JP,KP-1)-PROP(JP-1,KP-1))*PRR
  900 WPROP=WPROP1+(WPROP2-WPROP1)*(TMP-TMPA(KP-1))/
     1(TMPA(KP)-TMPA(KP-1))
      RETURN
      END
      SUBROUTINE DTANEW(ISEIKO,IPCAR,KONOP,LIMIT,SLIMIT,TLIMIT,TAUCRE,
     * SAC1,SAC2,SACAN1,SACAN2,SACAN3,QGLHO1,QGLHO2,QGLHO3,QGLHO4,SAC3)
C
C
C       INPUT DATA DESCRIPTION
C
C
C       ISEIKO IS A FLAG FOR TIME STEP SELECTION
C       ISEIKO=0  ...  NO UPPER BOUND SELECTION FOR DELT
C       ISEIKO=1  ...  TINCRE IS THE UPPER BOUND FOR DELT
C
C       IPCAR IS A OPTION TO PRINT CARDS FOR REINITIALIZATION
C       IPCAR=0  ...  REINITIALIZATION CARDS ARE PRINTED
C       IPCAR.NE.0  ...  REINITILIZATION CARDS ARE NOT PRINTED
C
C       KONOP IS A FUEL-CLAD CONTACT OPTION TO STOP THE CASE AT TLIMIT
C       KONOP=0  ...  SLIP CONTACT IS CONSIDERED
C       KONOP.NE.0  ...  STICK CONTACT IS CONSIDERED
C
C       LIMIT IS A REINITIALIZATION FLAG
C       LIMIT.NE.0  ...  REINITIALIZATION INPUT DATA MUST BE SUPPLIED
C
C       SLIMIT IS THE STRESS LIMIT FOR THIS RUN
C       SLIMIT USUALLY TAKEN AS 50 PERCENT OF VINDE AND LUND SCC THRESHOLD
C
C       TLIMIT IS THE TIME LIMIT FOR THIS RUN
C
C       TAUCRE IS THE TIME THAT CREEP ENHANCEMENT STARTS
```

```
C
CC      SAC1, SAC2 AND SAC3 ARE USED TO CALIBRATE THE GAS RELEASE MODEL
C
CC      SACAN1, SACAN2 AND SACAN3 ARE USED TO CALIBRATE THE SWELLING MODEL
C
CC      QGLHO1, QGLHO2, QGLHO3 AND QGLHO4 ARE USED FOR CREEP ENHANCEMENT
C
C
      READ(5,10) ISEIKO,IPCAR,KONOP,LIMIT
      READ(5,20)SLIMIT,TLIMIT,TAUCRE
      READ(5,20) SAC1,SAC2,SAC3
      READ(5,20)SACAN1,SACAN2,SACAN3
      READ(5,20)QGLHO1,QGLHO2,QGLHO3,QGLHO4
   10 FORMAT(8I10)
   20 FORMAT(5E15.8)
      RETURN
      END
      SUBROUTINE BEGINR(NN,XM6,RHO,C,R1B,RVB,REB,RUB,RH,RHOP,
     1SWS,GS,PRS,DEB,EBO,DER,DEC,DEZ,EPRO,EPCO,EPZO,DELTO,DUBO,RCAO,
     2R4BO,R4BI,R4B,RCA,FLO,FL,CLO,CL,JKL,MNO,POWA1,PPOW,PPRG,PTOUT,
     3PTIN,FM,DPRO,DPCO,DPZO,I,J,K,L,M,N,IT,CIM,IM,SF,SC,SSF,SSC,ALF0,
     4ALF1,FA11,FA12,FA21,FA22,FA31,FA32,DUB,FLNCO,NT,SIGRO,
     5SIGCO,SIGZO,EHP,PRSO,EHP6,SWS6)
      REAL*8 XM6,C,RH,RHOP,DUB,DUBO
      DIMENSION XM6(10,3),RHO(3),R1B(10),RVB(10),REB(10),
     1RUB(10),RH(10,3),RHOP(10,3),SWS(10,3),GS(10,3),PRS(10,4),
     2DEB(10,4),EBO(10,4),DER(10,4),DEC(10,4),DEZ(10,4),EPRO(10,4),
     3EPCO(10,4),EPZO(10,4),          DUBO(10),RCAO(10),R4BO(10),
     4R4BI(10),R4B(10),RCA(10),FM(10),DPRO(10,4),DPCO(10,4),DPZO(10,4),
     5ALF0(3),ALF1(3),DUB(10),PPRG(10),FLNCO(10),
     6SIGRO(10,4),SIGCO(10,4),SIGZO(10,4),EHP(10,3),PRSO(10,4),
     7EHP6(10,3),SWS6(10,3)
      READ(5,20) (DUB(N),N=1,NN)
      READ(5,20) (XM6(N,1),N=1,NN)
      READ(5,20) (XM6(N,2),N=1,NN)
      READ(5,20) (XM6(N,3),N=1,NN)
```

```
      READ(5,20) ((RH   (N,K),K=1,3),N=1,NN)
      READ(5,20) ((RHOP (N,K),K=1,3),N=1,NN)
      READ(5,20) ((SWS  (N,K),K=1,3),N=1,NN)
      READ(5,20) ((SWS6 (N,K),K=1,3),N=1,NN)
      READ(5,20) ((GS   (N,K),K=1,3),N=1,NN)
      READ(5,20) ((PRS  (N,K),K=1,4),N=1,NN)
      READ(5,20) ((PRSO (N,K),K=1,4),N=1,NN)
      READ(5,20) ((DEB  (N,K),K=1,4),N=1,NN)
      READ(5,20) ((EBO  (N,K),K=1,4),N=1,NN)
      READ(5,20) ((DER  (N,K),K=1,4),N=1,NN)
      READ(5,20) ((DEC  (N,K),K=1,4),N=1,NN)
      READ(5,20) ((DEZ  (N,K),K=1,4),N=1,NN)
      READ(5,20) ((SIGRO(N,K),K=1,4),N=1,NN)
      READ(5,20) ((SIGCO(N,K),K=1,4),N=1,NN)
      READ(5,20) ((SIGZO(N,K),K=1,4),N=1,NN)
      READ(5,20) ((EHP  (N,K),K=1,4),N=1,NN)
      READ(5,20) ((EPRO (N,K),K=1,4),N=1,NN)
      READ(5,20) ((EPCO (N,K),K=1,4),N=1,NN)
      READ(5,20) ((EPZO (N,K),K=1,4),N=1,NN)
      READ(5,20) (DUB(J),J=1,NN)
      READ(5,20) (DUBO (J),J=1,NN)
      READ(5,20) (FLNCO(J),J=1,NN)
      READ(5,20) (PPRG (J),J=1,NN)
      READ(5,20) (RCAO (J),J=1,NN)
      READ(5,20) (R4BO (J),J=1,NN)
      READ(5,20) (R4BI (J),J=1,NN)
      READ(5,20) (FM(I),I=1,NN)
      READ(5,20) ((DPRO(I,J),J=1,4),I=1,NN)
      READ(5,20) ((DPCO(I,J),J=1,4),I=1,NN)
      READ(5,20) ((DPZO(I,J),J=1,4),I=1,NN)
      READ(5,20) FLO,CLO,POWA1,PPOW,PTOUT
      READ(5,20) PTIN,CIM,DELTO,SF,SC
      READ(5,20) SSF,SSC,Z,ALF0(1)
      READ(5,20) ALF1(1),ALF0(2),ALF1(2),ALF0(3),ALF1(3)
      READ(5,20) EHP61,EHP62,EHP63
      EHP6(NN,1)=EHP61
```

```
      EHP6(NN,2)=EHP62
      EHP6(NN,3)=EHP63
      READ(5,10) I,J,K,L,M,N
      READ(5,10) JKL,MNO,IM,IT
   10 FORMAT(8I10)
   20 FORMAT(5E15.8)
      RETURN
      END
      SUBROUTINE BEGIN(NN,XM6,RHO,C,R1B,RVB,REB,RUB,RH,RHOP,
     1SWS,GS,PRS,DEB,EBO,DER,DEC,DEZ,EPRO,EPCO,EPZO,DELTO,DUBO,RCAO,
     2R4BO,R4BI,R4B,RCA,FLO,FL,CLO,CL,JKL,MNO,POWA1,PPOW,PPRG,PTOUT,
     3PTIN,FM,DPRO,DPCO,DPZO,I,J,K,L,M,N,IT,CIM,IM,SF,SC,SSF,SSC,ALF0,
     4ALF1,FA11,FA12,FA21,FA22,FA31,FA32,DUB,FLNCO,NT,SIGRO,
     5SIGCO,SIGZO,EHP,PRSO,EHP6,SWS6)
      REAL*8 XM6,C,RH,RHOP,DUB,DUBO
      DIMENSION XM6(10,3),RHO(3),R1B(10),RVB(10),REB(10),
     1RUB(10),RH(10,3),RHOP(10,3),SWS(10,3),GS(10,3),PRS(10,4),
     2DEB(10,4),EBO(10,4),DER(10,4),DEC(10,4),DEZ(10,4),EPRO(10,4),
     3EPCO(10,4),EPZO(10,4),          DUBO(10),RCAO(10),R4BO(10),
     4R4BI(10),R4B(10),RCA(10),FM(10),DPRO(10,4),DPCO(10,4),DPZO(10,4),
     5ALF0(3),ALF1(3),DUB(10),PPRG(10),FLNCO(10),
     6SIGRO(10,4),SIGCO(10,4),SIGZO(10,4),EHP(10,3),PRSO(10,4),
     7EHP6(10,3),SWS6(10,3)
      DO 186  N = 1,NN                                              7/25
      DUB(N) = RUB(N)
      XM6(N,1) = C*RHO(1)*(R1B(N)-RVB(N))*(R1B(N)+RVB(N))
      XM6(N,2) = C*RHO(2)*(REB(N)-R1B(N))*(REB(N)+R1B(N))
      XM6(N,3) = C*RHO(3)*(DUB(N)-REB(N))*(DUB(N)+REB(N))
      IF (N - NN) 310,311,311
  310 Z = FL/(NN-1)*(N -(NN/2.))*2.54
      GO TO 312
  311 Z =          (CL/2.)*2.54
  312 DO 185 K =1,3
      RH(N,K) = RHO(K)                                              7/25
      RHOP(N,K) = RHO(K)
      SWS(N,K) = 0.                                                 7/25
```

```
      SWS6(N,K) = 0.
185   GS(N,K) = 0.                                                  7/25
      DO 186 K = 1,4                                                7/25
      PRS(N,K) = 0.001
      PRSO(N,K) = 0.
      DEB(N,K) = 0.
      EBO(N,K) = 0.
      DER(N,K) = 0.                                                 7/25
      DEC(N,K) = 0.                                                 7/25
      DEZ(N,K) = 0.                                                 7/25
      SIGRO(N,K) = 0.
      SIGCO(N,K) = 0.
      SIGZO(N,K) = 0.
      EHP(N,K) = 0.
      EPRO(N,K) = 0.                                                7/25
      EPCO(N,K) = 0.                                                7/25
186   EPZO(N,K) = 0.                                                7/25
      DO 16 J=1,NN
      DUB(J) = RUB(J)
      DUBO(J) = DUB(J)
      FLNCO(J) = 0.
      PPRG(J) = 0.
      RCAO(J) = RCA(J)
      R4BO(J) = R4B(J)
16    R4BI(J)=R4B(J)
      FLO = FL
      CLO = CL
      JKL = 1
      MNO = 1
      POWA1 = 0.
      PPOW = 0.
      PTOUT = 68.
      PTIN = 68.
      DO 81 I=1,NN
      FM(I) = 0.4                                                   10/26
      DO 81 J = 1,4
```

```
      DPRO(I,J) = 0.
      DPCO(I,J) = 0.
      DPZO(I,J) = 0.
   81 CONTINUE
      DO 82  K = 1,3
   82 EHP6(NN,K) = 0.
      I = 1
      J =1
      K =1
      L =1
      M =1
      N =1
      IM = 0
      IT = 0
      CIM = 0.000001
      DELTO = 100000.
      SF = 0.                                                          7/25
      SC = 0.                                                          7/25
      SSF = 0.
      SSC = 0.
      ALF0(1) = FA11
      ALF1(1) = FA12
      ALF0(2) = FA21
      ALF1(2) = FA22
      ALF0(3) = FA31
      ALF1(3) = FA32
      RETURN
      END
      SUBROUTINE COMPO(EPR,EPC,EPZ,DELEP,JM,DPR,DPC,DPZ,SIGMA,          44
     1EQSGI,DDS,DSNX1,NN,ID,RW,PRS,SDEP,G,GNU,IRW,SDEP1,CPRS,TPR,TPC,
     2TPZ,SUMDS,DPNX,SS,DELT)
      DIMENSION EPR(10,4),EPC(10,4),EPZ(10,4),DELEP(4),DPR(10,4),
     1DPC(10,4),DPZ(10,4),EQSGI(4),SIGMA(4),DDS(4),
     2PRS(10,4),SD1(4),        G(4),GNU(4),CPRS(4),TPR(10,4),
     3TPC(10,4),TPZ(10,4),SS(10,4),W(4),EPR1(4),EPC1(4),EPZ1(4),EPR2(4),
     4 EPC2(4),EPZ2(4),XC(4,4),XCO(4,4),XCVO(4,4),EPR3(4),EPC3(4),
```

```
     5 EPZ3(4)
C***** BEING JANKUS' COMPOSITION #44, CONVEYING THE PLASTIC MESSAGE IN
C      ITS MOST ADVANCED FORM.  THE OBOE NOW CARRIES THE ELASTIC PART
C      AND THE PLASTIC MESSAGE OF THE BASOON IS TRANSMITTED IN ITS
C      UTMOST ELEGANCE AND PRECISION. *****
       COMMON PI,N3
       XL = 0.9E+06
       DSMX1 = 10.
       DPMX = 1.E-06
       IF(DDS(4)-XL) 17,17,15
   15  IT = 0
       SSS = SS(JM,1)+SS(JM,2)+SS(JM,3)+SS(JM,4)
       DO 16 K = 1,4
       W(K) = 4.*SS(JM,K)/SSS
       DO 16 L = 1,4
       XCVO(L,K) = 0.
    16 XCO(L,K) = 0.
       JNX = 0
       SMIN = 9.E+06
       SMN1 = 1.
       IF(JM-NN) 17,45,45
    45 W(4) = 1.
       DO 5 K = 1,3
       PRS(JM,K) = 0.
       SD1(K) = 0.
       CPRS(K) = 0.
       SIGMA(K) = 0.
   5   EQSGI(K) = 0.
   17  IT = IT+1
       SMDS = 0.
       SDP = 0.
       SDP1 = 0.
       TDEP = 0.
       DDS(4) = 1.
       XTRM2 = 0.
       XTRM = 0.
```

```
      K$=1
      IF(JM-NN)2,1,1
    1 K$=4
    2 DO 4 K=K$,4
3     C = SIGMA(K)/DELEP(K)/1.5
      BM = G(K)*(2.+2.*GNU(K))/(1.-2.*GNU(K))
      ER = EPR(JM,K)
      EC = EPC(JM,K)
      EZ = EPZ(JM,K)
      EB = (ER+EC+EZ)/3.
      DTR = (ER-EB-TPR(JM,K))*G(K)*2.
      DTC = (EC-EB-TPC(JM,K))*G(K)*2.
      DTZ = (EZ-EB-TPZ(JM,K))*G(K)*2.
      DSIGR = C*DPR(JM,K)
      DSIGC = C*DPC(JM,K)
      DSIGZ = C*DPZ(JM,K)
      CALL EQUISI(DTR,DTC,DTZ,SIGEQ)
      EQSGI(K) = SIGEQ
      SD2 = (DSIGR-DTR)**2+(DSIGC-DTC)**2+(DSIGZ-DTZ)**2
      S = SD2+3.*(PRS(JM,K)-CPRS(K))**2
      SD1(K) = SQRT(SD2*1.5)
      XS = DSIGR*DTC-DSIGC*DTR
      IF(XS) 26,27,27
26    SD1(K) = -SD1(K)
 27   SDP = SDP+(SD2/(2.*G(K))**2+3.*((PRS(JM,K)-CPRS(K))/BM)**2)*
     1W(K)**2
      XC(1,K) = (DSIGR - DTR)*W(K)/G(K)/ 2.
      XC(2,K) = (DSIGC - DTC)*W(K)/G(K)/ 2.
      XC(3,K) = (DSIGZ - DTZ)*W(K)/G(K)/ 2.
      XC(4,K) = ( PRS(JM,K) - CPRS(K))*W(K)*(1.73205) /BM
      DXTM2 = 0.
      DXTM = 0.
      DO 31 L = 1,4
      DXTM2 = DXTM2 + XC(L,K)*XCVO(L,K)
 31   DXTM = DXTM + XC(L,K)*XCO(L,K)
      XTRM2 = XTRM2 + DXTM2
```

```
      XTRM = XTRM + DXTM
      SDP1 = SDP1+(SD2/(2.*G(K))**2)*W(K)**2
      TDEP=TDEP+(ABS(DPR(JM,K))+ABS(DPC(JM,K))+ABS(DPZ(JM,K)))*W(K)
4     SMDS = SMDS+S*W(K)**2
      SUMDS = SQRT(SMDS)
      SDEP = SQRT(SDP)
      SDEP1 = SQRT(SDP1)
      ID = 0
      GO TO 57
20    ID = -1
      IF(SDEP-1.) 7,7,20
7     IF(SDEP-SMN1) 21,24,24
24     ID = -1
      GO TO 22
21    SMN1 = SDEP
      IF(SMN1-DPMX) 23,22,22
23    SMN1 = DPMX
      ID = 1
      GO TO 29
22    IF(SUMDS-SMIN) 8,25,25
25    IF(ID) 11,11,9
8     SMIN = SUMDS
      IF(SMIN-DSMX1) 33,9,9
33    SMIN = DSMX1
      IF(ID) 9,9,11
9     ID = 0
 11   DO 6 K = 1,4
      EPR3(K) = EPR2(K)
      EPC3(K) = EPC2(K)
      EPZ3(K) = EPZ2(K)
      EPR2(K) = EPR1(K)
      EPC2(K) = EPC1(K)
      EPZ2(K) = EPZ1(K)
      EPR1(K) = EPR(JM,K)
      EPC1(K) = EPC(JM,K)
      EPZ1(K) = EPZ(JM,K)
```

```
      DO 6 L = 1,4
      XCVO(L,K) = XCO(L,K)
    6 XCO(L,K) = XC(L,K)
      IF(ID) 10,18,29
   10 IF (JNX) 12,12,57
   12 JNX = 1
      ID = 0
      GO TO 34
   18 JNX = 0
   34 IF (IT - 2) 44,42,28
   42 XTPL2 = 0.
      XTPL1 = (SDP - XTRM)/(SDP + SDPO - 2.*XTRM)
      GO TO 43
   28 DTMN =  (SDP + SDPO - 2.*XTRM)*(SDP + SDPVO - 2.*XTRM2)
     1      - (SDP + XTRMO - XTRM - XTRM2)**2
      IF(DTMN)32,42,32
   32 XTPL1 = - (SDP*XTRMO - XTRM*XTRM2 + XTRM2*XTRM2 + XTRM*SDPVO
     1         - SDP*SDPVO - XTRM2*XTRMO) / DTMN
      XTPL2 = - (SDP*XTRMO - XTRM*XTRM2 + XTRM*XTRM + XTRM2*SDPO
     1         - SDP*SDPO - XTRM*XTRMO) / DTMN
   43 DO 30 K = 1,4
      EPR(JM,K)=EPR(JM,K)*(1.-XTPL1-XTPL2)+EPR2(K)*XTPL1+EPR3(K)*XTPL2
      EPC(JM,K)=EPC(JM,K)*(1.-XTPL1-XTPL2)+EPC2(K)*XTPL1+EPC3(K)*XTPL2
   30 EPZ(JM,K)=EPZ(JM,K)*(1.-XTPL1-XTPL2)+EPZ2(K)*XTPL1+EPZ3(K)*XTPL2
   44 SDPVO = SDPO
      SDPO = SDP
      XTRMO = XTRM
      GO TO 29
   57 IF(DELT-.001) 61,60,60
   61 IF(TDEP-.0001 ) 59,60,60
   60 IF(SUMDS-DSNX1) 58,29,29
   58 IF(SDEP-DPNX) 59,29,29
   59 ID = 1
   29 RETURN
      END
      SUBROUTINE CREEF(SIGOLD,EPSNEW,FLUX,TEMAV,DELT,SIGNEW,G6,FC,D)
```

```
      IT = 0                                                          7/15
      SIGNEW = 0.
C *** THESE ARE  GEAP-10054 CONSTANTS.
      IF(D-92.) 3,4,4
    3 D = 92.
    4 A = (1.376E-4)/(-90.5+D)
      A1 = (9.726 E+6)/(-87.7 + D)
      GD = 10.
      B = 0.8E-23
      FM = 4.5
      FN = 1.
      Q = 132000.
      Q1 = 90000.
      R = 8.314/1.8/4.186
      TEMAV = TEMAV + 460.
C *** TEMAV NOW IN DEG R
      FCO = 0.
      IF(EPSNEW) 20,20,22
   20 FC = 1.
      EPSNEW = 1.E-30
      SIGNEW = EPSNEW*G6*3.
      GO TO 25
   22 IF(SIGOLD) 310,310,312
  310 SIGOLD = 100.
  312 X1 = Q/(R*TEMAV)
      X9 = Q1/(R*TEMAV)
      IF(A.LE.0.) A=0.
      X2 = - X1 + ALOG( A )                                           6/27
      IF(A1.LE.0.) A1=0.
      IF(GD.LE.0.) GD=0.
      X5 = B*FLUX+EXP(-X9+ALOG(A1)-2.*ALOG(GD))
      SIG = SIGOLD
  399 SIGB =  SIG                                                     10/12
      IF(SIGB.LE.0.) SIGB=0.
      X3 = ALOG(SIGB)
      X4 = EXP( X2 + FM*X3 )                                          5/27
```

```
      IT = IT + 1                                                        7/15
      X6 = X5*SIGB**FN
      FC1 = (FM*X4+FN*X6)*DELT                                           10/12
      FCN = (X4+X6)*DELT
      X7 = ABS(FCN-FCO)/FCN
      FCO = FCN
      X = SIG
      SIG = SIG*(EPSNEW-FCN+FC1)/(FC1+SIG/G6/3.)
      IF(IT-100) 2,2,1
    1 WRITE (6,10) IT,X,SIG,FCN,X7
   10 FORMAT('0',' ***NUMERICAL GUESS OF CREEP WAS NOT SATISFACTORY AFTE
     1R',I4,' EXTRAPOLATIONS',/2X,'PREVIOUS SIGMA =',E15.8,' LAST SIGMA
     2=',E15.8,/2X,'FINAL CREEP =',E15.8,' HAS AN ESTIMATED FRACTIONAL E
     3RROR =',E15.8/)
      GO TO 401
    2 IF(X7-.0001) 26,399,399
   26 X8 = ABS(SIG-X)
      IF(X8-.5) 401,399,399
  401 SIGNEW = SIG
   24 FC = FCN/EPSNEW
   25 TEMAV = TEMAV-460.
C *** TEMAV NOW BACK TO DEG F
      RETURN
      END
      SUBROUTINE FLTMP(WFO,TFO,RFO,RHOT,RHO,XM,ALF0,ALF1,NOK,BT,A1,B1,C1
     1,A2,B2,C2,CM1,DHR,F,N,N1,DXM,TLR,RLR,TB,ATB,TL,RL,FD,JS,GDT,
     2 JBM,RHOZON)
      REAL*8 RFO,R,DR,SM,XM,XML,XM1,DM0,DM,DM1,RHO,XAR,X,PI2
      DIMENSION RHO(3),XM(3),CM1(2),DHR(2),F(14),DXM(3),TLR (4),RLR(4),
     1TB(3),ATB(3),TL(15),RL(15),XML(3),CM(2),ALF0(3),ALF1(3),FD(3),
     2GDT(15),ZHO(3)
      DIMENSION RHOZON(3)
      COMMON PI,N3
C
C ***  FLTMP CALCULATIONS IN UNITS OF WATTS,CM,HR,DEG C **** BUT,
C      FLTMP OUTPUT CONVERTED TO INCHES AND DEG F ETC.
```

```
      WFO = WFO*1000./30.48
C *** WFO NOW IN WATTS/CM
      TFO = (TFO-32.)*(5./9.)
C *** TFO NOW IN DEG C
      RFO = RFO*2.54
C  *  RFO NOW IN CM
      TLR(4) = TFO
   28 RLR(4) = RFO
      TL(N+1)= TFO
      RL(N+1)= RFO
      JNX = 0
      JNX1 = 0
      NI = 0
      XML(1) = 0.
      XML(2) = XM(1)
      XML(3) = XM(1) +XM(2)
      SM     = XML(3) + XM(3)
      X = PI
      PI2 = X*2.
      SF = 0.
      DO 1 I=1,N
    1 SF = SF + F(I)
      N2 = N * N1
      DM0 = -SM/N2
      XM1 = SM
      R  = RFO
      T  = TFO
      W  = WFO
      I = 3
      DM = DM0
      IF(DM+XM(3)) 25,24,24
   25 DM = -XM(3)
      DM1 = DM
      GO TO 2
  24  DM1 = 0.
    2 ST = 0.
```

```
      SAT = 0.
      SSF = 0.                                                          7/25
      P = 1.- RHO(I)/RHOT
      FP = (1.025/0.95)*((1. - P)/(1. + BT*P))
    3 DR = DM/(RHO(I)*R*PI2)
      XAR = 0.25 +DR/(2.*R)
      IF (XAR) 22,23,23
   22 XAR = 0.
      JNX1 = 1
      WRITE (6,270) JS
  270 FORMAT('1',' CENTRAL HOLE CLOSES IN AXIAL SECTION',I3,'STANDARD FI
     1XUP TAKEN')
      WRITE(6,271) I,NM,NI,R,DR,DM0,DM,DM1,XM(1),XM(2),XM(3)
  271 FORMAT(1X,3I10/2E16.8/6E16.8/)
      RFO = RFO-(DM+PI2*RHO(I)*R*R/2.)/(PI2*RHO(I)*RFO)
      GO TO 28
  23  DR = DR/(0.5+DSQRT(XAR))
      NI = NI + 1
   21 NM = (XM1/SM)*N+0.999999
      IF(NM) 26,26,27
   26 NM = 1
   27 W1 = WFO*N*F(NM)/SF/SM
      XJ = W/R/PI2
      W2 = W1*DM/DR
      XJ1 = (W2*R-W)/R**2/PI2
      DW = W1*DM
      IF(NOK-2) 4,5,5
C **  THERMAL CONDUCTIVITY EQUATION BASED UPON LYONS EQUATION FOR TD =
C **  0.95.  MAXWELL-EUCKEN RELATION USED WITH NORMALIZATION TO TD =
C **  0.95 AND WITH BETA = 0.5 (SEE MAIN).
    4 XK = (A1/(B1 + T) + C1*(T + 273.)**3)*FP
      XK1 = (-A1/(B1 + T)**2 + 3.*C1*(T + 273.)**2)*FP
      GO TO 6
   5  ZHO(I) = RHO(I)/RHOT
      XK = A2+1./((B2-C2*ZHO(I))*T)
      XK1 = -1./((B2-C2*ZHO(I))*T*T)
```

```
    6 X = -XJ*DR
      DT = (X/XK)*(1.+XK1*X/XK**2/2.) - XJ1*DR**2/XK/2.
      ST = ST + (T + DT/2)*DM
      Y = 20.
      SAT=SAT+(ALF0(I)*T+ALF1(I)*T*T/2.+(ALF0(I)+ALF1(I)*T)*DT/2.)*DM
     1-(ALF0(I)*Y+ALF1(I)*Y*Y/2.)*DM
      SSF = SSF + F(NM)*DM                                              7/25
      XM1 = XM1 + DM
      R  = R + DR
      W = W + DW
      T = T + DT
      TL(NM) = T
      RL(NM) = R
      GDT(NM) = DT/DR
      X = XML(I) - XM1
      IF (X - DM0) 7,7,8
    7 DM = DM0
      DM1 = 0.
      GO TO 3
    8 IF (X) 9,10,9
    9 DM = X
      DM1 = DM+DM1
      GO TO 3
   10 TLR(I) = T
      RLR(I) = R
      TB(I) =-ST/XM(I)
      ATB(I) =-SAT/XM(I)
      FD(I) = -SSF*N*RHO(I)/SM/SF/XM(I)                                 7/25
C**** FD IS THE NUMBER OF FISSIONS IN ONE IN**3 FOR ONE FISSION IN A     7/25
C**** SECTION OF WHOLE FUEL ROD OF ONE IN HEIGHT.                       7/25
      I = I-1
      IF (I-1) 14,11,11
   11 GRDT = -DT/DR
      Y = 0.1*(T - TFO)/RFO                                             .1=BGRFC
      IF (GRDT - Y) 12,13,13
   12 GRDT = Y
```

```
   13  TK = T+273
       IF (GRDT .LE. 0.000001)  GRDT = 0.000001
       XLC = ALOG(CM1(I))-1.5*ALOG(TK)+ALOG(GRDT)-DHR(I)/TK
       V = R
       VZZ = PI2
       XXX = XLC+ALOG(V)+ALOG(VZZ)
       CM(I)=EXP(XXX)
       DM=DM0-DM1
       X = XML(I) - XM1
       IF(X-DM) 24,24,20
    20 DM = X
       DM1 = DM1+DM
       GO TO 2
    14 DXM(3) = - CM(2)*RHO(3)/RHOZON(3)
       DXM(2) = CM(2)*RHO(3)/RHOZON(3) - CM(1)*RHO(2)/RHOZON(2)
       DXM(1) = CM(1)*RHO(2)/RHOZON(2)
C ***  NOW CONVERT BACK TO ENGLISH UNITS
       WFO = WFO*30.48/1000.
       TFO = 32. + TFO*1.8
       RFO = RFO/2.54
       NNN = N + 1
       DO 15 I=1,NNN
       RL(I) = RL(I)/2.54
   15  TL(I) = 32. + TL(I)*1.8
       DO 16 I = 1,3
       FD(I) = FD(I)*6.4516                                          7/25
   16  TB(I) = 32.+TB(I)*1.8
       DO 17  I = 1,4
       RLR(I) = RLR(I)/2.54
   17  TLR(I) = 32.+TLR(I)*1.8
C      BOUNDARY VELOCITY CHANGES RAPIDLY WITH TEMPERATURE AND TO OBTAIN
C      ACCURATE DISPLACEMENTS ONE SHOULD CHOSE SMALL TIME INTERVALS
C      SO THAT MASS CHANGES ARE MUCH SMALLER THAN T/DHR.
       RETURN
       END
       SUBROUTINE GASOUT(SS,NS,FL,DELT,GR,GRT,GS,POW,FD,JPLEN,IT,EBG)
```

```
      DIMENSION SS(10,4),GR(10),GS(10,3),POW(10),FRPT(3),FD(10,3),
     1REL(3),W(3),EBG(10,3)
      COMMON PI,N3
      COMMON/SACC/SAC1,SAC2,SACAN1,SACAN2,SACAN3,SAC3
      A91 = 9.3E+15
C***  UNITS -  3.1*10**10FISSIONS/WATT/SEC*1000WATTS/KWT/3600SEC/HR*
C***  1FT/12IN = 9.3*10**15 FISSIONS*FT/KW/HR/IN
      AF=0.27
C***   AF IS ATOMS OF GAS PER FISSION
      AN = 6.02E+23
C***  AN IS AVOGADRO'S NUMBER
   83 FNS = NS
      SL = FL/FNS
C
C
C      SAC1, SAC2, SAC3 ARE USED TO CALIBRATE THE GAS RELEASE MODEL
C      SAC1 ADJUSTS THE COLUMNAR GRAIN ZONE RELEASE
C      SAC2 ADJUSTS THE EQUIAXED GRAIN ZONE RELEASE
C      SAC3 ADJUSTS THE UNDISTURBED GRAIN ZONE RELEASE
C
C
      FRPT(1)=0.0005*SAC1
      FRPT(2)=0.00011*SAC2
      FRPT(3)=0.00005*SAC3
C***   FRPT IS FRACTION OF GAS RELEASED PER HOUR
      DO 74 J = 1,NS                                              7/29
      DFN = A91*POW(J)*DELT
C***   SAME AS IN SWELL SUBROUTINE
      GR(J) = 0.
      SSS = SS(J,1)+SS(J,2)+SS(J,3)
      DO 79  K = 1,3
      W(K) = SSS/SS(J,K)/3.
      VOL = PI*SS(J,K)*SL
      DGS = AF*VOL*FD(J,K)*DFN/AN
      GO = GS(J,K)
      EG = EBG(J,K)
```

```
      EHR = 0.
      IF(EG-0.25)  12,12,11
   11 EHR = (EG-0.25)/.01
   12 F = FRPT(K)+EHR*(FRPT(1)-FRPT(K))
      X = F*DELT
      IF(X-.1)  3,4,4
    3 Y = (1.-X/3.+X*X/12.)*X/2.
      Z = X-X*Y
      REL(K) = G0*Z+DGS*Y
      GS(J,K) = G0+DGS-REL(K)
      GO TO 79                                                    1/10
    4 IF(X-170.)  7,6,6
    6 GS(J,K) = DGS/X                                             1/11
      GO TO 8                                                     1/11
    7 GS(J,K) = DGS/X+(G0-DGS/X)*EXP(-X)
    8 REL(K) = G0+DGS-GS(J,K)                                     1/11
   79 GR(J) = GR(J)+REL(K)                                        1/10
   74  GRT = GRT+GR(J)
    2 RETURN
      END
      SUBROUTINE GOLDN(POWAV,QSF,TOUT,TIN,NN,RCLO,POW,TCLO,AFNA,FL,
     1HC1,TNA,TMPA,PRSA,SPHT,WCON,WVIS,WVOL,PO)
      DIMENSION QSF(10),TCLO(10),POW(10),RCLO(10),HC1(10),TNA(10),
     1TMPA(5),PRSA(5),SPHT(5,5),WCON(5,5),WVIS(5,5),WVOL(5,5)
C***** CALCULATES CLAD CD TEMPERATURE
      PI2=6.2831853
      AF=AFNA
      WB=POWAV*3415.2
C***** WB IS AVG POWER IN BTU/HR/FT
      DTMP=TOUT-TIN
      TPROP=(TOUT+TIN)/2.
   20 CPAV=WPROP(TPROP,PO,TMPA,PRSA,SPHT,5,5)
      TX=TIN
   25 WDOT=WB*(FL/12.)/(CPAV*DTMP)
   30 WVAV=WPROP(TPROP,PO,TMPA,PRSA,WVOL,5,5)
   35 WVEL=WDOT*WVAV/AF
```

```
      TNA(NN)=TOUT
      TCLO(NN)=TOUT
      POW(NN)=0.
      NF=NN-1
      XNF=NF
      S=0.
      DO 1 N=1,NF
    1 S=S+QSF(N)
      X=0.
      SW=0.
    5 DO 10 N=1,NF
      SW=SW+QSF(N)
      CPN=WPROP(TX,PO,TMPA,PRSA,SPHT,5,5)
      CPDT=CPAV*DTMP/CPN
      X=CPDT*(SW-QSF(N)/2.)/S
    6 TNA(N)=TIN+X
C**** THIS IS WATER TEMP AT AXIAL NODE N
      TX=TNA(N)
      W=WB*QSF(N)*XNF/S
      POW(N)=W/3415.2
C**** NOW CALCULATE HEAT TRANSFER COEFF.
      PWET=PI2*RCLO(N)/12.
      DEQ=4.*AF/PWET
      CP=WPROP(TX,PO,TMPA,PRSA,SPHT,5,5)
C**** CP IN BTU/LBM-DEG F
      WK=WPROP(TX,PO,TMPA,PRSA,WCON,5,5)
C**** WK IN BTU/HR-FT-DEG F
      XMU=WPROP(TX,PO,TMPA,PRSA,WVIS,5,5)
C**** XMU IN LBM/HR-FT
      VEE=WPROP(TX,PO,TMPA,PRSA,WVOL,5,5)
C**** VEE IN CU. FT/LBM
      VEL=WDOT*VEE/AF
      REY=(DEQ*VEL)/(VEE*XMU)
      PRAN=CP*XMU/WK
      XNU=0.023*(REY**0.8)*(PRAN**0.4)
      HC=XNU*WK/DEQ
```

```
    7 HC1(N)=HC
C****** NOW CALCULATE TCLO
      CNST=W/(PWET*HC)
    8 TCLO(N)=TX+CNST
   10 CONTINUE
      RETURN
      END
      SUBROUTINE READ1(EPR,EPC,EPZ,DPR,DPC,DPZ,TPR,TPC,TPZ,
     1DSR,DSC,DSZ,TSR,TSC,TSZ,SIGR,SIGC,SIGZ,WDISP,UDISP,RVB,R1B,
     2REB,RUB,RCA,R4B,NN,AFNA)
      DIMENSION EPR(10,4),EPC(10,4),EPZ(10,4),DPR(10,4),DPC(10,4),
     1DPZ(10,4),TPR(10,4),TPC(10,4),TPZ(10,4),DSR(10,4),DSC(10,4),
     2DSZ(10,4),TSR(10,4),TSC(10,4),TSZ(10,4),SIGR(10,4),SIGC(10,4),
     3SIGZ(10,4),WDISP(10,4),UDISP(10,6),RVB(10),R1B(10),REB(10),
     4RUB(10),RCA(10),R4B(10)
      READ(5,20)  ((EPR(N,M),M=1,4),N=1,NN)
      READ(5,20)  ((EPC(N,M),M=1,4),N=1,NN)
      READ(5,20)  ((EPZ(N,M),M=1,4),N=1,NN)
      READ(5,20)  ((DPR(N,M),M=1,4),N=1,NN)
      READ(5,20)  ((DPC(N,M),M=1,4),N=1,NN)
      READ(5,20)  ((DPZ(N,M),M=1,4),N=1,NN)
      READ(5,20)  ((TPR(N,M),M=1,4),N=1,NN)
      READ(5,20)  ((TPC(N,M),M=1,4),N=1,NN)
      READ(5,20)  ((TPZ(N,M),M=1,4),N=1,NN)
      READ(5,20)  ((DSR(N,M),M=1,4),N=1,NN)
      READ(5,20)  ((DSC(N,M),M=1,4),N=1,NN)
      READ(5,20)  ((DSZ(N,M),M=1,4),N=1,NN)
      READ(5,20)  ((TSR(N,M),M=1,4),N=1,NN)
      READ(5,20)  ((TSC(N,M),M=1,4),N=1,NN)
      READ(5,20)  ((TSZ(N,M),M=1,4),N=1,NN)
      READ(5,20)  (( SIGR(N,M),M=1,4),N=1,NN)
      READ(5,20)  (( SIGC(N,M),M=1,4),N=1,NN)
      READ(5,20)  (( SIGZ(N,M),M=1,4),N=1,NN)
      READ(5,20)  ((WDISP(N,M),M=1,4),N=1,NN)
      READ(5,20)  ((UDISP(N,M),M=1,6),N=1,NN)
      READ(5,20)   (RVB(N),N=1,NN)
```

```
      READ(5,20)   (R1B(N),N=1,NN)
      READ(5,20)   (REB(N),N=1,NN)
      READ(5,20)   (RUB(N),N=1,NN)
      READ(5,20)   (RCA(N),N=1,NN)
      READ(5,20)   (R4B(N),N=1,NN)
      READ(5,20) AFNA
C**** AFNA IS THE AVG WATER FLOW AREA IN FT**2
  20  FORMAT(5E15.8)
      RETURN
      END
      SUBROUTINE READ2(TMPA,PRSA,SPHT,WCON,WVIS,WVOL)
      DIMENSION TMPA(5),PRSA(5),SPHT(5,5),WCON(5,5),WVIS(5,5),WVOL(5,5)
      READ(5,10)  (TMPA(I),I=1,5)
      READ(5,10)  (PRSA(I),I=1,5)
      READ(5,15)  ((SPHT(N,M),N=1,5),M=1,5)
      READ(5,15)  ((WCON(N,M),N=1,5),M=1,5)
      READ(5,15)  ((WVIS(N,M),N=1,5),M=1,5)
      READ(5,15)   ((WVOL(N,M),N=1,5),M=1,5)
   10 FORMAT(5F10.1)
   15 FORMAT(5F10.5)
      RETURN
      END
      SUBROUTINE RITE1 (J,I,SIGR,SIGC,SIGZ,EPR,EPC,EPZ,U11,U12,U22,U32,
     1U41,U42,DPR,DPC,DPZ,TPR,TPC,TPZ,DSR,DSC,DSZ,TSR,TSC,TSZ,SWS6,EHP6)
      DIMENSION  SIGR(10,4),SIGC(10,4),SIGZ(10,4),EPR(10,4),EPC(10,4),
     1EPZ(10,4),DPR(10,4),DPC(10,4),DPZ(10,4),TPR(10,4),TPC(10,4),
     2TPZ(10,4),DSR(10,4),DSC(10,4),DSZ(10,4),TSR(10,4),TSC(10,4),
     3TSZ(10,4),SWS6(10,3),SWZ(3),CPRS(4),EHP6(10,3),HPR(3)
      DO 5 L = 1,4
   5  CPRS(L) = -(SIGR(J,L)+SIGC(J,L)+SIGZ(J,L))/3.
      WRITE (6,710) J
      WRITE (6,711) (SIGR(J,L),L=1,4)
      WRITE (6,712) (SIGC(J,L),L=1,4)
      WRITE (6,713) (SIGZ(J,L),L=1,4)
      WRITE(6,731) (CPRS(L),L=1,4)
      WRITE (6,714) (EPR(J,L),L=1,4)
```

```
      WRITE (6,715) (EPC(J,L),L=1,4)
      WRITE (6,716) (EPZ(J,L),L=1,4)
      WRITE (6,718)  ( DPR(J,L),L=1,4)
      WRITE (6,719)  ( DPC(J,L),L=1,4)
      WRITE (6,720)  ( DPZ(J,L),L=1,4)
      WRITE (6,721)   (TPR(J,L),L=1,4)
      WRITE (6,722)   (TPC(J,L),L=1,4)
      WRITE (6,723)   (TPZ(J,L),L=1,4)
      WRITE (6,724)  (DSR(J,L),L=1,4)
      WRITE (6,725)  (DSC(J,L),L=1,4)
      WRITE (6,726)  (DSZ(J,L),L=1,4)
      WRITE (6,727)  (TSR(J,L),L=1,4)
      WRITE (6,728)  (TSC(J,L),L=1,4)
      WRITE (6,729)  (TSZ(J,L),L=1,4)
      DO 1 L = 1,3
      HPR(L) = EHP6(J,L)/3.
    1 SWZ(L) = SWS6(J,L)/3.
      WRITE(6,730) (SWZ(L),L=1,3)
      WRITE (6,732) (HPR(L),L = 1,3)
      WRITE (6,717)   U11,U12,U22,U32,U41,U42
  710 FORMAT(20X,'AXIAL SECTION J =',I3)
  711 FORMAT(' ',3X,'SIGR(J,1)',8X,'SIGR(J,2)',8X,'SIGR(J,3)',8X,
     1'SIGR(J,4)'/4E17.8)
  712 FORMAT(' ',3X,'SIGC(J,1)',8X,'SIGC(J,2)',8X,'SIGC(J,3)',8X,
     1'SIGC(J,4)'/4E17.8)
  713 FORMAT(' ',3X,'SIGZ(J,1)',8X,'SIGZ(J,2)',8X,'SIGZ(J,3)',8X,
     1'SIGZ(J,4)'/4E17.8)
  714 FORMAT(' ',4X,'EPR(J,1)',9X,'EPR(J,2)',9X,'EPR(J,3)',9X,'EPR(J,4)'
     1/4E17.8)
  715 FORMAT(' ',4X,'EPC(J,1)',9X,'EPC(J,2)',9X,'EPC(J,3)',9X,'EPC(J,4)'
     1/4E17.8)
  716 FORMAT(' ',4X,'EPZ(J,1)',9X,'EPZ(J,2)',9X,'EPZ(J,3)',9X,'EPZ(J,4)'
     1/4E17.8)
  717 FORMAT('0',5X,'U11',14X,'U12',14X,'U22',14X,'U32',14X,'U41',14X,
     1'U42',/6E17.8)
  718 FORMAT(' ',4X,'DPR(J,1)',9X,'DPR(J,2)',9X,'DPR(J,3)',9X,
```

```
     1'DPR(J,4)',/4E17.8)
719   FORMAT(' ',4X,'DPC(J,1)',9X,'DPC(J,2)',9X,'DPC(J,3)',9X,
     1'DPC(J,4)',/4E17.8)
720   FORMAT(' ',4X,'DPZ(J,1)',9X,'DPZ(J,2)',9X,'DPZ(J,3)',9X,
     1'DPZ(J,4)',/4E17.8)
721   FORMAT(' ',4X,'TPR(J,1)',9X,'TPR(J,2)',9X,'TPR(J,3)',9X,
     1'TPR(J,4)'/4E17.8)
722   FORMAT(' ',4X,'TPC(J,1)',9X,'TPC(J,2)',9X,'TPC(J,3)',9X,
     1'TPC(J,4)'/4E17.8)
723   FORMAT(' ',4X,'TPZ(J,1)',9X,'TPZ(J,2)',9X,'TPZ(J,3)',9X,
     1'TPZ(J,4)'/4E17.8)
724   FORMAT(' ',4X,'DSR(J,1)',9X,'DSR(J,2)',9X,'DSR(J,3)',9X,
     1'DSR(J,4)'/4E17.8)
725   FORMAT(' ',4X,'DSC(J,1)',9X,'DSC(J,2)',9X,'DSC(J,3)',9X,
     1'DSC(J,4)'/4E17.8)
726   FORMAT(' ',4X,'DSZ(J,1)',9X,'DSZ(J,2)',9X,'DSZ(J,3)',9X,
     1'DSZ(J,4)'/4E17.8)
727   FORMAT(' ',4X,'TSR(J,1)',9X,'TSR(J,2)',9X,'TSR(J,3)',9X,
     1'TSR(J,4)',/4E17.8)
728   FORMAT(' ',4X,'TSC(J,1)',9X,'TSC(J,2)',9X,'TSC(J,3)',9X,
     1'TSC(J,4)',/4E17.8)
729   FORMAT(' ',4X,'TSZ(J,1)',9X,'TSZ(J,2)',9X,'TSZ(J,3)',9X,
     1'TSZ(J,4)',/4E17.8)
730   FORMAT(5X,'SSW(J,1)',9X,'SSW(J,2)',9X,'SSW(J,3)',/3E17.8)
731   FORMAT(6X,'CPRS(1)',10X,'CPRS(2)',10X,'CPRS(3)',10X,'CPRS(4)',
     1/4E17.8)
 732  FORMAT(5X,'HPR(J,1)',9X,'HPR(J,2)',9X,'HPR(J,3)', /3E17.8)
      RETURN
      END
      SUBROUTINE RITE2(NN,NI,ITERNO,NT,NOK,RVB,R1B,REB,RUB,RCA,R4B,
     1FL,CL,PTCP,PO,FKA1,FKB1,FKC1,FKA2,FKB2,FKC2,FA11,FA12,FA21,FA22,
     2FA31,FA32,CK1,CK2,CA1,CA2,CM1,DHR,RHO,RHOC,FQ,QSF,TOGAS,AFNA)
      DIMENSION RVB(10),R1B(10),REB(10),RUB(10),RCA(10),R4B(10),DHR(2),
     1RHO(3),FQ(14),QSF(10),CM1(2)
      WRITE(6,101)
 101  FORMAT('1',20X,'INITIAL VALUES INPUT',////)
```

```
      WRITE(6,105) NN,NI,ITERNO,NT,NOK
  105 FORMAT('0','NUMBER OF AXIAL SECTIONS =',I2/1X,'BEGIN DEFORMATION A
     1NALYSIS WITH SECTION',I2/,1X,'MAX ITERATIONS ALLOWED =',I2,5X,
     2'EQUAL MASS SECTIONS USED IN FLTMP =',I3/1X,'FUEL CONDUCTIVITY FUN
     3CTION =',I3,2X,'(STANDARD = 1, G.E. = MORE THAN 1)',/)
   10 WRITE(6,15 ) RVB(1),R1B(1),REB(1),RUB(1),RCA(1),R4B(1),AFNA
   15 FORMAT(' ',6X,'RVB(1)',11X,'R1B(1)',11X,'REB(1)',11X,'RUB(1)',11X,
     1'RCA(1)',11X,'R4B(1)',/,6(F15.8,2X),//,4X,'AFNA(FT2) =',F15.8,/)
   20 WRITE(6,107)FL,CL,PTOP,PO,FKA1,FKB1,FKC1,FKA2,FKB2,FKC2,FA11,FA12,
     1FA21,FA22,FA31,FA32,CK1,CK2,CA1,CA2
  107 FORMAT('0',1X,'FL,CL,PTOP,PO NEXT',/1X,4E17.8/1X,'FKA1,FKB1,FKC1,
     1FKA2,FKB2,FKC2 NEXT',/1X,6E17.8/1X,'FA11,FA12,FA21,FA22,FA31,FA32
     2NEXT',/1X,6E17.8/1X,'CK1,CK2,CA1,CA2 NEXT',/1X,5E17.8/)
      WRITE(6,109) (CM1(L),L=1,2),(DHR(L),L=1,2)
  109 FORMAT(' ',1X,'CM1(L),L=1,2 AND DHR(L),L=1,2 NEXT',/1X,4E17.8/)
      WRITE(6,108) (RHO(I),I=1,3),RHOC
  108 FORMAT('0',1X,'RHO(I),I=1,3 AND RHOC NEXT',/1X,4E17.8/)
      WRITE(6,113) (QSF(N),N=1,NN)
  113 FORMAT('0',1X,'AXIAL SHAPE FACTORS QSF(N),N=1,NN NEXT',/1X,
     110(F5.2,2X))
      WRITE(6,115) TOGAS
  115 FORMAT('0',1X,'INITIAL GAS MOLES IN PLENUM =',E15.8/)
      WRITE(6,120) (FQ(J),J=1,NT)
  120 FORMAT('0',1X,'RADIAL SHAPE FACTORS F(J),J=1,NT NEXT',/,
     12(7F10.5,/))
      RETURN
      END
      SUBROUTINE RITE3(NN,R4B,POW,TCLO,R,T,TBC,ATBC,HG1,RUB,RHOT,RH,
     1XMM6,EPZO,N3,F,DXM6,TLR6,RLR6,TBF6,ATBF6,TL6,RL6,GS,TOGAS,PLPR,
     2IT,TIT,POWAV,TOUT,TIN,TVZJ,SIGR,SIGC,SIGZ,EPR,EPC,EPZ,UDISP,DPR,
     3DPC,DPZ,TPR,TPC,TPZ,DSR,DSC,DSZ,TSR,TSC,TSZ,FL,CL,SSF,SSC,RCA,
     4REB,RVB,R1B,R4BI,DELT,HC1,TNA,SWS6,FLNC,F7,
     5DSMX1,SMEP,XPR12,XPR23,XPRG,IIRW,IM,SDPM,EHP6,GASI,JCRR)
      REAL*8 RH,XMM6,SM
      DIMENSION R4B(10),POW(10),TCLO(10),T(10,7),R(10,7),TBC(10),
     1ATBC(10),RUB(10),RH(10,3),XMM6(10,3),EPZO(10,4),F(14),DXM6(10,3),
```

```
     2TLR6(10,4),TBF6(10,3),ATBF6(10,3),TL6(10,15),RL6(10,15),
     3RHO(3),XM(3),DXM(3),TB(3),ATB(3),TLR(4),RLR(4),TL(15),RL(15),
     4GS(10,3),SIGR(10,4),SIGC(10,4),SIGZ(10,4),EPR(10,4),EPC(10,4),
     5EPZ(10,4),UDISP(10,6),DPR(10,4),DPC(10,4),DPZ(10,4),TPR(10,4),
     6TPZ(10,4),DSR(10,4),DSC(10,4),DSZ(10,4),TSR(10,4),TSC(10,4),
     7TSZ(10,4),TPC(10,4),RLR6(10,4),RCA(10),REB(10),RVB(10),R1B(10),
     8R4BI(10),HG1(10),HC1(10),TNA(10),SWS6(10,3),
     9FLNC(10),F7(10,14),XPR12(10),XPR23(10),
     AXPRG(10),IIRW(10),EHP6(10,3)
      COMMON/GRAPH/IGRAPH,KONVER
      IGRAPH=IGRAPH+1                                                  &7IA6
      WRITE (6,70)
570   IF(JCRR) 571,24,571
571   WRITE(6,23) IT
23    FORMAT(9X,'THE INPUT FOR STEP NO.',I2,' HAS BEEN MODIFIED AS FOLLO
     1WS')
  24  WRITE(6,709) IT,TIT,POWAV,TOUT,TIN,DELT,TVZJ
 709  FORMAT(1X ,'STEP NO.',I4,2X,'TIME(HRS)',F10.3,2X,'POWAV(KW/FT)',
     1F10.3,2X,'TOUT(F)',F10.3,2X,'TIN(F)',F10.3/2X,'DELT =',F10.5,
     2'    TLEFT =',F7.2,' SEC.')
 719  FORMAT(1X ,'STEP NO.',I4,2X,'TIME(HRS)',F10.3,2X,'POWAV(KW/FT)',
     1F10.3,2X,'TOUT(F)',F10.3,2X,'TIN(F)',F10.3/2X,'DELT =',F10.5,
     2'    TLEFT =',F7.2,' SEC   POW(',I2,') =',F7.3)
      WRITE(6,710) IM ,SDPM                                            4/1
710   FORMAT (' LARGEST NUMBER OF ITERATIONS IN THIS TIME STEP =',I4,
     1 ' ,SDPM = ',F12.8)                                              4/1
      WRITE(6,261)
261   FORMAT('0',10X,'GOLDN OUTPUT NEXT',//)
      WRITE(6,118)   (POW(L),L=1,NN)
118   FORMAT('0','POW(L),L=1,NN'/1X,10(F7.2,2X))
      WRITE(6,104)  (FLNC(L),L=1,NN)
104   FORMAT('0','FLUENCE(L),L=1,NN',/1X,10(E11.4))
      WRITE(6,100)  (TNA(L),L=1,NN)
100   FORMAT('0','COOLANT TEMPS AT THE MIDDLE OF EACH SECTION FOLLOW'/
     11X,10(F9.2))
 17   WRITE(6,121)  (TCLO(L),L=1,NN)
```

```
121  FORMAT('0','CLAD O.D.TEMPS AT THE MIDDLE OF EACH SECTION FOLLOW',/
    11X,10(F9.2))
     WRITE(6,271)
271  FORMAT('0',//,20X,'CLTMP OUTPUT NEXT',//)
     DO 1 J = 1,NN
     WRITE(6,273) J
273  FORMAT('0',1X,'AXIAL SECTION =',I2,/)
     WRITE(6,272) (J,K,R(J,K),J,K,T(J,K),K=1,7)
272  FORMAT(' ',1X,'R(',I2,',',I2,')=',E15.8,5X,'T(',I2,',',I2,')=',
    1E15.8)
     WRITE(6,274) J,TBC(J),ATBC(J)
274  FORMAT(2X,'TBC FOR SECTION',I3,'=',E15.8,3X,'ATBC FOR SAME SECTION
    1 =',E15.8)
 1   CONTINUE
     NF = NN-1
     N4 = N3-1
     WRITE(6,275)
275  FORMAT('0',//,20X,'FLTMP OUTPUT NEXT',//)
     DO 6 J = 1,NF
     HG = HG1(J)*144.
     HC=HC1(J)
     WFO = POW(J)
     TFO = TLR6(J,4)
     RFO = RLR6(J,4)
     SM = 0.
     DO 2 K = 1,3
     RHO(K) = RH(J,K)
     XM(K) = XMM6(J,K)/(1.+EPZO(J,K))
     DXM(K) = DXM6(J,K)
     TB(K) = TBF6(J,K)
     ATB(K) = ATBF6(J,K)
     SM = SM+XMM6(J,K)
 2   CONTINUE
     DO 3 K = 1,4
     TLR(K) = TLR6(J,K)
     RLR(K) = RLR6(J,K)
```

```
 3    CONTINUE
      DO 4 M = 1,N3
      TL(M) = TL6(J,M)
      RL(M) = RL6(J,M)
 4    CONTINUE
      SF = 0.
      DO 20 M = 1,N4
      F(M) = F7(J,M)
 20   SF = SF+F(M)
      DO 21 M = 1,N4
 21   F(M) = N4*F(M)/SF
      WRITE(6,273) J
      WRITE(6,444) HG,HC
444   FORMAT(2X,'HG =',E15.8,3X,'HC =',E15.8)
 5    WRITE(6,281) (RHC(M),M=1,3),RHOT,(XM(M),M=1,3),
     1(F(M),M=1,N4)
      WRITE(6,282) (RLR(M),M=1,4),(TLR(M),M=1,4),
     1(TB(M),M=1,3),(ATB(M),M=1,3),(RL(M),M=1,N3)
      WRITE(6,283) (TL(M),M=1,N3)
281   FORMAT('0',5X,'RHO(M),M=1,3',/5X,3E20.8,3X,'(THEORETICAL =',
     1E20.8,' )',/5X,'XM(M),M=1,3',/,
     25X,3E20.8/,5X,'F(M),M=1,N4'/(5X,6E15.8))
282   FORMAT(5X,'RLR(M),M=1,4'/5X,4E20.8/,5X,'TLR(M),M=1,4'/5X,4E20.8,
     1/5X,'TBM(M),M=1,3'/5X,3E20.8/5X,
     2'ATBM(M),M=1,3'/5X,3E20.8/5X,'RL(M),M=1,N3'/(5X,6E15.8,2X))
283   FORMAT(5X,'TL(M),M=1,N3'/(5X,6E15.8,2X))
 6    CONTINUE
      WRITE(6,10)
 10   FORMAT('0',//,20X,'GASOUT OUTPUT',//)
      TGS = 0.
      DO 7 J = 1,NF
      DO 7 K = 1,3
      TGS = TGS+GS(J,K)
      WRITE(6,12) J,K ,GS(J,K)
12    FORMAT(' ',5X,'AXIAL SECTION =',I2,5X,'RADIAL  ZONE   =',I2,5X,
     1'GAS REMAINING =',E15.8)
```

```
 7    CONTINUE
      X = TOGAS-GASI
      YP = 100.*X/(TGS+X)
      WRITE(6,14) X,YP
 14   FORMAT('0',5X,'CUMULATIVE GAS RELEASED =',E15.8,' MOLES,OR ',F5.2,
     1'% OF TOTAL FISSION GAS')
      WRITE(6,60) PLPR
 60   FORMAT('0',5X,'PLENUM PRESSURE =',E15.8)
      DO 8 J = 1,NN
      WRITE (6,70)
      POW1 = POW(J)
      WRITE(6,719) IT,TIT,POWAV,TOUT,TIN,DELT,TVZJ,J,POW1
      U11 = UDISP(J,1)
      U12 = UDISP(J,2)
      U22 = UDISP(J,3)
      U32 = UDISP(J,4)
      U41 = UDISP(J,5)
      U42 = UDISP(J,6)
      PR12 = XPR12(J)
      PR23 = XPR23(J)
      PRG = XPRG(J)
      IRW = IIRW(J)
      IF(J-NN) 488,80,80
 80   DO 81 LL=1,3
 81   SWS6(J,LL) = 0.
488   CALL RITE1(J,I1,SIGR,SIGC,SIGZ,EPR,EPC,EPZ,U11,U12,U22,U32,U41,
     1U42,DPR,DPC,DPZ,TPR,TPC,TPZ,DSR,DSC,DSZ,TSR,TSC,TSZ,SWS6,EHP6)
      DIM1A = RVB(J) + U11
      DIM1B = R1B(J) + U12
      DIM2B = REB(J) + U22
      DIM3B = RUB(J) + U32
      DIM4A = RCA(J) + U41
      DIM4B = R4B(J) + U42
      DDOD = ((DIM4B-R4BI(J))/R4BI(J))*100.
      IF(J-NN) 13,11,11
 11   DIM1A = 0.
```

```
      DIM1B = 0.
      DIM2B = 0.
      DIM3B = 0.
 13   WRITE(6,888) DIM1A,DIM1B,DIM2B,DIM3B,DIM4A,DIM4B
888   FORMAT(6X,'R1A',12X,'R1B',12X,'R2B',12X,'R3B',12X,'R4A',
     112X,'R4B  ',/6(F12.7,5X))
      WRITE(6,200) PLPR,PR12,PR23,PRG
200   FORMAT(6X,'PLPR',13X,'PR12',13X,'PR23',13X,'PRG',/4E17.8)
      IF(J.EQ.NN)GCTO 454
      IF(IRW) 451,452,453
451   WRITE(6,802)
      GO TO 454
452   WRITE(6,202)
      GO TO 454
453   WRITE(6,204)
202   FORMAT(54X,'GAP IS OPEN')                                        4/1
204   FORMAT(54X,'STICK ASSUMPTION IS VALID')                          4/1
802   FORMAT(54X,'SLIP ASSUMPTION IS IN EFFECT')                       4/1
454   WRITE(6,889) DDOD
889   FORMAT('0',5X,'PERCENT CHANGE IN  ORIGINAL O.D. =',F12.8)
 8    CONTINUE
      SSF = 0.
      SSC = 0.
      DO 9  J = 1,NN
      SSF = SSF+EPZ(J,1)
 9    SSC = SSC+EPZ(J,4)
      FFL = FL*(1.+(SSF-EPZ(NN,1))/(NN-1))
      CCL = FL*(1.+(SSC-EPZ(NN,4))/(NN-1 ))+(CL-FL)*(1.+EPZ(NN,4))
      WRITE(6,887) FFL,CCL
887   FORMAT(' 0',5X,'FUEL LENGTH =',F12.8,2X,'CLAD LENGTH =',F12.8)
1751  WRITE(6,212) DSMX1,SMEP,KONVER,IGRAPH
 212  FORMAT(1H,' DSMX1 =',E10.3,'    SMEP =',E10.3,/,' ****** >>>>
     1 NUMBER OF CONVERGED TIME STEPS =',I6,'     <<<< ******',//,' ****
     2** >>>>     NUMBER OF PRINTED TIME STEPS =',I6,'     <<<< ******',
     3//,' >> GO TO NEXT TIME STEP >> **********************************
     4**************************************************',//)
```

```
   70  FORMAT('1')
       RETURN
       END
       SUBROUTINE SWELL(SIGR,SIGC,SIGZ,J,TBAV,SS,POW,DELT,GS,FL,NF,TSR,   7/25
      1TSC,TSZ,SWS,SWS5,DSR,DSC,DSZ,FD,PRS,BM,EB,I1,PRSO,RHOT,RH,
      2 EHP,EHP6,ATB)
       DIMENSION SIGR(10,4),SIGC(10,4),SIGZ(10,4),TBAV(10,3),SS(10,4),
      1POW(10),GS(10,3),TSR(10,4),TSC(10,4),TSZ(10,4),SWS(10,3),SWS6(3), 7/25
      2DSR(10,4),DSC(10,4),DSZ(10,4),FD(10,3),PRS(10,4),BM(4),EB(3),
      3SWS5(10,3),PRSO(10,4),RH(3),BN(4),SWS7(3),EHP(10,3),EHP6(10,3),
      4 ATB(3)
       COMMON PI,N3
       COMMON/SACC/SAC1,SAC2,SACAN1,SACAN2,SACAN3,SAC3
       R9 = 8.31436*0.7376*12.
       SVPF = 0.70E-24
C***   NET SOLID VOLUME CREATED PER FISSION...R9 IS IDEAL GAS CONSTANT
C***   IN LBS*IN/MOLE/DEG K
       A91 = 9.3E+15
       DFN = A91*POW(J)*DELT
C***   DFN IS THE NUMBER OF FISSIONS IN THE CROSS-SECTION OF FUEL ROD
C***   OF ONE INCH IN HEIGHT.
C***   PG IS EFFECTIVE PRESSURE DUE TO SURFACE TENSION IN BUBBLE.
       DPG = 1.
       C = 5.56E+5
       QRK = 43800.
       DO 81 K = 1,3
       T          = (TBAV(J,K)-32.)*5./9.+273.
       CK = (DELT/2.)*(C/T)*EXP(-QRK/T)
       RHF = 1.-RH(K)/RHOT*(1.+3.*ATB(K))
       DSWS = SVPF*FD(J,K)*DFN
C***    FD IS EXPLAINED IN FLTMP SUBROUTINE
       SWS6(K) = SWS(J,K)+DSWS
       SWS6(K)=SACAN1*SWS6(K)
       SWS5(J,K) = SWS6(K)
       VOL = PI*SS(J,K)*FL/NF
       A2 = R9*T         *GS(J,K)/VOL
```

```
      A2=SACAN2*A2
C***  GS IS FISSION GAS IN MOLES CALCULATED IN GASOUT SUBROUTINE.
C**** BM(K) = (BULK MODULUS)*3.
      IF(K-2) 21,22,23
   21 PG = 500.
      GO TO 7
   22 PG = 1000.
      GO TO 7
   23 PG = 1000000.
      SWS6(K)=SWS6(K)+SACAN3*2.389*GS(J,K)/VOL
    7 CKNU = CK*(RHF - A2/(PRSO(J,K) + PG))                          7/22
      IF (CKNU) 15,16,16                                             7/22
   15 CKNU = 0.                                                      7/22
   16 SWS7(K) = SWS6(K) + EHP(J,K) - CKNU   * PRSO(J,K)              7/22
      A3 = A2                                                        7/22
      BN(K) = 1. / (1./BM(K) + CKNU  /3.)                            7/22
      C1 = (PG+(SWS7(K)/3.-EB(K))*BN(K))/2.
      C2 = A3*BN(K)/3.
      AW = C1*C1 + C2
      IF (AW)10,9,9
   10 SIG = PRSO(J,K)
      FSN = TSR(J,K)
      EHP6(J,K) = EHP(J,K)
      GO TO 8
    9 RT = SQRT( AW )
      IF(C1) 2,2,1
    1 X = C1+RT
      GO TO 3
    2 X = C2/(RT-C1)
    3 SIG = X-PG
      FSN = EB(K) + SIG/BM(K)
      Y = RHF-A2/X
      EHP6(J,K) = EHP(J,K)-CK*(SIG+PRSO(J,K))*Y
      IF(Y) 5,8,8
    5 IF(CK) 8,8,6
    6 CK = 0.
```

```
      GO TO 7
   8  PRS(J,K) = SIG
  33  DSR(J,K) = FSN-TSR(J,K)
      DSC(J,K) = FSN-TSC(J,K)
      DSZ(J,K) = FSN-TSZ(J,K)
      IF(FSN-1.) 81,4,4
   4  WRITE(6,100) T,CK,RHF,A2,A3,PRSO(J,K),BM(K),BN(K),SIG,K
 100  FORMAT(5E15.8/4E15.8,I15)
  81  CONTINUE
  14  RETURN
      END
      SUBROUTINE VZJRWW (J,NN,TPR,TPC,TPZ,TSR,TSC,TSZ,ATB,ATBC,RVB,R1B,
     1REB,RUB,RCA,R4B,ARTI,SS,FL,CL,RHO,RHOC,G,GNU,PLPR,PO,PTOP,PR12,
     2PR23,PRG,EPZO,EPZ,EPZM,EPZ4,FM,FMM,IRW,U41,U42)
      COMMON PI,N3
      DIMENSION TPR(10,4),TPC(10,4),TPZ(10,4),TSR(10,4),TSC(10,4),
     1TSZ(10,4),ATB(3),ATBC(10),RVB(10),R1B(10),REB(10),RUB(10),RCA(10),
     2R4B(10),ARTI(4),SS(10,4),RHO(3),G(4),GNU(4),EPZO(10,4),EPZ(10,4),
     3FM(10),FMM(10)
C *** GIVEN PLASTIC AND THERMAL DEFORMATIONS, VZJRWW CALCULATES TOTAL
C     AXIAL STRAINS AND INTERFACE PRESSURES IN AXIAL SECTION J *******
      IF(J-NN) 605,606,606
 605  CALL XHELP1(TPR,TPC,TSR,TSC,TSZ,ARTI,RVB,R1B,REB,G,GNU,PLPR,J,
     1X1,X2,X4,X5,X6,X7,X8,X9,X10,RUB )                              7/14
      CALL       XHELP2 (X1,X2,X4,X5,X6,X7,X8,X9,X10,PA0,PAZ,PAFC,PB0,  7/18
     1 PBZ,PBFC )                                                    7/18
C *** ASSUME GAP OPEN
 606    GNUC = GNU(4)
      GC  = G(4)
 555  CRO = R4B(J)
      CRI = RCA(J)
      IF(J-NN) 609,559,559
 609   FJ=J
 559  ZM =  (FL/(NN-1))*(FJ - 0.5)                                   7/10
 621  TPRC = TPR(J,4)
      TPCC = TPC(J,4)
```

```
      TPZC = TPZ(J,4)
      TSRC = TSR(J,4)
      TSCC = TSC(J,4)
      TSZC = TSZ(J,4)
  561 ATB4 = ATBC(J)
      R4BC = R4B(J)
      RCAC = RCA(J)
      IF (J-NN) 563,631,631
  631 CALL PHELPC(PLPR,PO,PTOP,GNUC,GC,CL,TPRC,TPCC,TPZC,TSRC,TSCC,TSZC,
     1ATB4,RHOC,CRO,CRI,P5,P6,P7,P8,FL)
      GO TO 567
  563 CALL PHELPM       (G,SS,GNU,ATB,TPR,TPC,TPZ,TSR,TSC,TSZ,RHO,RVB,
     1R1B,PLPR,PA0,PAZ,PAFC,REB,PB0,PBZ,PBFC,RUB,FL,ZM,P1,P2,P3,P4,J)
      CALL PHELP4(PLPR,PO,PTOP,GNUC,GC,CL,TPRC,TPCC,TPZC,TSRC,TSCC,TSZC,7/18
     1ATB4,RHOC,CRO,CRI,P5,P6,P7,P8,ZM)                                 7/18
  565 EPZ(J,1) =(P3*PLPR + P4)/P1
      EPZ(J,2) =EPZ(J,1)
      EPZ(J,3) =EPZ(J,1)
  567 EPZ(J,4) =(P7*PLPR+P8)/P5
      IF(J-NN)568,569,569
  568 EPZM = EPZ(J,1)
  569 EPZ4 = EPZ(J,4)
      IF(J-NN) 570,571,571
  570 PR23=(X6*(X4*EPZ(J,1)+X5)-X1*X9*EPZ(J,1)-X1*(X10-X8*PLPR))/(X1*X7 7/7
     1+X2*X6)
      PR12 = (X2*PR23-X4*EPZ(J,1)-X5)/X1
  571  PFC = PLPR
      PRG = PFC
      IF(J-NN) 613,578,578
  613  TPR33 = TPR(J,3)
  575 TPC33 = TPC(J,3)
      TSR33 = TSR(J,3)
      TSC33 = TSC(J,3)
      TSZ33 = TSZ(J,3)
      ARTI3 = ARTI(3)
      RUB3  = RUB(J)
```

```
      REB3  = REB(J)
      G33 = G(3)
      GNU3  = GNU(3)
      CALL ANQUAN(TPR33,TPC33,TSR33,TSC33,TSZ33,ARTI3,RUB3,REB3,RUB3,
     1G33,GNU3,ANA1,ANA2,ANA3,ANA4,AN31,AN32,AN33,AN34)                    7/14
  577 U3B =-AN31*PR23-AN32*PFC-AN33*EPZ(J,3)-AN34                          7/7
  578 TPR44 = TPR(J,4)
      TPC44 = TPC(J,4)
      TSR44 = TSR(J,4)
      TSC44 = ISC(J,4)
      TSZ44 = TSZ(J,4)
      ARTI4 = ARTI(4)
      R4B4  =R4B(J)
      RCA4  =RCA(J)
      G44   = G(4)
      GNU44 = GNU(4)
      CALL ANQUAN (TPR44,TPC44,TSR44,TSC44,TSZ44,ARTI4,R4B4,RCA4,RCA4,
     1G44,GNU44,AN41,AN42,AN43,AN44,ANB1,ANB2,ANB3,ANB4)                  7/14
  581 UCA = -AN41*PFC -AN42*PO -AN43*EPZ(J,4) -AN44
      U41 = UCA
      IF(J-NN) 585,582,582
  582 U42 = -ANB1*PFC -ANB2*PO -ANB3*EPZ(J,4) -ANB4                        7/14
      GO TO 907
  585 GAP = RCA(J) - RUB(J)
      FMM(J) = 0.7
      TV1 = UCA-U3B+ GAP
      IF(TV1) 701,701,907
C *** CHECK FOR GAP CLOSURE
  701 X11 = AN31
      X13 = AN33
      X12 = AN32 - AN41
      X14 = -AN43
      X15 = -AN42 *PO + AN34 -AN44 - RUB(J) + RCA(J)
      CALL PVHELP(X1,X2,X4,X5,X6,X7,X8,X9,X10,X11,X12,X13,X14,X15,
     1P1,P2,P3,P4,P5,P6,P7,P8,VV1,VV2,VV3, P9, P10, P11, P12,VV4,VV5,
     2VV6,VV7,EPZO,J)
```

```
      FMU = FM(J)                                                        10/26
      VV8 = FL*FMU*PI*RCA(J)
C *** ASSUME STICK
  731 EPZFC = VV6/VV7
      FRIC  = VV4*EPZFC + VV5
      PFC1 = (-(P9+P10)*EPZFC -P12)/P11
      PRG = PFC1
      EPZFU = EPZO(J,3)+EPZFC
      EPZCL = EPZO(J,4)+EPZFC
      PR23 = VV1*EPZFU+VV2*PFC1+VV3
      PR12 = (X2*PR23-X4*EPZFU-X5)/X1
      AFRIC = ABS( FRIC )                                                10/26
      FMM(J) = 0.8
      TV2 =AFRIC  - VV8*PFC1                                             10/26
      IF (TV2)  901,751,751
C *** CHECK FOR STICK
  751 FMU = FM(J)                                                        10/26
C 751 FMU = 0.7  MIGHT LEAD TO DIVERGENCIES.
      FMM(J) = 0.7
      VV8 = FL*FMU*PI*RCA(J) *FRIC/AFRIC                                 10/26
      CALL VHELP2(P1,P2,P3,P4,P5,P6,P7,P8,VV8,VV9,VV10,VV11,VV12)
      EPZM =  -(P10*VV12 +P11*VV10 +P12)/(P9+P10*VV11+ P11*VV9)
  753 EPZ4 = VV11*EPZM  + VV12
      EPZ(J,1) = EPZM+EPZO(J,1)
      EPZ(J,2) = EPZM+EPZO(J,2)
      EPZ(J,3) = EPZM+EPZO(J,3)
  943 EPZ(J,4) = EPZ4+EPZO(J,4)
      PFC2 =  VV9*EPZM +VV10
      PRG = PFC2
      PR23 = VV1*EPZ(J,3)+VV2*PFC2+VV3
      PR12 = (X2*PR23-X4*EPZ(J,3)-X5)/X1
      EPZM = EPZ(J,3)                                                    10/27
      EPZ4 = EPZ(J,4)                                                    10/27
      IRW = -1
      GO TO 907
  901 IRW = 1
```

```
      EPZ(J,1) = EPZO(J,1)+EPZFC
      EPZ(J,2) = EPZO(J,2)+EPZFC
      EPZ(J,3) = EPZO(J,3)+EPZFC
      EPZ(J,4) = EPZO(J,4)+EPZFC
      EPZM = EPZFU
      EPZ4 = EPZCL
  907 RETURN
      END
      SUBROUTINE ABDE(ERP2,ECP2,ERS2,ECS2,EZS2,GMOD,RI,RO,AR,BR,DR,ER,
     1 CR,FR )                                                          7/14
      S1 = RO*RO-RI*RI
      W = RO/RI
      W1 = W-1.
      IF(W1)8,8,9
    8 W = .0001
      WRITE(6,12)
   12 FORMAT(5X,'RO/RI WAS LESS THAN 1.0 IN ABDE',//)
    9 S2 = ALOG(W)*GMOD
      S3 =(S1/(RO*RO))*GMOD
      AR = (ERP2+ECP2)*S3
      BR = (ECP2-ERP2)*2.*S2
      CR =(-ERP2+ECP2)*S3                                               7/14
      DR = (ERS2+ECS2)*S3
      ER = (ECS2-ERS2)*2.*S2
      FR =(-ERS2+ECS2)*S3                                               7/14
      RETURN
      END
      SUBROUTINE AMQUAN(ERP5,ECP5,ERS5,ECS5,EZS5,ARTI5,RO5,RI5,G5,GNU5,
     1AM11,AM22,AM33,AM44,AM55,AM66,AM77)
      S10 = 1.-GNU5
      S11 = (1.-2.*GNU5)/(2.*G5)
      S12 = (RO5 * RO5 - RI5*RI5)
      S13 = (RO5*RO5)/S12
      S14 = ERS5 + ECS5 + EZS5
      S15 = (GNU5/(S10*RO5))*S14*S12/2.
      S16 = ((1.+GNU5)/(S10*RO5))*ARTI5
```

```
      CALL ABDE(ERP5,ECP5,ERS5,ECS5,EZS5,G5,RI5,RO5,AR,BR,DR,ER,CR,FR)   7/14
      S17 = ((S11*RO5)/(2.*S10))*(AR+DR-BR-ER)
      AM11 = S15 + S16 + S17
      AM22 = (RI5 *RI5*S13)/(2.*G5)
      AM33 = -AM22
      CALL D1D2(ERP5,ECP5,ERS5,ECS5,EZS5,ARTI5,RI5,RO5,G5,GNU5,D1,D2)
      AM44 = AM22*(D1+D2)
      AM66 = -S11* S13
      AM55 = -S11-AM66
      AM77 = -AM66 * (D1+D2)
      RETURN
      END
      SUBROUTINE ANQUAN(ERP6,ECP6,ERS6,ECS6,EZS6,ARTI6,RO6,RI6,R,G6,
     1GNU6,AN1A,AN2A,AN3A,AN4A,AN1B,AN2B,AN3B,AN4B )                     7/14
      CALL AMQUAN(ERP6,ECP6,ERS6,ECS6,EZS6,ARTI6,RO6,RI6,G6,GNU6,AM11,
     1AM22,AM33,AM44,AM55,AM66,AM77)
      RR = RI6                                                          7/14
      AN1A = -(AM22/RR) - (RR*AM55)
      AN2A = -(AM33/RR) - (RR*AM66)
      AN3A = GNU6 * RR
      AN4A = -((AM44/RR)+ RR*AM77 )                                     7/14
      RR = RO6                                                          7/14
      AN1B = -(AM22/RR) - (RR*AM55)
      AN2B = -(AM33/RR) - (RR*AM66)
      AN3B = GNU6 * RR
      AN4B = -((AM44/RR)+ RR*AM77 + AM11)                               7/14
      RETURN
      END
      SUBROUTINE CLTMP(LL,WFC,TCLO,RCLO,RCLI,A0,A1,ALF0,ALF1,R,T,TBC,
     1ATBC)
      DIMENSION  WFO(10),TCLO(10),RCLO(10),RCLI(10),R(10,7),T(10,7),
     1TBC(10),ATBC(10),A(7)
      COMMON PI,N3
C *** CLDTMP CALCULATIONS IN UNITS OF BTU,HR,IN,DEG F
      W = WFO(LL)/PI
      W = W*3414./12.
```

```
C *** W FROM KW/FT TO BTU/HR/IN
      AK =(A0 + A1*TCLO(LL)) /12.
C *** CONDUCTIVITY NOW IN BTU/HR/IN
      AK2 = AK*AK
      A(1) =  41./140.
      A(2) = 216./140.
      A(3) =  27./140.
      A(4) = 272./140.
      A(5) =  27./140.
      A(6) = 216./140.
      A(7) =  41./140.
C     INTEGRATION BY WEDDLE'S RULE = NEWTON-COTES-6
      DR =  (RCLO(LL)-RCLI(LL))/6.
      S=0.
      S1=0.
      DO 1  K = 1,7
      R(LL,K) = RCLI(LL) + DR*( K-1)
      XL = ALOG(RCLO(LL)/R(LL,K))
      T(LL,K) = TCLO(LL)+W*XL/(AK+SQRT(AK2+A1*W*XL/12.))
      S1 = S1 + A(K)*R(LL,K)*(ALF0*T(LL,K)+ALF1*T(LL,K)**2/2.
     1  -ALF0*68. -ALF1*2312.)
      S = S + A(K)*R(LL,K)*T(LL,K)
    1 CONTINUE
      TBC(LL)= S/(RCLO(LL)+RCLI(LL))/3.
      ATBC(LL) =  S1/(RCLO(LL)+RCLI(LL))/3.
      RETURN
      END
      SUBROUTINE CONVG(J,I1,SDEP,PR12,PR23,PRG,IRW,IM,SDPM,SUMDS,
     1CPRS,PRS,SUMDS1,SDEP2,NN,SIGRO,SIGCO,SIGZO,SIGR,SIGC,SIGZ,DEB,EB,
     2EBO,ATBF6,PRSO,DER,DEC,DEZ,EPR,EPC,EPZ,EPRO,EPCO,EPZO,DERO,DECO,
     3DEZO,DELTO,DELT,TVZJ,PRT,MNO,CIM)
      DIMENSION PRT(10),PRS(10,4),CPRS(4),   SIGRO(10,4),SIGCO(10,4),
     1SIGZO(10,4),SIGR(10,4),SIGC(10,4),SIGZ(10,4),DEB(10,4),EB(3),
     2EBO(10,4),ATBF6(10,3),PRSO(10,4),DER(10,4),DEC(10,4),DEZ(10,4),
     3EPR(10,4),EPC(10,4),EPZ(10,4),EPRO(10,4),EPCO(10,4),EPZO(10,4),
     4DERO(10,4),DECO(10,4),DEZO(10,4)
```

```
454   TVZJ = TLEFT(1.)/100.
      PRT(J) = PRG
      MNO = 1
      IF (IM - I1) 457,458,458
 457  IM = I1
 458  CIM = IM
      IF(SDPM-SDEP) 459,460,460
459   SDPM = SDEP
460   PRS(J,1) = CPRS(1)
      PRS(J,4) = CPRS(4)
      IF(SUMDS-SUMDS1) 486,486,485
485   SUMDS1 = SUMDS
486   IF(SDEP-SDEP2) 488,488,487
487   SDEP2 = SDEP
 488  K$ = 1
      IF(J-NN)428,430,430
 430  K$ = 4
 428  DO 188 K=K$,4
      SIGRO(J,K)=SIGR(J,K)
      SIGCO(J,K) = SIGC(J,K)
      SIGZO(J,K) = SIGZ(J,K)
      PRSO(J,K) = PRS(J,K)
      DER(J,K) = EPR(J,K) - EPRO(J,K)
      DEC(J,K) = EPC(J,K) - EPCO(J,K)
      DEZ(J,K) = EPZ(J,K) - EPZO(J,K)
      DERO(J,K) = DER(J,K)
      DECO(J,K) = DEC(J,K)
188   DEZO(J,K) = DEZ(J,K)
      DELTO = DELT
      RETURN
      END
      SUBROUTINE D1D2(ERP,ECP,ERS,ECS,EZS,ARTDR,RA,RB,GM,GNU,D1,D2)
      S4 =1./(2.*(1.-GNU))
      S5 = 2.*GM/(RB*RB*(1.-GNU))
      S6 = 1.-(2.*GNU)
      CALL ABDE(ERP,ECP,ERS,ECS,EZS,GM,RA,RB,AR,BR,DR,ER,CR,FR)
```

```
      S7 = ERS + ECS + EZS
      S8 = RB*RB-RA*RA
      D1 = S4*(S6*AR+BR)+S5*(1.+GNU)*ARTDR
      D2 = S4*(S6*DR+ER)+S5*GNU*S7*(S8/2.)
      RETURN
      END
      SUBROUTINE  DISPL (TPRX,TPCX,TSRX,TSCX,TSZX,ATBCX,ATBFX,RVBX,R1BX,
     1REBX,RUBX,RCAX,R4BX,GX,GNUX, JX,PLPRX,PR12X,PR23X,PRFCX,POX,EPZMX,
     2EPZCX,U11X,U12X,U22X,U32X,U41X,U42X,SSX)
      DIMENSION TPRX(10,4),TPCX(10,4),TSRX(10,4),TSCX(10,4),TSZX(10,4),
     1ATBCX(10),ATBFX(10,3),RVBX(10),R1BX(10),REBX(10),RUBX(10),RCAX(10)
     2,R4BX(10),GX(4),GNUX(4),SSX(10,4)
      DO 939 L =1,4
      TPRY = TPRX(JX,L)
      TPCY = TPCX(JX,L)
      TSRY = TSRX(JX,L)
      TSCY = TSCX(JX,L)
      TSZY = TSZX(JX,L)
      IF (L-3) 919,919,921
  919 ARTIY = ATBFX(JX,L)*SSX(JX,L) /2.                                  7/7
      GO TO  923
  921 ARTIY = ATBCX(JX)*SSX(JX,L) /2.                                    7/7
  923 RVBY = RVBX(JX)
      R1BY = R1BX(JX)
      REBY = REBX(JX)
      RUBY = RUBX(JX)
      RCAY = RCAX(JX)
      R4BY = R4BX(JX)
      GY   = GX(L)
      GNUY = GNUX(L)
      IF (L-3) 933,929,927
  927 CALL ANQUAN(TPRY,TPCY,TSRY,TSCY,TSZY,ARTIY,R4BY,RCAY,R4BY,GY,GNUY,
     1YNA1,YNA2,YNA3,YNA4,YNB1,YNB2,YNB3,YNB4)                          7/15
      U42X = -( YNB1*PRFCX + YNB2*POX +YNB3*EPZCX + YNB4)                7/15
      U41X = -(YNA1*PRFCX + YNA2*POX +YNA3*EPZCX + YNA4)                 7/15
      GO TO 939
```

```
  929 CALL ANQUAN(TPRY,TPCY,TSRY,TSCY,TSZY,ARTIY,RUBY,REBY,RUBY,GY,GNUY,
     1YNA1,YNA2,YNA3,YNA4,YNB1,YNB2,YNB3,YNB4)                          7/15
      U32X = -(YNB1*PR23X + YNB2*PRFCX + YNB3*EPZMX +YNB4)              7/15
      GO TO 939
  933 IF (L-1) 939,937,935
  935 CALL ANQUAN(TPRY,TPCY,TSRY,TSCY,TSZY,ARTIY,REBY,R1BY,RUBY,GY,GNUY,7/15
     1YNA1,YNA2,YNA3,YNA4,YNB1,YNB2,YNB3,YNB4)                          7/15
      U22X = -(YNB1*PR12X + YNB2*PR23X + YNB3*EPZMX +YNB4)              7/15
      GO TO 939
  937 CALL ANQUAN(TPRY,TPCY,TSRY,TSCY,TSZY,ARTIY,R1BY,RVBY,R1BY,GY,GNUY,
     1YNA1,YNA2,YNA3,YNA4,YNB1,YNB2,YNB3,YNB4)                          7/15
      U12X = -(YNB1*PLPRX +YNB2*PR12X +YNB3*EPZMX + YNB4)               7/15
      U11X = -(YNA1*PLPRX + YNA2*PR12X + YNA3*EPZMX + YNA4)             7/15
  939 CONTINUE
      RETURN
      END
      SUBROUTINE EQUIEP (EP1,EP2,EP3,EPSEQ)
      D1 = EP1 - EP2
      D2 = EP1 - EP3
      D3 = EP2 - EP3
      EPSEQ = SQRT((D1*D1+D2*D2+D3*D3)*2.)/3.
      RETURN
      END
      SUBROUTINE EQUISI (S1,S2,S3,SIGEQ)
      D4 = S1-S2
      D5 = S1-S3
      D6 = S2-S3
      SIGEQ = SQRT((D4*D4+D5*D5+D6*D6)/2.)
      RETURN
      END
      SUBROUTINE PHELP4 (PPLEN,PCOO,PTOP,CNU,CG,CL,CPRAV,CPCAV,CPZAV,   7/18
     1CSRAV,CSCAV,CSZAV,CATAV,CRHO,CRO,CRI,PP5,PP6,PP7,PP8,FZ)          7/18
      COMMON PI,N3
      GRAV = 0.036127                                                   7/10
C *** GRAV IS THE WEIGHT OF ONE CUBIC INCH OF WATER IN POUNDS.          7/15
      CARTI = CATAV*(CRO*CRO - CRI*CRI) / 2.                            7/7
```

```
      CALL AMQUAN(CPRAV,CPCAV,CSRAV,CSCAV,CSZAV,CARTI,CRO,CRI,CG,CNU,    7/7
     1CM11,CM22,CM33,CM44,CM55,CM66,CM77)
      PP5 = 1. + CNU
      PP6 = 1./(2.*CG*PI*(CRO*CRO-CRI*CRI))
      PP7 = (-2.*CNU*CM55)/(1.-2.*CNU)
   28 S25 = 1./(2.*CG*PI*(CRO*CRO-CRI*CRI))
      S26 = -PTOP -PI*(CRO*CRO*PCOO -CRI*CRI*PPLEN)
      S27 = -CRHO*GRAV*PI*(CRO*CRO-CRI*CRI)*(CL*(1.-(FZ/CL)))
      S28 = CPZAV +CSZAV +((1.+CNU)/(1.-CNU))*CATAV
      S29 = ((-2.*CNU)/(1.-2.*CNU))*(CM66*PCOO+CM77)
      S30 = CSRAV + CSCAV + CSZAV
      CALL ABDE(CPRAV,CPCAV,CSRAV,CSCAV,CSZAV,CG,CRI,CRO,ARC,BRC,DRC,
     1ERC,CRC,FRC)                                                      7/15
      X = CRO*CRO/(CRO*CRO -CRI*CRI)                                    7/15
      BB =(BRC - CRC)*X                                                 7/15
      EB =(ERC - FRC)*X                                                 7/15
      S31 = (CNU/(1.-CNU))*(S30-CPRAV-CSRAV+(BB +EB )/(2.*CG))          7/15
      PP8 = S25*(S26+S27)+S28+S29+S31
      RETURN
      END
      SUBROUTINE PHELPC (PPLEN,PCOO,PTOP,CNU,CG,CL,CPRAV,CPCAV,CPZAV,
     1CSRAV,CSCAV,CSZAV,CATAV,CRHO,CRO,CRI,PP5,PP6,PP7,PP8,FL)
      COMMON PI,N3
      GRAV = 0.036127                                                   7/10
C *** GRAV IS THE WEIGHT OF ONE CUBIC INCH OF WATER IN POUNDS.          7/15
      PP5 = 1. + CNU
      PP6 = 1./(2.*CG*PI*(CRO*CRO-CRI*CRI))
      CARTI = CATAV*(CRO*CRO - CRI*CRI) / 2.                            7/7
      CALL AMQUAN(CPRAV,CPCAV,CSRAV,CSCAV,CSZAV,CARTI,CRO,CRI,CG,CNU,   7/7
     1CM11,CM22,CM33,CM44,CM55,CM66,CM77)
      PP7 = (-2.*CNU*CM55)/(1.-2.*CNU)
      S25 = PP6
      S26 = -PTOP -PI*(CRO*CRO*PCOO -CRI*CRI*PPLEN)
      S27 = -CRHO*GRAV*PI*(CRO*CRO-CRI*CRI)*(2.*CL-FL)/2.
      S28 = CPZAV +CSZAV +((1.+CNU)/(1.-CNU))*CATAV
      S29 = ((-2.*CNU)/(1.-2.*CNU))*(CM66*PCOO+CM77)
```

```
      S30 = CSRAV + CSCAV + CSZAV
      CALL ABDE(CPRAV,CPCAV,CSRAV,CSCAV,CSZAV,CG,CRI,CRO,ARC,BRC,DRC,
     1ERC,CRC,FRC)                                                    7/15
      X = CRO*CRO/(CRO*CRO -CRI*CRI)                                  7/15
      BB =(BRC - CRC)*X                                               7/15
      EB =(ERC - FRC)*X                                               7/15
      S31 = (CNU/(1.-CNU))*(S30-CPRAV-CSRAV+(BB +EB )/(2.*CG))        7/15
      PP8 = S25*(S26+S27)+S28+S29+S31
      RETURN
      END
      SUBROUTINE  PHELPF(FNU,FG,FL,FPRAV,FPCAV,FPZAV,FSRAV,FSCAV,FSZAV, 7/18
     1FATAV,FRHO,FZ,FRO,FRI,PPLEN,PI0,PIZ,PIFC,P00,POZ,POFC,PP1,PP2,PP3,7/18
     2 PP4 )                                                          7/18
      COMMON PI,N3
      GRAV = 0.036127                                                 7/10
C *** GRAV IS THE WEIGHT OF ONE CUBIC INCH OF WATER IN POUNDS.        7/15
      FARTI = FATAV*(FRO*FRO - FRI*FRI) / 2.                          7/7
      CALL AMQUAN(FPRAV,FPCAV,FSRAV,FSCAV,FSZAV,FARTI,FRO,FRI,FG,FNU,  7/7
     1FM11,FM22,FM33,FM44,FM55,FM66,FM77)
      PP1 = 1. + FNU + 2.*FNU/(1.-2.*FNU)*(FM55*PIZ + FM66*POZ)       7/18
      PP2= (FZ-FL)/(2.*FG*PI*FL*(FRO*FRO-FRI*FRI))
      PP3 =       -2.*FNU/(1.-2.*FNU)*(FM55*PIFC + FM66*POFC)         7/18
      S20 = PPLEN + FRHO*GRAV*(FL-FZ)
      S21 = ((1.+FNU)/(1.-FNU))*FATAV
      S22 = ((-2.*FNU)/(1.-2.*FNU))*(FM55*PI0 + FM66*P00+ FM77)       7/18
      CALL ABDE(FPRAV,FPCAV,FSRAV,FSCAV,FSZAV,FG,FRI,FRO,ARF,BRF,DRF,
     1ERF,CRF,FRF)                                                    7/15
      S23 = FSRAV + FSCAV + FSZAV
      X = FRO*FRO/(FRO*FRO -FRI*FRI)                                  7/15
      BB =(BRF - CRF)*X                                               7/15
      EB =(ERF - FRF)*X                                               7/15
      S24 = (-FNU/(1.-FNU))*(FPRAV+FSRAV-S23-(BB +EB )/(2.*FG))       7/15
      PP4 = -S20/(2.*FG) + FPZAV+FSZAV+S21 +S22 +S24
      RETURN
      END
      SUBROUTINE PHELPM(G,SS,GNU,ATB,TPR,TPC,TPZ,TSR,TSC,TSZ,RHO,RVB,
```

```
     1R1B,PLPR,PA0,PAZ,PAFC,REB,PB0,PBZ,PBFC,RUB,FL,ZM,P1,P2,P3,P4,J)
      COMMON PI,N3
      DIMENSION G(4),SS(10,4),ATB(3),TPR(10,4),TPC(10,4),TPZ(10,4),
     1TSR(10,4),TSC(10,4),TSZ(10,4),RHO(3),RVB(10),R1B(10),REB(10),
     2RUB(10),W(3),GNU(4)
      SW = G(1)*SS(J,1)+G(2)*SS(J,2)+G(3)*SS(J,3)
      P1 = 0.                                                          7/18
      P2 = 0.                                                          7/18
      P3 = 0.                                                          7/18
      P4 = 0.                                                          7/18
      DO 197 K=1,3                                                     7/18
      GNUF = GNU(K)                                                    7/18
      GF = G(K)                                                        7/18
      W(K) = GF*SS(J,K)/SW                                             7/18
      ATBF = ATB(K)                                                    7/18
       PRAVF = TPR(J,K)                                                7/18
      PCAVF = TPC(J,K)                                                 7/18
      PZAVF = TPZ(J,K)                                                 7/18
      SRAVF = TSR(J,K)                                                 7/18
      SCAVF = TSC(J,K)                                                 7/18
      SZAVF = TSZ(J,K)                                                 7/18
      RHOF = RHO(K)                                                    7/18
      IF (K - 2) 193,194,195                                           7/18
  193 RI = RVB(J)                                                      7/18
      RO = R1B(J)                                                      7/18
      PI0 = PLPR
      PIZ = 0.                                                         7/18
      PIFC = 0.                                                        7/18
      PO0 = PA0                                                        7/18
      POZ = PAZ                                                        7/18
      POFC = PAFC                                                      7/18
      GO TO 196                                                        7/18
  194 RI = R1B(J)                                                      7/18
      RO = REB(J)                                                      7/18
      PI0= PA0                                                         7/18
      PIZ = PAZ                                                        7/18
```

```
      PIFC = PAFC                                                          7/18
      PO0 = PB0                                                            7/18
      POZ = PBZ                                                            7/18
      POFC = PBFC                                                          7/18
      GO TO 196                                                            7/18
  195 RI = REB(J)                                                          7/18
      RO = RUB(J)                                                          7/18
      PI0= PB0                                                             7/18
      PIZ = PBZ                                                            7/18
      PIFC = PBFC                                                          7/18
      PO0 = 0.                                                             7/18
      POZ = 0.                                                             7/18
      POFC = 1.                                                            7/18
  196 CALL PHELPF(GNUF,GF,FL,PRAVF,PCAVF,PZAVF,SRAVF,SCAVF,SZAVF,ATBF,     7/18
     1RHOF,ZM,RO  ,RI  ,PLPR,PI0,PIZ,PIFC,PO0,POZ,POFC, Y1, Y2, Y3, Y4)   7/18
      P1 = P1 +Y1*W(K)                                                     7/18
      P2 = P2+Y2*W(K)/3.                                                   7/25
      P3 = P3 +Y3*W(K)                                                     7/18
  197 P4 = P4 +Y4*W(K)                                                     7/18
      RETURN
      END
      SUBROUTINE PLENP (JJ,RLR,TLR,R,T,TOUT,FL,CL,TOGAS,PLPR)
C ***
C ***  THIS VERSION OF PLENP INCLUDES BOTH THE VOID VOLUME AND THE GAP
C ***  VOLUME IN ADDITION TO THE PLENUM VOLUME IN THE CALCULATION OF
C ***  THE PLENUM PRESSURE.
C ****  TO INCLUDE THIS MODEL MODIFICATION, IT IS NECESSARY TO CHANGE
C ****  THE SUBROUTINE CALL STATEMENT (537) IN THE MAIN PROGRAM TO :
C 537 CALL PLENP (NN,RLR6,TLR6,R,T,TOUT,FL,CL,TOGAS,PLPR)
C ***
      DIMENSION RLR(10,4),TLR(10,4),R(10,7),T(10,7)
      COMMON PI,N3
C ***
C ***  SET UP THE NUMBER OF AXIAL FUEL REGIONS.
C ***
      IF (JJ - 1)  10,10,20
```

```
   10 J = JJ
      GO TO 30
   20 J = JJ - 1
   30 CONTINUE
      RPLEN = R(JJ,1)
      VPLEN = PI*RPLEN*RPLEN*(CL - FL)
      TPLENK = (TOUT - 32.)*(5./9.) + 273.
C ***
C ***  INITIALIZE THE GAP AND VOID VOLUMES AND VOLUME/TEMPERATURE
C ***  QUOTIENTS.
C ***
   40 VVOID  = 0.0
      VGAP   = 0.0
      VTVOID = 0.0
      VTGAP  = 0.0
   50 DO 80  I = 1,J
      RVOID = RLR(I,1)
      ROFUEL = RLR(I,4)
      RICLAD = R(I,1)
C ***
C ***  CALCULATE THE GAP AND VOID VOLUMES.
C ***
      VVOIDI = PI*RVOID*RVOID*FL/FLOAT(J)
      VGAPI = PI*(RICLAD + ROFUEL)*(RICLAD - ROFUEL)*FL/FLOAT(J)
      VVOID = VVOID + VVOIDI
      VGAP = VGAP + VGAPI
   60 CONTINUE
      TVOIDK = (TLR(I,1) - 32.)*(5./9.) + 273.
      TOFUEL = (TLR(I,4) - 32.)*(5./9.) + 273.
      TICLAD =   (T(I,1) - 32.)*(5./9.) + 273.
      TGAPK = (TOFUEL + TICLAD)/2.
C ***
C ***  CALCULATE THE TEMPERATURE AVERAGED VOLUMES FOR VOID AND GAP.
C ***
   70 VTVOID = VTVOID + VVOIDI/TVOIDK
      VTGAP = VTGAP + VGAPI/TGAPK
```

```
   80 CONTINUE
C ***
C ***  CALCULATE THE TOTAL VOLUME AND VOLUME AVERAGED TEMPERATURE FOR
C ***  THE PIN GAS.
C ***
      VOLTOT = VPLEN + VVOID + VGAP
      VTTOT = VPLEN/TPLENK + VTVOID + VTGAP
      TAVGK = VOLTOT/VTTOT
C
C      RK IS IN LBS*IN/MOLE/DEG K
      RK = 8.31436*0.7376*12.
C ***
C ***  CALCULATE THE PLENUM GAS PRESSURE.
C ***
      PLPR = (TOGAS*RK*TAVGK)/VOLTOT
      RETURN
      END
      SUBROUTINE PVHELP(X1,X2,X4,X5,X6,X7,X8,X9,X10,X11,X12,X13,X14,X15,
     1P1,P2,P3,P4,P5,P6,P7,P8,VV1,VV2,VV3,PP9,PP10,PP11,PP12,VV4,VV5,
     2VV6,VV7,EPZO,J)
      DIMENSION EPZO(10,4)
      D = X2*X6 + X1*X7                                                  7/18
      VV2 = (X8*X1)/D                                                    7/18
      VV1 = (X6*X4-X1*X9)/D                                              7/18
      VV3 =     (X6*X5 -X1*X10)/D                                        7/18
      PP9 = X11*VV1 + X13
      PP10= X14
      PP11= X11*VV2 +X12
      PP12= X11*VV3 +X15
      VV4 = (P5*PP11 +P7*(PP9+PP10))/(P6*PP11)
      P4 = P4-P1*EPZO(J,3)
      P8 = P8-P5*EPZO(J,4)
      PP12 = PP12+PP9*EPZO(J,3)+PP10*EPZO(J,4)
      VV5 = (P7*PP12-PP11*P8)/(PP11*P6)
      VV6 = P2*VV5-(P3*PP12)/PP11+P4
      VV7 = P1 -P2*VV4 + P3*(PP9+PP10)/PP11
```

```
C *** COMPUTE VV8 IN MAIN PROGRAM
      RETURN
      END
      SUBROUTINE STRAIN  (RVB,R1B,REB,RUB,RCA,R4B,U11,U12,U22,U32,U41,
     1U42,PLPR,PR12,PR23,PRG,PO,TPR,TPC,TPZ,TSR,TSC,TSZ,ATBC,ATBF6,
     2EPZM,EPZ4,G,GNU,ARTI,J,NN,EPC,EPR)
      DIMENSION RVB(10),R1B(10),REB(10),RUB(10),RCA(10),R4B(10),TPR(10,4
     1),TPC(10,4),TPZ(10,4),TSR(10,4),TSC(10,4),TSZ(10,4),ATBC(10),
     2ATBF6(10,3),G(4),GNU(4),ARTI(4),EPC(10,4),EPR(10,4)
      K$ = 1
      IF(J-NN) 11,10,10
   10 K$ = 4
   11 DO 5 K=K$,4
      EEPR=TPR(J,K)
      EEPC = TPC(J,K)
      EEPZ = TPZ(J,K)
      ESR = TSR(J,K)
      ESC = TSC(J,K)
      ESZ = TSZ(J,K)
      XNU = GNU(K)
      XG = G(K)
      ARTI5 = ARTI(K)
      IF(K-3) 13,13,14
   13 AT = ATBF6(J,K)
      EZ = EPZM
      IF(K-2) 1,2,3
    1 RI = RVB(J)
      RO = R1B(J)
      UI = U11
      UO = U12
      PRI = PLPR
      PRO = PR12
      GO TO 4
    2 RI = R1B(J)
      RO = REB(J)
      UI = U12
```

```
      UO = U22
      PRI = PR12
      PRO = PR23
      GO TO 4
3     RI = REB(J)
      RO = RUB(J)
      UI = U22
      UO = U32
      PRI = PR23
      PRO = PRG
      GO TO 4
14    AT = ATBC(J)
      EZ = EPZ4
      RI = RCA(J)
      RO = R4B(J)
      UI = U41
      UO = U42
      PRI = PRG
      PRO = PO
4     CALL AMQUAN(EEPR,EEPC,ESR,ESC,ESZ,ARTI5,RO,RI,XG,XNU,AM1,AM2,AM3,
     1AM4,AM5,AM6,AM7)
      C1 = 2.*(ALOG(RO/RI))/(RO+RI)/(RO-RI)
      C2 = (1.-RI*RI*C1)/2.
      C3 = (1.-RO*RO*C1)/2.
      XNU1 = XNU/(1.-XNU)
      XNU2 = 1.+2.*XNU1
      XNU3 = (1.-XNU1)/2.
      ES = ESR+ESC+ESZ
      EC = C1*(AM2*PRI+AM3*PRO+AM4)+AM5*PRI+AM6*PRO-XNU*EZ+AM7+C2*(XNU1
     1*ES+XNU2*AT+XNU3*(EEPR+EEPC+ESR+ESC))+C3*XNU3*(-EEPR+EEPC-ESR+ESC)
      ER = -EC+2.*(UO*RO-UI*RI)/(RO+RI)/(RO-RI)
      EPC(J,K) = EC
      EPR(J,K) = ER
5     CONTINUE
      RETURN
      END
```

```
      SUBROUTINE STRESS(EPRW,EPCW,EPZW,ATBFW,ATBCW,TPRW,TPCW,TPZW,TSRW,
     1TSCW,TSZW,GW,GNUW,SIGRW,SIGCW,SIGZW,EQSI2,J8,NN,CPRS)
      DIMENSION  EPRW(10,4),EPCW(10,4),EPZW(10,4),ATBFW(10,3),ATBCW(10),
     1TPRW(10,4),TPCW(10,4),TPZW(10,4),TSRW(10,4),TSCW(10,4),TSZW(10,4),
     2GW(4),GNUW(4),SIGRW(10,4),SIGCW(10,4),SIGZW(10,4),EQSI2(4),CPRS(4)
      N$ = 1
      IF(J8-NN) 24,21,21
   21 N$ = 4
   24 DO 39 N=N$,4
      EPR5=EPRW(J8,N)
      EPC5 = EPCW(J8,N)
      EPZ5 = EPZW(J8,N)
      IF (N-3) 151,151,141
  141 ATB5 = ATBCW(J8)
      GO TO 153
  151 ATB5 = ATBFW(J8,N)
  153 TPR5 = TPRW(J8,N)
      TPC5 = TPCW(J8,N)
      TPZ5 = TPZW(J8,N)
      TSR5 = TSRW(J8,N)
      TSC5 = TSCW(J8,N)
      TSZ5 = TSZW(J8,N)
      GW5  = GW(N)
      GNU5 = GNUW(N)
      C1 = TSR5 + TSC5 + TSZ5
      C2 = EPR5 + EPC5 + EPZ5 - 3.*ATB5 -C1
      C3 = GNU5/(1.-2.*GNU5)
      C4 = 2.* GW5
      C5 = C3*C2  - ATB5
      SIGRW(J8,N) = C4*(EPR5 + C5 -TPR5 -TSR5)
      SIGCW(J8,N) = C4*(EPC5 + C5 -TPC5 -TSC5)
      SIGZW(J8,N) = C4*(EPZ5 + C5 -TPZ5 -TSZ5)
      SRW = SIGRW(J8,N)
      SCW = SIGCW(J8,N)
      SZW = SIGZW(J8,N)
      CPRS(N) =-C2*(2.+2.*GNU5)*GW5/(1.-2.*GNU5)/3.
```

```
      CALL EQUISI(SRW,SCW,SZW,EQSI9)
      EQSI2(N) = EQSI9
   39 CONTINUE
      RETURN
      END
      SUBROUTINE VHELP2(P1,P2,P3,P4,P5,P6,P7,P8,VV8,VV9,VV10,VV11,VV12)
      D = P2*VV8+P3
      VV9 = P1/D
      VV10 = -P4/D
      VV11 = VV9*(P6*VV8+P7)/P5
      VV12 = P8/P5+VV11*VV10/VV9
      RETURN
      END
      SUBROUTINE XHELP1(ERP7,ECP7,ERS7,ECS7,EZS7,ARTI7,RVB7,RCB7,REB7,
     1G7,GNU7,PPL7,N7,XX1,XX2,XX4,XX5,XX6,XX7,XX8,XX9,XX10,RUB7)          7/16
      DIMENSION ERP7(10,4),ECP7(10,4),ERS7(10,4),ECS7(10,4),EZS7(10,4),
     1ARTI7(4),RVB7(10),RCB7(10),REB7(10),G7(4),GNU7(4),RUB7(10)          7/16
      ERP7C= ERP7(N7,1)
      ECP7C= ECP7(N7,1)
      ERS7C= ERS7(N7,1)
      ECS7C= ECS7(N7,1)
      EZS7C= EZS7(N7,1)
      ARTIC= ARTI7(1)
      RCB77= RCB7(N7)
      RVB77= RVB7(N7)
      GC7 = G7(1)
      GNUC7=GNU7(1)
      CALL ANQUAN (ERP7C,ECP7C,ERS7C,ECS7C,EZS7C,ARTIC,RCB77,RVB77,
     1RCB77,GC7,GNUC7,AN1A,AN2A,AN3A,AN4A,AN1B,AN2B,AN3B,AN4B)            7/15
      ERP7E = ERP7(N7,2)
      ECP7E = ECP7(N7,2)
      ERS7E = ERS7(N7,2)
      ECS7E = ECS7(N7,2)
      EZS7E = EZS7(N7,2)
      ARTIE = ARTI7(2)
      REB77= REB7(N7)
```

```
 GE7 = G7(2)
 GNUE7 = GNU7(2)
 CALL  ANQUAN (ERP7E,ECP7E,ERS7E,ECS7E,EZS7E,ARTIE,REB77,RCB77,
1RCB77,GE7,GNUE7,AN1C,AN2C,AN3C,AN4C,AN1D,AN2D,AN3D,AN4D)          7/15
 XX1 = AN2B - AN1C                                                 7/15
 XX2 = AN2C
 XX4 = AN3B - AN3C                                                 7/15
 XX5 = AN4B - AN4C + AN1B*PPL7                                     7/15
 ERP7E = ERP7(N7,3)                                                7/15
 ECP7E = ECP7(N7,3)                                                7/15
 ERS7E = ERS7(N7,3)                                                7/15
 ECS7E = ECS7(N7,3)                                                7/15
 EZS7E = EZS7(N7,3)                                                7/15
 ARTIE = ARTI7(3)                                                  7/15
 REB77= RUB7(N7)                                                   7/15
 RCB77= REB7(N7)                                                   7/15
 GE7 = G7(3)                                                       7/15
 GNUE7 = GNU7(3)                                                   7/15
 CALL  ANQUAN (ERP7E,ECP7E,ERS7E,ECS7E,EZS7E,ARTIE,REB77,RCB77,    7/15
1RCB77,GE7,GNUE7,AN1E,AN2E,AN3E,AN4E,AN1F,AN2F,AN3F,AN4F)          7/15
 XX6 = AN1D                                                        7/15
 XX7 = AN2D - AN1E                                                 7/15
 XX8 = AN2E
 XX9 = AN3D - AN3E                                                 7/15
 XX10 = AN4D - AN4E                                                7/15
 RETURN
 END
 SUBROUTINE XHELP2 (X1,X2,X4,X5,X6,X7,X8,X9,X10,PA0,PAZ,PAFC,PB0,  7/18
1 PBZ,PBFC )                                                       7/18
 D = X7*X1 + X2*X6
 PA0 = -(X7*X5 + X2*X10)/D
 PAZ =    -(X7*X4 + X2*X9)/D                                       7/19
 PAFC = X2*X8/D
 PB0 = (X6*X5 - X1*X10)/D
 PBZ =  (X6*X4 - X1*X9)/D
 PBFC = X1*X8/D
```

```
      RETURN
      END
      SUBROUTINE XLAME(TBC,TBY,GX,GNUX,J,NN,RHO,RHOT)
      DIMENSION TBX(3),GX(4),GNUX(4),TBY(3),RHO(3)
      E00=3.16E+07
      EP = -2.35
      TLG=16300.
      ONU = .317
      ONUP = -.46
      AA3=4.770E+06
      AA4=-1.906E+03
      AA7=.387
      AA8=8.18E-5
      JNX = 0
      IF(J-NN) 9,10,10
9     DO 3  K = 1,3
      IF(TBY(K)-TLG+100.) 2,2,1
2     TBX(K) = TBY(K)
      GO TO 3
1     TBX(K) = TLG-100.
      JNX = 1
3     CONTINUE
      DO 7 K = 1,3
      P = -RHO(K)/RHOT + 1.
      E = E00*(1.+EP*P)*(1.-TBX(K)/TLG)
      GNU = ONU*(1.+ONUP*P)
      GNUX(K) = (GNU*(TLG-TBX(K))+0.5*(TBX(K)-77.))/(TLG-77.)
7     GX(K) = E/(2.+2.*GNUX(K))
 10   TBCX = TBC
6     GX(4) = AA3+AA4*TBCX
      GNUX(4)= AA7+AA8*TBCX
8     RETURN
      END
      SUBROUTINE TIMITR (DELT,DELTO,TIME1,TIME2,POWAV,PPOW,TOUT,PTOUT,
     1 TIN,PTIN,JKL,JKLM,KUTSTP,KONVRG,NEWTIM,NDTIME,NDTIM1,
     2TINCRE,ISEIKO,TAUCRE)
```

```
C **
C **   REVISED LIFE-1LWR ITERATION PATTERN TO DECREASE REQUIRED NUMBER
C **    OF ITERATIONS FOR EXECUTION TO A GIVEN TIME.
C **
      IF(TAUCRE.GT.TIME2) GO TO 11
   10 IF(DELT.GT.TINCRE.AND.ISEIKO.EQ.1) GO TO 1111
   11 IF (DELT .LE. (2.*DELTO))  GO TO 70
 1111 I = 0
      JKL = 2
      IF (NEWTIM .EQ. 1)  ITEST = 1
      IF (ITEST.EQ.1 .AND. KONVRG.EQ.1)  NDTIME = NDTIME - 1
      IF (NDTIME .LE. 1)  NDTIME = 1
      IF (ITEST.EQ.1 .AND. KUTSTP.NE.0)  NDTIME = NDTIME + 1
      IF (NDTIME .GT. NDTIM1)  NDTIME = NDTIM1
   20 CONTINUE
      TIME2 = TIME1 + DELT/2.
      POWAV = PPOW + (POWAV - PPOW)/2.
      TOUT = PTOUT + (TOUT - PTOUT)/2.
      TIN = PTIN + (TIN - PTIN)/2.
      DELT = DELT/2.
      IF (I .EQ. 1)  GO TO 90
      IF(TAUCRE.GT.TIME2) GO TO 21
      IF(DELT.GT.TINCRE.AND.ISEIKO.EQ.1) GO TO 20
   21 IF (DELT .GT. (2.*DELTO))  GO TO 20
      IF (NEWTIM.EQ.1 .AND. KUTSTP.EQ.0)  GO TO 60
      NEWTIM = 0
   30 CONTINUE
      IF (JKLM .EQ. 1)  GO TO 50
      IF (KUTSTP.GE.2 .AND. ITEST.EQ.0)  GO TO 80
      IF (KUTSTP.GE.1  .AND.  KONVRG.EQ.1 .OR. ITEST.EQ.0)  GO TO 80
      IF (NDTIME .GT. NDTIM1)  NDTIME = NDTIM1
   40 CONTINUE
      ITEST = 0
      IF (INDEX .GE. NDTIME)  GO TO 60
      INDEX = INDEX + 1
      I = 1
```

```
      GO TO 20
   50 CONTINUE
      IF (KUTSTP.GE.2 .AND. ITEST.EQ.0)  GO TO 80
      IF (KUTSTP.GE.1 .AND. KONVRG.EQ.1)  GO TO 80
      IF (KUTSTP.GE.1 .AND. ITEST.EQ.0)  NDTIME = NDTIME - 1
      IF (NDTIME .LE. 1)  NDTIME = 1
      IF (NDTIME .GT. NDTIM1)  NDTIME = NDTIM1
      GO TO 40
   60 CONTINUE
      INDEX = 1
   70 KUTSTP = 1
   80 ITEST = 1
   90 KUTSTP = KUTSTP - 1
      IF (KUTSTP .LE. 0)  KUTSTP = 0
      KONVRG = 1
      RETURN
      END
```

LIST OF REFERENCES

1) A. Garlick, "Fracture of Zircaloy Cladding Under Simulated Power Ramp Conditions", Journal of Nuclear Materials 49, 209-224 (1973/1974).

2) Donald R. Olander, "Fundamental Aspects of Nuclear Reactor Fuels", ERDA, 1976.

3) EPRI, "Evaluation of Fuel Performance in Maine Yankee Core I Task C", NP-218 Project 586-1 Final Report, November 1976.

4) Westinghouse Nuclear Energy Systems, "Reference Core Report 17x17".

5) R. Manzel and H. Stehle, "KWU-In-reactor Experience with LWR Fuel" in Proceedings of European Nuclear Conference, Progress in Nuclear Energy, Maturity vol. 3, 1975.

6) E. Duncomb, J. E. Meyer, W. A. Coffman, "Comparison with Experiment of Calculated Dimensional Changes and Failure-Analysis of Irradiated Bulk Oxide Fuel Test Rods Using CYGRO-1 Computer Program", WAPD-TM-583, September 1966.

7) G. Lucas and R. L. Coble, "MIT Course 22.72J", Class Notes Spring 1977.

8) Dúncan, Smerd, "Fuel Performance Experience in CE and KWU Pressurized Water Reactors", Transaction ANS vol. 18 page 251 (1974).

9) R. N. Duncan, Knoedler, Stehle, Knaab, "Fuel Performance Experience in CE and KWU Pressurized Water Reactors", Transaction ANS vol. 16, page 104 (1973).

10) J.A.L. Robertson, "Nuclear Failures: Their Causes and Remedies", Proc Joint ANS/CNA Topl Mtg Commercial Fuel Technology Today, Toronto, Canada (1973).

11) J. T. A. Roberts, E. Smith, N. Fuhrman, D. Cubicciotti, "On the Pellet-cladding Interaction Phenomenon", Nuclear Technology, August 1977.

12) Steinar Aas, "Effects of Load Following on Fuel Rods", Nuclear Eng and Design 33, 261-268 (1975).

13) Y. Yung Liu, A. L. Bement, "A Regression Approach for Zircaloy-2 in Reactor Creep Constitutive Equations", Trans 4th Intl Conf Str Mech in Reactor Tech C, Paper C3/3 (1977).

14) Dr. Ing Thomas A. Jaeger, "Discussion on Cylindrical Fuel Pellet Behavior and Mechanical Interaction Effects Between Fuel and Cladding", MIT Course 22314, Class Handouts, Fall 1976.

15) G. H. Gittus, D. A. Howl, H. Hughes, "Theoretical Analysis of Cladding Stresses and Strains Produced by Expansion of Cracked Fuel Pellets", Nuclear Applications and Technology vol. 9, July 1970.

16) R. D. Page, D. G. Hardy, A. J. Moradian, J. Howilson, G. R. Fanjoy and D. B. Nazzer, "Engineering and Performance of UO_2 Fuel Assemblies", Third U. N. Conf on Peaceful Use of Atomic Energy, Geneva, September 1964.

17) G. E. Lucas, "Modification of LIFE-1 for Prediction of Light Water Reactor Fuel Pin Behavior", MIT Dept of Nuclear Engineering (1975).

18) K. Vindem and L. Lunde, "Fuel Element Failures Caused by Iodine Stress Corrosion", in Proceedings of European Conference, Progress in Nuclear Energy, Maturity vol.3 (1975).

19) Su Chiang Shu Faya, "An Introduction to Current Modeling Techniques in Nuclear Fuel Performance Analysis", Dept of Nuclear Eng MIT, (1976).

20) J. E. Lunde and A. Hanevik, "Studies Conducted at the OECD Halden Reactor Project on Pellet Clad Mechanincal Interaction Mechanism", Institute for Atomenergy, Halden, Norway (1975).

21) EPRI, "Planning Support Document for the EPRI Light Water Reactor Fuel Rod Performance Program", SR-25 Special Report, December 1975.

22) Eliot Duncombe and Ivan Goldberg, "Axial Ratchetting of Fuel Under Pressure Cycling Conditions", Nuclear Applications and Technology vol. 9, July 1970.

23) Y. Mishima, T. Wada, Y. Wakashima, "Thermal Deformation of UO_2 Pellets in Thin-walled Small-clearance Fuel Pin", in Proceedings of the European Nuclear Conf, vol. 3 (1975).

24) Babcock & Wilcox, "Plant Operation",

25) J. T. Roberts, Personal Communication, MIT, June 1977.

26) D. L. Bell, "Utility Requirements for Analytical Fuel Rod Models", EPRI Utility Review Meeting for RP 397 Project.

27) EPRI, "A Power Shape Monitoring System to Evaluate the Effects of Core Power Maneuvers on Fuel Rod Reliability", Request for Proposal - Project Description RFP 4484.

28) G. Lysel, G. Valli, "Overpower Ramp Tests on Cirene Prototype Fuel Pins", Nuclear Fuel Performance Conference, London, 1973.

29) E. Rolstad, K. Sanholm, "Overpower-to-failure on a High

Burnup Fuel Rod", Nuclear Fuel Performance Conference, London 1973.

30) S. Aas, K. D. Olshausen, K. Vindem, "Fuel Failures Caused by Overpower Ramps", Nuclear Fuel Performance Conference, London 1973.

31) C. C. Busby, R. P. Tucker and J. E. McCauley, "Halogen Stress Corrosion Cracking of Zircaloy-4 Tubing", Journal of Nuclear Materials 55, 64-82 (1975).

32) D. O. Pickman, K. M. Rose and J. A. Robinson, "Endurance of SGHWR Fuel Elements Under Steady and Transient Conditions", in Proceedings of European Nuclear Conference, 1975.

33) R. K. Lo and J. C. Wood, "CANDU Fuel Power Ramp Performance Criteria", Nuclear Technology, vol. 34, July 1977.

34) D. Cordall, R. M. Cornell, K. W. Jones and J. S. Waddington, "Fuel Failures in the Dodeward Boiling Water Reactor", Nuclear Technology vol. 34, August 1977.

35) J. C. Wood, B. A. Surette, J. M. London and J. Baird, "Environmentally Induced Fracture of Zircaloy by Iodine and Cesium; The Effects of Strain Rate, Localized Stresses and Temperature", Journal of Nuclear Materials

57,155-179 (1975).

36) P. E. MacDonald, J. M. Broughton, "Cracked Pellet Gap Conductance Model: Comparison of Prap-S Calculations with Measured Fuel Centerline Temperatures", Conf-750360-2 (1975).

37) Su Chiang Shu Faya, "Survey on Fuel Pellet Cracking and Healing Phenomena in Reactor Operation", Dept of Nuclear Engineering, MIT 1977.

38) Mike Kramen, "Calibration of the CYGRO and LIFE Fuel Element Modeling Codes", N. E. Thesis, MIT 1977.

39) Westinghouse Nuclear Energy System, "Final Safety Analysis Report Angra I Nuclear Power Plant Furnas Centrais Eletricas S. A., Rio de Janeiro, Brazil", 1976.

40) Gilberto G. de Andrade, "Load Following Operation of a Pressurized Water Nuclear Power Plant", N. E. Thesis, MIT 1977.

41) W. Keller, "Pressurized Water Reactor Development, Mechanical-Structural Requirements and Problems", Siemens, Germany 1973

42) A. Accary, "Applications of Sintering in Nuclear Industry" Powder Metalurgy, vol. 2 #2 page 40-42 (1970).

43) Dr. Gary J. Busselman, "The Evolution of Nuclear Fuel Design", MIT Nuclear Eng Seminar, March 14, 1977.

44) J. R. Halmiton, "Babcock-205, A Standard 205 Fuel Assembly NSS", American Power Conf, Chicago, Illinois, April 1976.

45) Floyd Gelhaus, John Hallan and Tor Savar, "Reactor Fuel Reliability Constraints on Power Shape Control", Nuclear Engineering and Science 64, 684-693 (1977).

46) Scandpower Inc., "Scandpower Fuel Technology Program", (1976).

47) EPRI, "Nuclear Fuel Performance Evaluation", NP-409 Project 509-1 Final Report.

48) G. E. Lucas, "The Strength-Differential in Zirconium and its Effects on Clad Creepdown Analysis", MIT Dept of Nuclear Engineering, 1976.

49) Floyd E. Gelhaus, "The Cladding Flaw Growth Index: A Method for Corewide Fuel Rod Reliability Prediction", EPRI Special Report NP-324-SR, February 1977.

50) Scandpower International Consultants," The Scandpower Model for Fuel Failure Frequency Projection", 1976.

51) H. E. Williamson and Dana C. Ditmore, "Current BWR Fuel Design and Experience", Reactor Technology, vol. 14 #1, Spring 1971.

52) John E. Meyer, "Structural Mechanics in Nuclear Power Technology", Class Notes of MIT Course 22314, Fall 1976.

53) D. D. Lanning, "Power Reactors", Class Notes of MIT Course 22.32, Fall 1976.

54) Stanley Kass, "The Development of Zircaloys", Bettis Atomic Power Laboratory, Westinghouse Eletric Co.

55) R. D. MacDonald and A. S. Bain, "Canadian Report AECL-1159-1960.

56) F. A. Nichols, "Theory of the Creep of Zircaloy During Neutron Irradiation", Journal of Nuclear Materials 30, 249-270 (1969).

57) H. Stehle and H. Assmann, "The Dependence of IN-reactor UO_2 Densification of Temperature and Microstructure", Journal of Nuclear Materials 52, 303-308 (1974).

58) P. J. Pankaskie, "BUCKLE, An Analytical Computer Code for Calculating Creep Buckling of an Initially Oval Tube", Battelle Pacific Nothwest Laboratories, May 1974.

59) J. A. L. Robertson, "Irradiation Effects in Nuclear Fuels" American Nuclear Society.

60) V. Z. Jankus and R. W. Weeks, "LIFE-1, a FORTRAN-IV Computer Code for the Prediction of Fast-reactor Fuel-element Behavior,"